STUDY OF 1-D FLOW IN POROUS MEDIA

A Thesis submitted to Gujarat Technological University

for the award of

Doctor of Philosophy

in

Science - Maths

by

Mahendra A. Patel
Enrollment No.: 139997673006

under supervision of

Dr. Narendrasinh B. Desai

GUJARAT TECHNOLOGICAL UNIVERSITY
AHMEDABAD

JANUARY 2019

STUDY OF 1-D FLOW IN POROUS MEDIA

A Thesis submitted to Gujarat Technological University

for the award of

Doctor of Philosophy

in

Science - Maths

by

Mahendra A. Patel
Enrollment No.: 139997673006

under supervision of

Dr. Narendrasinh B. Desai

GUJARAT TECHNOLOGICAL UNIVERSITY
AHMEDABAD

JANUARY 2019

DECLARATION

I declare that the thesis entitled **"Study of 1-D Flow in Porous Media"** submitted by me for the degree of Doctor of Philosophy is the record of research work carried out by me during the period from **February 2014 to August 2018** under the supervision of **Prof. (Dr.) Narendrasinh B. Desai**, Head of Mathematics Department, A. D. Patel Institute of Technology, New V. V. Nagar, Anand and this has not formed the basis for the award of any degree, diploma, associateship, fellowship, titles in this or any other University or other institution of higher learning.

I further declare that the material obtained from other sources has been duly acknowledged in the thesis. I shall be solely responsible for any plagiarism or other irregularities, if noticed in the thesis.

Signature of the Research Scholar: Date: 15/01/2019

Name of Research Scholar: **Mahendra A. Patel**

Place: Gandhinagar.

CERTIFICATE

I certify that the work incorporated in the thesis **"Study of 1-D Flow in Porous Media"** submitted by Shri **Mahendrakumar Amrutbhai Patel** was carried out by the candidate under my supervision/guidance. To the best of my knowledge: (i) the candidate has not submitted the same research work to any other institution for any degree/diploma, Associateship, Fellowship or other similar titles, (ii) the thesis submitted is a record of original research work done by the Research Scholar during the period of study under my supervision, and (iii) the thesis represents independent research work on the part of the Research Scholar.

Signature of Supervisor: Date: 15/01/2019

Name of Supervisor: **Dr. Narendrasinh B. Desai**

Place: New V. V. Nagar.

Course-work Completion Certificate

This is to certify that **Mr. Mahendrakumar Amrutbhai Patel** enrollment no. **139997673006** is a PhD scholar enrolled for PhD program in the branch **Science - Maths** of Gujarat Technological University, Ahmedabad.

(Please tick the relevant option(s))

☐ He has been exempted from the course-work (successfully completed during M.Phil Course)

☐ He has been exempted from Research Methodology Course only (successfully completed during M.Phil Course)

☐ He has successfully completed the PhD course work for the partial requirement for the award of PhD Degree. His performance in the course work is as follows-

Grade Obtained in Research Methodology (PH001)	Grade Obtained in Self Study Course (Core Subject) (PH002)
BB	**BB**

Supervisor's Sign:

Name of Supervisor: **Dr. Narendrasinh B. Desai**

Originality Report Certificate

It is certified that PhD Thesis titled **"Study of 1-D Flow in Porous Media"** by **Mahendrakumar Amrutbhai Patel** has been examined by us. We undertake the following:

a. Thesis has significant new work / knowledge as compared already published or are under consideration to be published elsewhere. No sentence, equation, diagram, table, paragraph or section has been copied verbatim from previous work unless it is placed under quotation marks and duly referenced.

b. The work presented is original and own work of the author (i.e. there is no plagiarism). No ideas, processes, results or words of others have been presented as Author own work.

c. There is no fabrication of data or results which have been compiled / analysed.

d. There is no falsification by manipulating research materials, equipment or processes, or changing or omitting data or results such that the research is not accurately represented in the research record.

e. The thesis has been checked using **Turnitin** (copy of originality report attached) and found within limits as per GTU Plagiarism Policy and instructions issued from time to time (i.e. permitted similarity index $\leq 25\%$).

Signature of the Research Scholar: Date: 15/01/2019

Name of Research Scholar: **Mahendra A. Patel**

Place: Gandhinagar.

Signature of Supervisor: Date: 15/01/2019

Name of Supervisor: **Dr. Narendrasinh B. Desai**

Place: New V. V. Nagar.

Turnitin Originality Report

Study of 1-D Flow in Porous Media_05082018 by GEC Gandhinagar 013

From PG Project Report_47 (ME Final Dissertation_2)

Processed on 05-Aug-2018 21:53 IST
ID: 958702108
Word Count: 34951

Similarity Index	Similarity by Source	
24%	Internet Sources:	24%
	Publications:	14%
	Student Papers:	8%

sources:

1 6% match (Internet from 01-Aug-2018)
https://www.ripublication.com/gjpam16/gjpamv12n1_90.pdf

2 5% match (Internet from 01-Aug-2018)
http://ijmaa.in/v6n1-c/463-470.pdf

3 4% match (Internet from 01-Aug-2018)
https://easychair.org/publications/open/nQW

4 2% match (Internet from 17-Apr-2018)
http://www.nonlinearscience.com/downloads/0000000223.pdf

5 1% match (Internet from 01-Aug-2018)
https://www.ripublication.com/ijcam17/ijcamv12n3_01.pdf

6 1% match (Internet from 30-Mar-2014)
http://www.gigapaper.ir/Articles/math/abbasband/Shijun_Liao__Homotopy_analysis_method_in_nonlinear_differential_

7 1% match (student papers from 27-Jun-2018)
Submitted to Sardar Vallabhbhai National Inst. of Tech.Surat on 2018-06-27

8 1% match (Internet from 14-Apr-2018)
https://www.ijirset.com/upload/2015/august/95_21_An.pdf

9 1% match (publications)
Jacob Bear, Alexander H.-D. Cheng, "Modeling Groundwater Flow and Contaminant Transport", Springer Nature America, Inc, 2010

10 1% match (Internet from 01-Jun-2017)
http://journals.tubitak.gov.tr/math/issues/mat-16-40-5/mat-40-5-18-1508-3.pdf

11 1% match (Internet from 01-Dec-2016)
http://www.ejpam.com/index.php/ejpam/article/download/2506/443

paper text:

STUDY OF 1-D FLOW IN POROUS MEDIA A Thesis submitted to Gujarat Technological University for the award of Doctor of Philosophy in Mathematics by Mahendra A. Patel Enrollment No.: 139997673006 under supervision of Dr. Narendrasinh B. Desai GUJARAT TECHNOLOGICAL UNIVERSITY AHMEDABAD AUGUST 2018 Chapter 1 General Introduction 1.1 Introduction This chapter deals with the introductory nature and general introduction of the subject matter of the thesis viz, basic concepts of porous media, mathematical formulation of the fluid flow problems and homotopy analysis solution of the problems arising

PhD THESIS Non-Exclusive License to GUJARAT TECHNOLOGICAL UNIVERSITY

In consideration of being a PhD Research Scholar at GTU and in the interests of the facilitation of research at GTU and elsewhere, I, Mahendrakumar Amrutbhai Patel having enrollment no. 139997673006 hereby grant a non-exclusive, royalty free and perpetual license to GTU on the following terms:

a). GTU is permitted to archive, reproduce and distribute my thesis, in whole or in part, and/or my abstract, in whole or in part (referred to collectively as the "Work") anywhere in the world, for non-commercial purposes, in all forms of media;

b). GTU is permitted to authorize, sub-lease, sub-contract or procure any of the acts mentioned in paragraph (a);

c). GTU is authorized to submit the Work at any National / International Library, under the authority of their "Thesis Non-Exclusive License";

d). The Universal Copyright Notice (©) shall appear on all copies made under the authority of this license;

e). I undertake to submit my thesis, through my University, to any Library and Archives. Any abstract submitted with the thesis will be considered to form part of the thesis.

f). I represent that my thesis is my original work, does not infringe any rights of others, including privacy rights, and that I have the right to make the grant conferred by this non-exclusive license.

g). If third party copyrighted material was included in my thesis for which, under the terms of the Copyright Act, written permission from the copyright owners is required, I have obtained such permission from the copyright owners to do the acts mentioned in paragraph (a) above for the full term of copyright protection.

h). I retain copyright ownership and moral rights in my thesis, and may deal with the copyright in my thesis, in any way consistent with rights granted by me to my University in this non-exclusive license.

i). I further promise to inform any person to whom I may hereafter assign or license my copyright in my thesis of the rights granted by me to my University in this non-exclusive license.

j). I am aware of and agree to accept the conditions and regulations of PhD including all policy matters related to authorship and plagiarism.

Signature of the Research Scholar:
Name of Research Scholar: **Mahendra A. Patel**
Date: 15/01/2019 Place: Gandhinagar.

Signature of Supervisor:
Name of Supervisor: **Dr. Narendrasinh B. Desai**
Date: 15/01/2019 Place: New V. V. Nagar.
Seal:

Thesis Approval Form

The viva-voce of the PhD Thesis submitted by **Shri Mahendrakumar Amrutbhai Patel** (Enrollment No. 139997673006) entitled **"Study of 1-D Flow in Porous Media"** was conducted on Tuesday, 15 January 2019 at Gujarat Technological University.

(Please tick any one of the following option)

☐ The performance of the candidate was satisfactory. We recommend that he be awarded the PhD degree.

☐ Any further modifications in research work recommended by the panel after 3 months from the date of first viva-voce upon request of the Supervisor or request of Independent Research Scholar after which viva-voce can be re-conducted by the same panel again.

(briefly specify the modifications suggested by the panel)

☐ The performance of the candidate was unsatisfactory. We recommend that he should not be awarded the PhD degree.

(The panel must give justifications for rejecting the research work)

Name and Signature of Supervisor with Seal

1) (External Examiner:1) Name and Signature

2) (External Examiner:2) Name and Signature

3) (External Examiner:3) Name and Signature

ABSTRACT

The fluid flow through porous media is one of the most important concept in many areas of applied science and engineering such as hydrogeology, petroleum engineering, water resource engineering, soil mechanics, environmental engineering, chemical engineering, construction engineering, civil engineering, geophysics, biophysics etc.

In recent years, extensive research works have been carried out to study the fluid flow through porous media. This field has gained extensive attention due to its broad range of applications in science and industry. In particular, the modeling of fluid flow through porous media is a central problem within the field of various applications in such areas. The scope of the present study lies in an increasing importance of the hydrodynamics of single phase flow and multiphase flow through porous media. Due to vast scope of multiphase flow through porous media, the specific problems are almost unlimited and therefore it is reasonable to select such types of problems for discussion here. Accordingly a selection of more interesting problems of current interest have been made for mathematical treatment in the work. The investigated problems of the present study are concerned with the flow of immiscible and incompressible fluids.

This work has been devoted to study of 1-D flow in porous media and the development of mathematical model of fluid flow through porous media. The physical phenomena like as fingering phenomenon, imbibition phenomenon, fingero-imbibition phenomenon, infiltration phenomenon arise in fluid flow through porous medium which are encountered in many fields of science and engineering. The mathematical problems of different physical phenomena give us one dimensional nonlinear partial differential equations. These equations are solved using homotopy analysis method whose convergence is discussed by choosing proper value of convergence control parameter. The solution of the problems have been studied numerically and graphically with the help of Mathematica coding.

Acknowledgement

It is a matter of tremendous pleasure for me to submit my Ph.D. thesis entitled "Study of 1-D Flow in Porous Media" in the subject of Mathematics. My registration was done in the year 2014 for carrying out the work related to the subject which seemed to me to be herculean task ab initio but with the passing of time, everything seemed to be within the reach by god's grace.

I feel highly indebted to my guide Dr. Narendrasinh B. Desai, Head, Department of Mathematics, A. D. Patel Institute of Technology, New V. V. Nagar, Anand. He has been a consistent supporter during the course of my work. He has been the real guiding force behind this work who inspired me to go on with undaunted courage. My Doctorate Progress Committee members also guided me through all these years. I would like to thank Dr. H. C. Patel, Professor, L. D. College of Engineering, Ahmedabad and Dr. M. S. Joshi, Associate Professor, C. K. Pithawala College of Engineering & Technology, Surat, who have reviewed my research work time to time and given the valuable suggestion in my research work.

During the process of preparation of my thesis, I have refered many books and research papers for which I personally thank the authors who provided me a deep insight and inspiration for the solution of problems.

I sincerely thank my previous Principal Dr. C. B. Bhatt and my current Principal Dr. S. P. Dave and Dr. I. N. Trivedi, Head, General Department, who have allowed and cooperated to do this research work as a part time candidate along with my job responsibilities. Thanks are due to my colleagues like Mr. D. J. Prajapati, Dr. T. J. Patel, Mr. P. M. Gadhavi, Mr. M. I. Bosmia, Dr. P. L. Vihol and all the faculty members of Mathematics department, Government Engineering College, Sector-28, Gandhinagar. I am also thankful to Dr. R. K. Jain, Principal, A. D. Patel Institute of Technology for his cooperation.

No value is more precious than the value of the family hence, I sincerely thank my parents, my wife Shital for great help and constant inspiration throughout my work. They have done everything they could to make me feel relaxed and inspired.

At the end, I would like to appreciate all the help and support extended to me during this journey.

Mahendra A. Patel

Contents

List of Symbols

g	acceleration due to gravity
P_c	capillary pressure
ρ_o	constant density of oil
ρ_w	constant density of water
β	constant quantity
δ_o	constant viscosity of oil
δ_w	constant viscosity of water
c_0	convergence control parameter
q	embedding parameter
κ	hydraulic conductivity
θ	inclination of the bed
$\mathscr{L}$	linear operator
$\overline{P}$	mean pressure
Θ	moisture content
$\mathscr{N}$	nonlinear operator
K	permeability of the porous medium
P	porosity of porous medium
P_o	pressure of oil
P_w	pressure of water
k_o	relative permeability of oil
k_w	relative permeability of water
S_o	saturation of oil
S_w	saturation of water
D	soil water diffusivity
v_t	total velocity
v_o	velocity of oil
v_w	velocity of water

List of Figures

List of Tables

Dedicated to my son Vrund .....

CHAPTER 1

General Introduction

1.1 Introduction

This chapter deals with the introductory nature and general introduction of the subject matter of the thesis viz, basic concepts of porous media, mathematical formulation of the fluid flow problems and homotopy analysis solution of the problems arising from the fluid flow through porous media.

The scope of the present investigation lies in an increasing importance of single phase and double phase flow through porous media. The thesis discusses the approximate analytical solution of some problems of single phase and double phase flow through porous media. The mathematical formulation of the problems lead to one dimensional nonlinear partial differential equations which are solved with suitable conditions using homotopy analysis method. The fluid flow through porous media has a great importance in many areas of applied sciences and engineering such as environmental science, water resource engineering, petroleum engineering, hydrogeological engineering, civil engineering, geoscience etc. The common subject of study is the fluid flow through porous media and it has been of interest for a long time.

1.2 Structure of the thesis

The thesis consists basically of 8 main chapters. Subsequent to these introductory words, Chapter 2 gives an overview of basic concepts of porous media, fluid flow through porous media, fundamental equations for fluid flow through porous media and

basic terminology of homotopy analysis method which has helped us to solve nonlinear differential equations.

The next Chapter 3 is targeted to the problem of fingering phenomenon arising in fluid flow through homogeneous porous medium. We obtain the solution of governing equation with the help of homotopy analysis method.

Chapter 4 is focused on homotopy analysis solution of countercurrent imbibition phenomenon. In this chapter, the mathematical model is studied for the problem of countercurrent imbibition phenomenon in the inclined homogeneous porous medium. The mathematical problem yields to one dimensional nonlinear partial differential equation and solves it using appropriate boundary conditions. Using c_0-curves, we have obtained convergent solution.

Chapter 5 discusses the mathematical model for cocurrent imbibition phenomenon in the inclined homogeneous and heterogeneous porous medium. The solutions of the governing equations are discussed by homotopy analysis method. The solutions represent saturation of injected water. The graphical and numerical solutions are also discussed.

Chapter 6 explains the phenomenon of fingero-imbibition arising in fluid flow through heterogeneous porous medium. The mathematical model of the phenomenon of fingero-imbibition in heterogeneous porous medium with magnetic field effect is studied. The homotopy analysis method is used to solve the governing equations with boundary conditions. The graphical and numerical interpretations of solutions are given with the help of Mathematica software. The comparative numerical values of the solution for fingero-imbibition phenomenon without magnetic field effect and with magnetic field effect are given.

Chapter 7 is focused on the infiltration phenomenon in unsaturated homogeneous soil. Homotopy series solution of the Boussinesq's equation for infiltration phenomenon has been obtained. The numerical and graphical interpretations of solution has also been given.

The last Chapter 8 presents an analysis of investigations of the problem of one dimensional groundwater recharge in the vertical downward direction. When the groundwater is recharged by spreading of water on ground surface, the moisture content increases in soil. On the basis of linear and nonlinear conductivity and diffusivity functions, three cases are considered for Brooks-Corey model. The proper value of convergence control parameter for convergent solution has been chosen from c_0-curve.

Some of the results/solutions reported here are also published in scholarly, peer reviewed and indexed journals as well as presented in conferences.

The references are given alphabetically at the end.

1.3 Brief description on the state of the art of the research topic

Scheidegger [77] has introduced the physics of flow through porous media. The study of the physics of fluid flow through porous media has become basis for many scientific and engineering applications like as groundwater hydrology, ceramic engineering, petroleum engineering, water resource engineering, soil mechanics etc. All these branches of science and engineering have contributed a vast amount of literature on this topic.

The fluid flow through porous media can be classified into single phase flow and multiphase flow. Many researchers have discussed the single phase flow and multiple phase flow with different view points. Different type of problems of fluid flow through porous media in the various fields have been discussed by Muskat [47]. The theory of dynamics of fluids in porous media, as applicable to many disciplines of science and engineering are given in the book "Dynamics of fluids in porous media" by Bear [5]. It helps researchers to know where flow through porous media plays a fundamental role in several fields such as soil mechanics, soil physics, groundwater hydrology, petroleum engineering, drainage and irrigation engineering, chemical engineering and

sanitary engineering. By reading this literature, I have learnt which has made easier to understand and analyze my research topic. The phenomenon of fingering (instability) has great importance in various engineering fields like agriculture engineering, groundwater hydrology and petroleum engineering, soil mechanics [6, 8, 13, 71, 78, 82]. The phenomenon of fingering in homogeneous porous media without capillary pressure was examined from a statistical viewpoint by Scheidegger and Johnson [78]. The stabilization of fingers in a specific oil-water displacement process with capillary pressure has been statistically discussed for a heterogeneous porous medium by Verma [86].

Spontaneous imbibition is the one of most important phenomenon. Spontaneous imbibition may be classified as countercurrent or cocurrent. The cocurrent and countercurrent imbibition phenomena have been investigated by many researchers with different viewpoints [9, 11, 14, 19, 22, 24, 38, 43, 70, 77, 81, 93]. The simultaneous occurrence of both phenomena fingering and imbibition is known as fingero-imbibition phenomenon which is investigated by researchers with different viewpoints [19, 25, 44, 45, 52, 53, 57, 58, 79, 87].

Infiltration is the process by which the water on ground surface enters into soils and moves into rocks through pore spaces and cracks. The problem in groundwater infiltration has been studied by many authors with different aspects [15, 68, 80, 89, 91].

One dimensional groundwater recharge problem is related to hydrology, environmental engineering, soil mechanics, water resource engineering etc. The flow of water in unsaturated soil has been considered with some specific assumptions. The problem of groundwater flow has been discussed by many authors with different aspects [27, 30, 48, 74, 85].

1.4 Definition of the Problem

In the secondary oil recovery process, physical phenomena like as fingering phenomenon, countercurrent imbibition phenomenon, cocurrent imbibition

phenomenon, fingero-imbibition phenomenon occur in the two phase flow through porous medium. The mathematical models of 1-D flow in porous medium has been studied with some specific assumptions in the present work. The aim of the present study is to investigate the behavior of the saturation of injected water in different physical phenomena which are arising in fluid flow through homogeneous or heterogeneous porous medium. To study the infiltration phenomenon through unsaturated porous medium and the solution of the Boussinesq's equation for infiltration phenomenon. The objective of the work is to investigate the behavior of the moisture content of soil in the groundwater flow when excess water on the ground surface is spreading in the vertical direction through unsaturated porous medium.

1.5 Objective and Scope of work

The main goal of the present work is to study the 1-D flow in porous media. The primary objective of our study is to discuss the one dimensional mathematical problem arising in fluid flow through porous media. The secondary objective is to study the solution of one dimensional nonlinear partial differential equation by homotopy analysis method. The solution represents:

1. the saturation of the injected water which helps us to predict the amount of water required to inject for recovering oil,
2. the moisture content which helps us to predict the amount of water spread in the unsaturated soil.

This type of mathematical model is useful for predicting oil recovery from petroleum reservoir and for predicting moisture content increase in unsaturated soil. The scope of the current work is to study of problems of 2-D flow in porous media.

1.6 Original contribution by the thesis

The original contribution made by the study is created/modified mathematical models of countercurrent imbibition phenomenon in the inclined homogeneous porous

medium, cocurrent imbibition phenomenon in the inclined homogeneous and heterogeneous porous medium, and the phenomenon of fingero-imbibition in a heterogeneous porous medium with magnetic field effect.

The solutions of various problems of fluid flow through porous media are discussed using homotopy analysis method with appropriate boundary conditions. Comparative study of the phenomenon of fingero-imbibition with magnetic field effect and without magnetic field effect are given.

1.7 Methodology of Research and Results/Comparisons

We have studied various literatures related to fluid flow through porous media and done a comparative analysis to find out research gap and problem statement. The literature survey helped us to define an objective of the research.

We have used Mathematica BVPh package for nonlinear boundary value problems [36]. It is a combination of the homotopy analysis method and the computer algebra system Mathematica, and provides us a convenient analytic tool to solve many nonlinear differential equations. We have studied various problems of fluid flow through porous medium and according to research gap we create/modify the mathematical model for different physical phenomena arising in two phase flow through porous medium during secondary oil recovery process.

We have discussed the problems related to fingering phenomenon, cocurrent and countercurrent imbibition phenomenon, fingero-imbibition phenomenon, infiltration phenomenon, groundwater recharge. We have obtained the series solutions of one dimensional nonlinear partial differential equations which are arising in fluid flow through porous medium using homotopy analysis method. The convergence of homotopy series solution is dependent on convergence control parameter which is chosen from c_0-curve. We used Mathematica BVPh package to plot c_0-curves and to obtain numerical and graphical representations of solutions.

1.8 Achievements with respect to objectives

The mathematical models of the problems in fluid flow through porous media are created/modified for countercurrent imbibition phenomenon in the inclined homogeneous porous medium, cocurrent imbibition phenomenon in the inclined homogeneous and heterogeneous porous medium, and the phenomenon of fingero-imbibition in the heterogenous porous medium with magnetic field effect.

We have discussed the problems of fluid flow through porous media for oil-water displacement process (instability) in the homogeneous porous medium, countercurrent imbibition phenomenon occurring in the inclined homogeneous porous medium, cocurrent imbibition phenomenon in the inclined homogeneous and heterogeneous porous medium, fingero-imbibition phenomenon occurring in fluid flow through heterogeneous porous medium with and without magnetic field effect, the infiltration phenomenon through unsaturated porous medium and groundwater recharge in the vertical direction. The solutions of mathematical problems are obtained by homotopy analysis method with suitable boundary conditions.

1.9 Conclusion

We have studied the mathematical models of different physical phenomena like as fingering phenomenon, countercurrent imbibition phenomenon, cocurrent imbibition phenomenon, fingero-imbibition phenomenon which are arising during secondary oil recovery process. We have discussed the infiltration phenomenon through unsaturated porous medium and an approximate analytical solution of the Boussinesq's equation for infiltration phenomenon. Also we have investigated the mathematical model of groundwater recharge in vertical downward direction through unsaturated porous medium. All the problems are considered in one dimensional fluid flow and then the governing equations come in the form of one dimensional nonlinear partial differential equations. Homotopy analysis method is adopted to find solutions of nonlinear partial differential equations with appropriate boundary conditions. The solutions are

interpreted graphically as well as numerically using Mathematica BVPh package for homotopy analysis method.

CHAPTER 2

Basic Concepts

2.1 Introduction

This chapter is devoted to some basic concepts of fluid flow, porous media and homotopy analysis method. The appropriate notation will be introduced and thus, it will provide a base for the following chapters of the thesis.

2.2 Fluid flow through porous medium

A porous medium means a material consisting of a solid matrix with a certain amount of pores spaces (voids or interspaces), either connected or disconnected, dispersed within it in either a regular or random manner. These pores may contain a variety of fluids such as water, oil, air, gas etc. If the pores represent a certain portion of the bulk volume, a complex network can be formed which is permeable to contain fluids. Only these permeable porous media are taken into consideration in this volume. The interconnected pores allow the fluid flow through it. A porous medium is most often characterized by its porosity. Many natural substances such as rocks and soil (e.g. petroleum reservoirs, aquifers), biological tissues (e.g. muscles, bones), and man made materials such as ceramics and cements can be considered as porous media.

Various examples are given below where porous media plays an important role.

- In Soil Science: The soil (porous medium) contains water and nutrients, and transports them to plants.

- In Medical and Biological Science: Most of biological tissues of the body (e.g. bones, cardiac, muscles) are porous media.
- In Hydrology: The porous medium relates with water flow in the earth and sand structures, such as water flow to wells from water bearing formations and sea water intrusion in coastal areas.
- In Chemical Science: The porous medium is applied as filter or catalyst bed.
- In Petroleum Technology: The reservoir rock (porous medium) contains crude oil and natural gas.

We are mostly interested in porous medium with a connected pore space because we focus on fluid flow. Flow in porous media is a common research topic encountered in many branches of engineering, groundwater hydrology, petroleum engineering, medical and biological science, chemical engineering etc. In fluid mechanics, single phase flow occurs when the pores are completely saturated by only one fluid. Multiphase flow is simultaneous flow of different phases (i.e. gas, liquid or solid). Two-phase flow is a particular example of multiphase flow.

Basically one must distinguish between two groups of porous media: 1. intergranular 2. fractured. Porous materials having both intergranular and fractured porosity are known as dual porous media. On the other side, concerned with mechanical properties, it should distinguish between consolidated porous medium and unconsolidated porous medium. The particles of a consolidated porous medium are held together by a cementing material, like as sandstone, lime stone, concrete, cement, clothes, wood, human lung and in the other type the grains are loose, like as beach sand, glass beads, catalyst pellets.

2.3 Types of fluid flow

2.3.1 Steady and unsteady flow

Fluid flow can be steady or unsteady, depending on the fluid properties. The flow in which fluid properties at a point do not vary with the time is called *steady flow*. The flow in which fluid properties at a point vary with time is said to be *unsteady flow*.

2.3.2 Uniform and non-uniform flow

If the velocity at a given time is the same in both magnitude and direction throughout the flow domain, the flow is called *uniform flow*. The flow of fluid in which velocity at a given time changes from point to point, is called *non-uniform flow*.

2.3.3 Laminar and turbulent flow

Laminar flow occurs when a fluid flows in parallel layers with no disruption between the layers. The fluid flow in which the adjacent layer of fluid cross to each other and move in definite path is called *turbulent flow*. The ratio of the inertial force to viscous force is said to be the *Reynolds number* R_e which determines whether a flow is laminar or turbulent. It can be concluded that when the viscous forces are dominant (slow flow, low R_e) they are sufficient enough to take all the fluid particles in parallel line, so the flow is laminar. Very low R_e shows viscous creeping motion where inertia effects are avoidable. When the inertial forces dominate over the viscous forces, (when the fluid is flowing speedy and R_e is bigger) then the flow will be turbulent. Experiments have shown that if the Reynolds number is less than 2000, then the flow will be laminar. At Reynolds number between 2000 and 4000, the flow is volatile as a result of the inception of turbulence. This flow is sometimes known as *transitional flow*. If R_e is greater than 4000, the flow is turbulent.

2.3.4 Compressible and incompressible flow

Fluid flow can be compressible or incompressible, depending on whether you can easily compress the fluid. Usually liquids are impossible to compress, whereas gases (also considered a fluid) are much compressible. The fluid flow in which the density of fluid changes from point to point is called *compressible flow*. The flow in which density is constant (volume does not change) is called *incompressible flow*.

2.3.5 One, two and three dimensional flows

Term one, two or three dimensional flow refers to the number of space coordinates required to describe a flow. It appears that any physical flow is generally three-dimensional but some can be estimated to a two dimensional or even one dimensional flow to simplify the calculations without loosing too much accuracy. This is achieved by ignoring changes to flow in any of the directions, thus reducing the complexity.

2.4 Fundamental properties of porous media

A material or structure must have these two properties in order to come under a porous medium:

- It must contain interstices (voids or solid free spaces or pores), implanted in the solid or semi-solid matrix. The interstices usually contain some fluids like as air, water, oil or a mixture of different fluids.
- It must be permeable to a various fluids, i.e. fluids should be able to infiltrate through one face of a sample of material and appear on the other side.

Whereas fluid and structure properties such as porosity or permeability are well examined and known, the determination of the fluid-structure interaction still poses a

lot of questions. The porous medium may be classified as homogeneous porous medium or heterogeneous porous medium depending upon whether its properties are uniform throughout or variable. A porous medium domain is referred to as *homogeneous* if its permeability is the same at all points of the domain. If not, the porous medium domain is known as *heterogeneous*.

A porous medium is said to be *isotropic* at a point if the permeability is independent of direction at that point. Otherwise it is known as *anisotropic*. This behavior reflects the macroscopic effect of the geometrical configuration of the pore space.

2.4.1 Porosity

Porosity (P), a porous medium property, is defined as the ratio of volume of the void space V_P to the total volume V_T of a porous medium (say, of a rock sample)

$$P = \frac{V_P}{V_T} = \frac{V_T - V_s}{V_T} \tag{2.1}$$

where V_s is the volume of solids within V_T. The porosity is a dimensionless quantity. The porosity is dependent on the structure and texture of the porous material. The porosity changes from 25% to 90%.

2.4.2 Saturation

Usually pores may contain several fluids. The *saturation* of a certain fluid, say α-fluid is defined as

$$S_\alpha = \frac{\text{Volume of } \alpha \text{ phase in the porous media}(V_\alpha)}{\text{Effective pore volume of the porous media}(V_P)}. \tag{2.2}$$

Summing the saturations results in

$$\sum_\alpha S_\alpha = 1. \tag{2.3}$$

2.4.3 Wettability

A drop of fluid on a plane solid surface can take various shapes. The respective shape is dependent on the wettability of the considered fluid. Figure 2.1 explains that property. The water is wetting phase in the case of water and air, and the air is the wetting phase in case of mercury and air.

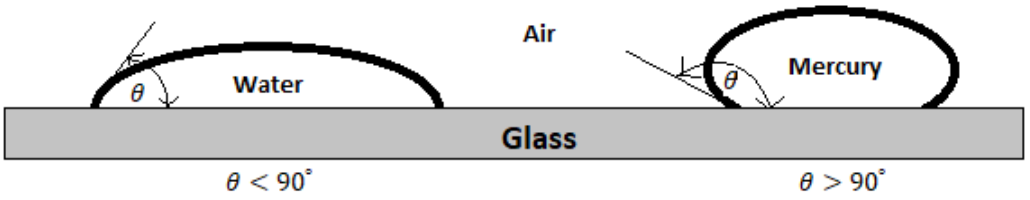

FIGURE 2.1: Comparison of wetting and nonwetting fluid.

The contact angle θ is used as a measure of wettability. When the contact angle is smaller than 90°, the fluid is known as *wetting fluid*. The fluid is called *nonwetting fluid* when the contact angle is greater than 90°.

2.4.4 Capillary pressure

In double phase flow, a discontinuity in fluid pressure arises across an interface between two immiscible fluids (eg. oil and water). The difference between the pressure of nonwetting phase P_o (eg. oil) and pressure of wetting phase P_w (eg. water) is known as *capillary pressure* P_c:

$$P_c = P_o - P_w. \tag{2.4}$$

2.4.5 Darcy's law

The volumetric flow rate of the fluid through homogeneous sand column is (a) proportional to the constant cross-sectional area A of the column and proportional to

the difference in fluid level elevations at inflow and outflow of the column, (b) inversely proportional to the length of the column. i.e.

$$Q = \kappa A \frac{h^{(1)} - h^{(2)}}{L} \tag{2.5}$$

where κ is the proportionality coefficient.

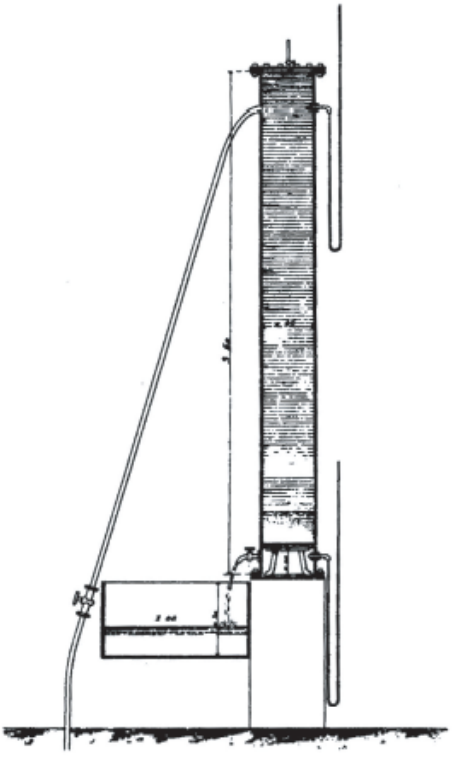

FIGURE 2.2: Darcy's column experiment.

2.4.6 Specific discharge

Specific discharge or *Darcy velocity* is defined as the volumetric flow rate of water per unit time through a unit cross-sectional area A, i.e.

$$v = \frac{Q}{A} = \kappa \frac{h^{(1)} - h^{(2)}}{L}. \tag{2.6}$$

Darcy's law was formulated from experiments on a vertical homogeneous sand column, it can be easily extended to the one dimensional flow in the inclined column

(see figure 2.3). The elevations $h^{(1)}$ and $h^{(2)}$ represent the hydraulic heads (piezometric heads) in the respective reservoirs, defined by

$$h = z + \frac{p}{\rho g}, \quad \rho g = \gamma \tag{2.7}$$

where z is the elevation of the point at which the piezometric head is being considered, above some datum level, p is the pressure of fluid, ρ is the density of fluid, γ is the specific weight of fluid and g is the acceleration due to gravity. The pressure head ψ is the internal energy of a fluid due to the pressure and is expressed as $\psi = \frac{p}{\rho g}$.

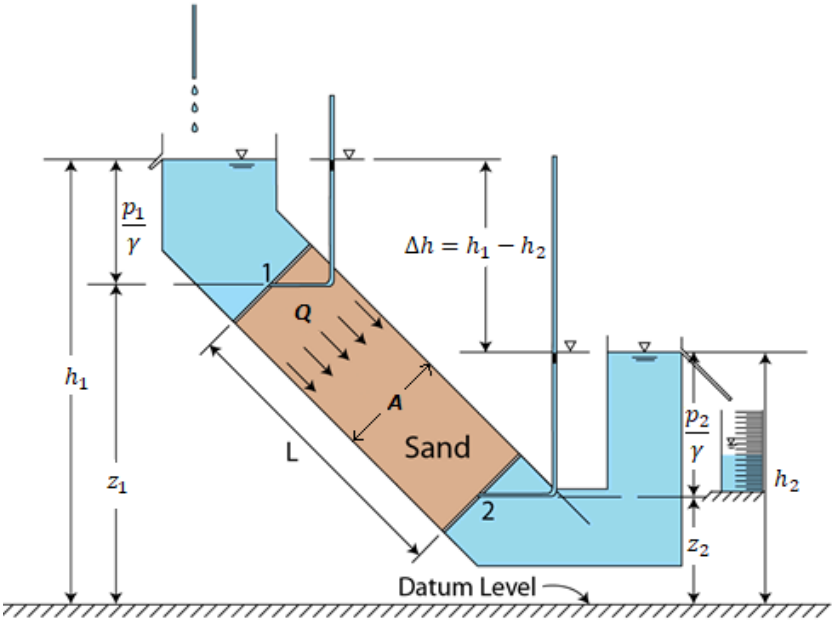

FIGURE 2.3: Darcy's Experiments in inclined sand filter.

In the inclined homogeneous reservoir, Darcy's law gives

$$v = \frac{Q}{A} = -\frac{\kappa}{\rho g}\left(\frac{\partial p}{\partial z} + \rho g sin\theta\right). \tag{2.8}$$

For one dimensional, horizontal flow (or when $\theta = 0$), Darcy's law takes the form

$$v = \frac{Q}{A} = -\frac{\kappa}{\rho g}\frac{\partial p}{\partial x}. \tag{2.9}$$

2.4.7 Hydraulic conductivity

Hydraulic conductivity κ indicates the ability of the aquifer to conduct water through it under hydraulic gradient. It is a combined property of the porous medium and the fluid flowing through it. Hydraulic conductivity is dependent on grain size, structure and texture of the soil matrix, type of soil fluid and saturation of the soil matrix. Important properties relevant to the solid matrix of the soil include pore size distribution, pore shape, tortuosity, specific surface and porosity. The effects of the various solid matrix (actually, void space) features are combined in the form of a coefficient called permeability.

The hydraulic conductivity κ is given by

$$\kappa = \frac{K\rho g}{\delta} = \frac{Kg}{\nu} \tag{2.10}$$

where K is the permeability, ρ is the density, g is the acceleration due to gravity, δ is the dynamic viscosity, ν is the kinematic viscosity. Permeability of the porous medium is the measure of ability of porous material to allow fluid to pass through it.

2.4.8 Permeability

The *permeability* is the most important physical property of a porous medium, which is a measure of the ability of a material to transmit fluid through it. The permeability K is a very important rock property because it controls the directional movement and the flow rate of the reservoir fluids in the formation.

2.4.9 Effective permeability

When there is only single fluid moving through porous medium, the permeability for this case is called *absolute permeability*. However, when there is more than one fluids present in a rock, the permeability of each fluid to flow is decreased because another fluid will also be flowing in the rock. The ability to preferentially flow or transmit a

particular fluid when other immiscible fluids are present in a rock is called the *effective permeability* of that fluid (e.g. effective permeability of gas in a gas-water reservoir). The effective permeability of each fluid is related to the properties of the geometrical configuration of the portion of pore space occupied by each fluid [6]. For each fluid, the effective permeability is dependent on the phase saturation.

2.4.10 Relative permeability

Underlying the extension of the motion equation of a single fluid to the simultaneous flow of two or more fluids is the concept of relative permeability. In multiphase flow through porous media, the *relative permeability* is the ratio of effective permeability of a particular fluid at a particular saturation to absolute permeability of that fluid at total saturation. If a single fluid is present in a rock, its relative permeability is 1.

For an isotropic porous medium, relative permeability to water and relative permeability to oil may be defined as [7]

$$k_w = \frac{k_{ew}(S_w)}{k_{sat}} \text{ and } k_o = \frac{k_{eo}(S_o)}{k_{sat}} \tag{2.11}$$

where k_{sat} is the permeability at full saturation $(S_w = 1)$, k_{ew} is the effective permeability to water and k_{eo} is the effective permeability to oil. The relative permeability is commonly used to describe permeability for multiphase flow in an isotropic porous medium. Note that $0 \leq k_w \leq 1$, and $0 \leq k_o \leq 1$.

2.4.11 Seepage velocity

At the particulate level, water takes the flow path through the void spaces (see figure 2.4). The portion of the area A available to flow fluid is PA. The *seepage velocity (average velocity)* of a fluid flowing through porous medium is

$$\frac{v}{P} = \frac{Q}{PA}. \tag{2.12}$$

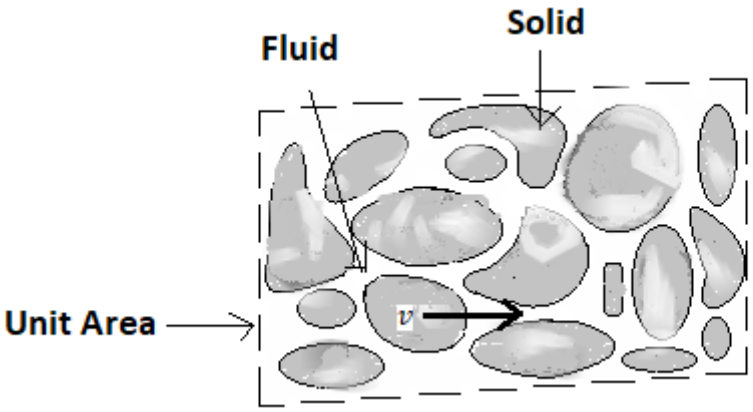

FIGURE 2.4: Porous medium cross-section.

2.4.12 Limitations of Darcy's law

It is difficult to predict the exact range of the validity of Darcy's law. Darcy's law is valid only for slow, viscous flow; fortunately, most groundwater flow cases fall in this category. In fluid mechanics, the Reynolds number R_e is used as a parameter to distinguish between the laminar flow and the turbulent flow. The Reynolds number expresses the ratio between inertial force and viscous force acting on a flowing fluid. The Reynolds number for fluid flow through porous medium is typically expressed as

$$R_e = \frac{vd}{\nu} \tag{2.13}$$

where d is some microscopic length characterizing the pore space, v is specific discharge and ν is the kinematic viscosity of fluid. Experimental tests have shown that Darcy's law is valid as long as Reynolds number doesn't exceed a value of 1 (but sometimes the upper limit can be extended up to 10).

2.5 Conservation of mass equation

For the time dependent problems involving fluid flow, Darcy's law has insufficient data to allow us to solve it. We must derive first a mathematical equation of the mass conservation principle in order to develop a governing equation to time dependent problems.

Assume that α-fluid is flowing through a one dimensional tube of constant cross-sectional area A. In particular, we focus on the region between two locations x and $x+\Delta x$.

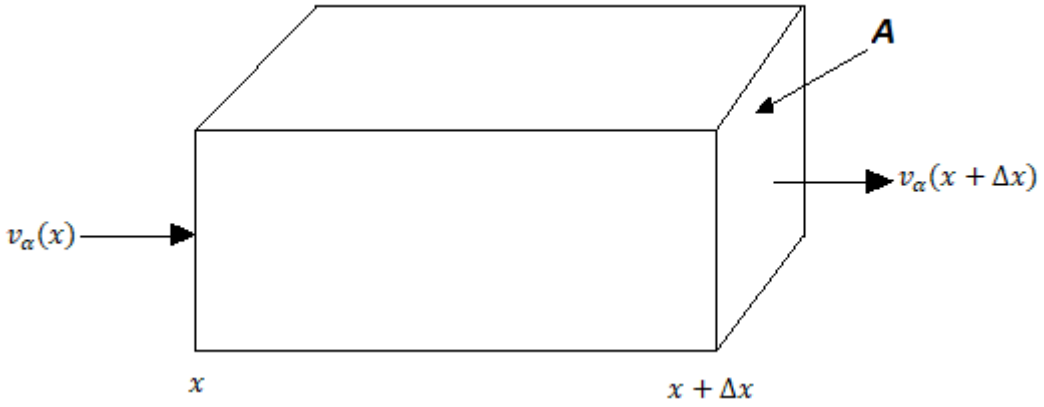

FIGURE 2.5: Region between two locations x and $x+\Delta x$.

Using the mass conservation principle, we get

$$\text{Mass flux in} - \text{Mass flux out} = \text{Increase in amount of mass stored.} \tag{2.14}$$

Note that the mass of the fluid property is conserved, not the volume of the fluid.

Consider that the α-fluid is moving from left to right through the region during the time duration between time t and time $t+\Delta t$. The mass flux in the region during this time increment will be

$$\text{Mass flux in} = A(x)\rho_\alpha(x)v_\alpha(x)\Delta t. \tag{2.15}$$

During this time increment, the mass flux out of the region will be

$$\text{Mass flux out} = A(x+\Delta x)\rho_\alpha(x+\Delta x)v_\alpha(x+\Delta x)\Delta t. \tag{2.16}$$

Suppose that the amount of mass of α-fluid stored in the region is m_α, thus the mass conservation equation takes place the form

$$[A(x)\rho_\alpha(x)v_\alpha(x) - A(x+\Delta x)\rho_\alpha(x+\Delta x)v_\alpha(x+\Delta x)]\Delta t = m_\alpha(t+\Delta t) - m_\alpha(t). \tag{2.17}$$

For one dimensional fluid flow through a cylindrical region, $A(x) = A = \text{constant}$. Now divide both sides of (2.17) by Δt and taking $\Delta t \to 0$, we get

$$-A[\rho_\alpha(x+\Delta x)v_\alpha(x+\Delta x) - \rho_\alpha(x)v_\alpha(x)] = \frac{\partial m_\alpha}{\partial t}. \tag{2.18}$$

But $m_\alpha = \rho_\alpha V_\alpha$, where V_α is the volume of α-fluid contained in the region between x and $x+\Delta x$. So,

$$m_\alpha = \rho_\alpha V_\alpha = \rho_\alpha S_\alpha V_P = \rho_\alpha S_\alpha P V_T = \rho_\alpha P S_\alpha A \Delta x. \tag{2.19}$$

Thus,

$$-A[\rho_\alpha(x+\Delta x)v_\alpha(x+\Delta x) - \rho_\alpha(x)v_\alpha(x)] = \frac{\partial(\rho_\alpha P S_\alpha)}{\partial t} A\Delta x. \tag{2.20}$$

Now divide both sides of (2.20) by $A\Delta x$ and taking $\Delta x \to 0$, we get

$$\frac{\partial(\rho_\alpha P S_\alpha)}{\partial t} + \frac{\partial(\rho_\alpha v_\alpha)}{\partial x} = 0. \tag{2.21}$$

This is the basic equation of conservation of mass for one dimensional flow in the porous medium.

2.6 Basic equation for immiscible fluid flow

The velocity of an immiscible fluid α governed by Darcy's law [5] is expressed as

$$v_\alpha = -\frac{k_\alpha}{\delta_\alpha} K \left[\frac{\partial P_\alpha}{\partial x} + \rho_\alpha g sin\theta \right] \tag{2.22}$$

where v_α is the velocity of α-fluid, k_α is the relative permeability of α-fluid, δ_α is the viscosity of α-fluid, K is the permeability, P_α is the pressure of α-fluid, ρ_α is the density of α-fluid, θ is the angle of inclination with porous medium and g is acceleration due to gravity.

2.7 Fundamental equations of groundwater flow

Groundwater flows through ground surface, flows in downward direction, firstly under the effect of gravity and assemble above some impervious porous stratum. We noted that the following two major zones are beneath the ground surface:

1. The saturated zone, in which relatively all pores and fractures are saturated with water.

2. The unsaturated zone, in which the pore space is partially filled by water and partially filled by air.

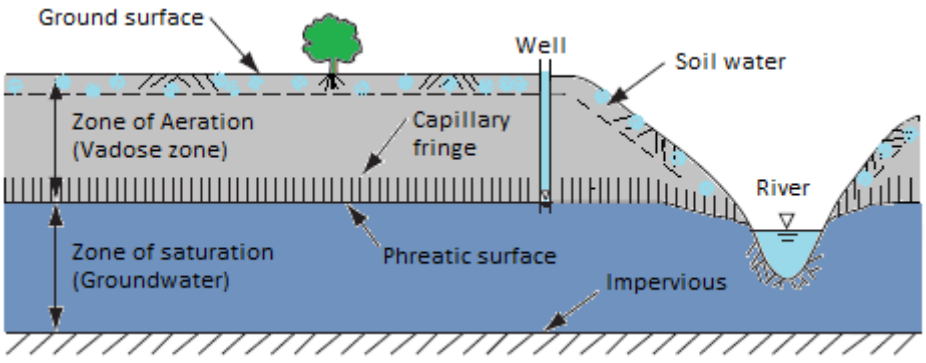

FIGURE 2.6: Subsurface zones [8].

The equation of continuity for water movement in unsaturated porous medium is governed by [5, 30]

$$\frac{\partial}{\partial t}(\rho\Theta) = -\nabla \cdot M \tag{2.23}$$

where ρ is the density, Θ is the moisture content and M is the mass flux of moisture.

Darcy's law for groundwater flow in porous medium is expressed as [5]

$$v = -\kappa\nabla\Phi \tag{2.24}$$

where v is the volume flux of moisture, κ is the hydraulic conductivity, $\nabla\Phi$ is the gradient of the whole moisture potential.

Consider the relation $\Phi = \psi - z$ for the system in which flow takes place in the vertical downward direction only where ψ is the pressure potential [5]. The vertical downward direction is considered as the positive direction of z-axis. We consider that Θ and ψ are related by single valued function and assume that $D = \kappa\frac{\partial\psi}{\partial\Theta}$ is the diffusivity co-efficient. For incompressible flow, (2.23) reduces to

$$\frac{\partial\Theta}{\partial t} = \frac{\partial}{\partial z}\left(D\frac{\partial\Theta}{\partial z}\right) - \frac{\partial\kappa}{\partial z}. \tag{2.25}$$

This equation is known as Richard's equation [3, 8, 30, 48, 75] which is one of the most important equations with broad applications in hydrology, engineering and soil sciences.

2.8 Physical phenomena

2.8.1 Fingering phenomenon

Fingering phenomenon is a physical phenomenon which frequently occurs in problems of petroleum technology. When a fluid having greater viscosity flowing through a porous medium is displaced by another fluid of lesser viscosity then, instead of regular

displacement of whole front, protuberances take place which shoot through the porous medium at a relatively very high speed, and fingers are developed during this process. This phenomenon is called *fingering (instability) phenomenon*. It is important in secondary oil recovery process of petroleum technology.

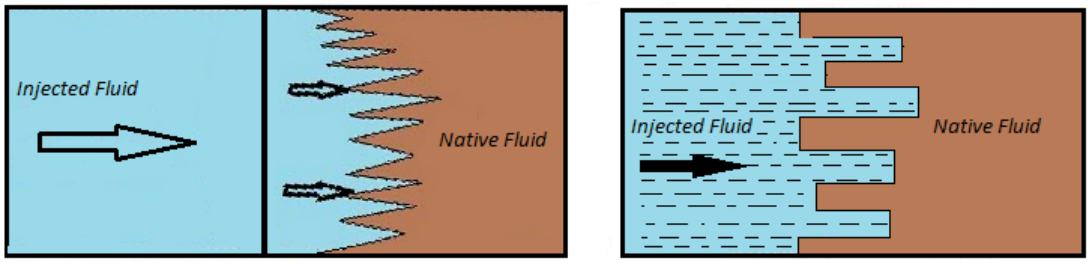

FIGURE 2.7: Representation of fingering phenomenon.

2.8.2 Imbibition phenomenon

When a porous medium filled with some nonwetting phase is brought into contact with another phase which preferentially wets the medium, then there is a spontaneous flow of the wetting phase into the medium and a counter flow of the nonwetting phase from the medium. This phenomenon occurring due to difference in wetting abilities of the phases, is said to be *imbibition phenomenon*. This phenomenon is applicable in oil recovery process, printing process, food industry, biological sciences, surface chemistry, composite materials, textiles and construction.

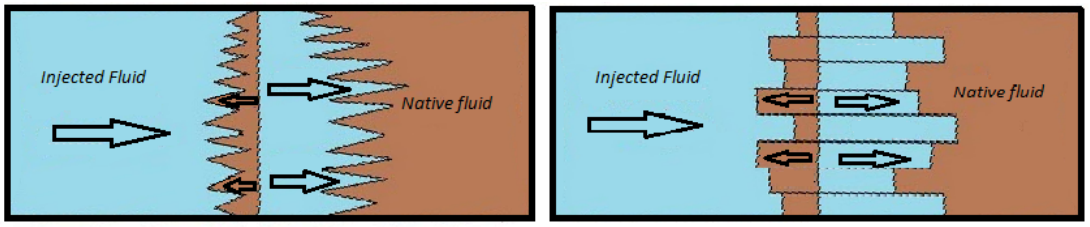

FIGURE 2.8: Representation of imbibition phenomenon.

2.8.3 Fingero-imbibition phenomenon

Fingero-imbibition phenomenon occurs during secondary oil recovery process. Simultaneous occurrence of fingering and imbibition phenomena is said to be *fingero-imbibition phenomenon* and it has been discussed by Verma [87].

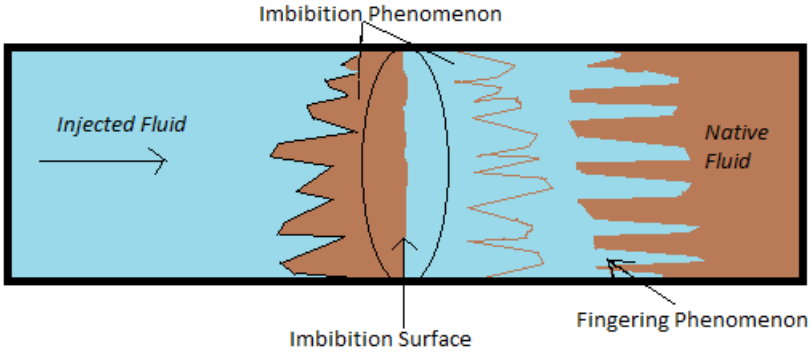

FIGURE 2.9: Representation of fingero-imbibition phenomenon.

2.8.4 Infiltration phenomenon

Infiltration phenomenon is the process by which water on ground surface enters into the subsurface soils and moves into rocks through pore spaces and cracks. The rate of infiltration depends on the different factors like as the amount of vegetative cover, soil texture and structure, the amount of precipitation, water content of the soil, the depth of the water table, storage capacity etc.

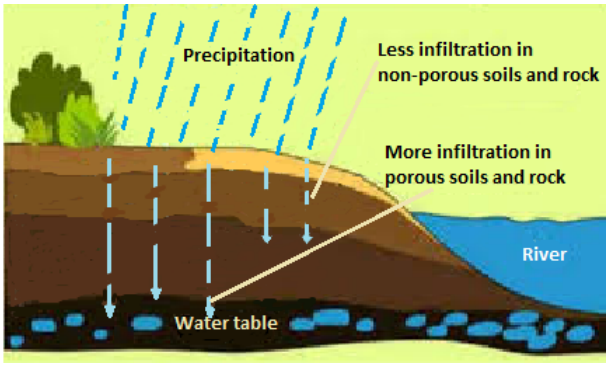

FIGURE 2.10: Infiltration phenomenon.

2.9 Homotopy analysis method (HAM)

2.9.1 Concepts of homotopy

In 1992, the homotopy analysis method [32] was first employed by Liao to solve nonlinear differential equations. This method is very powerful and has been successfully applied to various nonlinear differential equations. Here we shall introduce the basic terminology and fundamental concepts of the homotopy analysis method. Also the convergence of homotopy analysis solution will discussed by means of example.

Definition 2.9.1. Consider continuous functions $f(x)$ and $g(x)$ from a topological space X to a topological space Y. A *homotopy* between two continuous functions $f(x)$ and $g(x)$ is defined as a continuous function $\mathscr{F} : X \times [0,1] \longrightarrow Y$ such that $\mathscr{F}(x;0) = f(x)$ and $\mathscr{F}(x;1) = g(x)$, $\forall\, x \in X$. If such homotopy exists, we can say that f is *homotopic* to g, and is denoted by $f \simeq g$.

For example, let two continuous functions x^3 and $\frac{1-e^{-x}}{1-e^{-1}}$ be defined in the interval $X = [0,1]$ and construct a homotopy $\mathscr{F} : X \times [0,1] \longrightarrow Y$ for $Y = \mathbb{R}$ as

$$\mathscr{F}(x;q) = (1-q)x^3 + q\frac{1-e^{-x}}{1-e^{-1}}$$

where $q \in [0,1]$ is called *the embedding parameter* (*the homotopy parameter*), $\mathscr{F}$ depends on x and q both.

When $q = 0$ and $q = 1$, we have

$$\mathscr{F}(x;0) = x^3, \;\; \forall\, x \in [0,1]$$

and

$$\mathscr{F}(x;1) = \frac{1-e^{-x}}{1-e^{-1}}, \;\; \forall\, x \in [0,1]$$

respectively.

Thus as the homotopy parameter q increases from 0 to 1, the real function $\mathscr{F}(x;q)$ continuously changes from the function x^3 to $\frac{1-e^{-x}}{1-e^{-1}}$ (see figure 2.11).

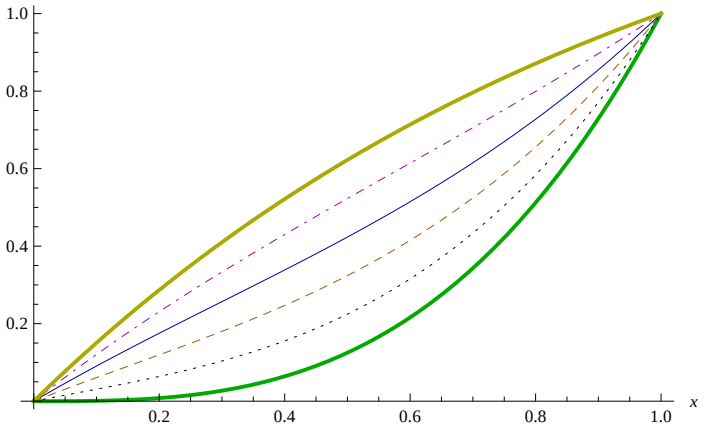

FIGURE 2.11: Continuous deformation of the homotopy $\mathscr{F}(x;q) = (1-q)x^3 + q\frac{1-e^{-x}}{1-e^{-1}}$. Thick line (Green): $q = 0$; Dotted line: $q = 1/5$; Dashed line: $q = 2/5$; Thin line: $q = 3/5$; DotDashed line: $q = 4/5$; Thick line (Yellow): $q = 1$.

2.9.2 Basic ideas of the homotopy analysis method

We consider the nonlinear differential equation

$$\mathscr{N}[u(\mathbf{r},t)] = 0 \tag{2.26}$$

where $\mathscr{N}$ is a nonlinear operator, $\mathbf{r}$ and t are independent variables, $u(\mathbf{r},t)$ is an unknown function.

Consider an auxiliary linear operator $\mathscr{L}$ with property $\mathscr{L}(0) = 0$ and construct the so-called homotopy of operators

$$\mathscr{F}(\mathscr{N},\mathscr{L};q)[u(\mathbf{r},t)] = \mathscr{F}(\mathscr{N}[u(\mathbf{r},t)],\mathscr{L}[u(\mathbf{r},t)];q) \tag{2.27}$$

such that

$$\mathscr{F}(\mathscr{N},\mathscr{L};0)[u(\mathbf{r},t)] = \mathscr{L}[u(\mathbf{r},t)] \tag{2.28}$$

and

$$\mathscr{F}(\mathscr{N},\mathscr{L};1)[u(\mathbf{r},t)] = \mathscr{N}[u(\mathbf{r},t)]. \tag{2.29}$$

Hence it makes sense to set a homotopy corresponding to the equation $\mathscr{N}[u(\mathbf{r},t)] = 0$ as $\mathscr{F}(\mathscr{N},\mathscr{L};q) = 0$. Thus, such a homotopy relates a nonlinear differential equation to a linear differential equation.

The zeroth-order deformation equation

Liao [32] construct a homotopy of functions

$$(1-q)\mathscr{L}[\phi(\mathbf{r},t;q) - u_0(\mathbf{r},t)] - c_0 q H(\mathbf{r},t)\mathscr{N}[\phi(\mathbf{r},t;q)] = 0 \tag{2.30}$$

where $q \in [0,1]$ is *the homotopy parameter* (*the embedding parameter*), $\mathscr{L}$ is the linear operator with property $\mathscr{L}(0) = 0$, $\phi(\mathbf{r},t;q)$ is the solution of (2.30) for $q \in [0,1]$, $u_0(\mathbf{r},t)$ is the initial guess (initial approximation) of $u(\mathbf{r},t)$, c_0 is a nonzero *convergence control parameter* (*auxiliary parameter*), $H(\mathbf{r},t)$ is a nonzero auxiliary function and $\mathscr{N}$ is a nonlinear operator.

We see that when $q = 0$ and $q = 1$, we have

$$\mathscr{L}[\phi(\mathbf{r},t;0) - u_0(\mathbf{r},t)] = 0 \tag{2.31}$$

and

$$c_0 H(\mathbf{r},t)\mathscr{N}[\phi(\mathbf{r},t;1)] = 0 \tag{2.32}$$

then due to the property $\mathscr{L}(0) = 0$ and $c_0 \neq 0,\ H(\mathbf{r},t) \neq 0$, (2.31) and (2.32) become

$$\phi(\mathbf{r},t;0) = u_0(\mathbf{r},t) \tag{2.33}$$

and

$$\mathscr{N}[\phi(\mathbf{r},t;1)] = 0. \tag{2.34}$$

So that the function $\phi(\mathbf{r},t;q)$ agrees the initial guess $u_0(\mathbf{r},t)$ at $q=0$ and from (2.34), we can say that the function $\phi(\mathbf{r},t;1)$ satisfies the nonlinear differential equation $\mathscr{N}[u(\mathbf{r},t)]=0$, i.e. $\phi(\mathbf{r},t;1)=u(\mathbf{r},t)$.

Thus, as the embedding parameter q increases from 0 to 1, the solution $\phi(\mathbf{r},t;q)$ of (2.30) varies continuously from initial guess $u_0(\mathbf{r},t)$ to the solution $u(\mathbf{r},t)$ of the original equation (2.26). In this regard, we call (2.30) as *the zeroth-order deformation equation*.

It is important in the homotopy analysis method that the convergence control parameter, linear operator, auxiliary function and initial approximation has great freedom to choose.

According to Taylor's theorem and (2.33), expanding $\phi(\mathbf{r},t;q)$ with respect to q we have

$$\phi(\mathbf{r},t;q)=u_0(\mathbf{r},t)+\sum_{m=1}^{\infty}u_m(\mathbf{r},t)q^m \tag{2.35}$$

where

$$u_m(\mathbf{r},t)=\frac{1}{m!}\frac{\partial^m\phi(\mathbf{r},t;q)}{\partial q^m}\bigg|_{q=0}. \tag{2.36}$$

Here, the series (2.35) is called *homotopy-Maclaurin series*. If the linear operator, initial approximation, auxiliary function and convergence control parameter are chosen in such a way that the series (2.35) converges at $q=1$. Then we have due to (2.34) *the homotopy series solution*

$$u(\mathbf{r},t)=u_0(\mathbf{r},t)+\sum_{m=1}^{\infty}u_m(\mathbf{r},t). \tag{2.37}$$

The high-order deformation equation

Define $\overrightarrow{u_m}=\{u_0(\mathbf{r},t),u_1(\mathbf{r},t),\ldots,u_m(\mathbf{r},t)\}$. Differentiating (2.30) m times with respect to the homotopy parameter q and then dividing them by $m!$ and finally setting $q=0$ we

have the so called *high-order deformation equation*

$$\mathscr{L}[u_m(\mathbf{r},t) - \chi_m u_{m-1}(\mathbf{r},t)] = c_0 H(\mathbf{r},t)\mathscr{R}_m(\overrightarrow{u_{m-1}}) \tag{2.38}$$

where

$$\mathscr{R}_m(\overrightarrow{u_{m-1}}) = \frac{1}{(m-1)!}\frac{\partial^{m-1}\mathscr{N}[\phi(\mathbf{r},t;q)]}{\partial q^{m-1}}\bigg|_{q=0} \tag{2.39}$$

and

$$\chi_m = \begin{cases} 0 & \text{if } m \leq 1, \\ 1 & \text{if } m > 1. \end{cases} \tag{2.40}$$

Applying $\mathscr{L}^{-1}$ both sides of (2.38), we get the special solution of (2.38)

$$u_m^*(\mathbf{r},t) = \chi_m u_{m-1}(\mathbf{r},t) + \mathscr{L}^{-1}[c_0 H(\mathbf{r},t)\mathscr{R}_m(\overrightarrow{u_{m-1}})]. \tag{2.41}$$

Then, it is easy to obtain general solution $u_m(\mathbf{r},t)$ of (2.38) for $m \geq 1$.

The homotopy series solution (2.37) of (2.26) contains the convergence control parameter c_0. As pointed out by Liao, the convergent homotopy analysis solution is strongly dependent on convergence control parameter c_0 and with the help of c_0-curve ($\hbar$-curve), the proper value of c_0 is chosen.

2.9.3 Some definition and related theorems

Definition 2.9.2. If ϕ is a function of the embedding parameter q, then

$$\mathscr{D}_m(\phi) = \frac{1}{m!}\frac{d^m\phi}{dq^m}\bigg|_{q=0} \tag{2.42}$$

is said to be *the mth-order homotopy derivative* of ϕ, where $m \geq 0$ is an integer, and $\mathscr{D}_m$ is known as *the mth-order homotopy derivative operator* [36].

Theorem 2.9.1. *Consider two arbitrary homotopy-Maclaurin series*

$$\phi = \sum_{i=0}^{\infty} u_i q^i \quad \Psi = \sum_{i=0}^{\infty} v_i q^i \tag{2.43}$$

where ϕ and Ψ are analytic in $q \in [0,a)$, then it satisfies

(a) $\mathscr{D}_m(\phi) = u_m$,

(b) $\mathscr{D}_m(q^k\phi) = \mathscr{D}_{m-k}(\phi)$,

(c) $\mathscr{D}_m(\phi\Psi) = \sum_{i=0}^{m} \mathscr{D}_i(\phi)\mathscr{D}_{m-i}(\Psi) = \sum_{i=0}^{m} u_i v_{m-i} = \sum_{i=0}^{m} \mathscr{D}_{m-i}(\phi)\mathscr{D}_i(\Psi) = \sum_{i=0}^{m} u_{m-i}v_i$,

(d) $\mathscr{D}_m(\phi^{n+1}) = \sum_{i=0}^{m} \mathscr{D}_i(\phi)\mathscr{D}_{m-i}(\phi^n) = \sum_{i=0}^{m} \mathscr{D}_{m-i}(\phi)\mathscr{D}_i(\phi^n)$,

(e) $\mathscr{D}_m(f\phi + g\Psi) = f\mathscr{D}_m(\phi) + g\mathscr{D}_m(\Psi) = fu_m + gv_m$,

where $m \geq 0$, $n \geq 1$, and $0 \leq k \leq m$ are integers, f and g are independent of q [36].

Theorem 2.9.2. *Let $\mathscr{L}$ be the linear operator independent of $q \in [0,1]$. Consider two arbitrary homotopy-Maclaurin series*

$$\phi = \sum_{i=0}^{\infty} u_i q^i \quad \Psi = \sum_{i=0}^{\infty} v_i q^i \tag{2.44}$$

where ϕ and Ψ are analytic in $q \in [0,a)$, then it satisfies

$$\mathscr{D}_m[\mathscr{L}(\phi)] = \mathscr{L}[\mathscr{D}_m(\phi)] = \mathscr{L}(u_m), \tag{2.45}$$

and

$$\mathscr{D}_m[\Psi\mathscr{L}(\phi)] = \sum_{i=0}^{m} \mathscr{D}_{m-i}(\Psi)\mathscr{L}[\mathscr{D}_i(\phi)] = \sum_{i=0}^{m} v_{m-i}\mathscr{L}(u_i), \tag{2.46}$$

where $m \geq 0$ is an integer [36].

Theorem 2.9.3. *Consider a homotopy-Maclaurin series*

$$\phi = \sum_{i=0}^{\infty} u_i q^i, \tag{2.47}$$

where $q \in [0,1]$ be the embedding parameter and linear operator $\mathscr{L}$ with the property $\mathscr{L}[0] = 0$ and is independent of q, then it satisfies

$$\mathscr{D}_m[(1-q)\mathscr{L}(\phi - u_0)] = \mathscr{L}(u_m - \chi_m u_{m-1}), \tag{2.48}$$

where χ_m is defined by (2.40) *[36].*

Theorem 2.9.4. *Let $\mathscr{L}$ be the linear operator with the property $\mathscr{L}(0) = 0$ and is independent of $q \in [0,1]$, $\mathscr{N}$ be a nonlinear operator, $u_0(\boldsymbol{r},t)$ be the initial guess of solution of $\mathscr{N}(u) = 0$, c_0 be the convergence control parameter independent of q, and $H(\boldsymbol{r},t)$ be an auxiliary function independent of q, where $\boldsymbol{r}$ is the spatial independent variable and t is the temporal independent variable. If*

$$\phi(\boldsymbol{r},t;q) = \sum_{i=0}^{\infty} u_i(\boldsymbol{r},t)q^i \tag{2.49}$$

is the homotopy-Maclaurin series of the zeroth-order deformation equation

$$(1-q)\mathscr{L}[\phi(\boldsymbol{r},t;q) - u_0(\boldsymbol{r},t)] = c_0 q H(\boldsymbol{r},t)\mathscr{N}(\phi(\boldsymbol{r},t;q)) \tag{2.50}$$

then the corresponding high-order deformation equation reads

$$\mathscr{L}[u_m(\boldsymbol{r},t) - \chi_m u_{m-1}(\boldsymbol{r},t)] = c_0 H(\boldsymbol{r},t)\mathscr{D}_{m-1}[\mathscr{N}(\phi(\boldsymbol{r},t;q))] \tag{2.51}$$

where χ_m is defined by (2.40) *and $\mathscr{D}_{m-1}$ is defined by* (2.42) *[36].*

Theorem 2.9.5. *Let $\mathscr{L}$ be the linear operator with the property $\mathscr{L}(0) = 0$ and is independent of $q \in [0,1]$, $\mathscr{N}$ be a nonlinear operator, $u_0(\boldsymbol{r},t)$ be the initial guess of solution of $\mathscr{N}(u) = 0$, c_0 be the convergence control parameter independent of q and $H(\boldsymbol{r},t)$ be an auxiliary function independent of q, where $\boldsymbol{r}$ is the spatial independent variable and t is the temporal independent variable. If*

$$\phi(\boldsymbol{r},t;q) = \sum_{i=0}^{\infty} u_i(\boldsymbol{r},t)q^i \tag{2.52}$$

is the homotopy-Maclaurin series of the zeroth-order deformation equation

$$(1-q)\mathscr{L}[\phi(\boldsymbol{r},t;q)-u_0(\boldsymbol{r},t)]=c_0qH(\boldsymbol{r},t)\mathscr{N}(\phi(\boldsymbol{r},t;q)) \tag{2.53}$$

where $u_m(\boldsymbol{r},t)$ *is governed by the corresponding high-order deformation equation*

$$\mathscr{L}[u_m(\boldsymbol{r},t)-\chi_m u_{m-1}(\boldsymbol{r},t)]=c_0H(\boldsymbol{r},t)\mathscr{D}_{m-1}[\mathscr{N}(\phi(\boldsymbol{r},t;q))] \tag{2.54}$$

where $\mathscr{D}_{m-1}$ *is defined by* (2.42) *and* χ_m *is defined by* (2.40)*. If the homotopy-series*

$$u(\boldsymbol{r},t)=\sum_{i=0}^{\infty}u_i(\boldsymbol{r},t) \tag{2.55}$$

converges, then

$$\sum_{i=0}^{\infty}\mathscr{D}_i[\mathscr{N}(\phi(\boldsymbol{r},t;q))]=0. \qquad \textit{[36]} \tag{2.56}$$

2.9.4 Example

As an example, we consider one dimensional nonlinear partial differential equation [28, 38, 59]

$$\frac{\partial S_w}{\partial T}=\frac{\partial}{\partial X}\left[(1-\alpha S_w)\frac{\partial S_w}{\partial X}\right] \tag{2.57}$$

where $S_w(X,T)$ is a function of X and T and $\alpha=1.11$.

We solve (2.57) with the following boundary conditions

$$S_w(0,T)=0.005T,\ 0.6\leq T\leq 1 \tag{2.58}$$

$$\frac{\partial S_w}{\partial X}(1,T)=0,\ 0.6\leq T\leq 1. \tag{2.59}$$

Homotopy analysis method suggests us to choose the initial guess according to our boundary conditions as

$$S_{w_0}(X,T) = 0.005T\left(e^{-X} + \frac{X}{e}\right). \tag{2.60}$$

We choose the linear operator

$$\mathscr{L}[\phi(X,T;q)] = \frac{\partial^2\phi(X,T;q)}{\partial X^2} \tag{2.61}$$

which satisfies the property $\mathscr{L}[0] = 0$. According to (2.57), we define a nonlinear operator $\mathscr{N}$ as

$$\mathscr{N}[\phi(X,T;q)] = \frac{\partial^2\phi(X,T;q)}{\partial X^2} - \alpha\phi(X,T;q)\frac{\partial^2\phi(X,T;q)}{\partial X^2} - \alpha\left\{\frac{\partial\phi(X,T;q)}{\partial X}\right\}^2 - \frac{\partial\phi(X,T;q)}{\partial T}. \tag{2.62}$$

Let $H(X,T) \neq 0$ be an auxiliary function, $c_0 \neq 0$ be the convergence control parameter [35] and $q \in [0,1]$ be the homotopy parameter. The zeroth-order deformation equation is

$$(1-q)\mathscr{L}[\phi(X,T;q) - S_{w_0}(X,T)] = c_0 qH(X,T)\mathscr{N}[\phi(X,T;q)]. \tag{2.63}$$

When $q = 0$, we get

$$\phi(X,T;0) = S_{w_0}(X,T). \tag{2.64}$$

When $q = 1$, we have

$$\phi(X,T;1) = S_w(X,T). \tag{2.65}$$

Thus as q increases from 0 to 1, $\phi(X,T;q)$ varies continuously from the initial guess $S_{w_0}(X,T)$ to the solution $S_w(X,T)$ of (2.57). Assume that the auxiliary linear operator, the initial guess, the convergence control parameter and the auxiliary function are chosen properly so that the expansion of $\phi(X,T;q)$ in powers of q as

$$\phi(X,T;q) = S_{w_0}(X,T) + \sum_{m=1}^{\infty} S_{w_m}(X,T)q^m \tag{2.66}$$

where

$$S_{w_m}(X,T) = \frac{1}{m!}\frac{\partial^m \phi(X,T;q)}{\partial q^m}\bigg|_{q=0} \tag{2.67}$$

converges at $q = 1$. Thus, we have the solution

$$S_w(X,T) = S_{w_0}(X,T) + \sum_{m=1}^{\infty} S_{w_m}(X,T). \tag{2.68}$$

Write $\overrightarrow{S_{w_n}} = \{S_{w_0}(X,T), S_{w_1}(X,T), \ldots, S_{w_n}(X,T)\}$. Differentiating the zeroth-order deformation equation (2.63) m times w.r.t. q and setting $q = 0$ and finally dividing them by $m!$, we have the high-order deformation equation

$$\mathscr{L}[S_{w_m}(X,T) - \chi_m S_{w_{m-1}}(X,T)] = c_0 H(X,T)\mathscr{R}_m(\overrightarrow{S_{w_{m-1}}}) \tag{2.69}$$

subject to

$$S_{w_m}(0,T) = 0 \text{ and } \frac{\partial S_{w_m}}{\partial X}(1,T) = 0,\ m \geq 1 \tag{2.70}$$

where χ_m is defined by (2.40) and

$$\begin{aligned}\mathscr{R}_m(\overrightarrow{S_{w_{m-1}}}) = {} & \frac{\partial^2 S_{w_{m-1}}(X,T)}{\partial X^2} - \alpha \sum_{j=0}^{m-1} S_{w_j}(X,T)\frac{\partial^2 S_{w_{m-1-j}}(X,T)}{\partial X^2} \\ & - \alpha \sum_{j=0}^{m-1} \frac{\partial S_{w_j}(X,T)}{\partial X}\frac{\partial S_{w_{m-1-j}}(X,T)}{\partial X} - \frac{\partial S_{w_{m-1}}(X,T)}{\partial T},\ m \geq 1.\end{aligned} \tag{2.71}$$

Assume that $H(X,T) = 1$. It is easy to obtain the solution of linear ODEs (2.69)-(2.71) with the initial guess and the linear operator. The special solution of (2.69) is

$$S^*_{w_m}(X,T) = \chi_m S_{w_{m-1}}(X,T) + c_0 \mathscr{L}^{-1}[\mathscr{R}_m(\overrightarrow{S_{w_{m-1}}})] \tag{2.72}$$

where $\mathscr{L}^{-1}$ denotes the inverse operator of $\mathscr{L}$. Thus, the solution of (2.69) is

$$S_{w_m}(X,T) = S^*_{w_m}(X,T) + C_1 X + C_2 \tag{2.73}$$

where the coefficients C_1 and C_2 are determined by (2.70). Hence

$$S_w(X,T) = 0.005T\left(e^{-X} + \frac{X}{e}\right) + 0.005c_0\left(Te^{-X} - e^{-X} - \frac{X}{2e} - \frac{X^3}{6e}\right.$$
$$- 0.005\alpha\frac{T^2X^2}{2e^2} - 0.0025\alpha T^2e^{-2X} - 0.005\alpha\frac{T^2Xe^{-X}}{e} + \frac{TX}{e}$$
$$\left. - T + 1 + 0.0025\alpha T^2\right) + \cdots \tag{2.74}$$

is the solution of (2.57). The equation (2.74) is the analytical expression of the solution of (2.57) which is obtained by homotopy analysis method. The convergence of series solution is strongly dependent on convergence control parameter c_0. The proper value of c_0 is chosen with the help of c_0-curve.

We first consider the convergence of some series like as $S_{w_{XX}}(1,1)$ and $S_{w_{XX}}(0,0.8)$. It is found that $S_{w_{XX}}(1,1)$ and $S_{w_{XX}}(0,0.8)$ are dependent on c_0. As pointed out by Liao [33], the corresponding series of $S_{w_{XX}}(1,1)$ and $S_{w_{XX}}(0,0.8)$ converge to the same value for each c_0. The curve of $S_{w_{XX}}(1,1)$ and $S_{w_{XX}}(0,0.8)$ v/s c_0 contains a line segment parallel to horizontal axis [2, 18, 21, 23, 33, 34, 54, 59, 61, 63, 83]. These curves are called *the c_0-curves* [33], which give the valid region of c_0.

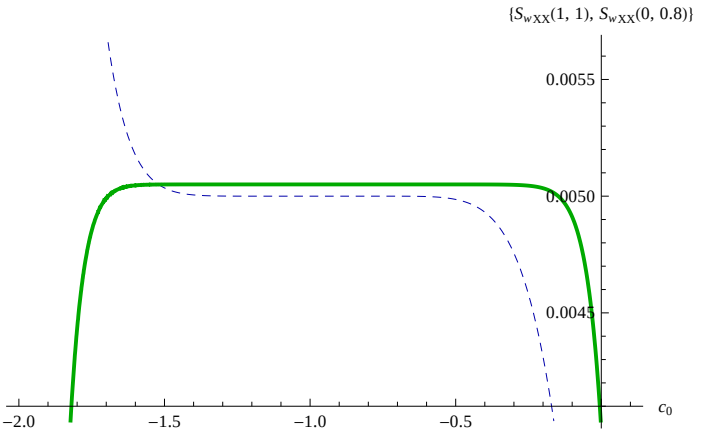

FIGURE 2.12: The c_0-curves of $S_{w_{XX}}(1,1)$(Dashed line) and $S_{w_{XX}}(0,0.8)$(Solid line) for 10th-order approximation.

The c_0-curves of $S_{w_{XX}}(1,1)$ and $S_{w_{XX}}(0,0.8)$ are plotted using Mathematica software [36]. Figure 2.12-2.14 show the c_0-curves of $S_{w_{XX}}(1,1)$ and $S_{w_{XX}}(0,0.8)$ for

different order approximations. The line segment parallel to horizontal axis in the c_0-curve gives us the valid region $-1.4 \leq c_0 \leq -0.5$. For different values of c_0 in the region $-1.4 \leq c_0 \leq -0.5$, the series of $S_{w_{XX}}(1,1)$ and $S_{w_{XX}}(0,0.8)$ given by solution expression converge to 0.00499997 and 0.00505032 respectively, as shown in Table 2.1.

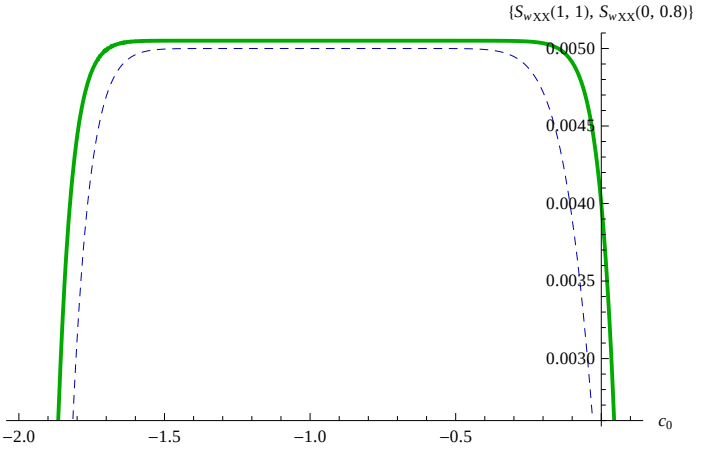

FIGURE 2.13: The c_0-curves of $S_{w_{XX}}(1,1)$(Dashed line) and $S_{w_{XX}}(0,0.8)$(Solid line) for 15th-order approximation.

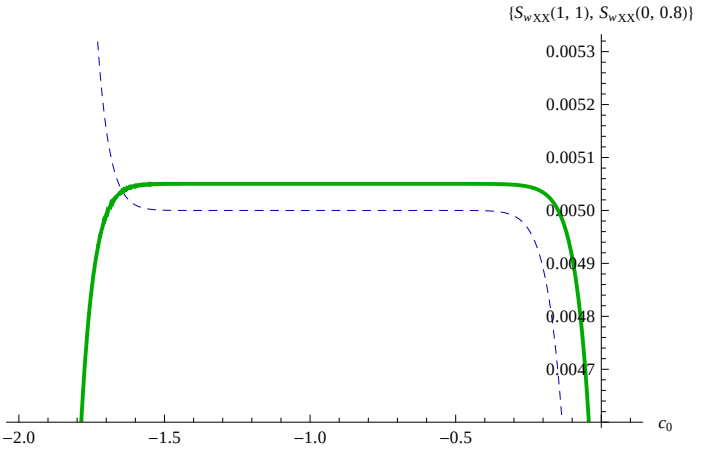

FIGURE 2.14: The c_0-curves of $S_{w_{XX}}(1,1)$(Dashed line) and $S_{w_{XX}}(0,0.8)$(Solid line) for 20th-order approximation.

The numerical interpretation of solution of (2.57) is given in Tables 2.2 and 2.3 for convergence control parameter $c_0 = -1$ and $c_0 = -0.8$ respectively.

We have discussed homotopy analysis method for nonlinear partial differential equation. We have discussed the convergence of homotopy series solution. The proper

TABLE 2.1: Approximations of $S_{wXX}(1,1)$ and $S_{wXX}(0,0.8)$ given by solution expression for different values of c_0.

Order	$S_{wXX}(1,1)$				$S_{wXX}(0,0.8)$			
	$c_0=-0.5$	$c_0=-0.8$	$c_0=-1$	$c_0=-1.3$	$c_0=-0.5$	$c_0=-0.8$	$c_0=-1$	$c_0=-1.3$
5^{th}	0.00470054	0.00499413	0.00499989	0.00495155	0.00500826	0.00504796	0.00505034	0.00505282
10^{th}	0.00498603	0.00499998	0.00499997	0.00500051	0.00504783	0.00505031	0.00505032	0.00505014
15^{th}	0.00499954	0.00499997	0.00499997	0.00499997	0.00505014	0.00505032	0.00505032	0.00505032
20^{th}	0.00499997	0.00499997	0.00499997	0.00499997	0.00505031	0.00505032	0.00505032	0.00505032

TABLE 2.2: Numerical values of solution $S_w(X,T)$ when $c_0=-1$ for 10th and 20th-order approximation.

X	$T=0.6$		$T=0.7$		$T=0.8$		$T=0.9$		$T=1.0$	
	10^{th} *order*	20^{th} *order*	10^{th} *order*	20^{th} *order*	10^{th} *order*	20^{th} *order*	10^{th} *order*	20^{th} *order*	10^{th} *order*	20^{th} *order*
0.0	0.00300000	0.00300000	0.00350000	0.00350000	0.00400000	0.00400000	0.00450000	0.00450000	0.00500000	0.00500000
0.1	0.00252446	0.00252446	0.00302420	0.00302420	0.00352393	0.00352393	0.00402367	0.00402367	0.00452340	0.00452340
0.2	0.00209926	0.00209926	0.00259876	0.00259876	0.00309826	0.00309826	0.00359776	0.00359776	0.00409726	0.00409726
0.3	0.00172431	0.00172431	0.00222360	0.00222360	0.00272289	0.00272289	0.00322218	0.00322218	0.00372147	0.00372147
0.4	0.00139951	0.00139951	0.00189863	0.00189863	0.00239774	0.00239774	0.00289685	0.00289685	0.00339596	0.00339596
0.5	0.00112481	0.00112481	0.00162377	0.00162377	0.00212273	0.00212273	0.00262169	0.00262169	0.00312065	0.00312065
0.6	0.00090014	0.00090014	0.00139898	0.00139898	0.00189781	0.00189781	0.00239665	0.00239665	0.00289548	0.00289548
0.7	0.00072544	0.00072544	0.00122419	0.00122419	0.00172293	0.00172293	0.00222167	0.00222167	0.00272040	0.00272040
0.8	0.00060069	0.00060069	0.00109936	0.00109936	0.00159803	0.00159803	0.00209670	0.00209670	0.00259537	0.00259537
0.9	0.00052585	0.00052585	0.00102448	0.00102448	0.00152311	0.00152311	0.00202174	0.00202174	0.00252037	0.00252037
1.0	0.00050090	0.00050090	0.00099952	0.00099952	0.00149814	0.00149814	0.00199675	0.00199675	0.00249537	0.00249537

TABLE 2.3: Numerical values of solution $S_w(X,T)$ when $c_0=-0.8$ for 10th and 20th-order approximation.

X	$T=0.6$		$T=0.7$		$T=0.8$		$T=0.9$		$T=1.0$	
	10^{th} *order*	20^{th} *order*	10^{th} *order*	20^{th} *order*	10^{th} *order*	20^{th} *order*	10^{th} *order*	20^{th} *order*	10^{th} *order*	20^{th} *order*
0.0	0.00300000	0.00300000	0.00350000	0.00350000	0.00400000	0.00400000	0.00450000	0.00450000	0.00500000	0.00500000
0.1	0.00252446	0.00252446	0.00302420	0.00302420	0.00352393	0.00352393	0.00402367	0.00402367	0.00452340	0.00452340
0.2	0.00209926	0.00209926	0.00259876	0.00259876	0.00309826	0.00309826	0.00359776	0.00359776	0.00409726	0.00409726
0.3	0.00172430	0.00172431	0.00222360	0.00222360	0.00272289	0.00272289	0.00322218	0.00322218	0.00372147	0.00372147
0.4	0.00139951	0.00139951	0.00189863	0.00189863	0.00239774	0.00239774	0.00289685	0.00289685	0.00339596	0.00339596
0.5	0.00112481	0.00112481	0.00162377	0.00162377	0.00212273	0.00212273	0.00262169	0.00262169	0.00312065	0.00312065
0.6	0.00090014	0.00090014	0.00139897	0.00139898	0.00189781	0.00189781	0.00239665	0.00239665	0.00289548	0.00289548
0.7	0.00072544	0.00072544	0.00122418	0.00122419	0.00172292	0.00172293	0.00222166	0.00222167	0.00272040	0.00272040
0.8	0.00060069	0.00060069	0.00109936	0.00109936	0.00159803	0.00159803	0.00209670	0.00209670	0.00259537	0.00259537
0.9	0.00052585	0.00052585	0.00102448	0.00102448	0.00152311	0.00152311	0.00202174	0.00202174	0.00252036	0.00252037
1.0	0.00050090	0.00050090	0.00099952	0.00099952	0.00149814	0.00149814	0.00199675	0.00199675	0.00249536	0.00249537

value of c_0 is chosen from the c_0-curves. Tables 2.2 and 2.3 show the numerical interpretation of the solution.

CHAPTER 3

Fingering Phenomenon

3.1 Introduction

The fingering phenomenon occurs during the displacement process of two immiscible fluids through porous medium which is frequently encountered in many fields of engineering and science like soil science, petroleum engineering, groundwater and hydrology and agriculture engineering [13, 71, 82]. This phenomenon arises in the secondary oil recovery process that takes place in oil reservoirs. It is common practice to inject water into oil field at certain spots in an attempt to drive towards the production well in the oil recovery technology. This stage of oil recovery process is known as secondary oil recovery process.

This chapter describes the importance of fingering phenomenon in fluid flow through homogeneous porous medium. If a porous medium is filled with some phase which is displaced by another phase of lesser viscosity, then instead of regular displacement of the whole front, protuberances take place which shoot through porous medium at a relatively great speed giving rise to fingers. This type of phenomenon is called phenomenon of fingering.

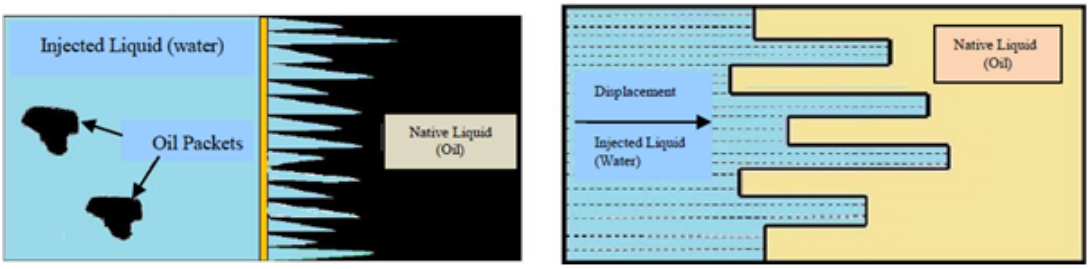

FIGURE 3.1: Schematic representation of fingers [26].

The fingering process is shown in the figure 3.1 for oil-water flow in a homogeneous porous medium. Assume that the macroscopic behavior of fingers is governed by a statistical treatment. We consider only average cross-sectional area occupied by fingers, while the shape and size of individual fingers are disregarded. The statistical behavior of fingering phenomenon in a homogeneous porous medium is discussed with the help of method of characteristics by Scheidegger and Johnson [78]. Verma [86] has discussed the stabilization of fingers in oil-water displacement process in heterogeneous porous medium. The problem of fingering phenomenon is solved using confluent hypergeometric function by Patel [55]. The solution of the instability phenomenon in homogeneous porous medium is examined with the help of group invariant method by Mehta and Joshi [41]. Mukherjee and Shome [46] have discussed the solution of fingering phenomenon in a homogeneous porous medium by means of calculus of variation and similarity theory. Joshi *et al.* [26] have discussed the solution of instability phenomenon by using product method.

In this chapter, homotopy analysis solution is discussed for nonlinear partial differential equation. This equation is arising in fingering phenomenon in a homogeneous porous medium. The numerical values of the solution are compared with exact values.

3.2 Statement of the problem

It is assumed that water is uniformly injected into the porous medium. Assume that the entire oil at the initial boundary $x = 0$ (x being measured in displacement direction) is displaced through a small distance due to injection of water. The permeability and porosity of homogeneous porous medium are considered as constant. For investigated flow problem, it is considered that Darcy's law is valid. The saturation of injected water $S_w(x,t)$ is defined as the average cross-sectional area occupied by injected water.

3.3 Mathematical formulation

During oil-water displacement process, the velocity of water v_w and the velocity of oil v_o are governed by Darcy's law [5]

$$v_w = -\frac{k_w}{\delta_w} K \frac{\partial P_w}{\partial x} \tag{3.1}$$

$$v_o = -\frac{k_o}{\delta_o} K \frac{\partial P_o}{\partial x} \tag{3.2}$$

where K is the permeability, k_w and k_o are the relative permeabilities of water and oil, δ_w and δ_o are the constant viscosities of water and oil, P_w and P_o are the pressures of water and oil.

The continuity equations are

$$P\frac{\partial S_w}{\partial t} + \frac{\partial v_w}{\partial x} = 0 \tag{3.3}$$

$$P\frac{\partial S_o}{\partial t} + \frac{\partial v_o}{\partial x} = 0 \tag{3.4}$$

where P is the porosity. According to the phase saturation, we have

$$S_w + S_o = 1. \tag{3.5}$$

The capillary pressure P_c is defined as [5]

$$P_c(S_w) = P_o - P_w. \tag{3.6}$$

The capillary pressure is expressed as [40],

$$P_c(S_w) = -\beta S_w \tag{3.7}$$

where β is a constant.

For the formulation of problem, we assume the relation between relative permeability and phase saturation as [78]

$$k_w = S_w. \tag{3.8}$$

Using (3.1)-(3.4), we get

$$P\frac{\partial S_w}{\partial t} = \frac{\partial}{\partial x}\left[K\frac{k_w}{\delta_w}\frac{\partial P_w}{\partial x}\right] \tag{3.9}$$

$$P\frac{\partial S_o}{\partial t} = \frac{\partial}{\partial x}\left[K\frac{k_o}{\delta_o}\frac{\partial P_o}{\partial x}\right]. \tag{3.10}$$

Using (3.6) in (3.9) results

$$P\frac{\partial S_w}{\partial t} = \frac{\partial}{\partial x}\left[K\frac{k_w}{\delta_w}\left(\frac{\partial P_o}{\partial x} - \frac{\partial P_c}{\partial x}\right)\right]. \tag{3.11}$$

Using (3.10) and (3.5), eliminating $\frac{\partial S_w}{\partial t}$ from (3.11), gives us

$$\frac{\partial}{\partial x}\left[\left(\frac{k_w}{\delta_w} + \frac{k_o}{\delta_o}\right)K\frac{\partial P_o}{\partial x} - \frac{k_w}{\delta_w}K\frac{\partial P_c}{\partial x}\right] = 0. \tag{3.12}$$

Integrating both sides of (3.12) w.r.t. x, results in

$$\left(\frac{k_w}{\delta_w} + \frac{k_o}{\delta_o}\right)K\frac{\partial P_o}{\partial x} - \frac{k_w}{\delta_w}K\frac{\partial P_c}{\partial x} = -C \tag{3.13}$$

where C is an integrating constant.
Solving (3.13) for $\frac{\partial P_o}{\partial x}$,

$$\frac{\partial P_o}{\partial x} = \frac{-C}{K\left(\frac{k_w}{\delta_w} + \frac{k_o}{\delta_o}\right)} + \frac{\frac{\partial P_c}{\partial x}}{1 + \frac{k_o}{k_w}\frac{\delta_w}{\delta_o}}. \tag{3.14}$$

Using (3.14) in (3.11) we have

$$P\frac{\partial S_w}{\partial t} + \frac{\partial}{\partial x}\left[\frac{K\frac{k_o}{\delta_o}\frac{\partial P_c}{\partial x} + C}{1 + \frac{k_o}{k_w}\frac{\delta_w}{\delta_o}}\right] = 0. \tag{3.15}$$

The pressure of oil can be expressed as the relation between mean pressure $\overline{P}$ and capillary pressure [67]

$$P_o = \frac{P_o + P_w}{2} + \frac{P_o - P_w}{2} = \overline{P} + \frac{1}{2}P_c \tag{3.16}$$

where $\overline{P}$ is constant, therefore (3.13) implies

$$C = \frac{K}{2}\left(\frac{k_w}{\delta_w} - \frac{k_o}{\delta_o}\right)\frac{\partial P_c}{\partial x}. \tag{3.17}$$

Hence (3.15) becomes

$$P\frac{\partial S_w}{\partial t} + \frac{1}{2}\frac{\partial}{\partial x}\left[\frac{k_w}{\delta_w}K\frac{dP_c}{dS_w}\frac{\partial S_w}{\partial x}\right] = 0. \tag{3.18}$$

Since $k_w = S_w$ and $P_c = -\beta S_w$, we have

$$P\frac{\partial S_w}{\partial t} - \frac{\beta}{2}\frac{K}{\delta_w}\frac{\partial}{\partial x}\left[S_w\frac{\partial S_w}{\partial x}\right] = 0. \tag{3.19}$$

Using dimensionless variables

$$X = \frac{x}{L},\ T = \frac{K\beta t}{2\delta_w L^2 P},$$

(3.19) reduces to

$$\frac{\partial S_w}{\partial T} = \frac{\partial}{\partial X}\left(S_w\frac{\partial S_w}{\partial X}\right) = S_w\frac{\partial^2 S_w}{\partial X^2} + \left(\frac{\partial S_w}{\partial X}\right)^2 \tag{3.20}$$

where $S_w(x,t) = S_w(X,T)$.

The boundary conditions are assumed as follows

$$S_w(0,T) = T \text{ and } S_w(1,T) = 1 - T. \tag{3.21}$$

3.4 Solution by homotopy analysis method

Homotopy analysis method is applied to (3.20), let

$$\mathscr{N}[\phi(X,T;q)] = 0 \tag{3.22}$$

be the nonlinear equation where $\mathscr{N}$ is defined as

$$\mathscr{N}[\phi(X,T;q)] = \phi(X,T;q)\frac{\partial^2\phi(X,T;q)}{\partial X^2} + \left\{\frac{\partial\phi(X,T;q)}{\partial X}\right\}^2 - \frac{\partial\phi(X,T;q)}{\partial T} \tag{3.23}$$

and $\phi(X,T;q)$ is an unknown function.

It is easy to choose the initial guess of solution according to boundary conditions (3.21) as

$$S_{w_0}(X,T) = (1-2T)X + T. \tag{3.24}$$

Let the linear operator be

$$\mathscr{L}[\phi(X,T;q)] = \frac{\partial^2\phi(X,T;q)}{\partial X^2} \tag{3.25}$$

with property $\mathscr{L}[0] = 0$.

Using the auxiliary function $H(X,T) = 1$, the zeroth-order deformation equation is constructed as

$$(1-q)\mathscr{L}[\phi(X,T;q) - S_{w_0}(X,T)] = c_0 q\mathscr{N}[\phi(X,T;q)] \tag{3.26}$$

where $q \in [0,1]$ is the embedding parameter and c_0 is a nonzero convergence control parameter.

When $q = 0$ and $q = 1$, (3.26) gives us

$$\phi(X,T;0) = S_{w_0}(X,T) \text{ and } \phi(X,T;1) = S_w(X,T). \tag{3.27}$$

Thus, as q increases from 0 to 1, the unknown function $\phi(X,T;q)$ deforms from $S_{w_0}(X,T)$ to $S_w(X,T)$. Expanding $\phi(X,T;q)$ w.r.t. q

$$\phi(X,T;q) = S_{w_0}(X,T) + \sum_{m=1}^{\infty} S_{w_m}(X,T)q^m \tag{3.28}$$

where

$$S_{w_m}(X,T) = \frac{1}{m!}\frac{\partial^m \phi(X,T;q)}{\partial q^m}\bigg|_{q=0}. \tag{3.29}$$

If the convergence control parameter, the linear operator and the initial guess are properly chosen that the homotopy series (3.28) converges at $q = 1$. Then we have due to (3.27)

$$S_w(X,T) = S_{w_0}(X,T) + \sum_{m=1}^{\infty} S_{w_m}(X,T). \tag{3.30}$$

Write $\overrightarrow{S_{w_n}} = \{S_{w_0}(X,T), S_{w_1}(X,T), \ldots, S_{w_n}(X,T)\}$. Differentiating (3.26) m times w.r.t. q and then dividing them by $m!$ and put $q = 0$ we get

$$\mathscr{L}[S_{w_m}(X,T) - \chi_m S_{w_{m-1}}(X,T)] = c_0 \mathscr{R}_m(\overrightarrow{S_{w_{m-1}}}) \tag{3.31}$$

where χ_m is defined by (2.40) and

$$\begin{aligned}\mathscr{R}_m(\overrightarrow{S_{w_{m-1}}}) = &\sum_{j=0}^{m-1} S_{w_j}(X,T)\frac{\partial^2 S_{w_{m-1-j}}(X,T)}{\partial X^2} + \sum_{j=0}^{m-1}\frac{\partial S_{w_j}(X,T)}{\partial X}\frac{\partial S_{w_{m-1-j}}(X,T)}{\partial X} \\ &- \frac{\partial S_{w_{m-1}}(X,T)}{\partial T},\ m \geq 1.\end{aligned} \tag{3.32}$$

Thus, the solution of (3.31) is

$$S_{w_m}(X,T) = \chi_m S_{w_{m-1}}(X,T) + c_0 \mathscr{L}^{-1}[\mathscr{R}_m(\overrightarrow{S_{w_{m-1}}})] + C_1 X + C_2 \tag{3.33}$$

subject to $S_{w_m}(0,T) = 0$ and $S_{w_m}(1,T) = 0$, where C_1 and C_2 are constants or functions of T.

It is easy to obtain $S_{w_m}(X,T)$ for $m = 1,2,3,\ldots$ from (3.33). For $m = 1$,

$$S_{w_1}(X,T) = c_0\left(-\frac{X}{3}+\frac{X^3}{3}+2TX-2TX^2-2T^2X+2T^2X^2\right),$$

$$\begin{aligned}S_{w_2}(X,T) = c_0\Bigg[&-\frac{X}{3}+\frac{X^3}{3}+2TX-2TX^2-2T^2X+2T^2X^2\\&+c_0\left(\frac{X}{6}-\frac{X^2}{3}-\frac{X^3}{3}+\frac{X^4}{2}-\frac{2TX}{3}+\frac{8TX^2}{3}-TX^3-TX^4\right.\\&\left.+2T^2X-8T^2X^2+6T^2X^3-2T^3X+6T^3X^2-4T^3X^3\right)\Bigg].\end{aligned}$$

Using initial approximation $S_{w_0}(X,T)$, the solution (3.30) becomes

$$\begin{aligned}S_w(X,T) = (X+T-2TX)+c_0\Bigg(&-\frac{X}{3}+\frac{X^3}{3}+2TX-2TX^2-2T^2X\\&+2T^2X^2\Bigg)+c_0\Bigg[-\frac{X}{3}+\frac{X^3}{3}+2TX-2TX^2-2T^2X+2T^2X^2\\&+c_0\left(\frac{X}{6}-\frac{X^2}{3}-\frac{X^3}{3}+\frac{X^4}{2}-\frac{2TX}{3}+\frac{8TX^2}{3}-TX^3-TX^4\right.\\&\left.+2T^2X-8T^2X^2+6T^2X^3-2T^3X+6T^3X^2-4T^3X^3\right)\Bigg]+\cdots. \qquad (3.34)\end{aligned}$$

This is the analytical expression of solution which gives the saturation of injected water for fingering phenomenon.

3.5 Numerical and graphical solution

The Mathematica package BVPh [36] has been used to obtain numerical representation of saturation of injected water (3.34). Table 3.1 indicates the numerical values of solution at different distance X and time T. The numerical values of exact solution [72] and the results obtained by homotopy analysis method are compared. We choose the proper value of c_0 from c_0-curves. Figure 3.2 represents the c_0-curve of $S_{w_{XX}}(0,0)$ for 5th, 8th and 10th-order of approximation. The proper value of $c_0 = -0.0001$ is chosen for numerical and graphical interpretations of solution.

Figure 3.3 represents the graph of solution $S_w(X,T)$ versus distance X for a fixed time $T = 0.001,\ 0.002,\ 0.003,\ 0.004,\ 0.005$ and $c_0 = -0.0001$.

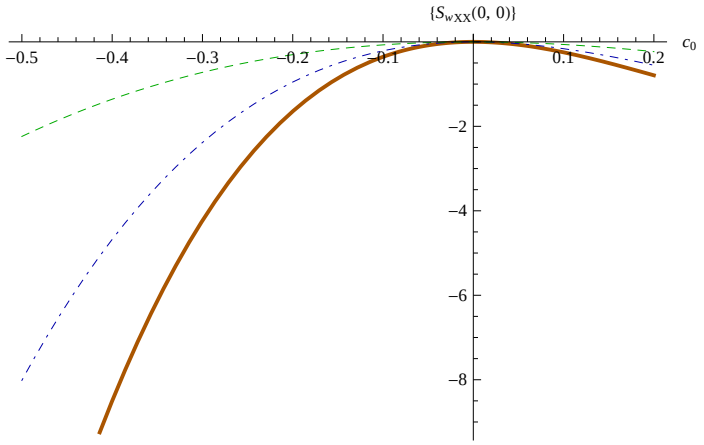

FIGURE 3.2: The c_0-curve for 5th (Dashed), 8th (DotDashed) and 10th (Thick)-order approximation.

TABLE 3.1: Numerical values of saturation of injected water $S_w(X,T)$ for fingering phenomenon.

X	Solution	Time T				
		0.001	0.002	0.003	0.004	0.005
0.1	HAM	0.100832826	0.101632647	0.102432467	0.103232289	0.104032110
	Exact	0.1008	0.1016	0.1024	0.1032	0.1040
0.2	HAM	0.200663688	0.201263369	0.201863051	0.202462733	0.203062416
	Exact	0.2006	0.2012	0.2018	0.2024	0.2030
0.3	HAM	0.300490587	0.300890168	0.301289751	0.301689333	0.302088917
	Exact	0.3004	0.3008	0.3012	0.3016	0.3020
0.4	HAM	0.400311523	0.400511044	0.400710567	0.400910090	0.401109614
	Exact	0.4002	0.4004	0.4006	0.4008	0.4010
0.5	HAM	0.500124496	0.500123997	0.500123500	0.500123004	0.500122508
	Exact	0.5	0.5	0.5	0.5	0.5

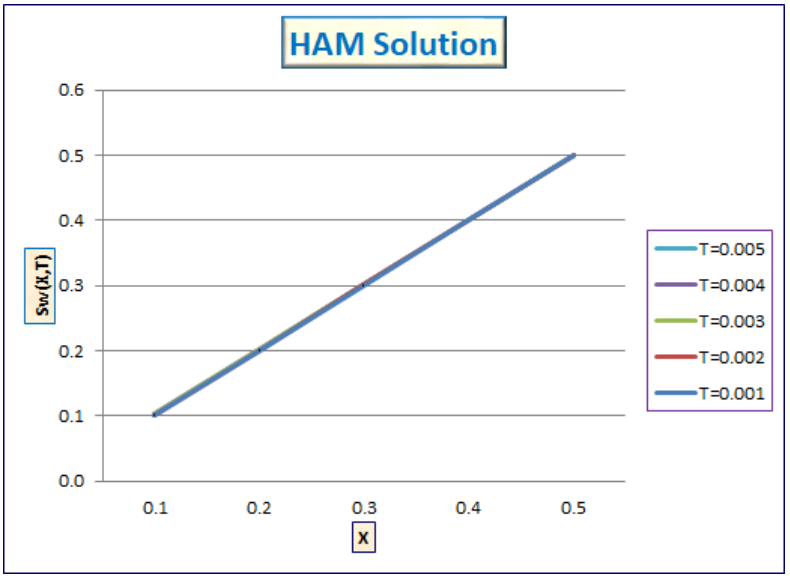

FIGURE 3.3: Graph of $S_w(X,T)$ versus X for a fixed $T = 0.001, 0.002, 0.003, 0.004, 0.005$ with $c_0 = -0.0001$.

3.6 Conclusion

Homotopy analysis method is used to represent an analytical expression of solution of one dimensional nonlinear partial differential equation. This equation is arising in fingering phenomenon in a homogeneous porous medium. The numerical values of exact solution [72] and the results obtained by homotopy analysis method are compared. It is concluded that the values of saturation of injected water in exact solution and homotopy analysis solution are much closer. Graphical representation of solution indicates that the saturation increases when distance increases for a given time.

CHAPTER 4

Countercurrent Imbibition Phenomenon

4.1 Introduction

Spontaneous imbibition is the one of the most important phenomenon which is driven by capillary pressure. There are two types of spontaneous imbibition: countercurrent and cocurrent. In the countercurrent imbibition both fluids flow in opposite directions while during cocurrent imbibition both wetting and nonwetting fluids flow in the same direction.

If a porous medium is filled with nonwetting phase which is brought into contact with wetting phase, then there is a spontaneous flow of wetting phase into the porous medium and a counter flow of nonwetting phase from the porous medium. This phenomenon is known as imbibition phenomenon (see figure 4.1). This phenomenon occurs due to the difference of wetting abilities of water and oil.

Many researchers have investigated the countercurrent imbibition phenomenon with different point of views [9, 14, 24, 43, 77, 81, 86]. Blair [9] has presented the numerical solution for countercurrent imbibition in porous rocks. Bourblaux and Kalaydjian [11] have performed the experiments for countercurrent and cocurrent imbibition phenomena with various boundary conditions. Pooladi-Darvish and Firoozabadi [70] have discussed the mathematical and physical differences between cocurrent and countercurrent imbibition phenomena. Yadav and Mehta [92] have studied the countercurrent imbibition in a curved homogeneous porous medium by using integral method. Joshi *et al.* [28] have studied the countercurrent imbibition

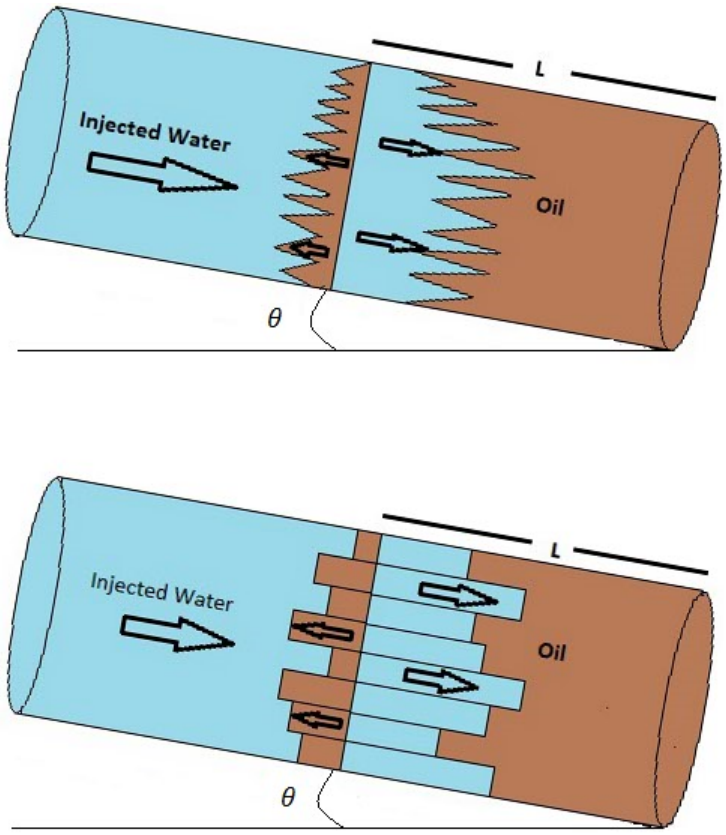

FIGURE 4.1: Representation of countercurrent imbibition phenomenon.

phenomenon by product method. Parikh *et al.* [51] have discussed the mathematical model of countercurrent imbibition phenomenon in vertical porous matrix.

In this chapter, we have studied the countercurrent imbibition in the inclined porous medium. The aim of study of this chapter is to calculate the saturation of water for the inclined porous medium ($\theta = 0^\circ,\ \theta = 5^\circ,\ 10^\circ$). The mathematical formulation of countercurrent imbibition gives us a nonlinear partial differential equation. The homotopy analysis method is adopted to obtain solution of governing equation with suitable conditions.

4.2 Statement of the problem

The velocity of oil and the velocity of water are assumed under the gravitational effect in the inclined homogeneous porous medium. Here the gravitational effect will be

deducted during imbibition of oil occurring in the opposite direction. For the mathematical formulation, it is assumed that Darcy's law is valid. For a homogeneous porous medium, the permeability K and porosity P are considered as constant. The densities of water ρ_w and oil ρ_o are also constants. The average cross-sectional area occupied by injected water gives us the saturation of injected water $S_w(x,t)$.

4.3 Mathematical model of the problem

According to Darcy's law, the velocity of injected water v_w and velocity of oil v_o can be written as follows [5, 8, 47, 77]:

$$v_w = -\frac{k_w}{\delta_w} K \left[\frac{\partial P_w}{\partial x} + \rho_w g sin\theta \right] \tag{4.1}$$

$$v_o = -\frac{k_o}{\delta_o} K \left[\frac{\partial P_o}{\partial x} - \rho_o g sin\theta \right] \tag{4.2}$$

where K is the permeability of porous medium, k_w and k_o are the relative permeabilities of water and oil, δ_w and δ_o are the constant viscosities, P_w and P_o are the pressures of water and oil, θ is the angle of inclination with porous matrix and g is acceleration due to gravity.

The continuity equation is

$$P\frac{\partial S_w}{\partial t} + \frac{\partial v_w}{\partial x} = 0. \tag{4.3}$$

The capillary pressure (P_c) is expressed as

$$P_c = P_o - P_w. \tag{4.4}$$

The capillary pressure (P_c) is assumed as a function saturation of water [40]

$$P_c = -\beta S_w \tag{4.5}$$

where β is a constant.

We consider the relation between relative permeability and phase saturation as [77, 78]

$$k_w = S_w \text{ and } k_o = 1 - \alpha S_w \tag{4.6}$$

where α is a constant.

The relation between the velocity of water and velocity of oil in countercurrent imbibition phenomenon [77] is expressed as

$$v_w + v_o = 0. \tag{4.7}$$

Using (4.1) and (4.2) in (4.7),

$$\frac{k_w}{\delta_w} K \left[\frac{\partial P_w}{\partial x} + \rho_w g sin\theta \right] + \frac{k_o}{\delta_o} K \left[\frac{\partial P_o}{\partial x} - \rho_o g sin\theta \right] = 0. \tag{4.8}$$

From (4.8) and (4.4)

$$\left(\frac{k_w}{\delta_w} + \frac{k_o}{\delta_o} \right) \frac{\partial P_o}{\partial x} - \frac{k_w}{\delta_w} \frac{\partial P_c}{\partial x} = - \left(\frac{k_w}{\delta_w} \rho_w - \frac{k_o}{\delta_o} \rho_o \right) g sin\theta. \tag{4.9}$$

Solving (4.9) for $\frac{\partial P_o}{\partial x}$

$$\frac{\partial P_o}{\partial x} = - \left[\frac{\left(\frac{k_w}{\delta_w} \rho_w - \frac{k_o}{\delta_o} \rho_o \right) g sin\theta - \frac{k_w}{\delta_w} \frac{\partial P_c}{\partial x}}{\frac{k_w}{\delta_w} + \frac{k_o}{\delta_o}} \right]. \tag{4.10}$$

From (4.2), we get

$$v_o = \frac{k_o}{\delta_o} K \left[\frac{\frac{k_w}{\delta_w} (\rho_w + \rho_o) g sin\theta - \frac{k_w}{\delta_w} \frac{\partial P_c}{\partial x}}{\frac{k_w}{\delta_w} + \frac{k_o}{\delta_o}} \right]. \tag{4.11}$$

Using (4.7) and (4.11)

$$v_w = - \frac{\frac{k_w}{\delta_w} \frac{k_o}{\delta_o}}{\frac{k_w}{\delta_w} + \frac{k_o}{\delta_o}} K \left[(\rho_w + \rho_o) g sin\theta - \frac{\partial P_c}{\partial x} \right]. \tag{4.12}$$

On substituting the value of v_w in (4.3),

$$P\frac{\partial S_w}{\partial t} - \frac{\partial}{\partial x}\left[\frac{\frac{k_w}{\delta_w}\frac{k_o}{\delta_o}}{\frac{k_w}{\delta_w}+\frac{k_o}{\delta_o}}K(\rho_w+\rho_o)gsin\theta\right] + \frac{\partial}{\partial x}\left[K\frac{\frac{k_w}{\delta_w}\frac{k_o}{\delta_o}}{\frac{k_w}{\delta_w}+\frac{k_o}{\delta_o}}\frac{\partial P_c}{\partial x}\right] = 0. \tag{4.13}$$

For the investigated flow system, according to Scheidegger [77], we have

$$\frac{\frac{k_w}{\delta_w}\frac{k_o}{\delta_o}}{\frac{k_w}{\delta_w}+\frac{k_o}{\delta_o}} \approx \frac{k_o}{\delta_o}. \tag{4.14}$$

On substituting values from (4.5), (4.6) and (4.14) into (4.13), we get

$$P\frac{\partial S_w}{\partial t} = \frac{K(\rho_w+\rho_o)gsin\theta}{\delta_o}\frac{\partial(1-\alpha S_w)}{\partial x} + \frac{K\beta}{\delta_o}\frac{\partial}{\partial x}\left[(1-\alpha S_w)\frac{\partial S_w}{\partial x}\right]. \tag{4.15}$$

Using dimensionless variables

$$X = \frac{x}{L},\ T = \frac{K\beta t}{\delta_o L^2 P},$$

(4.15) reduces to

$$\frac{\partial S_w}{\partial T} = \frac{\partial^2 S_w}{\partial X^2} - \alpha S_w\frac{\partial^2 S_w}{\partial X^2} - \alpha\left(\frac{\partial S_w}{\partial X}\right)^2 - \alpha A\frac{\partial S_w}{\partial X} \tag{4.16}$$

where $A = \frac{L(\rho_w+\rho_o)gsin\theta}{\beta}$ and $S_w(x,t) = S_w(X,T)$.

The equation (4.16) is the desired governing equation for countercurrent imbibition phenomenon which is solved with the following boundary conditions

$$S_w(0,T) = 0 \text{ and } S_w(1,T) = \frac{1+T}{3}. \tag{4.17}$$

4.4 Solution by homotopy analysis method

The equation (4.16) is solved by Homotopy analysis method [32]. According to boundary conditions (4.17), we choose the initial guess as

$$S_{w_0}(X,T) = \frac{(1+T)(X+X^2)}{6}. \tag{4.18}$$

We choose the linear operator $\mathscr{L}$ as

$$\mathscr{L}[\phi(X,T;q)] = \frac{\partial^2\phi(X,T;q)}{\partial X^2} \tag{4.19}$$

with $\mathscr{L}[0] = 0$ and $\phi(X,T;q)$ is an unknown function.

Here we choose a nonlinear operator $\mathscr{N}$ as

$$\begin{aligned}\mathscr{N}[\phi(X,T;q)] = \frac{\partial^2\phi(X,T;q)}{\partial X^2} - \alpha\phi(X,T;q)\frac{\partial^2\phi(X,T;q)}{\partial X^2} - \alpha\left\{\frac{\partial\phi(X,T;q)}{\partial X}\right\}^2 \\ - \alpha A\frac{\partial\phi(X,T;q)}{\partial X} - \frac{\partial\phi(X,T;q)}{\partial T}.\end{aligned} \tag{4.20}$$

Suppose that $c_0 \neq 0$ is the convergence control parameter, $q \in [0,1]$ is the homotopy parameter, $S_{w_0}(X,T)$ is the initial guess of $S_w(X,T)$ and $H(X,T) \neq 0$ is an auxiliary function. The zeroth-order deformation equation is

$$(1-q)\mathscr{L}[\phi(X,T;q) - S_{w_0}(X,T)] = c_0 q H(X,T)\mathscr{N}[\phi(X,T;q)]. \tag{4.21}$$

If $q = 0$ and $q = 1$, then

$$\phi(X,T;0) = S_{w_0}(X,T) \text{ and } \phi(X,T;1) = S_w(X,T). \tag{4.22}$$

Thus, as q increases from 0 to 1, the function $\phi(X,T;q)$ changes from $S_{w_0}(X,T)$ to the solution $S_w(X,T)$ of (4.16). Expanding $\phi(X,T;q)$ with respect to q we have

$$\phi(X,T;q) = S_{w_0}(X,T) + \sum_{m=1}^{\infty} S_{w_m}(X,T)q^m \tag{4.23}$$

where

$$S_{w_m}(X,T) = \frac{1}{m!}\frac{\partial^m \phi(X,T;q)}{\partial q^m}\bigg|_{q=0}. \tag{4.24}$$

If homotopy series converges at $q = 1$ then

$$S_w(X,T) = S_{w_0}(X,T) + \sum_{m=1}^{\infty} S_{w_m}(X,T). \tag{4.25}$$

Write $\overrightarrow{S_{w_n}} = \{S_{w_0}, S_{w_1}, \ldots, S_{w_n}\}$. Differentiating (4.21) m times w.r.t. q and then dividing them by $m!$ and put $q = 0$, we have the high-order deformation equation

$$\mathscr{L}[S_{w_m}(X,T) - \chi_m S_{w_{m-1}}(X,T)] = c_0 H(X,T)\mathscr{R}_m(\overrightarrow{S_{w_{m-1}}}) \tag{4.26}$$

where χ_m is defined by (2.40) and

$$\begin{aligned}\mathscr{R}_m(\overrightarrow{S_{w_{m-1}}}) = {} & \frac{\partial^2 S_{w_{m-1}}(X,T)}{\partial X^2} - \alpha \sum_{j=0}^{m-1} S_{w_j}(X,T)\frac{\partial^2 S_{w_{m-1-j}}(X,T)}{\partial X^2} \\ & - \alpha \sum_{j=0}^{m-1} \frac{\partial S_{w_j}(X,T)}{\partial X}\frac{\partial S_{w_{m-1-j}}(X,T)}{\partial X} - A\alpha \frac{\partial S_{w_{m-1}}(X,T)}{\partial X} \\ & - \frac{\partial S_{w_{m-1}}(X,T)}{\partial T},\ m \geq 1.\end{aligned} \tag{4.27}$$

For simplicity, assume $H(X,T) = 1$, then the general solution of (4.26) is

$$S_{w_m}(X,T) = \chi_m S_{w_{m-1}}(X,T) + c_0 \mathscr{L}^{-1}[\mathscr{R}_m(\overrightarrow{S_{w_{m-1}}})] + C_1 X + C_2 \tag{4.28}$$

subject to $S_{w_m}(0,T)=0$ and $S_{w_m}(1,T)=0$, $m\geq 1$ and C_1, C_2 are constants or functions of T. Hence,

$$\begin{aligned}S_w(X,T)=&\left(\frac{X}{6}+\frac{TX}{6}+\frac{X^2}{6}+\frac{TX^2}{6}\right)+c_0\Bigg(-\frac{X}{8}+\frac{\alpha X}{18}+\frac{5\alpha AX}{36}-\frac{TX}{6}\\&+\frac{\alpha TX}{9}+\frac{5\alpha ATX}{36}+\frac{\alpha T^2X}{18}+\frac{X^2}{6}-\frac{\alpha X^2}{72}-\frac{\alpha AX^2}{12}+\frac{TX^2}{6}\\&-\frac{\alpha TX^2}{36}-\frac{\alpha ATX^2}{12}-\frac{\alpha T^2X^2}{72}-\frac{X^3}{36}-\frac{\alpha X^3}{36}-\frac{\alpha AX^3}{18}-\frac{\alpha TX^3}{18}\\&-\frac{\alpha ATX^3}{18}-\frac{\alpha T^2X^3}{36}-\frac{X^4}{72}-\frac{\alpha X^4}{72}-\frac{\alpha TX^4}{36}-\frac{\alpha T^2X^4}{72}\Bigg)+\cdots\end{aligned}\tag{4.29}$$

is the solution of (4.16) which represents the saturation of injected water for countercurrent imbibition phenomenon. The values of constants are assumed as: $\alpha=1.11$, $\beta=0.1\ N/m^2$, $g=9.8\ m/s^2$, $L=1\ m$, $\rho_o=0.3\ kg/m^3$, $\rho_w=0.1\ kg/m^3$.

As discussed by Liao [32], homotopy series solution is dependent on c_0 which is important parameter to control convergence of series solution. We choose a proper value of c_0 to provide a convergent solution. The c_0-curves help us to choose proper value of c_0 which gives convergent homotopy series [1, 2, 23, 33, 54, 76].

With the help of BVPh package [36], we plotted the c_0-curves of $S_{w_X}(1,0)$, $S_{w_{XX}}(1,0)$, $S_{w_{XXX}}(1,0)$, $S_{w_X}(0,0)$, $S_{w_{XX}}(0,0)$, $S_{w_{XXX}}(0,0)$, $S_{w_X}(0.5,0.5)$, $S_{w_{XX}}(0.5,0.5)$, $S_{w_{XXX}}(0.5,0.5)$, $S_{w_X}(0,1)$, $S_{w_{XX}}(0,1)$ and $S_{w_{XXX}}(0,1)$ in the figures 4.2-4.6 for $\theta=0^\circ$. Using c_0-curves, we choose the value of $c_0=-0.9$.

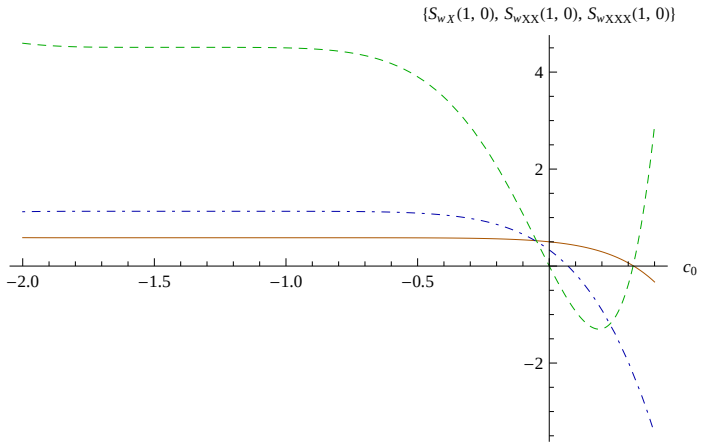

FIGURE 4.2: The c_0-curves of $S_{w_X}(1,0)$ (Solid line), $S_{w_{XX}}(1,0)$ (DotDashed line) and $S_{w_{XXX}}(1,0)$ (Dashed line) for 10th order approximation ($\theta=0^\circ$).

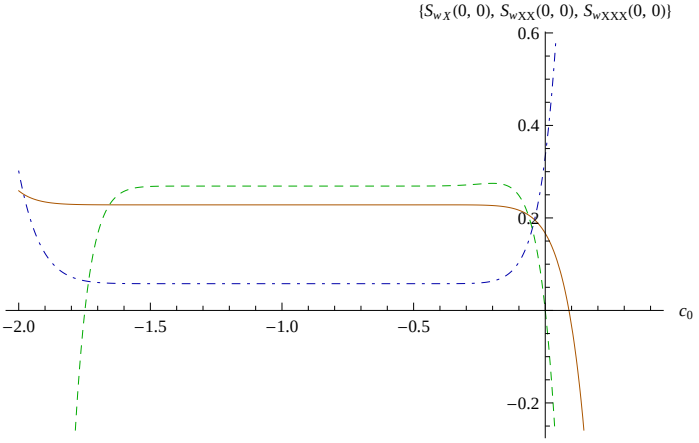

FIGURE 4.3: The c_0-curves of $S_{w_X}(0,0)$ (Solid line), $S_{w_{XX}}(0,0)$ (DotDashed line) and $S_{w_{XXX}}(0,0)$ (Dashed line) for 15th order approximation $(\theta = 0^\circ)$.

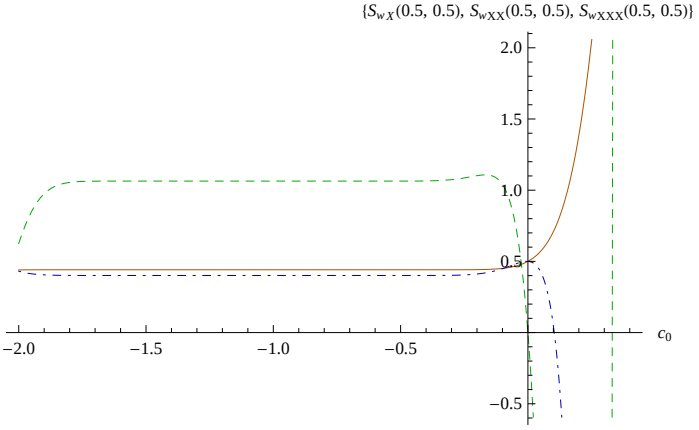

FIGURE 4.4: The c_0-curves of $S_{w_X}(0.5,0.5)$ (Solid line), $S_{w_{XX}}(0.5,0.5)$ (DotDashed line) and $S_{w_{XXX}}(0.5,0.5)$ (Dashed line) for 20th order approximation $(\theta = 0^\circ)$.

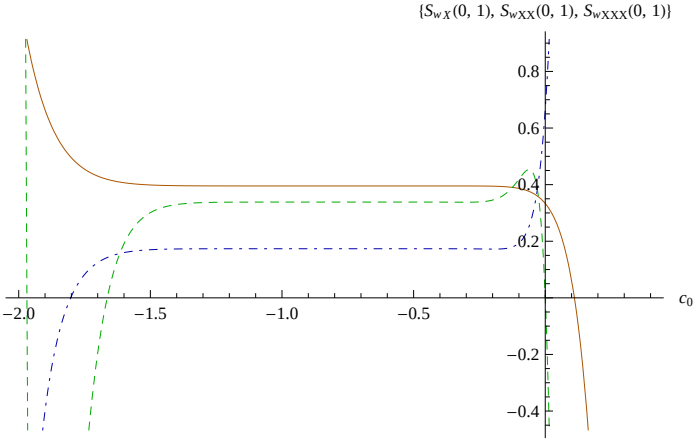

FIGURE 4.5: The c_0-curves of $S_{w_X}(0,1)$ (Solid line), $S_{w_{XX}}(0,1)$ (DotDashed line) and $S_{w_{XXX}}(0,1)$ (Dashed line) for 25th order approximation $(\theta = 0^\circ)$.

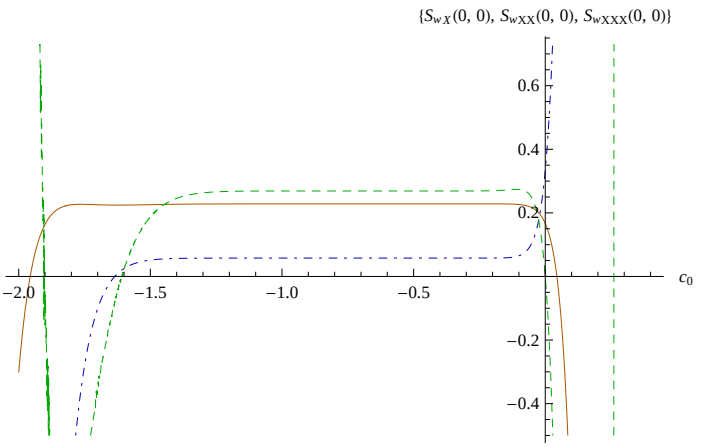

FIGURE 4.6: The c_0-curves of $S_{w_X}(0,0)$ (Solid line), $S_{w_{XX}}(0,0)$ (DotDashed line) and $S_{w_{XXX}}(0,0)$ (Dashed line) for 30th order approximation $(\theta = 0^\circ)$.

For inclination $\theta = 5^\circ$, we plotted the c_0-curves of $S_{w_X}(0,1)$, $S_{w_{XX}}(0,1)$, $S_{w_{XXX}}(0,1)$, $S_{w_X}(0,0)$, $S_{w_{XX}}(0,0)$, $S_{w_{XXX}}(0,0)$ $S_{w_X}(0.5,0.5)$, $S_{w_{XX}}(0.5,0.5)$ and $S_{w_{XXX}}(0.5,0.5)$ in the figures 4.7-4.9. We choose proper value of $c_0 = -0.5$.

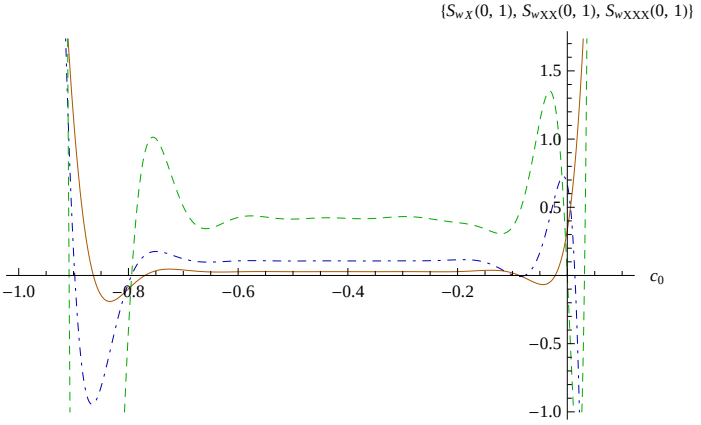

FIGURE 4.7: The c_0-curves of $S_{w_X}(0,1)$ (Solid line), $S_{w_{XX}}(0,1)$ (DotDashed line) and $S_{w_{XXX}}(0,1)$ (Dashed line) for 25th order approximation $(\theta = 5^\circ)$.

For inclination $\theta = 10^\circ$, we plotted the c_0-curves of $S_{w_X}(0,0)$ and $S_{w_{XX}}(0,0)$ for 30th-order approximation in the figures 4.10-4.11. Using these c_0-curves, we choose the value of $c_0 = -0.25$.

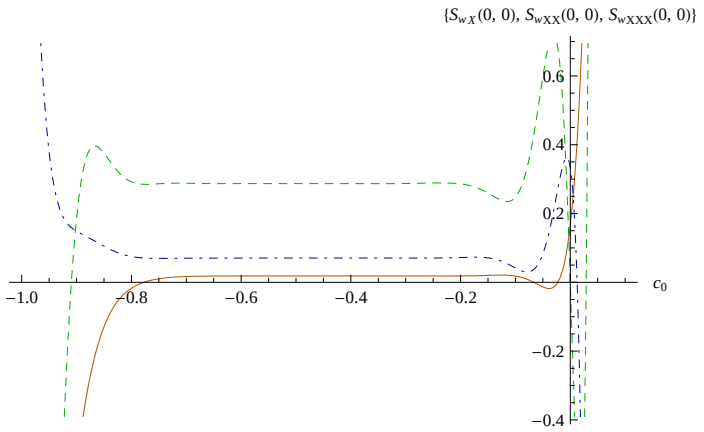

FIGURE 4.8: The c_0-curves of $S_{w_X}(0,0)$ (Solid line), $S_{w_{XX}}(0,0)$ (DotDashed line) and $S_{w_{XXX}}(0,0)$ (Dashed line) for 30th order approximation $(\theta = 5^\circ)$.

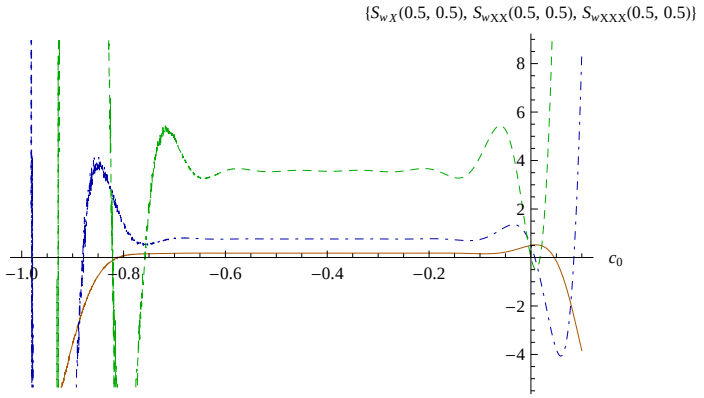

FIGURE 4.9: The c_0-curves of $S_{w_X}(0.5,0.5)$ (Solid line), $S_{w_{XX}}(0.5,0.5)$ (DotDashed line) and $S_{w_{XXX}}(0.5,0.5)$ (Dashed line) for 30th order approximation $(\theta = 5^\circ)$.

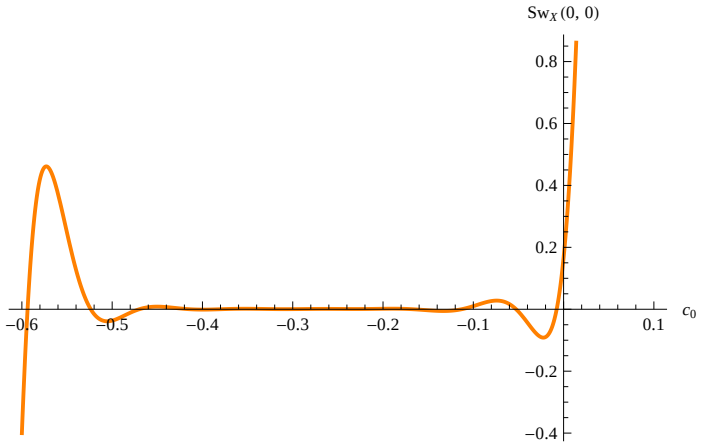

FIGURE 4.10: The c_0-curve of $S_{w_X}(0,0)$ $(\theta = 10^\circ)$.

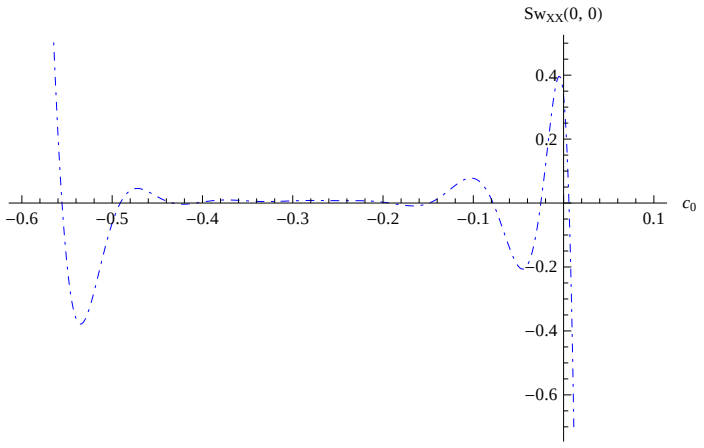

FIGURE 4.11: The c_0-curve of $S_{wXX}(0,0)$ $(\theta = 10^\circ)$.

4.5 Results and discussion

4.5.1 Without inclination $(\theta = 0^\circ)$

For the case, we put $\theta = 0^\circ$ in (4.29) and we obtained numerical and graphical presentations of solution. We choose the convergence control parameter $c_0 = -0.9$. Table 4.1 indicates the numerical values of solution.

TABLE 4.1: Numerical values of the saturation of injected water for $\theta = 0^\circ$.

T	Distance X									
	0.1	0.2	0.3	0.4	0.5	0.6	0.7	0.8	0.9	1.0
0.0	0.0231599	0.0471921	0.0724362	0.0992933	0.1282463	0.1598903	0.1949826	0.2345284	0.2799370	0.3333333
0.1	0.0254093	0.0518122	0.0795584	0.1090685	0.1408571	0.1755716	0.2140553	0.2574587	0.3074506	0.3666667
0.2	0.0275444	0.0562090	0.0863562	0.1184278	0.1529744	0.1907019	0.2325514	0.2798426	0.3345601	0.4000000
0.3	0.0295647	0.0603800	0.0928225	0.1273579	0.1645762	0.2052483	0.2504250	0.3016224	0.3612071	0.4333333
0.4	0.0314699	0.0643225	0.0989504	0.1358455	0.1756402	0.2191763	0.2676272	0.3227338	0.3873230	0.4666667
0.5	0.0332594	0.0680341	0.1047336	0.1438776	0.1861439	0.2324508	0.2841057	0.3431054	0.4128262	0.5000000
0.6	0.0349331	0.0715126	0.1101658	0.1514414	0.1960650	0.2450354	0.2998057	0.3626584	0.4376200	0.5333333
0.7	0.0364906	0.0747557	0.1152411	0.1585248	0.2053812	0.2568935	0.3146691	0.3813058	0.4615895	0.5666667
0.8	0.0379317	0.0777617	0.1199538	0.1651157	0.2140708	0.2679879	0.3286359	0.3989530	0.4845984	0.6000000
0.9	0.0392563	0.0805287	0.1242988	0.1712029	0.2221125	0.2782818	0.3416440	0.4154975	0.5064860	0.6333333
1.0	0.0404642	0.0830552	0.1282712	0.1767756	0.2294857	0.2877385	0.3536303	0.4308301	0.5270634	0.6666667

Figure 4.12 represents the graph of solution $S_w(X,T)$ versus X for a fixed $T = 0.1, 0.2, \ldots, 1$ and figure 4.13 represents the graph of solution $S_w(X,T)$ versus time T for a fixed distance $X = 0.1, 0.2, \ldots, 1$.

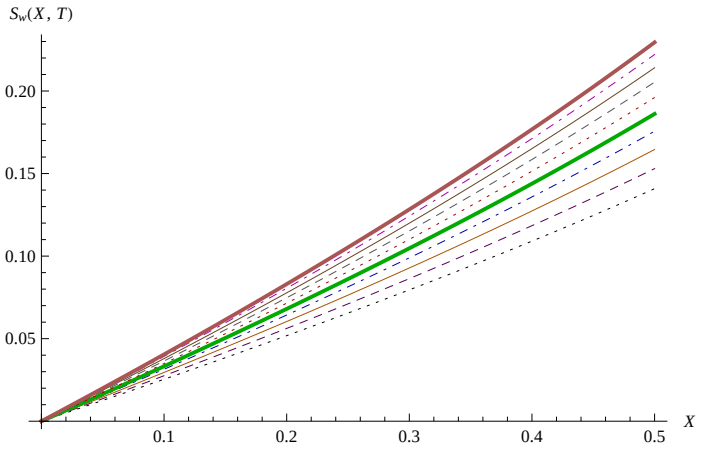

FIGURE 4.12: Graph of $S_w(X,T)$ versus X for a fixed $T = 0.1$(lowermost graph), 0.2, ..., 1(uppermost graph) for $\theta = 0^\circ$.

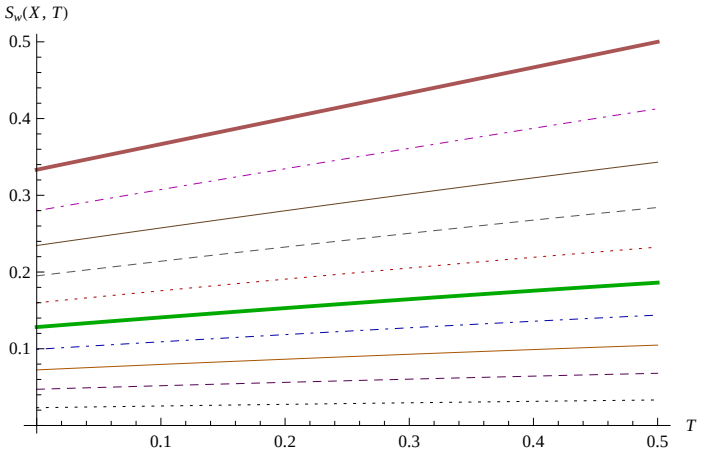

FIGURE 4.13: Graph of $S_w(X,T)$ versus T for a fixed $X = 0.1$(lowermost graph), 0.2, ..., 1(uppermost graph) for $\theta = 0^\circ$.

4.5.2 With inclination $(\theta = 5^\circ \& \theta = 10^\circ)$

In the case of inclination $\theta = 5^\circ$, we have chosen a value of $c_0 = -0.5$ to discuss the numerical and graphical interpretations of solution. Table 4.2 indicates the numerical values of (4.29) with $\theta = 5^\circ$.

Figure 4.14 represents the graph of solution $S_w(X,T)$ versus distance X for a fixed time $T = 0.1, 0.2, \ldots, 1$ with inclination $\theta = 5^\circ$. The numerical and graphical representations of solution are indicate that the saturation of water increases when distance increases for a given time.

TABLE 4.2: Numerical values of the saturation of injected water for $\theta = 5^\circ$.

T	Distance X									
	0.1	0.2	0.3	0.4	0.5	0.6	0.7	0.8	0.9	1.0
0.0	0.0022572	0.0055912	0.0105527	0.0179908	0.0292399	0.0464591	0.0733081	0.1164850	0.1900465	0.3333333
0.1	0.0024311	0.0060196	0.0113537	0.0193412	0.0314102	0.0498805	0.0787155	0.1252695	0.2054031	0.3666667
0.2	0.0025899	0.0064107	0.0120855	0.0205756	0.0333963	0.0530169	0.0836900	0.1334087	0.2198668	0.4000000
0.3	0.0027342	0.0067665	0.0127513	0.0216997	0.0352066	0.0558795	0.0882439	0.1409096	0.2334094	0.4333333
0.4	0.0028650	0.0070887	0.0133547	0.0227190	0.0368498	0.0584797	0.0923902	0.1477818	0.2460060	0.4666667
0.5	0.0029827	0.0073791	0.0138987	0.0236391	0.0383351	0.0608292	0.0961419	0.1540373	0.2576363	0.5000000
0.6	0.0030882	0.0076393	0.0143865	0.0244656	0.0396719	0.0629403	0.0995117	0.1596906	0.2682853	0.5333333
0.7	0.0031819	0.0078706	0.0148208	0.0252039	0.0408711	0.0648263	0.1025111	0.1647596	0.2779447	0.5666667
0.8	0.0032643	0.0080744	0.0152043	0.0258595	0.0419449	0.0665025	0.1051486	0.1692662	0.2866140	0.6000000
0.9	0.0033358	0.0082516	0.0155391	0.0264379	0.0429084	0.0679874	0.1074276	0.1732382	0.2943027	0.6333333
1.0	0.0033966	0.0084028	0.0158268	0.0269445	0.0437808	0.0693059	0.1093420	0.1767127	0.3010336	0.6666667

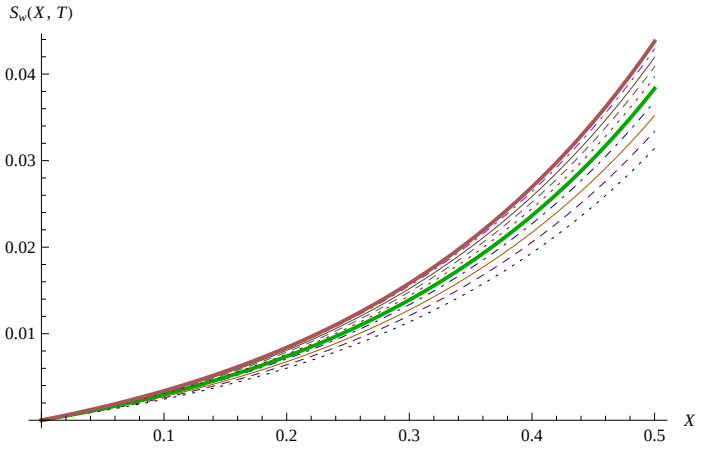

FIGURE 4.14: Graph of $S_w(X,T)$ versus X for a fixed $T = 0.1$(lowermost graph), 0.2, $\ldots$, 1(uppermost graph) for $\theta = 5^\circ$.

In the case of $\theta = 10^\circ$, $c_0 = -0.25$ is chosen to discuss the numerical values of solution (4.29). Table 4.3 indicates its numerical values.

TABLE 4.3: Numerical values of the saturation of injected water for $\theta = 10^\circ$.

T	Distance X									
	0.1	0.2	0.3	0.4	0.5	0.6	0.7	0.8	0.9	1.0
0.0	0.0001494	0.0004312	0.0009835	0.0021512	0.0047436	0.0105918	0.0236846	0.0529370	0.1228759	0.3333333
0.1	0.0001731	0.0004843	0.0010749	0.0023011	0.0050114	0.0111801	0.0251603	0.0564768	0.1316964	0.3666667
0.2	0.0002023	0.0005480	0.0011799	0.0024579	0.0052527	0.0116669	0.0264483	0.0597091	0.1398476	0.4000000
0.3	0.0002387	0.0006266	0.0013066	0.0026349	0.0054820	0.0120552	0.0275404	0.0626465	0.1473343	0.4333333
0.4	0.0002840	0.0007246	0.0014644	0.0028483	0.0057194	0.0123519	0.0284247	0.0653022	0.1541616	0.4666667
0.5	0.0003400	0.0008471	0.0016637	0.0031175	0.0059912	0.0125691	0.0290851	0.0676895	0.1603343	0.5000000
0.6	0.0004086	0.0009991	0.0019163	0.0034656	0.0063318	0.0127265	0.0295012	0.0698217	0.1658559	0.5333333
0.7	0.0004915	0.0011859	0.0022344	0.0039192	0.0067846	0.0128540	0.0296475	0.0717116	0.1707268	0.5666667
0.8	0.0005902	0.0014123	0.0026310	0.0045082	0.0074038	0.0129952	0.0294939	0.0733709	0.1749431	0.6000000
0.9	0.0007060	0.0016830	0.0031189	0.0052660	0.0082555	0.0132115	0.0290053	0.0748090	0.1784942	0.6333333
1.0	0.0008396	0.0020015	0.0037107	0.0062288	0.0094193	0.0135871	0.0281430	0.0760315	0.1813605	0.6666667

Figure 4.15 represents the graph of solution $S_w(X,T)$ versus distance X for a fixed time $T = 0.1, 0.2, \ldots, 1$ with $\theta = 10^\circ$. Clearly, the graphical and numerical

interpretations of solution show that the saturation of water increases when distance increases for a given time.

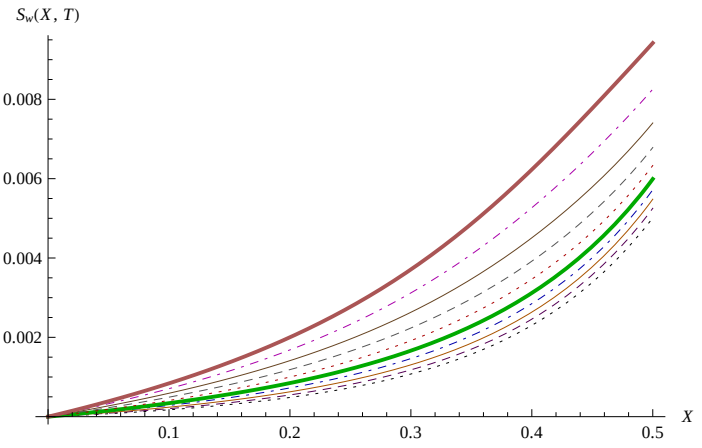

FIGURE 4.15: Graph of $S_w(X,T)$ versus X for a fixed $T = 0.1$(lowermost graph), 0.2, ..., 1(uppermost graph) for $\theta = 10^\circ$.

4.6 Conclusion

The countercurrent imbibition phenomenon is investigated in the inclined homogeneous porous medium and its mathematical model gives us a nonlinear partial differential equation. The solution of governing equation is discussed by homotopy analysis method which represents the saturation of injected water. The graphical and numerical interpretations of solution are discussed which show that the solution increases when distance and time increase. It is concluded that the saturation of injected water increases as distance increases for a given time in both horizontal and inclined porous medium. In inclined porous medium, the saturation of injected water is less than the saturation of injected water in horizontal porous medium.

CHAPTER 5

Cocurrent Imbibition Phenomenon

Present chapter discusses the mathematical modeling and the analysis of the problem of cocurrent imbibition phenomenon in fluid flow porous medium. The problem of cocurrent imbibition has been discussed in the inclined homogeneous and heterogeneous porous medium with the help of homotopy analysis method. The permeability and porosity of a homogeneous porous medium are considered as constant and in a heterogeneous porous medium both are considered as functions of x only. This chapter is divided into two parts corresponding to the type of porous medium as:

(A) Cocurrent imbibition phenomenon in the inclined homogeneous porous medium.

(B) Cocurrent imbibition phenomenon in the inclined heterogeneous porous medium.

5.1 PART (A): Cocurrent imbibition phenomenon in the inclined homogeneous porous medium

5.1.1 Introduction

In the oil recovery technology, the spontaneous imbibition is one of the most important phenomenon which is driven by capillary force. Countercurrent and cocurrent are types of spontaneous imbibition. The main difference between these two imbibitions is the direction of flow. In the countercurrent imbibition both fluids flow in opposite directions while during cocurrent imbibition both wetting and nonwetting fluids flow in the same direction. Cocurrent imbibition is more efficient than countercurrent imbibition in the

oil recovery process [11, 70, 93]. Imbibition in water-wet matrix of fractured porous media is commonly considered to be countercurrent [11, 19, 22, 38, 70, 92]. When the porous medium is partly filled with wetting fluid, flow is dominated by cocurrent imbibition, not countercurrent.

Many authors have investigated cocurrent imbibition phenomenon with different aspects [11, 22, 38, 70, 93]. Bourblaux and Kalaydjian [11] have performed flow experiments involving cocurrent and countercurrent. The mathematical and physical differences between cocurrent and countercurrent imbibition are studied by Pooladi-Darvish and Firoozabadi [70]. Yadav and Mehta [93] have discussed the series solution of cocurrent imbibition. Mcwhorter and Sunada [38] have presented the exact, quasi-analytical solutions for both cocurrent and countercurrent. Fazeli *et al.* [22] have studied the cocurrent and countercurrent imbibition by homotopy perturbation method.

During secondary oil recovery process, it is common practice to inject water into fractured oil formatted porous medium. Then cocurrent imbibition phenomenon occurs. The velocities of water and oil are considered under gravitational and inclination effects. For flow problem, the permeability K and porosity P are considered as constants. The densities of water ρ_w and oil ρ_o are also constants. The average cross-sectional area occupied by injected water gives us saturation of injected water $S_w(x,t)$.

Here we studied the cocurrent imbibition in inclined homogeneous porous medium with the help of homotopy analysis method. Homotopy series solution describes the saturation of injected water for cocurrent imbibition phenomenon. We discussed the graphical and numerical solutions with the proper choice of the convergence control parameter.

5.1.2 Mathematical modeling

5.1.2.1 Fundamental equations

According to the generalized Darcy's law, the velocity of injected water v_w and velocity of oil v_o can be written as follows [5, 47, 77]:

$$v_w = -\frac{k_w}{\delta_w} K \left(\frac{\partial P_w}{\partial x} + \rho_w g sin\theta \right) \tag{5.1}$$

$$v_o = -\frac{k_o}{\delta_o} K \left(\frac{\partial P_o}{\partial x} + \rho_o g sin\theta \right) \tag{5.2}$$

where δ_w and δ_o are the constant viscosities of water and oil, k_w and k_o are the relative permeabilities of water and oil, P_w and P_o are the pressures of water and oil, g is acceleration due to gravity and θ is the angle of inclination with porous matrix.

The continuity equation is

$$P \frac{\partial S_w}{\partial t} + \frac{\partial v_w}{\partial x} = 0. \tag{5.3}$$

The relation between the velocity of water and velocity of oil in cocurrent imbibition [31, 38] is expressed as

$$v_w + v_o = v_t \tag{5.4}$$

where v_t is the total velocity.

5.1.2.2 Standard relations

The capillary pressure (P_c) is expressed as [5]:

$$P_c(S_w) = P_o - P_w. \tag{5.5}$$

The relation between capillary pressure and saturation of water is considered as [40]

$$P_c(S_w) = -\beta S_w \tag{5.6}$$

where β is a constant.

We consider the relation between relative permeability and phase saturation as [77, 78]

$$k_w = S_w \text{ and } k_o = 1 - \alpha S_w \tag{5.7}$$

where α is a constant.

5.1.2.3 Equation of motion for saturation

Using (5.1), (5.2) and (5.4), we get

$$-\frac{k_w}{\delta_w}K\left(\frac{\partial P_w}{\partial x} + \rho_w g sin\theta\right) - \frac{k_o}{\delta_o}K\left(\frac{\partial P_o}{\partial x} + \rho_o g sin\theta\right) = v_t. \tag{5.8}$$

Using (5.5) in (5.8)

$$\frac{k_w}{\delta_w}K\left(\frac{\partial P_w}{\partial x} + \rho_w g sin\theta\right) + \frac{k_o}{\delta_o}K\left(\frac{\partial P_c}{\partial x} + \frac{\partial P_w}{\partial x} + \rho_o g sin\theta\right) = -v_t. \tag{5.9}$$

Solving (5.9) for $\frac{\partial P_w}{\partial x}$

$$\frac{\partial P_w}{\partial x} = -\left(K\frac{k_w}{\delta_w} + K\frac{k_o}{\delta_o}\right)^{-1}\left(K\left(\frac{k_o}{\delta_o}\rho_o + \frac{k_w}{\delta_w}\rho_w\right)g sin\theta + K\frac{k_o}{\delta_o}\frac{\partial P_c}{\partial x} + v_t\right). \tag{5.10}$$

Combining (5.1) and (5.10) results in

$$v_w = -\frac{k_w}{\delta_w}\left(\frac{k_w}{\delta_w} + \frac{k_o}{\delta_o}\right)^{-1}\left(K\frac{k_o}{\delta_o}(\rho_w - \rho_o)g sin\theta - K\frac{k_o}{\delta_o}\frac{\partial P_c}{\partial x} - v_t\right). \tag{5.11}$$

The pressure of water can be expressed as the relation between capillary pressure P_c and mean pressure $\bar{P}$ [67]

$$P_w = \frac{P_w + P_o}{2} + \frac{P_w - P_o}{2} = \bar{P} - \frac{1}{2}P_c \tag{5.12}$$

where $\bar{P}$ is a constant, therefore (5.9) reduces to

$$K\left(\frac{k_w}{\delta_w}\rho_w + \frac{k_o}{\delta_o}\rho_o\right) gsin\theta + \frac{K}{2}\left(\frac{k_o}{\delta_o} - \frac{k_w}{\delta_w}\right)\frac{\partial P_c}{\partial x} = -v_t. \tag{5.13}$$

Therefore (5.11) implies

$$v_w = \frac{K}{2}\frac{k_w}{\delta_w}\frac{\partial P_c}{\partial x} - K\frac{k_w}{\delta_w}\rho_w gsin\theta. \tag{5.14}$$

Substituting (5.14) into (5.3), we get

$$P\frac{\partial S_w}{\partial t} + \frac{\partial}{\partial x}\left[\frac{K}{2}\frac{k_w}{\delta_w}\frac{\partial P_c}{\partial x} - K\frac{k_w}{\delta_w}\rho_w gsin\theta\right] = 0. \tag{5.15}$$

Since $k_w = S_w$ and $P_c = -\beta S_w$, we have

$$P\frac{\partial S_w}{\partial t} - \frac{K\beta}{2\delta_w}\frac{\partial}{\partial x}\left[S_w\frac{\partial S_w}{\partial x}\right] - \frac{K\rho_w gsin\theta}{\delta_w}\frac{\partial S_w}{\partial x} = 0. \tag{5.16}$$

Using dimensionless variables

$$X = \frac{x}{L},\ T = \frac{\beta Kt}{2\delta_w L^2 P},$$

(5.16) reduces to

$$\frac{\partial S_w}{\partial T} = \frac{\partial}{\partial X}\left[S_w\frac{\partial S_w}{\partial X}\right] + A\frac{\partial S_w}{\partial X} \tag{5.17}$$

where $S_w(x,t) = S_w(X,T)$ and $A = \frac{2L\rho_w gsin\theta}{\beta}$.

The equation (5.17) is the governing equation for the cocurrent imbibition phenomenon and $S_w(X,T)$ gives the saturation of injected water. Now we solve (5.17)

with boundary conditions:

$$S_w(0,T) = 0 \text{ and } S_w(1,T) = \frac{2(1+T)}{5}. \tag{5.18}$$

5.1.3 Solution by homotopy analysis method

We apply HAM to (5.17). Consider

$$\mathscr{N}[\phi(X,T;q)] = 0 \tag{5.19}$$

where $\phi(X,T;q)$ is the unknown function, $q \in [0,1]$ is the embedding parameter and

$$\mathscr{N}[\phi(X,T;q)] = \phi(X,T;q)\frac{\partial^2\phi(X,T;q)}{\partial X^2} + \left\{\frac{\partial\phi(X,T;q)}{\partial X}\right\}^2 + A\frac{\partial\phi(X,T;q)}{\partial X} - \frac{\partial\phi(X,T;q)}{\partial T}. \tag{5.20}$$

We define the linear operator $\mathscr{L}$ as

$$\mathscr{L}[\phi(X,T;q)] = \frac{\partial^2\phi(X,T;q)}{\partial X^2}. \tag{5.21}$$

According to (5.18), it is straightforward to choose $S_{w_0}(X,T)$ as the initial guess of $S_w(X,T)$, as follows

$$S_{w_0}(X,T) = \frac{2(X^2+TX)}{5}. \tag{5.22}$$

Let $H(X,T) \neq 0$ be an auxiliary function and $c_0 \neq 0$ be the convergence control parameter [35]. The zeroth-order deformation equation [32] is

$$(1-q)\mathscr{L}[\phi(X,T;q) - S_{w_0}(X,T)] = c_0 q H(X,T)\mathscr{N}[\phi(X,T;q)]. \tag{5.23}$$

If $q = 0$ and $q = 1$, we get

$$\phi(X,T;0) = S_{w_0}(X,T) \text{ and } \phi(X,T;1) = S_w(X,T). \tag{5.24}$$

Thus as q increases from 0 to 1, $\phi(X,T;q)$ continuously changes from $S_{w_0}(X,T)$ to $S_w(X,T)$. Expanding $\phi(X,T;q)$ w.r.t. q, we have

$$\phi(X,T;q) = S_{w_0}(X,T) + \sum_{m=1}^{\infty} S_{w_m}(X,T)q^m \tag{5.25}$$

where

$$S_{w_m}(X,T) = \frac{1}{m!}\frac{\partial^m \phi(X,T;q)}{\partial q^m}\bigg|_{q=0}. \tag{5.26}$$

According to proper selection of the convergence control parameter, initial guess, linear operator and auxiliary function we get the convergent homotopy-Maclaurin series at $q = 1$, that is the homotopy series solution

$$S_w(X,T) = S_{w_0}(X,T) + \sum_{m=1}^{\infty} S_{w_m}(X,T). \tag{5.27}$$

Write $\overrightarrow{S_{w_n}} = \{S_{w_0}, S_{w_1}, \ldots, S_{w_n}\}$. Differentiating (5.23) m times w.r.t. q, then put $q = 0$ and dividing them by $m!$, we have the high-order deformation equation

$$\mathscr{L}[S_{w_m}(X,T) - \chi_m S_{w_{m-1}}(X,T)] = c_0 H(X,T)\mathscr{R}_m(\overrightarrow{S_{w_{m-1}}}) \tag{5.28}$$

with $S_{w_m}(0,T) = 0$ and $S_{w_m}(1,T) = 0,\ m \geq 1$, where χ_m is defined by (2.40) and

$$\mathscr{R}_m(\overrightarrow{S_{w_{m-1}}}) = \sum_{i=0}^{m-1} S_{w_i}\frac{\partial^2 S_{w_{m-1-i}}}{\partial X^2} + \sum_{i=0}^{m-1}\frac{\partial S_{w_i}}{\partial X}\frac{\partial S_{w_{m-1-i}}}{\partial X} + A\frac{\partial S_{w_{m-1}}}{\partial X} - \frac{\partial S_{w_{m-1}}}{\partial T},\ m \geq 1. \tag{5.29}$$

We consider $H(X,T) = 1$. The solution of (5.28) is

$$S_{w_m}(X,T) = \chi_m S_{w_{m-1}}(X,T) + c_0\mathscr{L}^{-1}[\mathscr{R}_m(\overrightarrow{S_{w_{m-1}}})] + C_1 X + C_2 \tag{5.30}$$

where $\mathscr{L}^{-1}$ denotes the inverse operator of $\mathscr{L}$ and C_1 & C_2 are determined by the boundary conditions.

For $m = 1$,

$$S_{w_1}(X,T) = c_0\bigg(-\frac{X}{75}-\frac{2AX}{15}-\frac{4TX}{25}-\frac{ATX}{5}-\frac{2T^2X}{25}+\frac{ATX^2}{5}+\frac{2T^2X^2}{25} -\frac{X^3}{15}+\frac{2AX^3}{15}+\frac{4TX^3}{25}+\frac{2X^4}{25}\bigg)$$

$m = 2$,

$$\begin{aligned}S_{w_2}(X,T) = c_0\bigg[&-\frac{X}{75}-\frac{2AX}{15}-\frac{4TX}{25}-\frac{ATX}{5}-\frac{2T^2X}{25}+\frac{ATX^2}{5}+\frac{2T^2X^2}{25}\\ &-\frac{X^3}{15}+\frac{2AX^3}{15}+\frac{4TX^3}{25}+\frac{2X^4}{25}+c_0\bigg(-\frac{7X}{375}-\frac{7AX}{750}+\frac{A^2X}{30}-\frac{TX}{75}\\ &+\frac{ATX}{25}+\frac{A^2TX}{30}+\frac{AT^2X}{75}-\frac{AX^2}{150}-\frac{A^2X^2}{15}-\frac{2TX^2}{375}-\frac{2ATX^2}{15}\\ &-\frac{A^2TX^2}{10}-\frac{8T^2X^2}{125}-\frac{3AT^2X^2}{25}-\frac{4T^3X^2}{125}+\frac{8X^3}{375}-\frac{AX^3}{50}-\frac{14TX^3}{375}\\ &-\frac{2ATX^3}{25}+\frac{A^2TX^3}{15}+\frac{8AT^2X^3}{75}-\frac{4T^2X^3}{125}+\frac{4T^3X^3}{125}-\frac{AX^4}{30}+\frac{A^2X^4}{30}\\ &-\frac{TX^4}{25}+\frac{13ATX^4}{75}+\frac{12T^2X^4}{125}-\frac{13X^5}{375}+\frac{26AX^5}{375}+\frac{12TX^5}{125}+\frac{4X^6}{125}\bigg)\bigg].\end{aligned}$$

Hence

$$\begin{aligned}S_w(X,T) = &\frac{2X^2}{5}+\frac{2TX}{5}+c_0\bigg(-\frac{X}{75}-\frac{2AX}{15}-\frac{4TX}{25}-\frac{ATX}{5}-\frac{2T^2X}{25}\\ &+\frac{ATX^2}{5}+\frac{2T^2X^2}{25}-\frac{X^3}{15}+\frac{2AX^3}{15}+\frac{4TX^3}{25}+\frac{2X^4}{25}\bigg)+c_0\bigg[-\frac{X}{75}\\ &-\frac{2AX}{15}-\frac{4TX}{25}-\frac{ATX}{5}-\frac{2T^2X}{25}+\frac{ATX^2}{5}+\frac{2T^2X^2}{25}-\frac{X^3}{15}+\frac{2AX^3}{15}\\ &+\frac{4TX^3}{25}+\frac{2X^4}{25}+c_0\bigg(-\frac{7X}{375}-\frac{7AX}{750}+\frac{A^2X}{30}-\frac{TX}{75}+\frac{ATX}{25}\\ &+\frac{A^2TX}{30}+\frac{AT^2X}{75}-\frac{AX^2}{150}-\frac{A^2X^2}{15}-\frac{2TX^2}{375}-\frac{2ATX^2}{15}-\frac{A^2TX^2}{10}\\ &-\frac{8T^2X^2}{125}-\frac{3AT^2X^2}{25}-\frac{4T^3X^2}{125}+\frac{8X^3}{375}-\frac{AX^3}{50}-\frac{14TX^3}{375}-\frac{2ATX^3}{25}\\ &+\frac{A^2TX^3}{15}+\frac{8AT^2X^3}{75}-\frac{4T^2X^3}{125}+\frac{4T^3X^3}{125}-\frac{AX^4}{30}+\frac{A^2X^4}{30}-\frac{TX^4}{25}\\ &+\frac{13ATX^4}{75}+\frac{12T^2X^4}{125}-\frac{13X^5}{375}+\frac{26AX^5}{375}+\frac{12TX^5}{125}+\frac{4X^6}{125}\bigg)\bigg]+\cdots\end{aligned} \tag{5.31}$$

is the solution of (5.17) which gives the saturation of injected water for cocurrent imbibition phenomenon.

5.1.4 Results and discussion

The convergence of homotopy series solution has been discussed with the help of c_0-curve by many researchers; Darvishi and Khani [18], Abbasbandy *et al.* [2], Ghotbi *et al.* [23], Fariborzi and Naghshband [21], Patel and Desai [59].

The line segment parallel to the horizontal axis in c_0-curve gives the valid interval of c_0 [2, 18, 21, 23, 59, 61]. Mathematica BVPh package [36] has helped us to find the c_0-curves. The values of constants are considered as $g = 9.8\ m/s^2$, $\beta = 2\ N/m^2$, $\rho_w = 0.1\ kg/m^3$, $L = 1\ m$ to discuss numerical and graphical representations of solution.

5.1.4.1 Without inclination with porous matrix i.e. $\theta = 0^\circ$.

Figure 5.1 shows the c_0-curve of $S_{w_{XX}}(0,0)$ for 30th-order approximation. The value of $c_0 = -0.1$ is chosen from this c_0-curve..

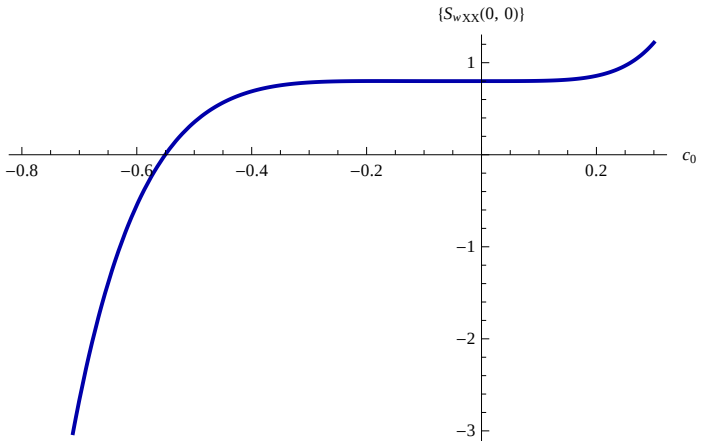

FIGURE 5.1: The c_0-curve of $S_{w_{XX}}(0,0)$ for $\theta = 0^\circ$.

Using the series solution (5.31) with the values of constants, we interpret the numerical and graphical solutions. Table 5.1 indicates the numerical values of saturation of injected water. The graph of solution $S_w(X,T)$ versus distance X for a

fixed time $T = 0.1, 0.2, \ldots, 1$ is presented in figure 5.2. The graphical and numerical interpretations of solution clearly show that the saturation of water increases when distance increases for a given time.

TABLE 5.1: Numerical values of $S_w(X,T)$ in a homogeneous porous medium ($\theta = 0^\circ$).

T	Distance X									
	0.1	0.2	0.3	0.4	0.5	0.6	0.7	0.8	0.9	1.0
0.1	0.0098380	0.0286652	0.0568974	0.0942209	0.1397092	0.1920183	0.2496140	0.3109845	0.3747994	0.4400000
0.2	0.0188183	0.0458898	0.0812903	0.1244648	0.1743800	0.2297261	0.2891245	0.3512995	0.4151905	0.4800000
0.3	0.0281635	0.0636062	0.1061190	0.1549784	0.2091191	0.2673299	0.3284301	0.3913983	0.4554402	0.5200000
0.4	0.0378634	0.0817849	0.1313386	0.1857117	0.2438835	0.3048009	0.3675183	0.4312809	0.4955529	0.5600000
0.5	0.0479077	0.1003971	0.1569063	0.2166188	0.2786345	0.3421151	0.4063802	0.4709492	0.5355336	0.6000000
0.6	0.0582861	0.1194149	0.1827813	0.2476568	0.3133380	0.3792522	0.4450099	0.5104064	0.5753876	0.6400000
0.7	0.0689884	0.1388107	0.2089248	0.2787865	0.3479635	0.4161957	0.4834038	0.5496570	0.6151205	0.6800000
0.8	0.0800042	0.1585579	0.2353000	0.3099718	0.3824845	0.4529325	0.5215607	0.5887067	0.6547380	0.7200000
0.9	0.0913235	0.1786304	0.2618722	0.3411796	0.4168781	0.4894526	0.5594816	0.6275619	0.6942459	0.7600000
1.0	0.1029360	0.1990029	0.2886084	0.3723799	0.4511243	0.5257485	0.5971686	0.6662294	0.7336501	0.8000000

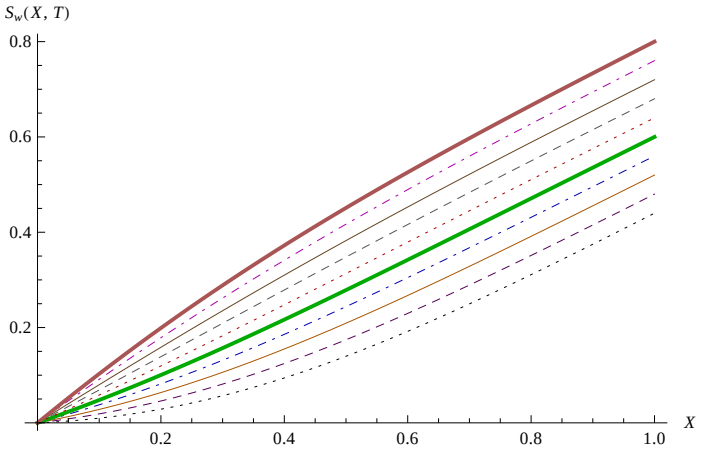

FIGURE 5.2: Saturation of injected water versus distance X for a fixed time $T = 0.1$(lowermost graph), 0.2, …, 1(uppermost graph) for $\theta = 0^\circ$.

5.1.4.2 $\theta = 5^\circ$ inclination with porous matrix.

Figure 5.3 shows the c_0-curve of $S_{w_{XX}}(0,0)$ for 30th-order approximation and the proper value of $c_0 = -0.1$ chosen for numerical and graphical representations of solution (with $\theta = 5^\circ$).

Table 5.2 indicates the numerical values of saturation of injected water for $\theta = 5^\circ$. The graph of solution $S_w(X,T)$ versus distance X for a fixed time $T = 0.1, 0.2, \ldots, 1$ is presented in figure 5.4.

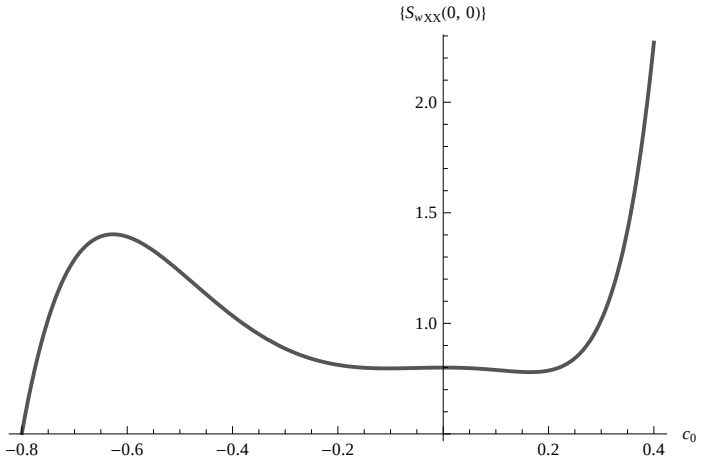

FIGURE 5.3: The c_0-curve of $S_{w_{XX}}(0,0)$ for $\theta = 5^\circ$.

TABLE 5.2: Numerical values of $S_w(X,T)$ in a homogeneous porous medium $(\theta = 5^\circ)$.

T	Distance X									
	0.1	0.2	0.3	0.4	0.5	0.6	0.7	0.8	0.9	1.0
0.1	0.0134242	0.0353242	0.0658915	0.1046419	0.1505559	0.2022832	0.2583616	0.3174084	0.3782527	0.4400000
0.2	0.0229441	0.0533840	0.0912083	0.1357445	0.1859259	0.2404929	0.2981836	0.3578808	0.4186973	0.4800000
0.3	0.0328201	0.0719041	0.1169061	0.1670467	0.2212909	0.2785331	0.3377509	0.3981061	0.4589871	0.5200000
0.4	0.0430415	0.0908550	0.1429412	0.1985016	0.2566122	0.3163803	0.3770560	0.4380880	0.4991283	0.5600000
0.5	0.0535977	0.1102079	0.1692718	0.2300657	0.2918555	0.3540153	0.4160945	0.4778315	0.5391275	0.6000000
0.6	0.0644781	0.1299345	0.1958584	0.2616994	0.3269906	0.3914225	0.4548646	0.5173427	0.5789915	0.6400000
0.7	0.0756722	0.1500076	0.2226633	0.2933660	0.3619913	0.4285900	0.4933666	0.5566289	0.6187269	0.6800000
0.8	0.0871694	0.1704004	0.2496513	0.3250324	0.3968351	0.4655087	0.5316030	0.5956982	0.6583407	0.7200000
0.9	0.0989593	0.1910873	0.2767889	0.3566684	0.4315026	0.5021724	0.5695778	0.6345590	0.6978398	0.7600000
1.0	0.1110315	0.2120431	0.3040445	0.3882467	0.4659777	0.5385776	0.6072965	0.6732204	0.7372307	0.8000000

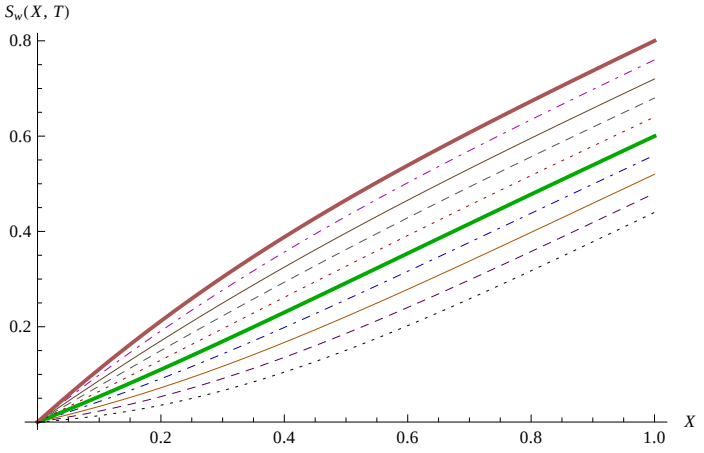

FIGURE 5.4: Saturation of injected water versus distance X for a fixed time $T = 0.1$(lowermost graph), $0.2, \ldots, 1$(uppermost graph) for $\theta = 5^\circ$.

5.1.4.3 $\theta = 10^\circ$ inclination with porous matrix.

The c_0-curve of $S_{w_{XX}}(0,0)$ is plotted for 30th-order approximation; see figure 5.5. Here we use $c_0 = -0.1$ to interpret the numerical and graphical solutions.

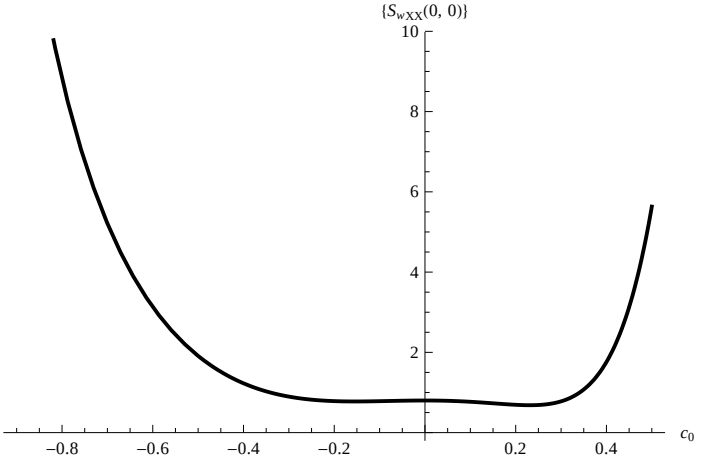

FIGURE 5.5: The c_0-curve of $S_{w_{XX}}(0,0)$ for $\theta = 10^\circ$.

The numerical values of solution $S_w(X,T)$ for $\theta = 10^\circ$ are obtained (see Table 5.3). Figure 5.6 shows the graph of solution $S_w(X,T)$ versus distance X for a fixed time $T = 0.1, 0.2, \ldots, 1$.

TABLE 5.3: Numerical values of $S_w(X,T)$ in a homogeneous porous medium ($\theta = 10^\circ$).

T	Distance X									
	0.1	0.2	0.3	0.4	0.5	0.6	0.7	0.8	0.9	1.0
0.1	0.0171217	0.0421112	0.0749611	0.1150472	0.1612894	0.2123590	0.2668863	0.3236290	0.3815786	0.4400000
0.2	0.0271826	0.0609980	0.1011812	0.1469785	0.1973249	0.2510391	0.3069950	0.3642431	0.4220696	0.4800000
0.3	0.0375898	0.0803124	0.1277266	0.1790391	0.2332829	0.2894859	0.3468013	0.4045810	0.4623935	0.5200000
0.4	0.0483324	0.1000247	0.1545544	0.2111850	0.2691290	0.3276812	0.3863026	0.4446497	0.5025581	0.5600000
0.5	0.0593993	0.1201059	0.1816243	0.2433760	0.3048336	0.3656107	0.4254988	0.4844573	0.5425715	0.6000000
0.6	0.0707798	0.1405281	0.2088981	0.2755751	0.3403706	0.4032635	0.4643923	0.5240130	0.5824417	0.6400000
0.7	0.0824630	0.1612641	0.2363397	0.3077490	0.3757182	0.4406321	0.5029872	0.5633266	0.6221768	0.6800000
0.8	0.0944381	0.1822875	0.2639152	0.3398674	0.4108576	0.4777116	0.5412894	0.6024085	0.6617847	0.7200000
0.9	0.1066946	0.2035727	0.2915928	0.3719031	0.4457736	0.5144999	0.5793063	0.6412692	0.7012731	0.7600000
1.0	0.1192218	0.2250951	0.3193426	0.4038318	0.4804535	0.5509968	0.6170462	0.6799197	0.7406496	0.8000000

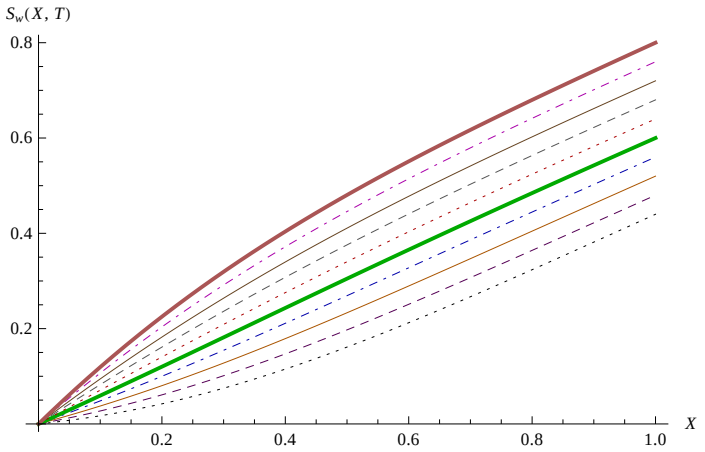

FIGURE 5.6: Saturation of injected water versus distance X for a fixed time $T = 0.1$(lowermost graph), $0.2, \ldots, 1$(uppermost graph) for $\theta = 10^{\circ}$.

5.2 PART (B): Cocurrent imbibition phenomenon in the inclined heterogeneous porous medium

5.2.1 Introduction

Here we have studied the cocurrent imbibition in the inclined heterogeneous porous medium. Most of all the authors have studied cocurrent imbibition in a homogeneous porous medium with different point of views [11, 22, 63, 70, 93]. Many researchers have investigated the problem of fluid flow through a heterogeneous porous medium. The behavior of fingering phenomenon in a heterogeneous porous medium is studied by Verma [86]. Patel *et al.* [58] have discussed imbibition phenomenon in a heterogeneous porous medium. Patel and Desai [61, 65] have discussed the fingero-imbibition in a heterogeneous porous medium with and without magnetic field effect.

For the mathematical formulation, we consider that the permeability and porosity are functions of x only. The mathematical model is studied for cocurrent imbibition phenomenon in the inclined heterogeneous porous medium. With the help of homotopy analysis method, we obtained the solution of governing equation.

5.2.2 Mathematical modeling

The permeability and porosity in a heterogeneous porous medium are assumed as [86],

$$P = P(x) = \frac{1}{a_1 - a_2 x} \tag{5.32}$$

$$K = K(x) = K_0(1 + bx) \tag{5.33}$$

where a_1, a_2, K_0 and b are positive constants. Since $P(x)$ can't exceed unity, we assume that $a_1 - a_2 x \geq 1$.

For the simplicity, we consider $K \propto P$ [16, 58],

$$K = K_c P \tag{5.34}$$

where K_c is a constant.
Using $K = K_c P$, $k_w = S_w$ and $P_c = -\beta S_w$ in (5.15), we get

$$\frac{\partial S_w}{\partial t} = \frac{K_c \beta}{2\delta_w}\left[\frac{\partial}{\partial x}\left(S_w \frac{\partial S_w}{\partial x}\right) + S_w \frac{\partial S_w}{\partial x}\frac{1}{P}\frac{\partial P}{\partial x}\right] + \frac{K_c \rho_w g sin\theta}{\delta_w}\left[\frac{\partial S_w}{\partial x} + S_w \frac{1}{P}\frac{\partial P}{\partial x}\right]. \tag{5.35}$$

Now

$$\frac{1}{P}\frac{\partial P}{\partial x} = \frac{\partial(\log P)}{\partial x} = \frac{\partial}{\partial x}\left(\frac{a_2 x}{a_1} - \log a_1\right) (\text{neglecting higher order terms of } x) = \frac{a_2}{a_1}.$$

Using dimensionless variables

$$X = \frac{x}{L},\ T = \frac{\beta K_c t}{2\delta_w L^2},$$

(5.35) becomes

$$\frac{\partial S_w}{\partial T} = \frac{\partial}{\partial X}\left[S_w \frac{\partial S_w}{\partial X}\right] + A\frac{\partial S_w}{\partial X} + BS_w \frac{\partial S_w}{\partial X} + ABS_w \tag{5.36}$$

where $A = \frac{2L\rho_w g sin\theta}{\beta}$, $B = \frac{a_2 L}{a_1}$ and $S_w(x,t) = S_w(X,T)$
is the governing equation for cocurrent imbibition phenomenon and $S_w(X,T)$ is the

solution of (5.36) which represents the saturation of injected water. The boundary conditions are given by

$$S_w(0,T) = 0 \text{ and } S_w(1,T) = \frac{1+T}{3}. \tag{5.37}$$

5.2.3 Solution by homotopy analysis method

According to (5.36), a nonlinear operator $\mathscr{N}$ is defined as

$$\begin{aligned}\mathscr{N}[\phi(X,T;q)] = \phi(X,T;q)\frac{\partial^2\phi(X,T;q)}{\partial X^2} + \left\{\frac{\partial\phi(X,T;q)}{\partial X}\right\}^2 + A\frac{\partial\phi(X,T;q)}{\partial X} \\ + B\phi(X,T;q)\frac{\partial\phi(X,T;q)}{\partial X} + AB\phi(X,T;q) - \frac{\partial\phi(X,T;q)}{\partial T}.\end{aligned} \tag{5.38}$$

The boundary conditions (5.37) suggest us to choose the initial approximation as

$$S_{w_0}(X,T) = \frac{TX+X^2}{3}. \tag{5.39}$$

Then the solution of (5.28) with $H(X,T) = 1$ reads

$$S_{w_m}(X,T) = \chi_m S_{w_{m-1}}(X,T) + c_0\mathscr{L}^{-1}[\mathscr{R}_m(\overrightarrow{S_{w_{m-1}}})] + C_1X + C_2 \tag{5.40}$$

where the coefficients C_1 and C_2 are determined by the boundary conditions and

$$\begin{aligned}\mathscr{R}_m(\overrightarrow{S_{w_{m-1}}}) = \sum_{i=0}^{m-1} S_{w_i}\frac{\partial^2 S_{w_{m-1-i}}}{\partial X^2} + \sum_{i=0}^{m-1}\frac{\partial S_{w_i}}{\partial X}\frac{\partial S_{w_{m-1-i}}}{\partial X} + A\frac{\partial S_{w_{m-1}}}{\partial X} \\ + B\sum_{i=0}^{m-1} S_{w_i}\frac{\partial S_{w_{m-1-i}}}{\partial X} + ABS_{w_{m-1}} - \frac{\partial S_{w_{m-1}}}{\partial T},\ m \geq 1.\end{aligned} \tag{5.41}$$

Using (5.21), (5.38), (5.39) and (5.40), the solution of (5.36) takes the form:

$$S_w(X,T) = \frac{TX+X^2}{3} + c_0\Bigg(-\frac{AX}{9} - \frac{BX}{90} - \frac{ABX}{36} - \frac{TX}{9} - \frac{ATX}{6} - \frac{BTX}{36} - \frac{ABTX}{18} - \frac{T^2X}{18} - \frac{BT^2X}{54} + \frac{ATX^2}{6} + \frac{T^2X^2}{18} - \frac{X^3}{18} + \frac{AX^3}{9} + \frac{TX^3}{9} + \frac{ABTX^3}{18} + \frac{BT^2X^3}{54} + \frac{X^4}{18} + \frac{ABX^4}{36} + \frac{BTX^4}{36} + \frac{BX^5}{90}\Bigg) + \cdots . \tag{5.42}$$

The solution (5.42) gives us the saturation of injected water for cocurrent imbibition phenomenon in the inclined heterogeneous porous medium.

5.2.4 Results and discussion

The c_0-curve helps us to discover the valid range of c_0. Many authors have discussed homotopy series solution with the help of c_0-curve [2, 18, 21, 23, 59, 61–63, 83]. Using BVPh package [36], we plotted the c_0-curves. The values of constants are considered as $g = 9.8\ m/s^2$, $\beta = 2\ N/m^2$, $\rho_w = 0.1\ kg/m^3$, $L = 1\ m$, $a_1 = 2$, $a_2 = 1\ m^{-1}$.

5.2.4.1 The c_0-curves of $S_{w_{XX}}(0,0)$

Figure 5.7-5.9 show the c_0-curve of $S_{w_{XX}}(0,0)$ for 30th-order approximation for angle of inclination $\theta = 0^\circ,\ \theta = 5^\circ$ and $\theta = 10^\circ$. The value of $c_0 = -0.05$ chosen for convergent homotopy series solution in the inclined ($\theta = 0^\circ,\ \theta = 5^\circ,\ \theta = 10^\circ$) heterogeneous porous medium.

5.2.4.2 Numerical interpretation of solution

Table 5.4-5.6 indicate the numerical values of solution $S_w(X,T)$ with $\theta = 0^\circ,\ \theta = 5^\circ$ and $\theta = 10^\circ$. The numerical representations of solution show that the saturation of water increases when distance increases for a given time.

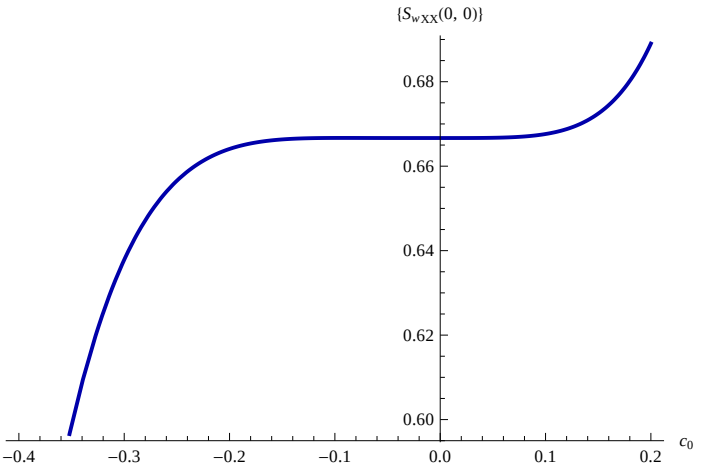

FIGURE 5.7: The c_0-curve of $S_{w_{XX}}(0,0)$ for $\theta = 0°$.

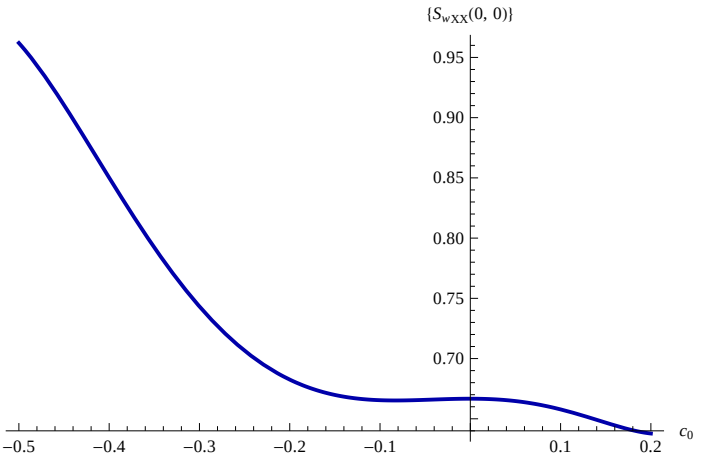

FIGURE 5.8: The c_0-curve of $S_{w_{XX}}(0,0)$ for $\theta = 5°$.

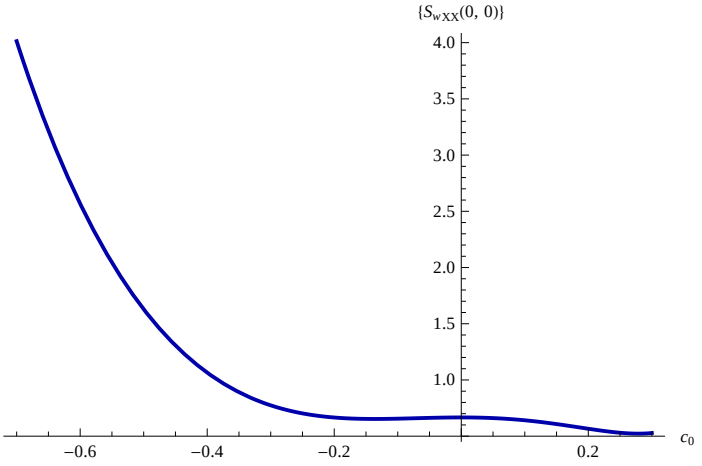

FIGURE 5.9: The c_0-curve of $S_{w_{XX}}(0,0)$ for $\theta = 10°$.

TABLE 5.4: Numerical values of $S_w(X,T)$ in a heterogeneous porous medium with $\theta = 0^\circ$.

T	Distance X									
	0.1	0.2	0.3	0.4	0.5	0.6	0.7	0.8	0.9	1.0
0.1	0.0079782	0.0229830	0.0451758	0.0744627	0.1105000	0.1527179	0.2003618	0.2525440	0.3083037	0.3666667
0.2	0.0133488	0.0335191	0.0605489	0.0942292	0.1341183	0.1795746	0.2298015	0.2839035	0.3409435	0.4000000
0.3	0.0188933	0.0443428	0.0762660	0.1143454	0.1580524	0.2066856	0.2594209	0.3153679	0.3736254	0.4333333
0.4	0.0246107	0.0554496	0.0923181	0.1347989	0.1822872	0.2340357	0.2892065	0.3469273	0.4063442	0.4666667
0.5	0.0304996	0.0668349	0.1086968	0.1555773	0.2068084	0.2616102	0.3191453	0.3785725	0.4390952	0.5000000
0.6	0.0365589	0.0784942	0.1253933	0.1766686	0.2316017	0.2893949	0.3492251	0.4102946	0.4718739	0.5333333
0.7	0.0427874	0.0904228	0.1423990	0.1980608	0.2566535	0.3173762	0.3794342	0.4420854	0.5046763	0.5666667
0.8	0.0491838	0.1026161	0.1597055	0.2197422	0.2819502	0.3455407	0.4097613	0.4739368	0.5374984	0.6000000
0.9	0.0557468	0.1150696	0.1773042	0.2417012	0.3074788	0.3738759	0.4401959	0.5058417	0.5703367	0.6333333
1.0	0.0624751	0.1277785	0.1951868	0.2639264	0.3332267	0.4023695	0.4707278	0.5377931	0.6031880	0.6666667

TABLE 5.5: Numerical values of $S_w(X,T)$ in a heterogeneous porous medium with $\theta = 5^\circ$.

T	Distance X									
	0.1	0.2	0.3	0.4	0.5	0.6	0.7	0.8	0.9	1.0
0.1	0.0097402	0.0263320	0.0498361	0.0800617	0.1165793	0.1587506	0.2057738	0.2567388	0.3106864	0.3666667
0.2	0.0153699	0.0373119	0.0657641	0.1004253	0.1407763	0.1861178	0.2356193	0.2883755	0.3434644	0.4000000
0.3	0.0211738	0.0485766	0.0820285	0.1211262	0.1652728	0.2137213	0.2656271	0.3201035	0.3762768	0.4333333
0.4	0.0271506	0.0601216	0.0986205	0.1421519	0.1900538	0.2415462	0.2957843	0.3519133	0.4091187	0.4666667
0.5	0.0332993	0.0719420	0.1155312	0.1634900	0.2151052	0.2695781	0.3260784	0.3837961	0.4419858	0.5000000
0.6	0.0396183	0.0840332	0.1327518	0.1851284	0.2404128	0.2978030	0.3564976	0.4157435	0.4748738	0.5333333
0.7	0.0461065	0.0963905	0.1502736	0.2070551	0.2659630	0.3262076	0.3870306	0.4477477	0.5077790	0.5666667
0.8	0.0527625	0.1090090	0.1680879	0.2292583	0.2917427	0.3547791	0.4176667	0.4798013	0.5406978	0.6000000
0.9	0.0595849	0.1218839	0.1861862	0.2517265	0.3177388	0.3835051	0.4483957	0.5118973	0.5736268	0.6333333
1.0	0.0665724	0.1350106	0.2045600	0.2744484	0.3439388	0.4123736	0.4792079	0.5440292	0.6065632	0.6666667

TABLE 5.6: Numerical values of $S_w(X,T)$ in a heterogeneous porous medium with $\theta = 10^\circ$.

T	Distance X									
	0.1	0.2	0.3	0.4	0.5	0.6	0.7	0.8	0.9	1.0
0.1	0.0115398	0.0297336	0.0545446	0.0856902	0.1226614	0.1647585	0.2111404	0.2608814	0.3130304	0.3666667
0.2	0.0174309	0.0411593	0.0710275	0.1066482	0.1474320	0.1926297	0.2413846	0.2927896	0.3459433	0.4000000
0.3	0.0234964	0.0528669	0.0878390	0.1279308	0.1724855	0.2207190	0.2717739	0.3247755	0.3788830	0.4333333
0.4	0.0297350	0.0648515	0.1049701	0.1495254	0.1978072	0.2490118	0.3022959	0.3568301	0.4118449	0.4666667
0.5	0.0361453	0.0771083	0.1224118	0.1714196	0.2233830	0.2774940	0.3329385	0.3889451	0.4448250	0.5000000
0.6	0.0427259	0.0896324	0.1401552	0.1936011	0.2491988	0.3061521	0.3636904	0.4211126	0.4778194	0.5333333
0.7	0.0494755	0.1024189	0.1581913	0.2160580	0.2752414	0.3349730	0.3945407	0.4533251	0.5108246	0.5666667
0.8	0.0563926	0.1154630	0.1765116	0.2387786	0.3014975	0.3639443	0.4254792	0.4855757	0.5438373	0.6000000
0.9	0.0634758	0.1287596	0.1951072	0.2617513	0.3279545	0.3930539	0.4564960	0.5178580	0.5768546	0.6333333
1.0	0.0707237	0.1423040	0.2139694	0.2849648	0.3546000	0.4222902	0.4875820	0.5501657	0.6098736	0.6666667

5.2.4.3 Graphical interpretation of solution

The graph of solution $S_w(X,T)$ versus distance X for a fixed time $T = 0.1, 0.2, \ldots, 1$ for $\theta = 0^\circ$ is given in figure 5.10. Figure 5.11 shows the graph of solution $S_w(X,T)$ versus distance X for a fixed time $T = 0.1, 0.2, \ldots, 1$ for $\theta = 5^\circ$. The graph of solution $S_w(X,T)$ versus distance X for a fixed time $T = 0.1, 0.2, \ldots, 1$ for $\theta = 10^\circ$ is shown in figure 5.12. The graphical representations of solution show that the saturation of water increases when distance increases for a given time.

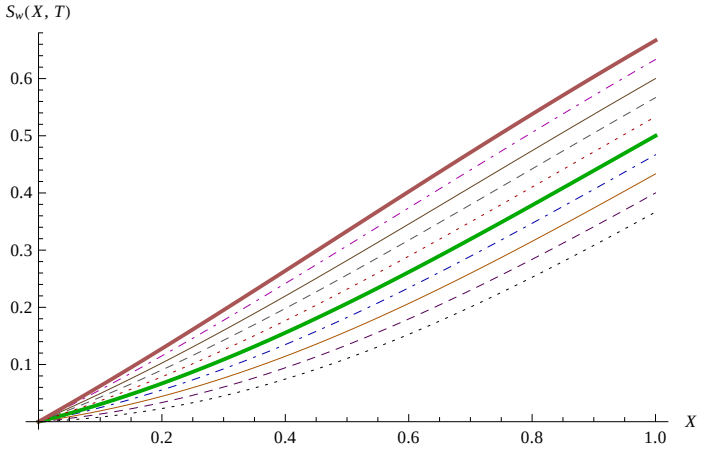

FIGURE 5.10: Saturation of water versus distance for a fixed time $T = 0.1$(lowermost graph), 0.2, ..., 1(uppermost graph) for $\theta = 0^\circ$.

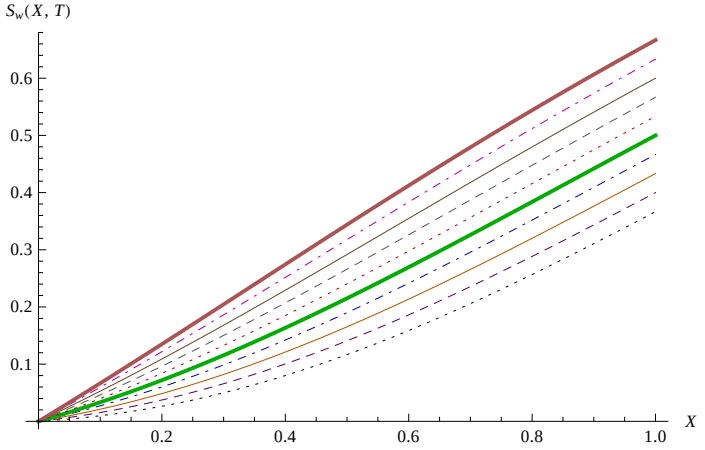

FIGURE 5.11: Saturation of water versus distance for a fixed time $T = 0.1$(lowermost graph), 0.2, ..., 1(uppermost graph) for $\theta = 5^\circ$.

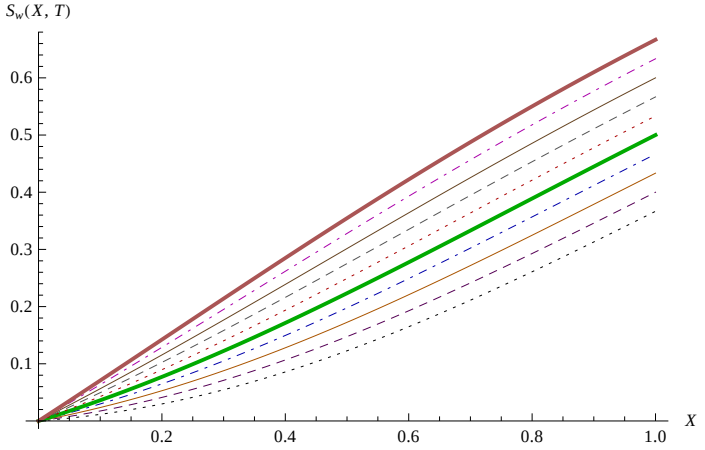

FIGURE 5.12: Saturation of water versus distance for a fixed time $T = 0.1$(lowermost graph), 0.2, ..., 1(uppermost graph) for $\theta = 10^\circ$.

5.3 Conclusion

We have discussed cocurrent imbibition phenomenon in the inclined homogeneous and heterogeneous porous medium and its mathematical models are derived. Homotopy series solutions are discussed for cocurrent imbibition phenomenon. The solutions satisfy both conditions. We have discussed the numerical and graphical interpretations of solutions for different angle of inclination. We conclude that in both the cases the saturation of injected water increases when distance increases for a given time.

CHAPTER 6

Fingero-imbibition Phenomenon

This chapter is divided into two parts:
(A) Fingero-imbibition phenomenon in a heterogeneous porous medium.
(B) Fingero-imbibition phenomenon in a heterogeneous porous medium with magnetic field effect.
In each part, the approximate analytical solutions have been discussed with some certain conditions and assumptions.

6.1 PART (A): Fingero-imbibition phenomenon in a heterogeneous porous medium

6.1.1 Introduction

During the secondary oil recovery process, fingero-imbibition phenomenon arises. If a porous medium filled with some phase (nonwetting phase) is brought into contact with another phase (wetting phase), then there is a spontaneous flow of wetting phase into the porous medium and a counter flow of nonwetting phase from the porous medium. This phenomenon is referred to as imbibition phenomenon. Besides this if a porous medium is filled with some phase which is displaced by another less viscous phase, instead of regular displacement of the whole front, protuberances may occur which shoot through porous medium at relatively great speed giving rise to the fingering. Thus two phenomena i.e. fingering and imbibition occur simultaneously which are known as fingero-imbibition phenomenon (see figure 6.1).

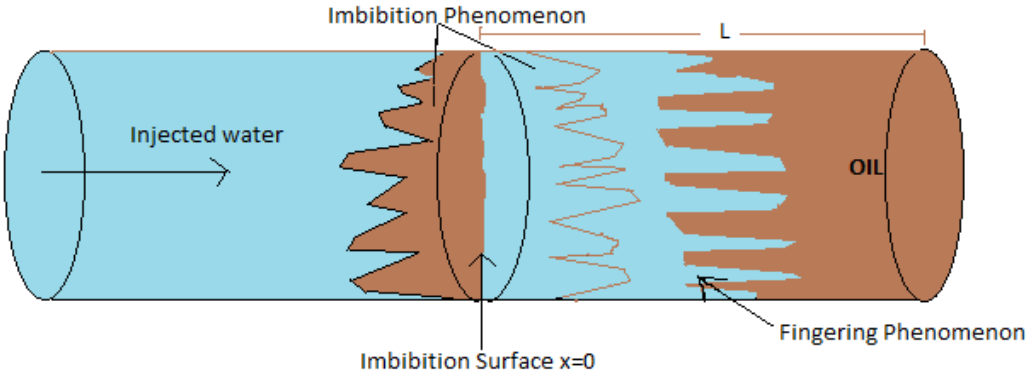

FIGURE 6.1: Fingero-imbibition phenomenon.

This phenomenon is one of the most important phenomena which is frequently encountered in various engineering fields such as hydrogeology, agriculture engineering, soil science, petroleum engineering etc. Many authors have discussed fingero-imbibition phenomenon with different point of views; Verma [87], Mehta and Verma [44], Shah and Verma [79], Desai [19], Patel *et al.* [57], Parikh *et al.* [52], Patel *et al.* [58], Iyiola and Folarin [25].

Our particular interest in present work is to measure the saturation of injected water for the phenomenon of fingero-imbibition in a heterogeneous porous medium. The mathematical formulation gives us a one dimensional nonlinear partial differential equation and it is solved with suitable conditions using homotopy analysis method.

6.1.2 Statement of the problem

Assume that there is a uniform water injection in oil formatted heterogeneous porous medium. The rock properties like permeability and porosity of heterogeneous porous medium may vary from one place to another. For heterogeneous porous medium, the permeability and porosity are assumed as the functions of x only.

It is considered that Darcy's law is valid for investigated problem. The shape and size of fingers are irregular and different. It is assumed that the fingers are rectangles and only the average cross-sectional area occupied by fingers are observed. The average

cross-sectional area occupied by injected water gives us the saturation of injected water for fingero-imbibition phenomenon.

6.1.3 Mathematical model of the problem

According to Darcy's law, the velocity of injected water v_w and the velocity of oil v_o can be expressed as [5, 47, 77]:

$$v_w = -\frac{k_w}{\delta_w} K \frac{\partial P_w}{\partial x} \tag{6.1}$$

$$v_o = -\frac{k_o}{\delta_o} K \frac{\partial P_o}{\partial x} \tag{6.2}$$

where $K = K(x)$ is the permeability of heterogeneous porous medium, k_w and k_o are the relative permeabilities of water and oil, δ_w and δ_o are the constant viscosities of water and oil, P_w and P_o are the pressures of water and oil respectively.

The equation of continuity of injected water is

$$P \frac{\partial S_w}{\partial t} + \frac{\partial v_w}{\partial x} = 0 \tag{6.3}$$

where $P = P(x)$ is the porosity.

It is considered that the permeability and porosity are the functions of x only for heterogeneous porous medium [86],

$$K = K(x) = K_0(1 + bx) \tag{6.4}$$

$$P = P(x) = \frac{1}{a_1 - a_2 x} \tag{6.5}$$

where a_1, a_2, K_0 and b are positive constants. Since $P(x)$ can't exceed unity, we assume that $a_1 - a_2 x \geq 1$.

For simplicity, we consider $K \propto P$ [16, 58],

$$K = K_c P \tag{6.6}$$

where K_c is a constant.

The pressure difference of nonwetting fluid (oil) and wetting fluid (water) is defined as the capillary pressure P_c

$$P_c = P_o - P_w. \tag{6.7}$$

The capillary pressure is considered as [40]

$$P_c = -\beta S_w \tag{6.8}$$

where β is a constant.

The relation between relative permeability and phase saturation is assumed as [77, 78]

$$k_w = S_w \text{ and } k_o = 1 - \alpha S_w \tag{6.9}$$

where α is a constant.

The condition for countercurrent imbibition phenomenon can be expressed as [77]

$$v_w + v_o = 0. \tag{6.10}$$

Using (6.1) and (6.2) in (6.10), we get

$$\frac{k_w}{\delta_w} K \frac{\partial P_w}{\partial x} + \frac{k_o}{\delta_o} K \frac{\partial P_o}{\partial x} = 0. \tag{6.11}$$

From (6.7) and (6.11)

$$\left(\frac{k_w}{\delta_w} + \frac{k_o}{\delta_o}\right) \frac{\partial P_w}{\partial x} + \frac{k_o}{\delta_o} \frac{\partial P_c}{\partial x} = 0. \tag{6.12}$$

Thus, (6.12) reduces to

$$\frac{\partial P_w}{\partial x} = -\frac{k_o}{\delta_o} \left(\frac{k_w}{\delta_w} + \frac{k_o}{\delta_o}\right)^{-1} \frac{\partial P_c}{\partial x}. \tag{6.13}$$

On substituting the value of $\frac{\partial P_w}{\partial x}$ in (6.1), we get

$$v_w = K\frac{k_w}{\delta_w}\frac{k_o}{\delta_o}\left(\frac{k_w}{\delta_w}+\frac{k_o}{\delta_o}\right)^{-1}\frac{\partial P_c}{\partial x}. \tag{6.14}$$

Substituting (6.14) into (6.3), we get

$$P\frac{\partial S_w}{\partial t}+\frac{\partial}{\partial x}\left[K\frac{k_w}{\delta_w}\frac{k_o}{\delta_o}\left(\frac{k_w}{\delta_w}+\frac{k_o}{\delta_o}\right)^{-1}\frac{\partial P_c}{\partial x}\right]=0. \tag{6.15}$$

According to Scheidegger [77], it is assumed that

$$\frac{k_w}{\delta_w}\frac{k_o}{\delta_o}\left(\frac{k_w}{\delta_w}+\frac{k_o}{\delta_o}\right)^{-1}\approx\frac{k_o}{\delta_o} \tag{6.16}$$

(6.15) reduces to

$$P\frac{\partial S_w}{\partial t}+\frac{\partial}{\partial x}\left[K\frac{k_o}{\delta_o}\frac{\partial P_c}{\partial S_w}\frac{\partial S_w}{\partial x}\right]=0. \tag{6.17}$$

Using (6.6), (6.8) and (6.9) into (6.17), we get

$$\begin{aligned}\frac{\partial S_w}{\partial t} &= \frac{\beta K_c}{\delta_o P}\frac{\partial}{\partial x}\left[P(1-\alpha S_w)\frac{\partial S_w}{\partial x}\right]\\ &= \frac{\beta K_c}{\delta_o}\frac{\partial}{\partial x}\left[(1-\alpha S_w)\frac{\partial S_w}{\partial x}\right]+\frac{\beta K_c}{\delta_o P}(1-\alpha S_w)\frac{\partial S_w}{\partial x}\frac{\partial P}{\partial x}.\end{aligned} \tag{6.18}$$

Since,

$$\begin{aligned}\frac{1}{P}\frac{\partial P}{\partial x}=\frac{\partial(\log P)}{\partial x} &= \frac{\partial}{\partial x}\left(-\log a_1+\frac{a_2 x}{a_1}\right)\text{(neglecting higher order terms of } x)\\ &= \frac{a_2}{a_1}\end{aligned}$$

(6.18) becomes

$$\frac{\partial S_w}{\partial t}=\frac{\beta K_c}{\delta_o}\frac{\partial}{\partial x}\left[(1-\alpha S_w)\frac{\partial S_w}{\partial x}\right]+\frac{a_2\beta K_c}{a_1\delta_o}(1-\alpha S_w)\frac{\partial S_w}{\partial x}. \tag{6.19}$$

Using dimensionless variables

$$X = \frac{x}{L},\ T = \frac{\beta K_c t}{\delta_o L^2},$$

(6.19) reduces to

$$(1-\alpha S_w)\frac{\partial^2 S_w}{\partial X^2} - \alpha\left(\frac{\partial S_w}{\partial X}\right)^2 + A\frac{\partial S_w}{\partial X} - A\alpha S_w\frac{\partial S_w}{\partial X} - \frac{\partial S_w}{\partial T} = 0. \tag{6.20}$$

where $A = \frac{La_2}{a_1}$ and $S_w(x,t) = S_w(X,T)$.

The equation (6.20) describes the governing equation for the phenomenon of fingero-imbibition in a heterogeneous porous medium. The solution $S_w(X,T)$ of (6.20) represents the saturation of injected water at distance X and time T. The following boundary conditions are considered to solve (6.20) by homotopy analysis method

$$S_w(0,T) = \frac{T}{5} \text{ and } S_w(1,T) = \frac{1+3T}{5}. \tag{6.21}$$

6.1.4 Solution by homotopy analysis method

We apply HAM [32] to (6.20). According to (6.20), we define a nonlinear operator as

$$\begin{aligned}\mathscr{N}[\phi(X,T;q)] = {} & \frac{\partial^2\phi(X,T;q)}{\partial X^2} - \alpha\phi(X,T;q)\frac{\partial^2\phi(X,T;q)}{\partial X^2} - \alpha\left\{\frac{\partial\phi(X,T;q)}{\partial X}\right\}^2 \\ & + A\frac{\partial\phi(X,T;q)}{\partial X} - A\alpha\phi(X,T;q)\frac{\partial\phi(X,T;q)}{\partial X} - \frac{\partial\phi(X,T;q)}{\partial T}.\end{aligned} \tag{6.22}$$

Using the boundary conditions (6.21), we assume appropriate initial guess as

$$S_{w_0}(X,T) = \frac{T+X^2+T(X+X^2)}{5}. \tag{6.23}$$

Let the linear operator $\mathscr{L}$ be

$$\mathscr{L}[\phi(X,T;q)] = \frac{\partial^2\phi(X,T;q)}{\partial X^2} \tag{6.24}$$

with $\mathscr{L}[0] = 0$, where $q \in [0,1]$ is the embedding parameter and $\phi(X,T;q)$ is an unknown function.

The zeroth-order deformation equation is

$$(1-q)\mathscr{L}[\phi(X,T;q) - S_{w_0}(X,T)] = c_0 q H(X,T)\mathscr{N}[\phi(X,T;q)] \tag{6.25}$$

where $c_0 \neq 0$ is the convergence control parameter, $H(X,T) \neq 0$ is an auxiliary function and $S_{w_0}(X,T)$ is the initial approximation of $S_w(X,T)$.

When $q = 0$ and $q = 1$ one has

$$\phi(X,T;0) = S_{w_0}(X,T) \text{ and } \phi(X,T;1) = S_w(X,T). \tag{6.26}$$

Thus as the embedding parameter q increases from 0 to 1, the solution $\phi(X,T;q)$ varies from the initial approximation $S_{w_0}(X,T)$ to the solution $S_w(X,T)$ of (6.20). Using Taylor series expansion of $\phi(X,T;q)$ w.r.t. q we get

$$\phi(X,T;q) = S_{w_0}(X,T) + \sum_{m=1}^{\infty} S_{w_m}(X,T)q^m \tag{6.27}$$

where

$$S_{w_m}(X,T) = \frac{1}{m!}\frac{\partial^m \phi(X,T;q)}{\partial q^m}\bigg|_{q=0}. \tag{6.28}$$

The series (6.27) is the homotopy series. Assume that the convergence control parameter, the initial approximation, the linear operator and the auxiliary function are in such a way that the series (6.27) converges at $q = 1$, we have

$$S_w(X,T) = S_{w_0}(X,T) + \sum_{m=1}^{\infty} S_{w_m}(X,T). \tag{6.29}$$

Define the vector $\overrightarrow{S_{w_n}} = \{S_{w_0}, S_{w_1}, \ldots, S_{w_n}\}$. Differentiating (6.25) m times w.r.t. q and dividing them by $m!$ and putting $q = 0$, we have the high-order deformation equation

$$\mathscr{L}[S_{w_m}(X,T) - \chi_m S_{w_{m-1}}(X,T)] = c_0 H(X,T)\mathscr{R}_m(\overrightarrow{S_{w_{m-1}}}) \tag{6.30}$$

where χ_m is defined by (2.40) and

$$\mathscr{R}_m(\overrightarrow{S_{w_{m-1}}}) = \frac{\partial^2 S_{w_{m-1}}}{\partial X^2} - \alpha \sum_{i=0}^{m-1} S_{w_i} \frac{\partial^2 S_{w_{m-1-i}}}{\partial X^2} - \alpha \sum_{i=0}^{m-1} \frac{\partial S_{w_i}}{\partial X} \frac{\partial S_{w_{m-1-i}}}{\partial X} + A\frac{\partial S_{w_{m-1}}}{\partial X} - A\alpha \sum_{i=0}^{m-1} S_{w_i} \frac{\partial S_{w_{m-1-i}}}{\partial X} - \frac{\partial S_{w_{m-1}}}{\partial T},\ m \geq 1. \tag{6.31}$$

For simplicity, assume $H(X,T) = 1$. Then the solution of (6.30) is

$$S_{w_m}(X,T) = \chi_m S_{w_{m-1}}(X,T) + c_0 \mathscr{L}^{-1}[\mathscr{R}_m(\overrightarrow{S_{w_{m-1}}})] + C_1 X + C_2 \tag{6.32}$$

subject to $S_{w_m}(0,T) = 0$ and $S_{w_m}(1,T) = 0,\ m \geq 1$ and $C_1,\ C_2$ are constants or functions of T. Hence,

$$\begin{aligned} S_w(X,T) = \frac{T + X^2 + TX + TX^2}{5} + c_0 \Bigg[& -\frac{X}{20} + \frac{X^2}{10} - \frac{X^3}{30} - \frac{X^4}{60} - \frac{TX}{5} \\ & + \frac{TX^2}{5} + \frac{A}{5}\left(-\frac{X}{3} + \frac{X^3}{3} - \frac{5TX}{6} + \frac{TX^2}{2} + \frac{TX^3}{3} \right) - \frac{\alpha}{25}\left(-\frac{X}{2} \right. \\ & \left. + \frac{X^4}{2} - 3TX + TX^2 + TX^3 + TX^4 - 3T^2X + \frac{3T^2X^2}{2} + T^2X^3 \right. \\ & \left. + \frac{T^2X^4}{2} \right) - \frac{A\alpha}{25}\left(-\frac{X}{10} + \frac{X^5}{10} - \frac{47TX}{60} + \frac{TX^3}{3} + \frac{TX^4}{4} + \frac{TX^5}{5} \right. \\ & \left. - \frac{27T^2X}{20} + \frac{T^2X^2}{2} + \frac{T^2X^3}{2} + \frac{T^2X^4}{4} + \frac{T^2X^5}{10} \right) \Bigg] + \cdots \end{aligned} \tag{6.33}$$

is the solution of governing equation (6.20) which gives us the saturation of injected water for the phenomenon of fingero-imbibition arising in fluid flow through heterogeneous porous medium.

We use the following values of constants involved in solution $L = 1\ m$, $\alpha = 1.11$, $a_1 = 2$, $a_2 = 1\ m^{-1}$. With the help of the c_0-curves, we choose appropriate value of c_0. Using BVPh package [36], a Mathematica package for nonlinear boundary value problems, we plotted the c_0-curves for 20th-order approximation of homotopy series solution. The c_0-curves of $S_{w_X}(0,1)$, $S_{w_{XX}}(0,1)$ & $S_{w_{XXX}}(0,1)$ gives us the interval $[-1.2,-0.5]$ as the valid region for c_0; see figure 6.2, the c_0-curves of $S_{w_X}(0,0)$, $S_{w_{XX}}(0,0)$ & $S_{w_{XXX}}(0,0)$ gives us the valid region $[-1.3,-0.3]$ for c_0 as shown in

figure 6.3 and the c_0-curves of $S_{w_X}(0.5,0.5)$, $S_{w_{XX}}(0.5,0.5)$ & $S_{w_{XXX}}(0.5,0.5)$ (see figure 6.4) gives the valid interval $[-1.45,-0.2]$ for c_0. The proper value of c_0 is chosen as $c_0 = -0.8$ to discuss numerical and graphical representations of series solution.

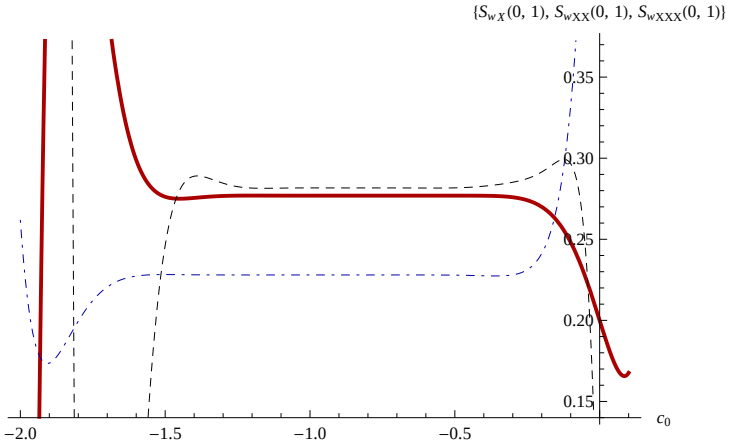

FIGURE 6.2: The c_0-curves of $S_{w_X}(0,1)$ (Solid), $S_{w_{XX}}(0,1)$ (DotDashed) and $S_{w_{XXX}}(0,1)$ (Dashed).

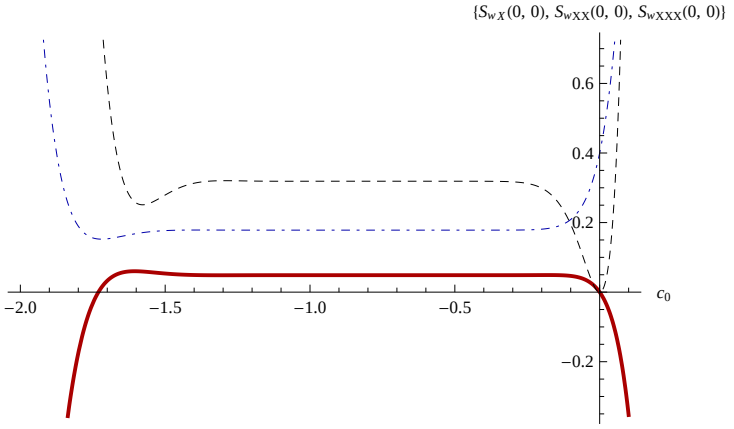

FIGURE 6.3: The c_0-curves of $S_{w_X}(0,0)$ (Solid), $S_{w_{XX}}(0,0)$ (DotDashed) and $S_{w_{XXX}}(0,0)$ (Dashed).

6.1.5 Results and discussion

Numerical and graphical interpretations are discussed with the help of Mathematica BVPh package. Table 6.1 indicates the numerical values of solution (6.33) for 20th-order approximation.

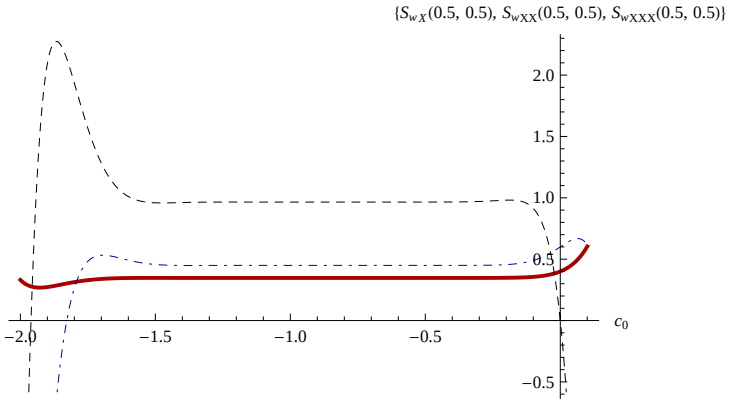

FIGURE 6.4: The c_0-curves of $S_{w_X}(0.5,0.5)$ (Solid), $S_{w_{XX}}(0.5,0.5)$ (DotDashed) and $S_{w_{XXX}}(0.5,0.5)$ (Dashed).

TABLE 6.1: Numerical values of the saturation of injected water for fingero-imbibition phenomenon.

T	Distance X									
	0.1	0.2	0.3	0.4	0.5	0.6	0.7	0.8	0.9	1.0
0.1	0.0294301	0.0408938	0.0547358	0.0713267	0.0910823	0.1144897	0.1421481	0.1748322	0.2136012	0.2600000
0.2	0.0527940	0.0675938	0.0847656	0.1047151	0.1279096	0.1549123	0.1864360	0.2234330	0.2672591	0.3200000
0.3	0.0758961	0.0938046	0.1141118	0.1372578	0.1637642	0.1942783	0.2296453	0.2710370	0.3201998	0.3800000
0.4	0.0987202	0.1194901	0.1427143	0.1688671	0.1985275	0.2324355	0.2715902	0.3174333	0.3722302	0.4400000
0.5	0.1212496	0.1446122	0.1705089	0.1994478	0.2320674	0.2692088	0.3120477	0.3623551	0.4230855	0.5000000
0.6	0.1434674	0.1691316	0.1974281	0.2288975	0.2642381	0.3043986	0.3507520	0.4054637	0.4723947	0.5600000
0.7	0.1653563	0.1930080	0.2234018	0.2571074	0.2948806	0.3377792	0.3873886	0.4463292	0.5196290	0.6200000
0.8	0.1868992	0.2162010	0.2483583	0.2839637	0.3238244	0.3691004	0.4215907	0.4844107	0.5640233	0.6800000
0.9	0.2080794	0.2386705	0.2722254	0.3093505	0.3508905	0.3980903	0.4529401	0.5190400	0.6044621	0.7400000
1.0	0.2288809	0.2603777	0.2949326	0.3331515	0.3758960	0.4244623	0.4809749	0.5494194	0.6393273	0.8000000

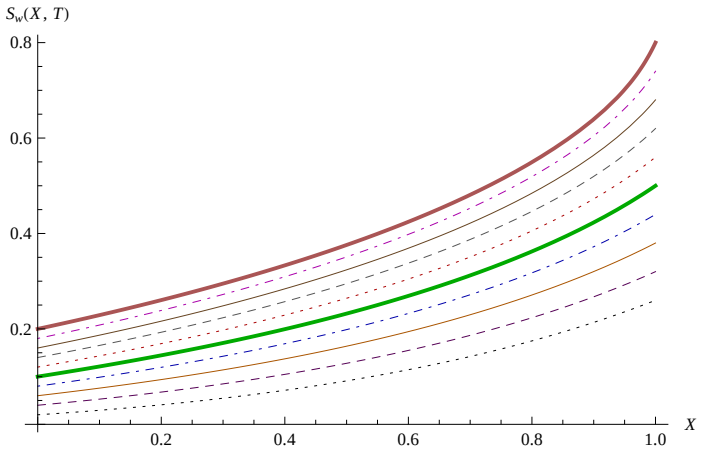

FIGURE 6.5: Saturation of injected water versus distance X for a fixed time $T = 0.1$(lowermost graph), 0.2, ..., 1(uppermost graph).

Figure 6.5 shows the graph of saturation of injected water $S_w(X,T)$ versus X for fixed $T = 0.1, 0.2, \ldots, 1$ and figure 6.6 represents the graph of saturation of injected water $S_w(X,T)$ versus time T for a fixed distance $X = 0.1, 0.2, \ldots, 1$. Figure 6.7 represents the graph of saturation of injected water $S_w(X,T)$ versus distance X & time T. Clearly, the graphical and numerical interpretations of solution show that the saturation of water increases when distance increases for a given time.

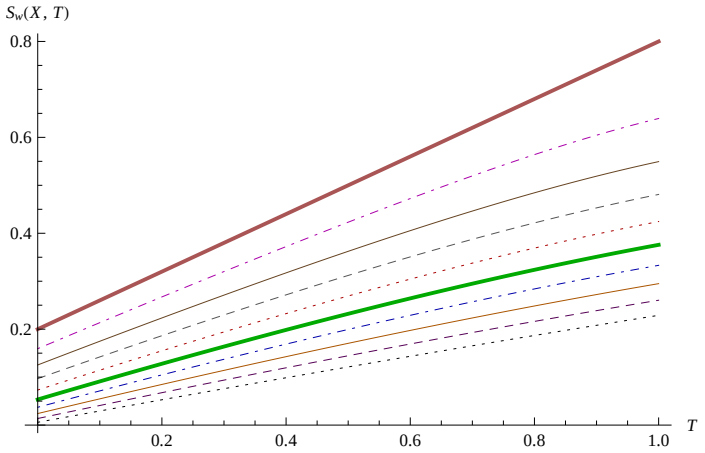

FIGURE 6.6: Saturation of injected water versus time T for a fixed distance $X = 0.1$(lowermost graph), 0.2, ..., 1(uppermost graph).

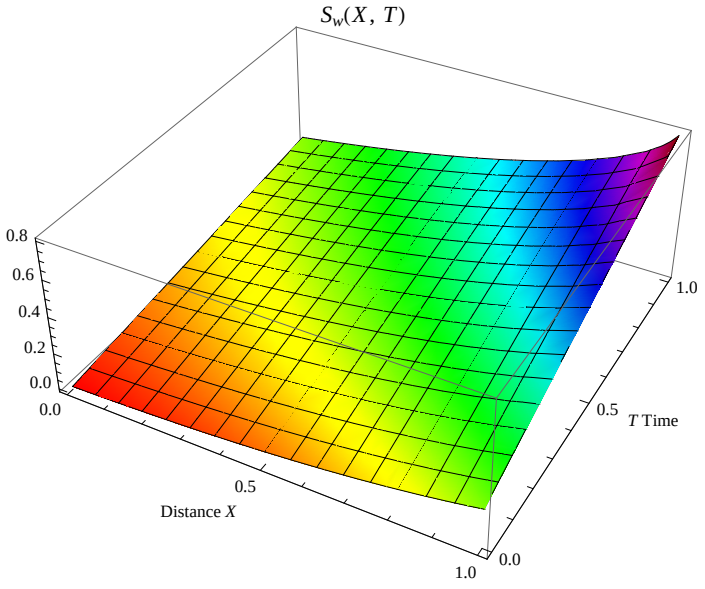

FIGURE 6.7: $S_w(X,T)$ versus X & T.

6.2 PART (B): Fingero-imbibition phenomenon in a heterogeneous porous medium with magnetic field effect

6.2.1 Introduction

The fingering phenomenon will occur simultaneously with imbibition for a less viscous and preferentially wetting phase which describes the phenomenon of fingero-imbibition for which the injection is started by imbibition and resulting displacement produce fingers. This simultaneous occurrence of both phenomena fingering and imbibition is known as fingero-imbibition phenomenon (see figure 6.8).

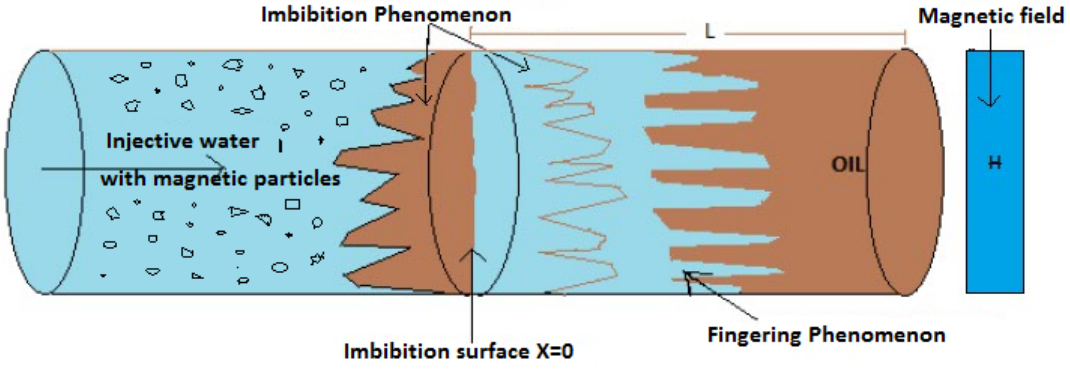

FIGURE 6.8: Fingero-imbibition phenomenon with magnetic field effect.

The imbibition phenomenon has been investigated by many researchers with different aspects. Mishra and Verma [45] have discussed imbibition in the double phase flow with magnetic field. Shah and Verma [79] have obtained the numerical solution of fingero-imbibition phenomenon through homogeneous porous media with magnetic fluid in the injected water. Pradhan and Verma [73] have discussed the finite element treatment of imbibition phenomenon involving magnetic fluid in the injected phase. Parikh *et al.* [53] have discussed mathematical modeling of fingero-imbibition phenomenon in homogeneous porous medium with magnetic field effect in vertical downward direction. Patel *et al.* [66] have discussed the phenomenon of

fingero-imbibition in displacement process through slightly dipping porous medium involving magnetic fluid in water.

In the present work, we have developed the mathematical model for fingero-imbibition phenomenon in a heterogeneous porous medium with magnetic field effect. The mathematical formulation leads to a one dimensional nonlinear partial differential equation. The solution of the problem has been obtained using homotopy analysis method [32]. The main purpose of this work is to find the solution (the saturation of injected water) of the fingero-imbibition phenomenon in a heterogeneous porous medium with magnetic field effect.

6.2.2 Statement of the problem

Here we consider the cylindrical piece of heterogeneous porous matrix of length L which is filled with oil. Consider the flow of water with magnetic particles and oil in a heterogeneous porous medium. In this work it is assumed that the injected water is conductive while the oil is non-conductive and the effect of a variable magnetic field is to increase the velocity of injected water by gradient of $\frac{\omega H^2}{8\pi}$ where ω is permeability of magnetic field H. It is considered that the Darcy's law is valid for this fluid flow problem.

6.2.3 Mathematical model

The velocity of injected water v_w can be represented due to Darcy's law as [5, 77]

$$v_w = -\frac{k_w}{\delta_w} K \left(\frac{\partial P_w}{\partial x} + \frac{\omega H}{4\pi} \frac{\partial H}{\partial x} \right) \tag{6.34}$$

and velocity of oil v_o is defined by (6.2), where ω is permeability of magnetic field H.

Using (6.2), (6.7) and (6.34) in (6.10), we get

$$\frac{\partial P_w}{\partial x} = -\left(\frac{k_w}{\delta_w} + \frac{k_o}{\delta_o} \right)^{-1} \left(\frac{k_o}{\delta_o} \frac{\partial P_c}{\partial x} + \frac{k_w}{\delta_w} \frac{\omega H}{4\pi} \frac{\partial H}{\partial x} \right). \tag{6.35}$$

On substituting the value of $\frac{\partial P_w}{\partial x}$ with (6.16) in (6.34), we get

$$v_w = K\frac{k_o}{\delta_o}\left(\frac{\partial P_c}{\partial x} - \frac{\omega H}{4\pi}\frac{\partial H}{\partial x}\right). \tag{6.36}$$

Substituting (6.36) into (6.3), we get

$$P\frac{\partial S_w}{\partial t} + \frac{\partial}{\partial x}\left[K\frac{k_o}{\delta_o}\frac{\partial P_c}{\partial x} - K\frac{k_o}{\delta_o}\frac{\omega H}{4\pi}\frac{\partial H}{\partial x}\right] = 0. \tag{6.37}$$

Considering the magnetic field in the x- direction only, we write H as [4, 88]

$$H = \lambda x^n \tag{6.38}$$

where λ is a constant parameter and n is an integer.

Using the value of H for $n = 1$ in (6.37) with (6.6), (6.8) and (6.9), we get

$$\frac{\partial S_w}{\partial t} = \frac{\beta K_c}{\delta_o P}\frac{\partial}{\partial x}\left[P(1-\alpha S_w)\frac{\partial S_w}{\partial x}\right] + \frac{K_c\omega\lambda^2}{4\pi\delta_o P}\frac{\partial}{\partial x}\left[P(1-\alpha S_w)x\right]. \tag{6.39}$$

Using dimensionless variables

$$X = \frac{x}{L},\ T = \frac{\beta K_c t}{\delta_o L^2},$$

(6.39) becomes,

$$\frac{\partial S_w}{\partial T} = \frac{1}{P}\frac{\partial}{\partial X}\left[P(1-\alpha S_w)\frac{\partial S_w}{\partial X}\right] + \frac{\omega\lambda^2 L^2}{4\pi\beta P}\frac{\partial}{\partial X}\left[P(1-\alpha S_w)X\right]. \tag{6.40}$$

Now,

$$\frac{1}{P}\frac{\partial P}{\partial X} = \frac{\partial(\log P)}{\partial X} = \frac{\partial}{\partial X}\left(\frac{a_2 LX}{a_1} - \log a_1\right)(\text{neglecting higher order terms of } X) = \frac{a_2 L}{a_1}.$$

Therefore (6.40) reduces to

$$\begin{aligned}\frac{\partial S_w}{\partial T} = \frac{\partial}{\partial X}\left[(1-\alpha S_w)\frac{\partial S_w}{\partial X}\right] + A(1-\alpha S_w)\frac{\partial S_w}{\partial X} + B\frac{\partial}{\partial X}\left[(1-\alpha S_w)X\right] \\ + AB(1-\alpha S_w)X\end{aligned} \tag{6.41}$$

where $A = \frac{a_2 L}{a_1}$, $B = \frac{\omega \lambda^2 L^2}{4\pi\beta}$ and $S_w(x,t) = S_w(X,T)$.

The equation (6.41) is the desired governing equation for fingero-imbibition phenomenon in a heterogeneous porous medium with magnetic field effect. The homotopy analysis method is used to obtain solution $S_w(X,T)$ of (6.41) with boundary conditions (6.21).

6.2.4 Solution by homotopy analysis method

According to (6.41), a nonlinear operator $\mathscr{N}$ is defined as

$$\begin{aligned}\mathscr{N}[\phi(X,T;q)] = {} & \frac{\partial^2\phi(X,T;q)}{\partial X^2} - \alpha\phi(X,T;q)\frac{\partial^2\phi(X,T;q)}{\partial X^2} - \alpha\left\{\frac{\partial\phi(X,T;q)}{\partial X}\right\}^2 \\ & + (A - B\alpha X)\frac{\partial\phi(X,T;q)}{\partial X} - A\alpha\phi(X,T;q)\frac{\partial\phi(X,T;q)}{\partial X} \\ & - (B\alpha + AB\alpha X)\phi(X,T;q) + ABX + B - \frac{\partial\phi(X,T;q)}{\partial T}. \end{aligned} \tag{6.42}$$

According to (6.21), it is straightforward to choose initial approximation as

$$S_{w_0}(X,T) = \frac{T + X^2 + T(X + X^2)}{5}. \tag{6.43}$$

Here we consider the auxiliary function as $H(X,T) = 1$. Then the solution of (6.30) becomes

$$S_{w_m}(X,T) = \chi_m S_{w_{m-1}}(X,T) + c_0\mathscr{L}^{-1}[\mathscr{R}_m(\overrightarrow{S_{w_{m-1}}})] + C_1X + C_2 \tag{6.44}$$

where C_1 & C_2 are determined by $S_{w_m}(0,T) = 0$ & $S_{w_m}(1,T) = 0$, $m \geq 1$, $\mathscr{L}$ is defined by (6.24) and

$$\begin{aligned}\mathscr{R}_m(\overrightarrow{S_{w_{m-1}}}) = {} & \frac{\partial^2 S_{w_{m-1}}}{\partial X^2} - \alpha\sum_{i=0}^{m-1} S_{w_i}\frac{\partial^2 S_{w_{m-1-i}}}{\partial X^2} - \alpha\sum_{i=0}^{m-1}\frac{\partial S_{w_i}}{\partial X}\frac{\partial S_{w_{m-1-i}}}{\partial X} \\ & + A\frac{\partial S_{w_{m-1}}}{\partial X} - B\alpha X\frac{\partial S_{w_{m-1}}}{\partial X} - A\alpha\sum_{i=0}^{m-1} S_{w_i}\frac{\partial S_{w_{m-1-i}}}{\partial X} - B\alpha S_{w_{m-1}} \\ & - AB\alpha X S_{w_{m-1}} + (B + ABX)(1 - \chi_m) - \frac{\partial S_{w_{m-1}}}{\partial T},\ m \geq 1. \end{aligned} \tag{6.45}$$

The equation (6.44) gives $S_{w_1}(X,T), S_{w_2}(X,T)$ and so on. Hence the homotopy series solution of (6.41) is as

$$\begin{aligned} S_w(X,T) = \frac{T+X^2+TX+TX^2}{5} + c_0\Bigg[& -\frac{X}{20}+\frac{X^2}{10}-\frac{X^3}{30}-\frac{X^4}{60}-\frac{TX}{5}+\frac{TX^2}{5} \\ & +\frac{A}{5}\left(-\frac{X}{3}+\frac{X^3}{3}-\frac{5TX}{6}+\frac{TX^2}{2}+\frac{TX^3}{3}\right)-\frac{\alpha}{25}\left(-\frac{X}{2}+\frac{X^4}{2}\right. \\ & \left.-3TX+TX^2+TX^3+TX^4-3T^2X+\frac{3T^2X^2}{2}+T^2X^3+\frac{T^2X^4}{2}\right) \\ & -\frac{A\alpha}{25}\left(-\frac{X}{10}+\frac{X^5}{10}-\frac{47TX}{60}+\frac{TX^3}{3}+\frac{TX^4}{4}+\frac{TX^5}{5}-\frac{27T^2X}{20}\right. \\ & \left.+\frac{T^2X^2}{2}+\frac{T^2X^3}{2}+\frac{T^2X^4}{4}+\frac{T^2X^5}{10}\right)-\frac{BX}{2}+\frac{BX^2}{2}-\frac{B\alpha}{5}\left(-\frac{X}{4}\right. \\ & \left.+\frac{X^4}{4}-\frac{13TX}{12}+\frac{TX^2}{2}+\frac{TX^3}{3}+\frac{TX^4}{4}\right)-\frac{ABX}{6}+\frac{ABX^3}{6} \\ & -\frac{AB\alpha}{5}\left(-\frac{X}{20}+\frac{X^5}{20}-\frac{3TX}{10}+\frac{TX^3}{6}+\frac{TX^4}{12}+\frac{TX^5}{20}\right)\Bigg]+\cdots. \end{aligned} \tag{6.46}$$

The solution (6.46) represents the saturation of injected water for the phenomenon of fingero-imbibition arising in fluid flow through heterogeneous porous medium with magnetic field effect.

As pointed out by Liao, the convergence of the homotopy series solution depends upon the value of convergence control parameter c_0. With the help of Mathematica package for nonlinear BVPs [36], the so-called c_0-curves are plotted for 20th-order approximation. This helps us to discover the range for the admissible values of c_0, which corresponds to the horizontal line segment. It is obvious that the valid domain of c_0 is $-1.2 \leq c_0 \leq -0.4$ from the c_0-curves (see figures 6.9-6.11). This means that the series (6.46) converges for these values of c_0.

6.2.5 Results and discussion

The following values of constants are assumed as: $L = 1\ m$, $\alpha = 1.11$, $a_1 = 2$, $a_2 = 1\ m^{-1}$, $\beta = 0.1\ N/m^2$, $\omega = 0.1\ N/A^2$, $\lambda = 0.1\ A/m^2$, $c_0 = -0.8$. We have considered

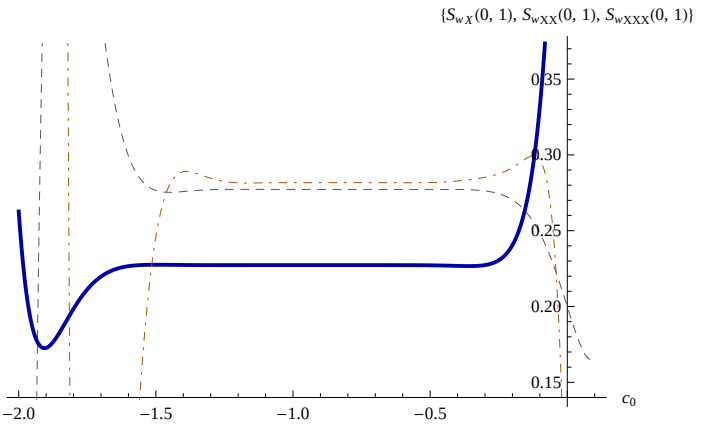

FIGURE 6.9: The c_0-curves of $S_{w_X}(0,1)$ (Dashed line), $S_{w_{XX}}(0,1)$ (Solid line) and $S_{w_{XXX}}(0,1)$ (DotDashed line).

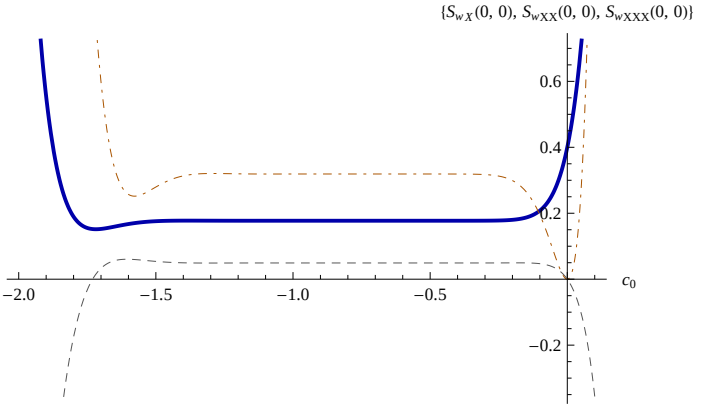

FIGURE 6.10: The c_0-curves of $S_{w_X}(0,0)$ (Dashed line), $S_{w_{XX}}(0,0)$ (Solid line) and $S_{w_{XXX}}(0,0)$ (DotDashed line).

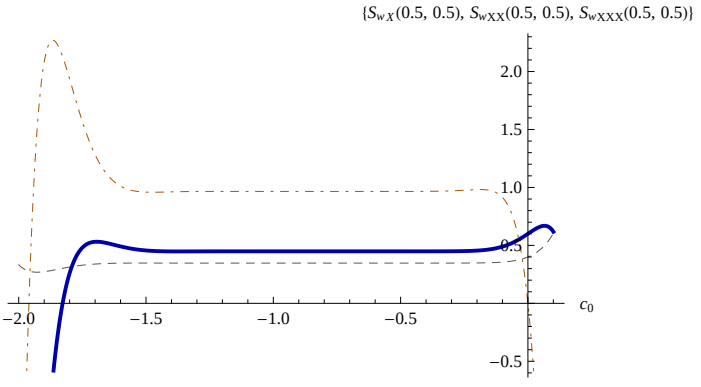

FIGURE 6.11: The c_0-curves of $S_{w_X}(0.5,0.5)$ (Dashed line), $S_{w_{XX}}(0.5,0.5)$ (Solid line) and $S_{w_{XXX}}(0.5,0.5)$ (DotDashed line).

first 20 terms of series solution for numerical and graphical representations. Table 6.2 indicates the numerical values of solution (6.46).

TABLE 6.2: Numerical values of the saturation of injected water for fingero-imbibition phenomenon with magnetic field effect.

T	Distance X									
	0.1	0.2	0.3	0.4	0.5	0.6	0.7	0.8	0.9	1.0
0.1	0.0294702	0.0409648	0.0548286	0.0714324	0.0911921	0.1145950	0.1422402	0.1749026	0.2136411	0.2600000
0.2	0.0528328	0.0676626	0.0848556	0.1048177	0.1280162	0.1550146	0.1865255	0.2235014	0.2672979	0.3200000
0.3	0.0759336	0.0938712	0.1141989	0.1373570	0.1638673	0.1943772	0.2297319	0.2711031	0.3202373	0.3800000
0.4	0.0987564	0.1195543	0.1427983	0.1689628	0.1986268	0.2325306	0.2716734	0.3174967	0.3722661	0.4400000
0.5	0.1212845	0.1446740	0.1705897	0.1995398	0.2321627	0.2692999	0.3121271	0.3624155	0.4231194	0.5000000
0.6	0.1435009	0.1691909	0.1975056	0.2289855	0.2643291	0.3044852	0.3508272	0.4055203	0.4724262	0.5600000
0.7	0.1653884	0.1930648	0.2234759	0.2571912	0.2949670	0.3378610	0.3874590	0.4463816	0.5196575	0.6200000
0.8	0.1869300	0.2162553	0.2484289	0.2840434	0.3239060	0.3691771	0.4216559	0.4844582	0.5640480	0.6800000
0.9	0.2081090	0.2387224	0.2722926	0.3094260	0.3509672	0.3981617	0.4529997	0.5190818	0.6044820	0.7400000
1.0	0.2289092	0.2604273	0.2949965	0.3332228	0.3759679	0.4245282	0.4810286	0.5494552	0.6393414	0.8000000

Graphical presentation of the saturation of injected water is obtained by using Mathematica software. The graph of saturation of injected water $S_w(X,T)$ versus distance X for a fixed time $T = 0.1, 0.2, \ldots, 1$ is given in figure 6.12 and figure 6.13 represents the graph of saturation of injected water $S_w(X,T)$ versus time T for a fixed distance $X = 0.1, 0.2, \ldots, 1$.

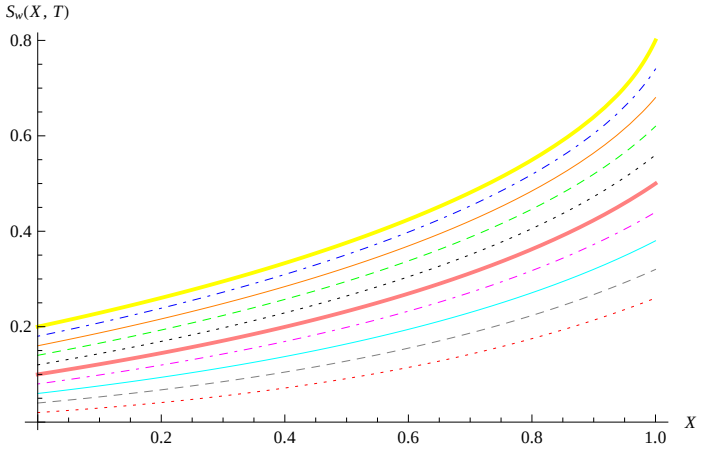

FIGURE 6.12: Saturation of injected water versus distance X for a fixed time $T =$ 0.1(lowermost graph), 0.2, ..., 1(uppermost graph).

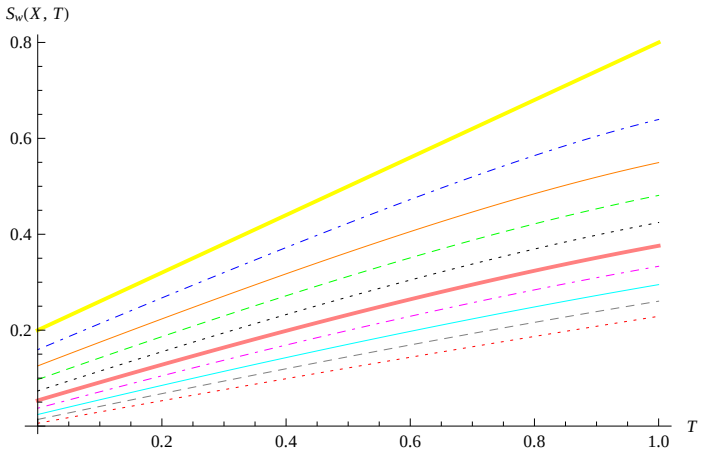

FIGURE 6.13: Saturation of injected water versus time T for a fixed distance $X = 0.1$(lowermost graph), 0.2, ..., 1(uppermost graph).

6.2.6 Comparative study with fingero-imbibition phenomenon in a heterogeneous porous medium without magnetic field effect

Table 6.3 shows the comparative numerical values of the saturation of injected water of fingero-imbibition phenomenon without magnetic field effect [61] and with magnetic field effect.

TABLE 6.3: Comparative numerical values of the saturation of injected water without magnetic field effect and with magnetic field effect.

T	Distance X									
	0.1	0.2	0.3	0.4	0.5	0.6	0.7	0.8	0.9	1.0
0.1	0.0294301	0.0408938	0.0547358	0.0713267	0.0910823	0.1144897	0.1421481	0.1748322	0.2136012	0.2600000
	0.0294702	0.0409648	0.0548286	0.0714324	0.0911921	0.1145950	0.1422402	0.1749026	0.2136411	0.2600000
0.2	0.0527940	0.0675938	0.0847656	0.1047151	0.1279096	0.1549123	0.1864360	0.2234330	0.2672591	0.3200000
	0.0528328	0.0676626	0.0848556	0.1048177	0.1280162	0.1550146	0.1865255	0.2235014	0.2672979	0.3200000
0.3	0.0758961	0.0938046	0.1141118	0.1372578	0.1637642	0.1942783	0.2296453	0.2710370	0.3201998	0.3800000
	0.0759336	0.0938712	0.1141989	0.1373570	0.1638673	0.1943772	0.2297319	0.2711031	0.3202373	0.3800000
0.4	0.0987202	0.1194901	0.1427143	0.1688671	0.1985275	0.2324355	0.2715902	0.3174333	0.3722302	0.4400000
	0.0987564	0.1195543	0.1427983	0.1689628	0.1986268	0.2325306	0.2716734	0.3174967	0.3722661	0.4400000
0.5	0.1212496	0.1446122	0.1705089	0.1994478	0.2320674	0.2692088	0.3120477	0.3623551	0.4230855	0.5000000
	0.1212845	0.1446740	0.1705897	0.1995398	0.2321627	0.2692999	0.3121271	0.3624155	0.4231194	0.5000000
0.6	0.1434674	0.1691316	0.1974281	0.2288975	0.2642381	0.3043986	0.3507520	0.4054637	0.4723947	0.5600000
	0.1435009	0.1691909	0.1975056	0.2289855	0.2643291	0.3044852	0.3508272	0.4055203	0.4724262	0.5600000
0.7	0.1653563	0.1930080	0.2234018	0.2571074	0.2948806	0.3377792	0.3873886	0.4463292	0.5196290	0.6200000
	0.1653884	0.1930648	0.2234759	0.2571912	0.2949670	0.3378610	0.3874590	0.4463816	0.5196575	0.6200000
0.8	0.1868992	0.2162010	0.2483583	0.2839637	0.3238244	0.3691004	0.4215907	0.4844107	0.5640233	0.6800000
	0.1869300	0.2162553	0.2484289	0.2840434	0.3239060	0.3691771	0.4216559	0.4844582	0.5640480	0.6800000
0.9	0.2080794	0.2386705	0.2722254	0.3093505	0.3508905	0.3980903	0.4529401	0.5190400	0.6044621	0.7400000
	0.2081090	0.2387224	0.2722926	0.3094260	0.3509672	0.3981617	0.4529997	0.5190818	0.6044820	0.7400000
1.0	0.2288809	0.2603777	0.2949326	0.3331515	0.3758960	0.4244623	0.4809749	0.5494194	0.6393273	0.8000000
	0.2289092	0.2604273	0.2949965	0.3332228	0.3759679	0.4245282	0.4810286	0.5494552	0.6393414	0.8000000

6.3 Conclusion

We have discussed the phenomenon of fingero-imbibition in a heterogeneous porous medium with and without magnetic field effect under certain assumptions. The homotopy series solutions are obtained which represent the saturation of injected water. The numerical and graphical representations clearly indicate the saturation of water increases when distance and time increase in both the cases. Due to additional magnetic field effect the saturation of injected water is more increasing than the saturation of injected water without magnetic field effect. We can conclude that the magnetic field effect plays an important role in the fingero-imbibition phenomenon in a heterogeneous porous medium.

CHAPTER 7

Infiltration Phenomenon

7.1 Introduction

The groundwater flow has great importance in many fields of engineering and science like as soil science, water resource engineering, environmental engineering, hydrology, fluid mechanics [5, 8, 19, 68, 69, 77]. We investigate problem related to fluid flow in fluid mechanics.

Infiltration is the process by which the water on ground surface or the water of reservoir enters into soils and moves into rocks through pore spaces and cracks. Once water has infiltrated into the soil, it may stay in the soil for a long time. The rate of infiltration is dependent on the different factors like as soil texture and structure, the amount of precipitation, water content of the soil, the depth of the water table, storage capacity, the amount of vegetative cover over the area.

Many researchers have investigated infiltration phenomenon with different aspects: Boussinesq [12], Philip [68], Srivastava and Yeh [80], Witelski [89], Wojnar [91], Vázquez [84], Borana *et al.* [10], Patel *et al.* [56], Chavan and Panchal [15], Parikh [50], Desai [20].

The main objective of the investigated problem is to obtain solution of Boussinesq's equation for infiltration phenomenon. Boussinesq's equation is solved by homotopy analysis method [32] with suitable conditions. The solution of the problem represents the height of free surface of the water table in unsaturated soil. The convergence of the homotopy series solution is discussed with the help of the c_0-curve.

7.2 Mathematical formulation

Consider that the groundwater reservoir has maximum height h_{max} and surrounding of groundwater reservoir is unsaturated soil. Infiltration is the process in which the groundwater has entered into the unsaturated homogeneous soil through vertical permeable wall. The bottom of groundwater reservoir is assumed impervious bed (which we label as $z = 0$), so water can't move in a downward direction. The infiltrated groundwater will enter in unsaturated soil then the infiltrated groundwater will develop a curve between unsaturated soil and saturated soil, which is called a water table. The dotted arc below the curve is saturated by infiltrated groundwater and above the curve is the dry region of unsaturated soil. The height of the free surface is zero, when $x = L$. The figure 7.1 demonstrates the infiltration phenomenon and it shows a vertical cross-section of the reservoir. We considered that there is no region of partial saturation. The main aim of the study of infiltration phenomenon is to measure the height of free surface.

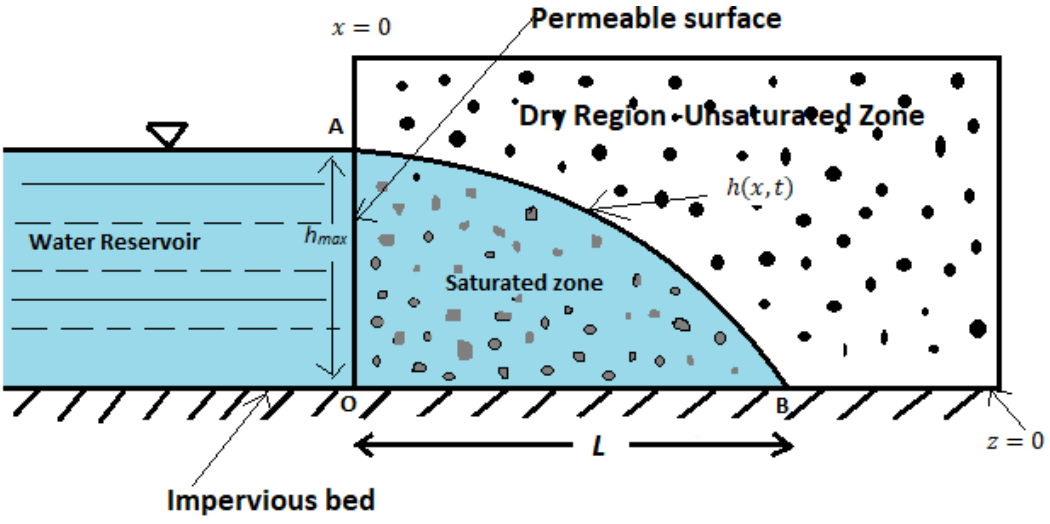

FIGURE 7.1: The infiltration phenomenon.

For mathematical formulation, we consider the following assumptions:

1) the transversal variable y is ignored,

2) a region occupied by infiltrated water is described as

$$\Omega = \{(x,z) \in R^2 : 0 \leq z \leq h(x,t)\}.$$

Obviously, $0 \leq h(x,t) \leq h_{max}$ and $h(x,t)$ is an unknown function. We assume that the flow has an almost horizontal speed $\mathbf{u} \sim (u,0)$. Thus the vertical component of the momentum equation gives

$$\rho\left(\frac{dw}{dt} + \mathbf{u}\cdot\nabla w\right) = -\frac{\partial p}{\partial z} - \rho g. \tag{7.1}$$

We neglected the left side of (7.1) and integrate it with respect to z gives

$$p + \rho g z = constant. \tag{7.2}$$

Assume $p = 0$ on the free surface $z = h(x,t)$. Thus,

$$p = \rho g(h - z). \tag{7.3}$$

We take a section $S = (a,x) \times (0,C)$, where C is the free surface $z = h(x,t)$. Then the mass conservation law give us

$$P\frac{\partial}{\partial t}\int_a^x \int_0^h dz dx = -\int_{\partial S} \mathbf{u}\cdot\mathbf{n}\, dl. \tag{7.4}$$

So,

$$P\frac{\partial}{\partial t}\int_a^x h dx = -\int_{\partial S} \mathbf{u}\cdot\mathbf{n}\, dl. \tag{7.5}$$

where P is the porosity and $\mathbf{u}$ is the velocity of water, which follows Darcy's law

$$\mathbf{u} = -\frac{K}{\delta}\nabla(p + \rho g z) = -\frac{K}{\delta}\nabla(\rho g h) \tag{7.6}$$

where δ is the viscosity, K is the permeability.

Now $\mathbf{u}\cdot\mathbf{n} \approx (u,0)\cdot(1,0) = u = -\frac{\rho g K}{\delta}\frac{\partial h}{\partial x}$. Differentiating (7.5) with respect to x, we get

$$P\frac{\partial h}{\partial t} = \frac{\rho g K}{\delta}\frac{\partial}{\partial x}\int_0^h \frac{\partial h}{\partial x}dz. \tag{7.7}$$

Thus

$$\frac{\partial h}{\partial t} = \frac{\rho g K}{2P\delta}\frac{\partial^2(h^2)}{\partial x^2} \tag{7.8}$$

is the Boussinesq's equation which describes infiltration phenomenon.

Using dimensionless variables

$$\mathscr{H} = \frac{h}{L},\ X = \frac{x}{L},\ T = \frac{\rho g K t}{P\delta L},$$

(7.8) gives us

$$\frac{\partial \mathscr{H}}{\partial T} = \mathscr{H}\frac{\partial^2 \mathscr{H}}{\partial X^2} + \left\{\frac{\partial \mathscr{H}}{\partial X}\right\}^2. \tag{7.9}$$

Homotopy analysis method is used to solve it with suitable conditions. The height of free surface is represented by the solution $\mathscr{H}(X,T)$. We assume the boundary conditions:

$$\mathscr{H}(0,T) = h_{max} \text{ and } \mathscr{H}(1,T) = 0. \tag{7.10}$$

7.3 Solution by homotopy analysis method

We apply HAM to (7.9) with (7.10). We define such a nonlinear equation

$$\mathscr{N}[\phi(X,T;q)] = 0 \tag{7.11}$$

where

$$\mathscr{N}[\phi(X,T;q)] = \phi(X,T;q)\frac{\partial^2\phi(X,T;q)}{\partial X^2} + \left\{\frac{\partial\phi(X,T;q)}{\partial X}\right\}^2 - \frac{\partial\phi(X,T;q)}{\partial T} \quad (7.12)$$

and $\phi(X,T;q)$ is an unknown function.

The zeroth-order deformation equation is [32]

$$(1-q)\mathscr{L}[\phi(X,T;q) - \mathscr{H}_0(X,T)] = c_0 qH(X,T)\mathscr{N}[\phi(X,T;q)] \quad (7.13)$$

where $\mathscr{H}_0(X,T)$ is the initial approximation of the solution $\mathscr{H}(X,T)$, $\mathscr{L}$ is the linear operator, $q \in [0,1]$ the homotopy parameter, $H(X,T) \neq 0$ is an auxiliary function and $c_0 \neq 0$ is the convergence control parameter.

We choose the linear operator $\mathscr{L}[\phi(X,T;q)] = \frac{\partial^2\phi(X,T;q)}{\partial X^2}$ and the initial approximation of $\mathscr{H}(X,T)$ as $\mathscr{H}_0(X,T) = (h_{max} - TX)(1-X^2)e^{-X}$.

When $q = 0$ and $q = 1$, (7.13) give us

$$\phi(X,T;0) = \mathscr{H}_0(X,T) \text{ and } \phi(X,T;1) = \mathscr{H}(X,T). \quad (7.14)$$

Thus the function $\phi(X,T;q)$ continuously varies from $\mathscr{H}_0(X,T)$ to $\mathscr{H}(X,T)$ as q increases from 0 to 1. According to Taylor's theorem, the expansion of $\phi(X,T;q)$ with respect to q gives

$$\phi(X,T;q) = \mathscr{H}_0(X,T) + \sum_{m=1}^{\infty} \mathscr{H}_m(X,T)q^m \quad (7.15)$$

where

$$\mathscr{H}_m(X,T) = \frac{1}{m!}\frac{\partial^m\phi(X,T;q)}{\partial q^m}\bigg|_{q=0}. \quad (7.16)$$

Assume the initial approximation, the linear operator, the convergence control parameter and the auxiliary function are in such a way that the series (7.15) converges

at $q = 1$. i.e.

$$\mathscr{H}(X,T) = \mathscr{H}_0(X,T) + \sum_{m=1}^{\infty} \mathscr{H}_m(X,T). \tag{7.17}$$

Write $\overrightarrow{\mathscr{H}_n} = \{\mathscr{H}_0(X,T), \mathscr{H}_1(X,T), \ldots, \mathscr{H}_n(X,T)\}$. Differentiating (7.13) m times w.r.t. q and dividing them by $m!$ and then put $q = 0$, we get the high-order deformation equation

$$\mathscr{L}[\mathscr{H}_m(X,T) - \chi_m \mathscr{H}_{m-1}(X,T)] = c_0 H(X,T) \mathscr{R}_m(\overrightarrow{\mathscr{H}_{m-1}}) \tag{7.18}$$

subject to

$$\mathscr{H}_m(0,T) = 0 \text{ and } \mathscr{H}_m(1,T) = 0,\ m \geq 1, \tag{7.19}$$

$$\mathscr{R}_m(\overrightarrow{\mathscr{H}_{m-1}}) = \sum_{i=0}^{m-1} \mathscr{H}_i \frac{\partial^2 \mathscr{H}_{m-1-i}}{\partial X^2} + \sum_{i=0}^{m-1} \frac{\partial \mathscr{H}_i}{\partial X} \frac{\partial \mathscr{H}_{m-1-i}}{\partial X} - \frac{\partial \mathscr{H}_{m-1}}{\partial T},\ m \geq 1 \tag{7.20}$$

and χ_m is defined by (2.40).

We consider $H(X,T) = 1$. Thus the solution of (7.18) is

$$\mathscr{H}_m(X,T) = \chi_m \mathscr{H}_{m-1}(X,T) + c_0 \mathscr{L}^{-1}[\mathscr{R}_m(\overrightarrow{\mathscr{H}_{m-1}})] + C_1 X + C_2 \tag{7.21}$$

where C_1 and C_2 are constants or functions of T. Hence the solution takes the form

$$\begin{aligned}
\mathscr{H}(X,T) = {} & e^{-X}\left(h_{max} - h_{max}X^2 - TX + TX^3\right) + c_0 e^{-X}\{-22 - 17X - 6X^2 \\
& - X^3\} + c_0 e^{-2X}\left\{\frac{h_{max}^2}{2} - h_{max}TX + \frac{T^2X^2}{2} - h_{max}^2X^2 + 2h_{max}TX^3\right. \\
& \left. - T^2X^4 + \frac{h_{max}^2X^4}{2} - h_{max}TX^5 + \frac{T^2X^6}{2}\right\} + c_0\left\{22 - \frac{h_{max}^2}{2} + 46Xe^{-1}\right. \\
& \left. - 22X + \frac{h_{max}^2X}{2}\right\} + \cdots .
\end{aligned} \tag{7.22}$$

The solution (7.22) represents the height of free surface for infiltration

phenomenon. The convergence of homotopy series solution depends on convergence control parameter c_0. With the help of c_0-curve, the convergence of homotopy series solution has discussed by many authors [29, 33, 49, 59–62, 64, 83]. Mathematica BVPh package [36] is used to plot the c_0-curve of $\mathscr{H}_{XX}(1,1)$ for 10th-order approximation (see figure 7.2). We choose proper value of $c_0 = -0.014$ from valid region.

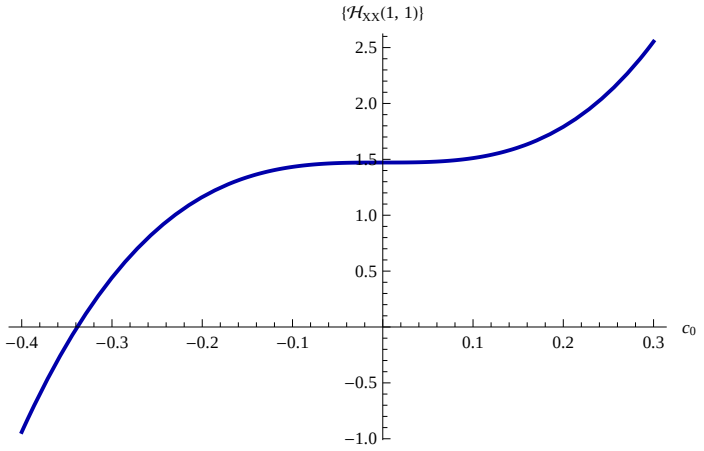

FIGURE 7.2: The c_0-curve of $\mathscr{H}_{XX}(1,1)$ (Thick line) for $h_{max} = 1$.

The numerical and graphical representations of the height of free surface are obtained by Mathematica software [36]. The numerical values of the height free surface $\mathscr{H}$ are given in the table 7.1. The graphical representation of the height of free surface versus length X for a fixed time $T = 0.1, 0.2, \ldots, 1$ in the figure 7.3.

TABLE 7.1: Numerical values of the height of free surface $\mathscr{H}$ for $h_{max} = 1$.

T	Length X										
	0.0	0.1	0.2	0.3	0.4	0.5	0.6	0.7	0.8	0.9	1.0
0.1	1.0000000	0.8953185	0.7858909	0.6747501	0.5643396	0.4566071	0.3530792	0.2549220	0.1629947	0.0778948	0.0000000
0.2	1.0000000	0.8874137	0.7717887	0.6563064	0.5434690	0.4352064	0.3329633	0.2377733	0.1503233	0.0710117	0.0000000
0.3	1.0000000	0.8794994	0.7576567	0.6378121	0.5225341	0.4137387	0.3127889	0.2205825	0.1376292	0.0641219	0.0000000
0.4	1.0000000	0.8715756	0.7434946	0.6192669	0.5015348	0.3922039	0.2925558	0.2033493	0.1249121	0.0572254	0.0000000
0.5	1.0000000	0.8636423	0.7293024	0.6006707	0.4804707	0.3706016	0.2722636	0.1860737	0.1121721	0.0503222	0.0000000
0.6	1.0000000	0.8556994	0.7150801	0.5820233	0.4593416	0.3489315	0.2519122	0.1687555	0.0994091	0.0434122	0.0000000
0.7	1.0000000	0.8477470	0.7008276	0.5633245	0.4381471	0.3271934	0.2315013	0.1513945	0.0866231	0.0364956	0.0000000
0.8	1.0000000	0.8397850	0.6865447	0.5445740	0.4168870	0.3053870	0.2110307	0.1339907	0.0738140	0.0295722	0.0000000
0.9	1.0000000	0.8318135	0.6722314	0.5257717	0.3955610	0.2835119	0.1905002	0.1165439	0.0609817	0.0226421	0.0000000
1.0	1.0000000	0.8238324	0.6578875	0.5069174	0.3741689	0.2615679	0.1699094	0.0990539	0.0481262	0.0157053	0.0000000

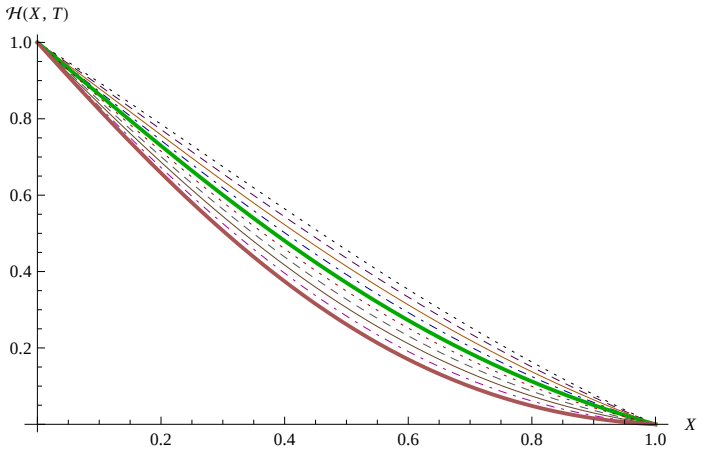

FIGURE 7.3: The height of free surface versus length X for a fixed time $T = 0.1$(uppermost graph), $0.2, \ldots, 1$(lowermost graph) $(h_{max} = 1)$.

7.4 Conclusion

The infiltration phenomenon is discussed and the mathematical formulation for infiltration phenomenon in unsaturated homogeneous soil leads to Boussinesq equation. Homotopy analysis solution is obtained for Boussinesq equation. The convergence of homotopy series solution is discussed with the help of c_0-curve. The solution decreases when length increases for a given time. We conclude that the height of free surface decreases when length increases for a given time.

CHAPTER 8

Groundwater Recharge

8.1 Introduction

One dimensional groundwater recharge problem is related to hydrology, environmental engineering, soil mechanics, water resource engineering etc. The flow of water in unsaturated soil has been considered with some specific assumptions. The zone in which relatively all pores and fractures are saturated with water is called the saturated zone. In the unsaturated zone, the pore space is partly filled by air and partly by water. The unsaturated zone is the part of the subsurface between the ground surface and the groundwater table (see figure 8.1). Moisture content is the quantity of water contained in a soil. Moisture content is used in a wide range of scientific and technical areas. In the dry soil there is no moisture, so its value 0 and is 1 when the medium is fully saturated by water. So the range of moisture content is 0 (completely dry) to 1 (fully saturated by water). The water flow in the unsaturated zone is complicated by the fact that the soil's permeability to water depends on its water saturation [3]. The water flow through soil is unsteady and slightly saturated because the moisture content is time dependent function and all pores are not completely filled with water.

The Richard's equation is one of the most well-known equations to describe the behavior of unsaturated zones in soil. One dimensional groundwater recharge has great importance in many branches of science and engineering. The problem of groundwater flow has been discussed by many researchers with different aspects, like as Klute [30] reduced diffusion equation to an ordinary differential equation and applied a forward integration and iteration method, Verma [85] obtained solution of a one dimensional groundwater recharge for constant diffusivity and linear conductivity by Laplace

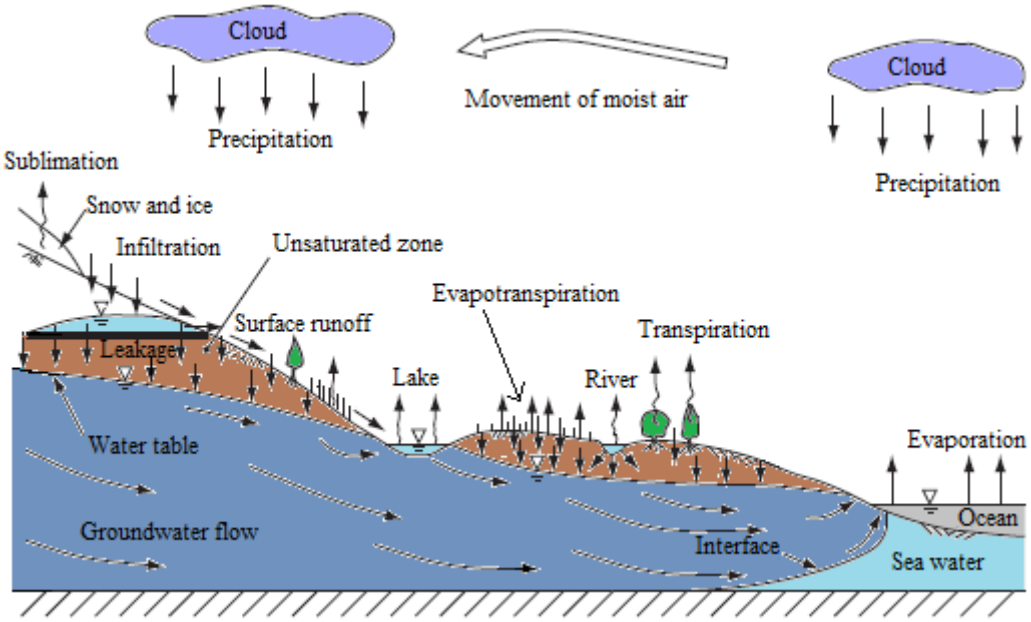

FIGURE 8.1: The hydrological cycle [8].

transform, Mehta [39] obtained singular perturbation solution of one dimensional flow in unsaturated porous media with small diffusivity coefficient, Prasad *et al.* [74] developed numerical model to simulate moisture flow through unsaturated zones using the finite element method, Desai [19] obtained composite expansion solution for groundwater recharge in vertical direction, Mehta and Patel [42] obtained solution of Burger's equation for one dimensional groundwater recharge by spreading in porous media, Joshi *et al.* [27] obtained solution of one dimensional vertical groundwater recharge by group theoretical approach, Nasseri *et al.* [48] studied traveling wave solution of advection-diffusion equation with typical forms of conductivity and diffusivity functions proposed by Brooks and Corey.

Our goal of the present work is to obtain solution of one dimensional groundwater recharge by spreading. It is assumed that the groundwater recharge takes place over the large basin of such geological location that the sides are bounded by rigid boundaries while the bottom by a thick layer of water table for investigated flow problem. Here the flow takes place in the vertical downward direction through unsaturated porous medium up to depth L (L is length of basin). On the basis of linear and nonlinear conductivity and diffusivity functions, three cases are considered for Brooks-Corey model. The mathematical formulation gives us a one dimensional nonlinear partial

equation which is solved by homotopy analysis method. The solution is expressed in series form and it gives moisture content of soil.

8.2 Mathematical formulation

The equation of continuity for water flow through unsaturated porous medium is governed by [5, 30]

$$\frac{\partial}{\partial t}(\rho\Theta) = -\nabla \cdot M \tag{8.1}$$

where ρ is the density of fluid, Θ is the moisture content and M is a mass flux of moisture.

Darcy's law for the motion of water in unsaturated porous medium is expressed as [5]

$$v = -\kappa\nabla\Phi \tag{8.2}$$

where v is the volume flux of moisture, κ is the hydraulic conductivity, $\nabla\Phi$ is the gradient of the whole moisture potential. The mass flux of moisture M is the product of fluid density ρ and volume flux of moisture v, i.e. $M = \rho v$. Thus (8.1) and (8.2) gives us

$$\frac{\partial}{\partial t}(\rho\Theta) = \nabla(\rho\kappa\nabla\Phi). \tag{8.3}$$

Consider the relation $\Phi = \psi - z$ for the system in which flow takes place in the vertical downward direction only where ψ is the pressure potential [5]. The vertical downward direction is considered as the positive direction of z-axis. Considering only the one dimensional vertical flow for incompressible fluid, (8.3) becomes

$$\frac{\partial\Theta}{\partial t} = \frac{\partial}{\partial z}\left(\kappa\frac{\partial\psi}{\partial z}\right) - \frac{\partial\kappa}{\partial z}. \tag{8.4}$$

Consider that Θ and ψ are related by single valued function and assume that the soil water diffusivity as $D = \kappa \frac{\partial \psi}{\partial \Theta}$. Thus (8.4) reduces to

$$\frac{\partial \Theta}{\partial t} = \frac{\partial}{\partial z}\left(D\frac{\partial \Theta}{\partial z}\right) - \frac{\partial \kappa}{\partial z}. \tag{8.5}$$

This equation is known as Richard's equation [3, 8, 30, 48, 75] which is one of the most important equations expressing water content in unsaturated porous medium with various applications in soil science, hydrology and engineering.

8.3 Discussion

We consider three nonlinear forms of Richard's equation (8.5) for linear and nonlinear conductivity and diffusivity functions. We will focus on Brooks-Corey model, conductivity and diffusivity are assumed to be of the form, $\kappa = \kappa_0 \Theta^k$ and $D = D_0 \Theta^n$ with $k \geq 1,\ n \geq 0$ [17, 48, 90]. We used Brooks-Corey model [17, 48, 90] for the three cases as (i) Linear diffusivity and nonlinear conductivity (ii) Linear diffusivity and linear conductivity (iii) Nonlinear diffusivity and linear conductivity.

8.3.1 Linear diffusivity and nonlinear conductivity

For the case, consider the constant D as $D = D_0$ and the nonlinear conductivity is represented as $\kappa = \kappa_0 \Theta^2$, $\kappa_0 = \frac{D_0}{2L}$ [39]. Then (8.5) results

$$\frac{\partial \Theta}{\partial t} = D_0 \frac{\partial^2 \Theta}{\partial z^2} - \frac{D_0}{L}\Theta\frac{\partial \Theta}{\partial z}. \tag{8.6}$$

Using dimensionless variables,

$$Z = \frac{z}{L} \text{ and } T = \frac{tD_0}{L^2}$$

(8.6) reduces to the governing equation

$$\frac{\partial \Theta}{\partial T} = \frac{\partial^2 \Theta}{\partial Z^2} - \Theta \frac{\partial \Theta}{\partial Z}. \tag{8.7}$$

8.3.2 Linear diffusivity and linear conductivity

Assume the linear diffusivity D as $D = D_0\Theta$ and the linear conductivity is represented as $\kappa = \kappa_0\Theta$, $\kappa_0 = \frac{D_0}{2L}$ [39]. Then (8.5) becomes

$$\frac{\partial \Theta}{\partial t} = D_0\Theta \frac{\partial^2 \Theta}{\partial z^2} + D_0 \left\{ \frac{\partial \Theta}{\partial z} \right\}^2 - \frac{D_0}{2L} \frac{\partial \Theta}{\partial z}. \tag{8.8}$$

Using dimensionless variables,

$$Z = \frac{z}{L} \text{ and } T = \frac{tD_0}{L^2}$$

(8.8) gives us

$$\frac{\partial \Theta}{\partial T} = \Theta \frac{\partial^2 \Theta}{\partial Z^2} + \left\{ \frac{\partial \Theta}{\partial Z} \right\}^2 - \frac{1}{2} \frac{\partial \Theta}{\partial Z}. \tag{8.9}$$

8.3.3 Nonlinear diffusivity and linear conductivity

For this case, we have taken D as $D = D_0\Theta^2$ and the hydraulic conductivity is taken as $\kappa = \kappa_0\Theta$, $\kappa_0 = \frac{D_0}{2L}$ [39]. Then (8.5) reduces to

$$\frac{\partial \Theta}{\partial t} = D_0\Theta^2 \frac{\partial^2 \Theta}{\partial z^2} + 2D_0\Theta \left\{ \frac{\partial \Theta}{\partial z} \right\}^2 - \frac{D_0}{2L} \frac{\partial \Theta}{\partial z}. \tag{8.10}$$

Using dimensionless variables,

$$Z = \frac{z}{L} \text{ and } T = \frac{tD_0}{L^2}$$

(8.10) becomes

$$\frac{\partial \Theta}{\partial T} = \Theta^2 \frac{\partial^2 \Theta}{\partial Z^2} + 2\Theta \left\{ \frac{\partial \Theta}{\partial Z} \right\}^2 - \frac{1}{2} \frac{\partial \Theta}{\partial Z}. \tag{8.11}$$

The equations (8.7), (8.9) and (8.11) are solved with boundary conditions by homotopy analysis method. The solutions of these equations represent moisture content $\Theta(Z,T)$ of soil at a depth Z and time T. For definiteness of the physical problem, water will flow vertical downward direction and hence set of boundary conditions are given by

$$\Theta(0,T) = 0.01 \text{ and } \Theta(1,T) = 1. \tag{8.12}$$

8.4 Homotopy analysis method

Homotopy analysis method is used to solve the nonlinear differential equations. Many researchers have successfully employed this technique to solve different types of nonlinear ODEs and PDEs [18, 23, 29, 32, 33, 36, 37, 49, 59–61, 63, 64, 83]. Liao [32, 33, 36, 37] has discussed homotopy analysis solutions of nonlinear ordinary and partial differential equations, Darvishi and Khani [18] have discussed homotopy series solution of the foam drainage equation, Ghotbi *et al.* [23] have discussed an analytical approach of infiltration in unsaturated soils by HAM, Kheiri *et al.* [29] have obtained approximate solutions of modified Burgers-Korteweg-de Vries equation and the Newell -Whitehead equation by using HAM, Vajravelu and Van Gorder [83] have discussed solutions of nonlinear ordinary and partial differential equations by HAM, Patel and Desai [59–61, 63, 64] have discussed convergent solution of nonlinear partial differential equation arising in double phase flow through porous medium by HAM with the help of c_0-curve.

Let $\mathscr{N}[\phi(Z,T;q)] = 0$ denote a nonlinear partial differential equation, $\phi(Z,T;q)$ be an unknown function which represents Θ at depth Z for a given time T for $0 \leq q \leq 1$.

We use the linear operator $\mathscr{L}[\phi(Z,T;q)] = \frac{\partial^2 \phi(Z,T;q)}{\partial Z^2}$ and the initial approximation of $\Theta(Z,T)$ is $\Theta_0(Z,T) = (1+T)Z + 0.01(1-Z^2) - TZ^3$ which satisfy both boundary conditions.

The zeroth-order deformation equation [32] is constructed as

$$(1-q)\mathscr{L}[\phi(Z,T;q) - \Theta_0(Z,T)] = c_0 q H(Z,T)\mathscr{N}[\phi(Z,T;q)] \tag{8.13}$$

where $q \in [0,1]$ is the homotopy parameter, c_0 is a nonzero convergence control parameter and $H(Z,T)$ is a nonzero auxiliary function.

When $q = 0$ and $q = 1$, (8.13) gives us

$$\phi(Z,T;0) = \Theta_0(Z,T) \text{ and } \phi(Z,T;1) = \Theta(Z,T). \tag{8.14}$$

According to (8.14) as q increases from 0 to 1, $\phi(Z,T;q)$ continuously varies from $\Theta_0(Z,T)$ to $\Theta(Z,T)$. The solution is considered as

$$\phi(Z,T;q) = \Theta_0(Z,T) + \sum_{m=1}^{\infty} \Theta_m(Z,T) q^m \tag{8.15}$$

where

$$\Theta_m(Z,T) = \frac{1}{m!} \frac{\partial^m \phi(Z,T;q)}{\partial q^m}\bigg|_{q=0}. \tag{8.16}$$

The initial guess, the linear operator, the convergence control parameter and the auxiliary function are assumed in such a way that the series of $\phi(Z,T;q)$ with respect to q at $q = 1$

$$\Theta(Z,T) = \Theta_0(Z,T) + \sum_{m=1}^{\infty} \Theta_m(Z,T) \tag{8.17}$$

converges.

Define $\overrightarrow{\Theta_n} = \{\Theta_0(Z,T), \Theta_1(Z,T), \ldots, \Theta_n(Z,T)\}$. Differentiating the zeroth-order deformation equation (8.13) m times w.r.t. q and putting $q = 0$ and then finally dividing

them by $m!$, we have the high-order deformation equation

$$\mathscr{L}[\Theta_m(Z,T) - \chi_m \Theta_{m-1}(Z,T)] = c_0 H(Z,T) \mathscr{R}_m(\overrightarrow{\Theta_{m-1}}) \tag{8.18}$$

subject to

$$\Theta_m(0,T) = 0 \text{ and } \Theta_m(1,T) = 0,\ m \geq 1 \tag{8.19}$$

where χ_m is defined by (2.40) and

$$\mathscr{R}_m(\overrightarrow{\Theta_{m-1}}) = \frac{1}{(m-1)!} \frac{\partial^{m-1} \mathscr{N}[\phi(Z,T;q)]}{\partial q^{m-1}}\bigg|_{q=0},\ m \geq 1. \tag{8.20}$$

For simplicity, we assume that $H(Z,T) = 1$. Thus the solution of the high-order deformation equation (8.18) is

$$\Theta_m(Z,T) = \chi_m \Theta_{m-1}(Z,T) + c_0 \mathscr{L}^{-1}[\mathscr{R}_m(\overrightarrow{\Theta_{m-1}})] + C_1 Z + C_2 \tag{8.21}$$

where C_1 and C_2 are constants or functions of T. Hence the homotopy analysis solution can be expressed as

$$\Theta(Z,T) = \Theta_0(Z,T) + \Theta_1(Z,T) + \Theta_2(Z,T) + \cdots. \tag{8.22}$$

As discussed by many researchers [18, 23, 29, 33, 37, 49, 59–61, 63, 64, 83], the convergent homotopy series solution is strongly dependent on convergence control parameter c_0 which occurs in solution (8.22). The proper value of c_0 is chosen with the help of c_0-curve which is suggested by Liao [33].

8.4.1 Solution of equation for the linear diffusivity and nonlinear conductivity

According to (8.7), we define a nonlinear operator $\mathscr{N}$ as

$$\mathscr{N}[\phi(Z,T;q)] = \frac{\partial^2\phi(Z,T;q)}{\partial Z^2} - \phi(Z,T;q)\frac{\partial\phi(Z,T;q)}{\partial Z} - \frac{\partial\phi(Z,T;q)}{\partial T}. \tag{8.23}$$

Apply homotopy analysis method with above mentioned linear operator and initial approximation, we have (8.20) as

$$\mathscr{R}_m(\overrightarrow{\Theta_{m-1}}) = \frac{\partial^2\Theta_{m-1}}{\partial Z^2} - \sum_{i=0}^{m-1}\Theta_i\frac{\partial\Theta_{m-1-i}}{\partial Z} - \frac{\partial\Theta_{m-1}}{\partial T},\ m \geq 1 \tag{8.24}$$

and the solution (8.22) is of the form

$$\begin{aligned}\Theta(Z,T) = (1+T)Z + 0.01(1-Z^2) - TZ^3 + c_0\Big\{&0.29581Z - 0.015Z^2 \\ &- 0.3333Z^3 + 0.0025Z^4 + 0.04999Z^5 + 1.135TZ - 0.005TZ^2 \\ &- \frac{4TZ^3}{3} + 0.005TZ^4 + \frac{TZ^5}{5} - \frac{0.005TZ^6}{3} + \frac{4T^2Z}{105} - \frac{T^2Z^3}{6} \\ &+ \frac{T^2Z^5}{5} - \frac{T^2Z^7}{14}\Big\} + \cdots.\end{aligned} \tag{8.25}$$

Here the c_0-curves of $\Theta_Z(0.5,0.5)$ and $\Theta_Z(1,0)$ are used to choose proper value of c_0. Figure 8.2 represents the c_0-curves of $\Theta_Z(0.5,0.5)$ (DotDashed) and $\Theta_Z(1,0)$ (Thick) for 10th-order approximation which are plotted using Mathematica BVPh package [36]. The line segment almost parallel to horizontal axis gives valid interval of c_0 [33]. We chosen $c_0 = -0.5$ from valid range of c_0 (see figure 8.2).

The approximate analytical solution of (8.7) is expressed in the series form which represents the moisture content $\Theta(Z,T)$ of soil at depth Z for a given time T. The numerical representation of the solution is obtained using Mathematica coding [36]. Table 8.1 indicates the numerical values of $\Theta(Z,T)$.

The graphical representation of solution (8.25) is also obtained using Mathematica coding [36]. Figure 8.3 represents the graph of $\Theta(Z,T)$ versus depth Z and time T.

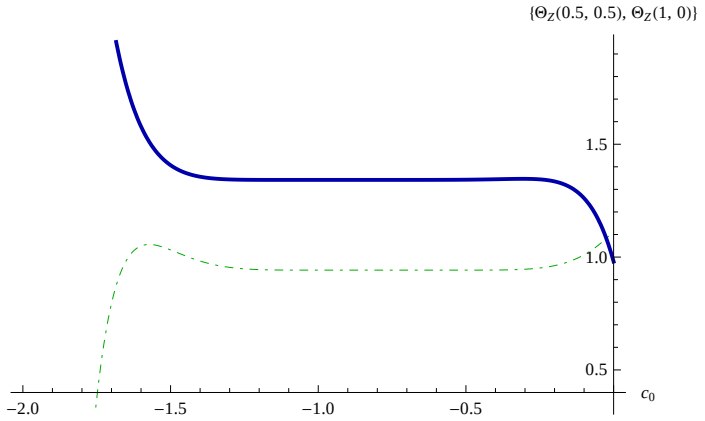

FIGURE 8.2: The c_0-curves of $\Theta_Z(0.5,0.5)$ (DotDashed) and $\Theta_Z(1,0)$ (Thick).

TABLE 8.1: Numerical values of the moisture content Θ.

T	Depth Z										
	0.0	0.1	0.2	0.3	0.4	0.5	0.6	0.7	0.8	0.9	1.0
0.1	0.01000	0.09433	0.17946	0.26614	0.35517	0.44743	0.54394	0.64587	0.75463	0.87196	1.00000
0.2	0.01000	0.09433	0.17946	0.26614	0.35517	0.44744	0.54395	0.64589	0.75465	0.87197	1.00000
0.3	0.01000	0.09433	0.17946	0.26614	0.35518	0.44745	0.54397	0.64590	0.75467	0.87199	1.00000
0.4	0.01000	0.09433	0.17947	0.26615	0.35519	0.44747	0.54399	0.64592	0.75469	0.87200	1.00000
0.5	0.01000	0.09434	0.17948	0.26617	0.35521	0.44749	0.54400	0.64594	0.75470	0.87201	1.00000
0.6	0.01000	0.09434	0.17949	0.26619	0.35523	0.44751	0.54403	0.64596	0.75472	0.87202	1.00000
0.7	0.01000	0.09435	0.17951	0.26621	0.35526	0.44753	0.54405	0.64598	0.75473	0.87203	1.00000
0.8	0.01000	0.09436	0.17953	0.26623	0.35529	0.44756	0.54407	0.64600	0.75474	0.87204	1.00000
0.9	0.01000	0.09438	0.17955	0.26626	0.35532	0.44759	0.54410	0.64601	0.75475	0.87205	1.00000
1.0	0.01000	0.09439	0.17958	0.26630	0.35536	0.44763	0.54413	0.64603	0.75476	0.87205	1.00000

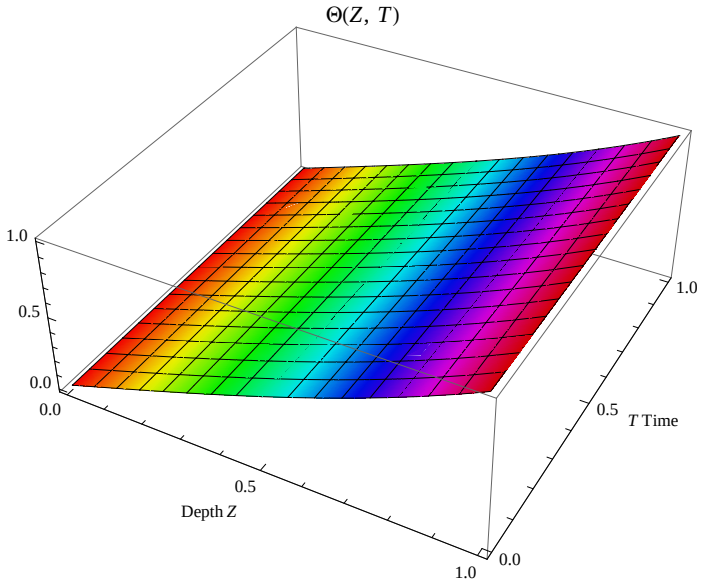

FIGURE 8.3: Graph of $\Theta(Z,T)$ versus Z and T.

8.4.2 Solution of equation for the linear diffusivity and linear conductivity

Apply homotopy analysis method to nonlinear partial differential equation (8.9) with nonlinear operator

$$\mathscr{N}[\phi(Z,T;q)] = \phi(Z,T;q)\frac{\partial^2\phi(Z,T;q)}{\partial Z^2} + \left\{\frac{\partial\phi(Z,T;q)}{\partial Z}\right\}^2 - \frac{1}{2}\frac{\partial\phi(Z,T;q)}{\partial Z} - \frac{\partial\phi(Z,T;q)}{\partial T}. \tag{8.26}$$

Then (8.20) becomes

$$\mathscr{R}_m(\overrightarrow{\Theta_{m-1}}) = \sum_{i=0}^{m-1}\Theta_i\frac{\partial^2\Theta_{m-1-i}}{\partial Z^2} - \sum_{i=0}^{m-1}\frac{\partial\Theta_i}{\partial Z}\frac{\partial\Theta_{m-1-i}}{\partial Z} - \frac{1}{2}\frac{\partial\Theta_{m-1}}{\partial Z} - \frac{\partial\Theta_{m-1}}{\partial T},\ m \geq 1 \tag{8.27}$$

and the homotopy analysis solution of (8.9) is

$$\begin{aligned}\Theta(Z,T) = (1+T)Z + 0.01(1-Z^2) - TZ^3 + c_0\Big\{ &-0.12495Z + 0.2499Z^2 \\ &- 0.175Z^3 + 0.00005Z^4 + 0.05Z^5 + 0.135TZ + 0.75TZ^2 - 0.02TZ^3 \\ &- 0.875TZ^4 + 0.01TZ^5 + 0.5T^2Z^2 - T^2Z^4 + 0.5T^2Z^6\Big\} + \cdots\end{aligned} \tag{8.28}$$

which gives the moisture content at depth Z for time T.

Using Mathematica, we plotted the c_0-curves of $\Theta_Z(0.5,0.5)$ (DotDashed) and $\Theta_Z(1,0)$ (Thick) (see figure 8.4) and the proper value of $c_0 = -0.5$ is chosen from this c_0-curve.

The numerical values of solution are given in table 8.2 and graphical interpretation is obtained (see figure 8.5). Figure 8.5 presents the graph of $\Theta(Z,T)$ versus depth Z and time T.

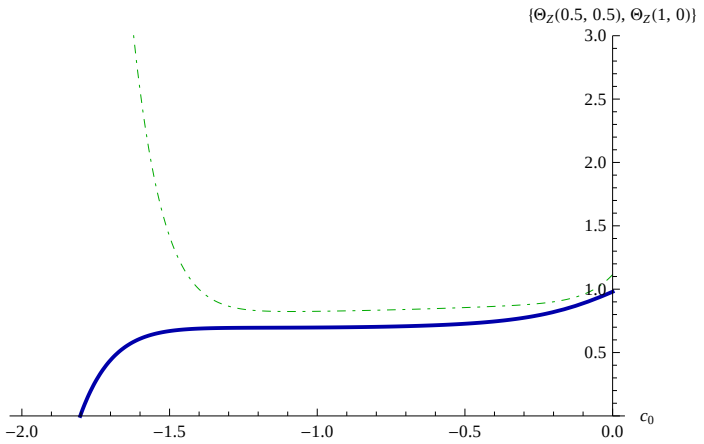

FIGURE 8.4: The c_0-curves of $\Theta_Z(0.5,0.5)$ (DotDashed) and $\Theta_Z(1,0)$ (Thick).

TABLE 8.2: Numerical values of the moisture content Θ.

T	Depth Z										
	0.0	0.1	0.2	0.3	0.4	0.5	0.6	0.7	0.8	0.9	1.0
0.1	0.01000	0.17640	0.30690	0.41732	0.51574	0.60640	0.69164	0.77285	0.85093	0.92650	1.00000
0.2	0.01000	0.18033	0.31083	0.42024	0.51767	0.60760	0.69238	0.77331	0.85122	0.92665	1.00000
0.3	0.01000	0.18412	0.31459	0.42315	0.51974	0.60903	0.69333	0.77392	0.85158	0.92681	1.00000
0.4	0.01000	0.18778	0.31822	0.42605	0.52194	0.61065	0.69448	0.77468	0.85201	0.92700	1.00000
0.5	0.01000	0.19133	0.32174	0.42896	0.52426	0.61244	0.69578	0.77555	0.85252	0.92720	1.00000
0.6	0.01000	0.19477	0.32516	0.43188	0.52668	0.61437	0.69724	0.77654	0.85308	0.92742	1.00000
0.7	0.01000	0.19811	0.32850	0.43481	0.52919	0.61643	0.69882	0.77763	0.85371	0.92767	1.00000
0.8	0.01000	0.20135	0.33176	0.43775	0.53177	0.61861	0.70052	0.77882	0.85439	0.92792	1.00000
0.9	0.01000	0.20451	0.33496	0.44071	0.53443	0.62088	0.70232	0.78009	0.85512	0.92820	1.00000
1.0	0.01000	0.20758	0.33811	0.44368	0.53715	0.62324	0.70421	0.78143	0.85590	0.92849	1.00000

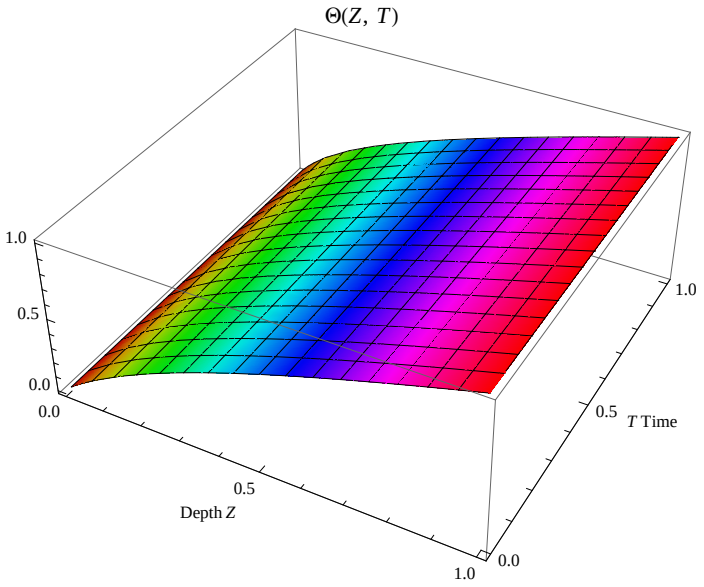

FIGURE 8.5: Graph of $\Theta(Z,T)$ versus Z and T.

8.4.3 Solution of equation for the nonlinear diffusivity and linear conductivity

Consider the nonlinear operator $\mathscr{N}$ from (8.11) as

$$\mathscr{N}[\phi(Z,T;q)] = \phi(Z,T;q)^2\frac{\partial^2\phi(Z,T;q)}{\partial Z^2} + 2\phi(Z,T;q)\left\{\frac{\partial\phi(Z,T;q)}{\partial Z}\right\}^2 - \frac{1}{2}\frac{\partial\phi(Z,T;q)}{\partial Z} - \frac{\partial\phi(Z,T;q)}{\partial T}. \tag{8.29}$$

Using (8.29) in (8.20), we get

$$\mathscr{R}_m(\overrightarrow{\Theta_{m-1}}) = \sum_{j=0}^{m-1}\Theta_j\sum_{i=0}^{m-1-j}\Theta_i\frac{\partial^2\Theta_{m-1-j-i}}{\partial Z^2} - 2\sum_{j=0}^{m-1}\Theta_j\sum_{i=0}^{m-1-j}\frac{\partial\Theta_i}{\partial Z}\frac{\partial\Theta_{m-1-j-i}}{\partial Z} - \frac{1}{2}\frac{\partial\Theta_{m-1}}{\partial Z} - \frac{\partial\Theta_{m-1}}{\partial T},\ m \geq 1 \tag{8.30}$$

and (8.22) gives us the homotopy analysis solution of (8.11) as

$$\begin{aligned}\Theta(Z,T) = {} & (1+T)Z + 0.01(1-Z^2) - TZ^3 + c_0\Big\{0.031767Z - 0.240001Z^2 \\ & + \frac{0.5044Z^3}{3} - 0.009999Z^4 + 0.0501Z^5 - \frac{0.000001Z^6}{3} + 0.1251TZ \\ & - 0.23TZ^2 + 0.9997TZ^3 + 0.085TZ^4 - 0.9997TZ^5 + 0.02TZ^6 \\ & - 0.0001TZ^7 + 0.01T^2Z^2 + T^2Z^3 - 0.03T^2Z^4 - 2T^2Z^5 + 0.03T^2Z^6 \\ & + T^2Z^7 - 0.01T^2Z^8 + \frac{T^3Z^3}{3} - T^3Z^5 + T^3Z^7 - \frac{T^3Z^9}{3}\Big\} + \cdots.\end{aligned} \tag{8.31}$$

The convergent homotopy analysis solution is obtained using the proper value of c_0. We plotted the c_0-curves of $\Theta_Z(0.5,0.5)$ (DotDashed) and $\Theta_Z(1,0)$ (Thick) in figure 8.6. The proper value of $c_0 = -0.5$ is chosen for numerical and graphical representations of solution.

The numerical values of the moisture content are given in table 8.3. In the figure 8.7, the graph of $\Theta(Z,T)$ versus depth Z and time T is presented.

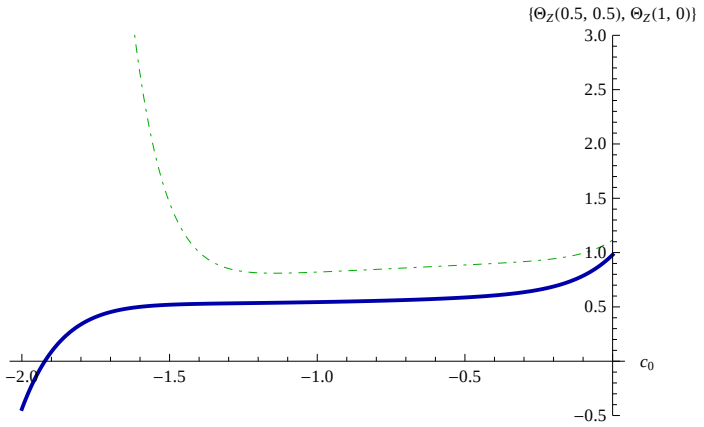

FIGURE 8.6: The c_0-curves of $\Theta_Z(0.5,0.5)$ (DotDashed) and $\Theta_Z(1,0)$ (Thick).

TABLE 8.3: Numerical values of the moisture content Θ.

T	Depth Z										
	0.0	0.1	0.2	0.3	0.4	0.5	0.6	0.7	0.8	0.9	1.0
0.1	0.01000	0.12580	0.25712	0.39116	0.51643	0.62666	0.72116	0.80265	0.87461	0.93981	1.00000
0.2	0.01000	0.13388	0.27120	0.40647	0.52880	0.63465	0.72559	0.80498	0.87586	0.94040	1.00000
0.3	0.01000	0.14194	0.28480	0.42071	0.54007	0.64204	0.72996	0.80745	0.87720	0.94098	1.00000
0.4	0.01000	0.14994	0.29789	0.43396	0.55038	0.64899	0.73431	0.81004	0.87860	0.94157	1.00000
0.5	0.01000	0.15788	0.31047	0.44628	0.55990	0.65558	0.73864	0.81272	0.88007	0.94216	1.00000
0.6	0.01000	0.16575	0.32253	0.45775	0.56877	0.66191	0.74297	0.81547	0.88159	0.94277	1.00000
0.7	0.01000	0.17355	0.33408	0.46845	0.57709	0.66803	0.74728	0.81829	0.88316	0.94338	1.00000
0.8	0.01000	0.18125	0.34513	0.47848	0.58496	0.67398	0.75159	0.82115	0.88478	0.94400	1.00000
0.9	0.01000	0.18886	0.35568	0.48790	0.59245	0.67978	0.75588	0.82406	0.88643	0.94463	1.00000
1.0	0.01000	0.19637	0.36576	0.49678	0.59963	0.68546	0.76016	0.82699	0.88812	0.94527	1.00000

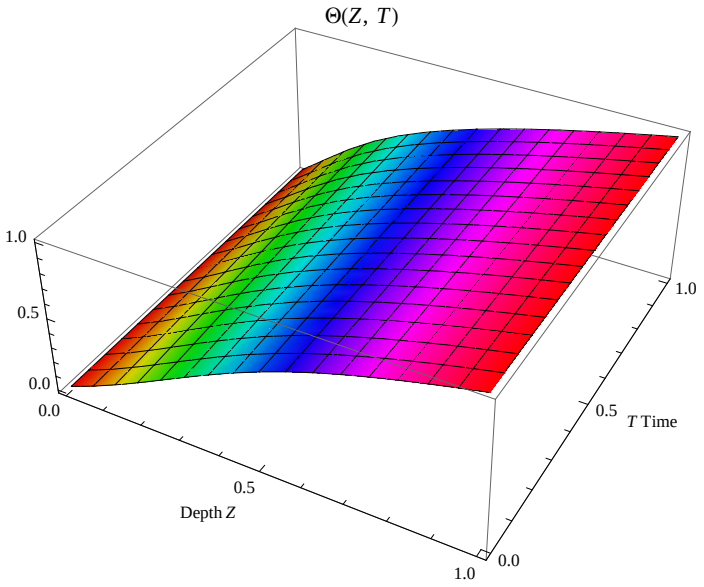

FIGURE 8.7: Graph of $\Theta(Z,T)$ versus Z and T.

8.5 Conclusion

Here we have discussed the one dimensional groundwater recharge by spreading through unsaturated porous medium. The homotopy analysis method is adopted to solve the governing equations. The series solutions are obtained for the equations which presented on the basis of linear and nonlinear conductivity and diffusivity functions. The solutions are satisfy both boundary conditions. The numerical and graphical representations of solutions are given. Moisture content of soil increases when depth increases for a given time.

References

[1] S Abbasbandy and E Shivanian, Solution of singular linear vibrational BVPs by the homotopy analysis method, *Journal of Numerical Mathematics and Stochastics*, **1(1)**, (2009), 77–84.

[2] S Abbasbandy, E Shivanian and K Vajravelu, Mathematical properties of $\hbar$-curve in the frame work of the homotopy analysis method, *Communications in Nonlinear Science and Numerical Simulation*, **16(11)**, (2011), 4268–4275.

[3] M B Allan, Numerical modeling of multiphase flow in porous media, *Advances in Water Resources*, **8(4)**, (1985), 162–187.

[4] A C Banerji and K M Srivastava, Radial oscillations of variable magnetic star and the origin of the planetary system, vol. 33(A), Proceedings of the National Academy of Sciences, India (1963), 125–148.

[5] J Bear, Dynamics of fluids in porous media, American Elsevier Publishing Company, Inc., New York (1972).

[6] J Bear and Y Bachmat, Introduction to modeling of transport phenomena in porous media, Kluwer Academic Publishers, Dordrecht, Netherlands (1990).

[7] J Bear, C Braester and P Menier, Effective and relative permeabilities of anisotropic porous-media, *Transport in Porous Media*, **2**, (1987), 301–316.

[8] J Bear and A H D Cheng, Modeling groundwater flow and contaminant transport: Theory and applications of transport in porous media, Springer Dordrecht, Heidelberg, London, New York (2010).

[9] P M Blair, Calculation of oil displacement by countercurrent water imbibition, *Society of Petroleum Engineers*, **4(3)**, (1964), 195–202.

[10] R N Borana, V H Pradhan and M N Mehta, Numerical solution of Boussinesq equation arising in one dimensional infiltration phenomenon by using finite difference method, *International Journal of Research in Engineering and Technology*, **2(8)**, (2013), 202–209.

[11] B J Bourblaux and F J Kalaydjian, Experimental study of cocurrent and countercurrent flows in natural porous media, *Society of Petroleaum Engineers*, **5(3)**, (1990), 361–368.

[12] J Boussinesq, Recherches théoriques sur l'écoulement des nappes d'eau infiltrées dans le sol et sur le débit des sources, *Journal de Mathématiques Pures et Appliquées*, **10**, (1904), 5–78.

[13] I Brailovsky, A Babchin, M Frankel and G Sivashinsky, Fingering instabilities in water-oil displacement, *Transport in Porous Media*, **63**, (2006), 363–380.

[14] E R Brownscobe and A B Dyes, A water imbibition displacement - A possibility for the spraberry, American Petroleum Institute (1952), 383–390.

[15] S S Chavan and M M Panchal, Solution of porous medium equation arising in fluid flow through porous media by homotopy perturbation method using Elzaki transform, *International Journal of Futuristic Trends in Engineering and Technology*, **1(10)**, (2014), 32–35.

[16] Z Cheng, Reservoir simulation: Mathematical techniques in oil recovery, Society for Industrial and Applied Mathematics, Philadelphia (2007).

[17] A T Corey, Mechanics of immiscible fluids in porous media, Water Resources Publications, Littleton, Colorado (1994).

[18] M T Darvishi and F Khani, A series solution of the foam drainage equation, *Computers and Mathematics with Applications*, **58**, (2009), 360–368.

[19] N B Desai, The study of problems arises in single phase and multiphase flow through porous media, Ph.D. thesis, South Gujarat University, Surat, India (2002).

[20] N B Desai, Similarity solution of nonlinear Boussinesq's equation arising in infiltration of incompressible fluid flow, *International Journals of Advanced Research in Computer Science and Software Engineering*, **7(6)**, (2017), 59–67.

[21] M A Fariborzi Araghi and S Naghshband, On convergence of homotopy analysis method to solve the Schrodinger equation with a power law nonlinearity, *International Journal of Industrial Mathematics*, **5(4)**, (2013), 367–374.

[22] H Fazeli, R Fathi and A Atashdehghan, Application of homotopy perturbation method to nonlinear equations describing cocurrent and countercurrent imbibition in fractured porous media, *Journal of Chemical and Petroleum Engineering*, **46(1)**, (2012), 13–29.

[23] A R Ghotbi, M Omidvar and A Barari, Infiltration in unsaturated soils - An analytical approach, *Computers and Geotechnics*, **38**, (2011), 777–782.

[24] J W Graham and J G Richardson, Theory and application of imbibition phenomena in recovery of oil, *Society of Petroleum Engineers*, **11(2)**, (1959), 65–69.

[25] O S Iyiola and S B Folarin, Approximate analytical study of fingero-imbibition phenomena of time-fractional type in double phase flow through porous media, *European Journal of Pure and Applied Mathematics*, **7(2)**, (2014), 210–229.

[26] M S Joshi, N B Desai and M N Mehta, An analytic solution of instability phenomenon arising in fluid flow through homogenous porous media, *International Journal of Applied Mathematics and Mechanics*, **6(16)**, (2010), 93–102.

[27] M S Joshi, N B Desai and M N Mehta, One dimensional and unsaturated fluid flow through porous media, *International Journal of Applied Mathematics and Mechanics*, **6(18)**, (2010), 66–79.

[28] M S Joshi, N B Desai and M N Mehta, An analytical solution of countercurrent imbibition phenomenon arising in fluid flow through homogeneous porous media, *International Journal of Applied Mathematics and Mechanics*, **7(11)**, (2011), 21–32.

[29] H Kheiri, N Alipour and R Dehghani, Homotopy analysis and homotopy pade methods for the modified Burgers-Korteweg-de Vries and the Newell -Whitehead equations, *Mathematical Sciences*, **5(1)**, (2011), 33–50.

[30] A Klute, A numerical method for solving the flow equation for water in unsaturated materials, *Soil Science*, **73(2)**, (1952), 105–116.

[31] M C Leverett, Capillary behavior in porous solids, *Transactions of the AIME*, **142**, (1941), 152–169.

[32] S J Liao, The proposed homotopy analysis technique for the solution of nonlinear problems, Ph.D. thesis, Shanghai Jiao Tong University, Shanghai, China (1992).

[33] S J Liao, Beyond perturbation: Introduction to the homotopy analysis method, Chapman and Hall/CRC Press, Boca Raton (2003).

[34] S J Liao, An analytic solution of unsteady boundary-layer flows caused by an impulsively stretching plate, *Communications in Nonlinear Science and Numerical Simulation*, **11(3)**, (2006), 326–339.

[35] S J Liao, Notes on the homotopy analysis method: Some definitions and theorems, *Communications in Nonlinear Science and Numerical Simulation*, **14**, (2009), 983–997.

[36] S J Liao, Homotopy analysis method in nonlinear differential equations, Higher Education Press, Beijing and Springer-Verlag Berlin Heidelberg (2012).

[37] S J Liao, Advances in the homotopy analysis method, World Scientific, Singapore (2013).

[38] D B Mcwhorter and D K Sunada, Exact integral solutions for two-phase flow, *Water Resources Research*, **26(3)**, (1990), 399–413.

[39] M N Mehta, A singular perturbation solution of one-dimensional flow in unsaturated porous media with small diffusivity coefficient, Proceeding of the National Conference on Fluid Mechanics and Fluid Power (1975), E1–E4.

[40] M N Mehta, Asymptotic expansions of fluid flow through porous media, Ph.D. thesis, South Gujarat University, Surat, India (1977).

[41] M N Mehta and M S Joshi, Solution by group invariant method of instability phenomenon arising in fluid flow through porous media, *International Journal of Engineering Research and Industrial Applications*, **2(1)**, (2009), 35–48.

[42] M N Mehta and T R Patel, A solution of the Burger's equation type one dimensional ground water recharge by spreading in porous media, *Journal of the Indian Academy of Mathematics*, **28(1)**, (2006), 25–32.

[43] M N Mehta and A P Verma, A singular perturbation solution of double phase flow due to differential wettability, *Indian Journal of Pure and Applied Mathematics*, **8(5)**, (1977), 523–526.

[44] M N Mehta and A P Verma, Composite expansion solution of fingero-imbibition in double phase flow through underground porous medium, vol. 87(2), Proceedings of the Indian Academy of Sciences-Mathematical Sciences, Springer Netherlands (1978), 65–70.

[45] S K Mishra and A P Verma, Imbibition in the flow of two immiscible fluids with magnetic field, *The Physics of fluids*, **17(6)**, (1974), 1338–1340.

[46] B Mukherjee and P Shome, An analytic solution of fingering phenomenon arising in fluid flow through porous media by using techniques of calculus of variation and similarity theory, *Journal of Mathematics Research*, **1(2)**, (2009), 1338–1340.

[47] M Muskat, The flow of homogeneous fluids through porous media, 1st ed., McGraw-Hill Book Company, Inc., New York and London (1937).

[48] M Nasseri, Y Daneshbod, M D Pirouz, G R Rakhshandehroo and A Shirzad, New analytical solution to water content simulation in porous media, *Journal of Irrigation and Drainage Engineering*, **138(4)**, (2012), 328–335.

[49] Z M Odibat, A study on the convergence of homotopy analysis method, *Applied Mathematics and Computation*, **217**, (2010), 782–789.

[50] A K Parikh, Numerical solution of Boussinesq's equation in groundwater infiltration phenomenon by differential quadrature method, *Paripex - Indian Journal of Research*, **4(6)**, (2015), 165–167.

[51] A K Parikh, M N Mehta and V H Pradhan, Mathematical model and analysis of countercurrent imbibition in vertical downward homogeneous porous media, *British Journal of Mathematics & Computer Science*, **3(4)**, (2013), 478–489.

[52] A K Parikh, M N Mehta and V H Pradhan, Mathematical modeling and analysis of fingero-imbibition phenomenon in vertical downward cylindrical homogeneous porous matrix, Nirma University International Conference on Engineering, Ahmedabad, India (2013).

[53] A K Parikh, M N Mehta and V H Pradhan, Mathematical modeling and analysis of fingero-imbibition phenomenon in homogeneous porous medium with magnetic field effect in vertical downward direction, *International Journal of Latest Technology in Engineering, Management & Applied Science*, **3(10)**, (2014), 17–23.

[54] M Paripour, E Babolian and J Saeidian, Analytic solutions to diffusion equations, *Mathematical and Computer Modelling*, **51**, (2010), 649–657.

[55] D M Patel, The classical solution approach of problems arising in fluid flow through porous media, Ph.D. thesis, South Gujarat University, Surat, India (1998).

[56] K K Patel, M N Mehta and T R Singh, A solution of Boussinesq's equation for infiltration phenomenon in unsaturated porous media by homotopy analysis method, *IOSR Journal of Engineering*, **4(2)**, (2014), 1–8.

[57] K R Patel, M N Mehta and T R Patel, Power series solution of fingero-imbibition in double phase flow through homogeneous porous media, *International Journal of Applied Mathematics and Mechanics*, **7(8)**, (2011), 65–77.

[58] K R Patel, M N Mehta and T R Patel, A mathematical model of imbibition phenomenon in heterogeneous porous media during secondary oil recovery process, *Applied Mathematical Modelling*, **37**, (2013), 2933–2942.

[59] M A Patel and N B Desai, Homotopy analysis solution of countercurrent imbibition phenomenon in inclined homogeneous porous medium, *Global Journal of Pure and Applied Mathematics*, **12(1)**, (2016), 1035–1052.

[60] M A Patel and N B Desai, An approximate analytical solution of the Burger's equation for longitudinal dispersion phenomenon arising in fluid flow through porous medium, *International Journal on Recent and Innovation Trends in Computing and Communication*, **5(5)**, (2017), 1103–1107.

[61] M A Patel and N B Desai, Homotopy analysis method for fingero-imbibition phenomenon in heterogeneous porous medium, *Nonlinear Science Letters A: Mathematics, Physics and Mechanics*, **8(1)**, (2017), 90–100.

[62] M A Patel and N B Desai, Homotopy analysis method for nonlinear partial differential equation arising in fluid flow through porous medium, *International Journal of Computer & Mathematical Sciences*, **6(5)**, (2017), 14–18.

[63] M A Patel and N B Desai, A mathematical model of cocurrent imbibition phenomenon in inclined homogeneous porous medium, vol. 2, Kalpa Publications in Computing, ICRISET2017, Selected Papers in Computing (2017), 51–61.

[64] M A Patel and N B Desai, Mathematical modelling and analysis of cocurrent imbibition phenomenon in inclined heterogeneous porous medium, *International Journal of Computational and Applied Mathematics*, **12(3)**, (2017), 639–652.

[65] M A Patel and N B Desai, Mathematical modelling of fingero-imbibition phenomenon in heterogeneous porous medium with magnetic field effect, *PRAJNA - Journal of Pure and Applied Sciences*, **24-25**, (2017), 15–22.

[66] P S Patel, K A Patel and P H Bhathawala, Numerical solutions of fingero-imbibition in a slightly dipping porous media involving magnetic fluid, *IOSR Journal of Mathematics*, **12(3)**, (2016), 49–53.

[67] D W Peaceman, Fundamentals of numerical reservoir simulation, Elsevier Scientific Publishing Company, New York (1977).

[68] J R Philip, The theory of infiltration: 1. The infiltration equation and its solution, *Soil science*, **83(5)**, (1957), 345–358.

[69] P Y Polubarinova-Kochina, Theory of ground water movement, Princeton University Press, Princeton (1962).

[70] M Pooladi-Darvish and A Firoozabadi, Cocurrent and countercurrent imbibition in a water-wet matrix block, *Society of Petroleaum Engineers*, **5(1)**, (2000), 3–11.

[71] A Posadas, R Quiroz, A Tannus, S Crestana and C M Vaz, Characterizing water fingering phenomena in soils using magnetic resonance imaging and multifractal theory, *Nonlinear Processes in Geophysics*, **16**, (2009), 159–168.

[72] V H Pradhan, M N Mehta and T R Patel, A numerical solution of nonlinear equation representing one dimensional instability phenomena in porous media by finite element technique, *International Journal of Advanced Engineering Technology*, **2(1)**, (2011), 221–227.

[73] V H Pradhan and A P Verma, Finite element treatment of imbibition phenomenon involving magnetic fluid, *Indian Journal of Engineering and Materials Sciences*, **5**, (1998), 465–468.

[74] K Prasad, M M Kumar and M Sekhar, Modeling flow through unsaturated zone: Sensitivity to unsaturated soil properties, *Sadhana*, **26(6)**, (2001), 517–528.

[75] L A Richards, Capillary conduction of liquids through porous mediums, *Physics*, **1**, (1931), 318–333.

[76] J Saeidian and S Javadi, Some notes on the convergence control parameter in the framework of the homotopy analysis method, *Journal of Mathematics and Computer Science*, **9**, (2014), 103–110.

[77] A E Scheidegger, The physics of flow through porous media, Revised edition, University of Toronto Press, Toronto (1960).

[78] A E Scheidegger and E F Johnson, The statistically behaviour of instabilities in displacement process in porous media, *Canadian Journal of Physics*, **39(2)**, (1961), 326–334.

[79] R C Shah and A P Verma, Fingero-imbibition phenomenon through porous media with magnetic fluid, *Indian Journal of Engineering and Materials Sciences*, **5**, (1998), 411–415.

[80] R Srivastava and T C J Yeh, Analytical solutions for one-dimensional, transient infiltration toward the water table in homogeneous and layered soils, *Water Resources Research*, **27(5)**, (1991), 753–762.

[81] Z Tavassoli, R W Zimmerman and M J Blunt, Analysis of countercurrent imbibition with gravity in weakly water-wet systems, *Journal of Petroleum Science and Engineering*, **48(1-2)**, (2005), 94–104.

[82] B P Tullis and S J Wright, Wetting front instabilities: a three dimensional experimental investigation, *Transport in Porous Media*, **70**, (2007), 335–353.

[83] K Vajravelu and R A Van Gorder, Nonlinear flow phenomena and homotopy analysis: Fluid flow and Heat transfer, Higher Education Press, Beijing and Springer-Verlag Berlin Heidelberg (2012).

[84] J L Vázquez, The porous medium equation: Mathematical theory, Oxford University Press, USA (2007).

[85] A P Verma, The laplace transform solution of a one dimensional groundwater recharge by spreading, *Annals of Geophysics*, **22(1)**, (1969), 25–31.

[86] A P Verma, Statistical behaviour of fingering in a displacement process in heterogeneous porous medium with capillary pressure, *Canadian Journal of Physics*, **47(3)**, (1969), 319–324.

[87] A P Verma, Fingero-imbibition in artificial replenishment ground water through cracked porous medium, *Water Resources Research*, **6(3)**, (1970), 906–911.

[88] A P Verma, Instabilities in two phase flow through porous media with magnetic field, *Multiphase transport: Fundamentals, Reactor Safety, Applications (Ed. T. N. Veziroglu), Hemisphere Publication Corporation, Washington*, **3**, (1980), 1323–1335.

[89] T P Witelski, Horizontal infiltration into wet soil, *Water Resources Research*, **34(7)**, (1998), 1859–1863.

[90] T P Witelski, Motion of wetting fronts moving into partially pre-wet soil, *Advances in Water Resources*, **28**, (2005), 1133–1141.

[91] R Wojnar, Boussinesq equation for flow in an aquifer with time dependent porosity, *Bulletin of Polish Academy of Sciences: Technical Sciences*, **58(1)**, (2010), 165–170.

[92] S R Yadav and M N Mehta, Mathematical model and similarity solution of countercurrent imbibition phenomenon in banded porous matrix, *International Journal of Applied Mathematics and Mechanics*, **5(5)**, (2009), 76–86.

[93] S R Yadav and M N Mehta, Analytical approximate expression for cocurrent imbibition during immiscible two-phase flow through porous media, *Mathematical Problems in Engineering*, (2014), 1–6.

List of Publications

List of Publications

1. An approximate analytical solution of nonlinear differential equation arising in fluid flow through homogeneous porous media, *International Journal of Innovative Research in Science, Engineering and Technology*, 4(8), (2015), 7655-7662.
2. Homotopy analysis solution of countercurrent imbibition phenomenon in inclined homogeneous porous medium, *Global Journal of Pure and Applied Mathematics*, 12(1), (2016), 1035-1052.
3. Homotopy analysis method for fingero-imbibition phenomenon in heterogeneous porous medium, *Nonlinear Science Letters A: Mathematics, Physics and Mechanics*, 8(1), (2017), 90-100.
4. Homotopy analysis method for nonlinear partial differential equation arising in fluid flow through porous medium, *International Journal of Computer & Mathematical Sciences*, 6(5) (2017), 14-18.
5. Mathematical modelling and analysis of cocurrent imbibition phenomenon in inclined heterogeneous porous medium, *International Journal of Computational and Applied Mathematics*, 12(3) (2017), 639-652.
6. An approximate analytical solution of the Burger's equation for longitudinal dispersion phenomenon arising in fluid flow through porous medium, *International Journal on Recent and Innovation Trends in Computing and Communication*, 5(5) (2017), 1103-1107.
7. Mathematical modelling of fingero-imbibition phenomenon in heterogeneous porous medium with magnetic field effect, *PRAJNA - Journal of Pure and Applied Sciences*, 24-25 (2017), 15-22.
8. An approximate analytical solution of Boussinesq's equation for infiltration phenomenon in unsaturated porous medium, *International Journal of Mathematics And Its Applications*, 6(1-C) (2018), 463-470.

Details of the Work Accepted

1. An approximate analytical solution of one-dimensional groundwater recharge by spreading, *TWMS Journal of Applied and Engineering Mathematics*.

Details of the Work Presented in Conference

1. The paper entitled as "A mathematical model of cocurrent imbibition phenomenon in inclined homogeneous porous medium" presented in *ICRISET2017* at B. V. M. Engineering College, V. V. Nagar, Anand (Gujarat) on 17^{th} February, 2017 and published in Kalpa Publications in Computing, ICRISET2017, Selected Papers in Computing, 2, (2017), 51-61.

Global Journal of Pure and Applied Mathematics.
ISSN 0973-1768 Volume 12, Number 1 (2016), pp. 1035-1052

http://www.ripublication.com/gjpam.htm

Homotopy Analysis Solution of Countercurrent Imbibition Phenomenon in Inclined Homogeneous Porous Medium

Mahendra A. Patel

Assistant Professor,
Government Engineering College,
Gandhinagar-382028, Gujarat (INDIA).

N. B. Desai

Head, Department of Mathematics,
A. D. Patel Institute of Technology,
New V. V. Nagar-388121, Gujarat (INDIA).

Abstract

In this paper, the mathematical model is developed for the problem of countercurrent imbibition phenomenon occurring in inclined oil formatted homogeneous porous medium. During the secondary oil recovery process, when the water is injected in inclined homogeneous porous medium, at the common interface the countercurrent imbibition phenomenon occurs due to the difference of wetting abilities of water and oil. The mathematical formulation leads to one dimensional nonlinear partial differential equation. The homotopy analysis method has been applied to solve nonlinear partial differential equation using appropriate initial and boundary conditions. The c_0-curves are obtained using Mathematica software.

AMS subject classification:
Keywords: Countercurrent Imbibition phenomenon, Fluid flow, Porous medium, Homotopy Analysis Method, The c_0-curve.

1. Introduction

Spontaneous imbibition is the process in which the wetting phase is drawn into a porous medium by means of capillary pressures and the curved interfaces between the wetting and non-wetting phase without any external force. There are two types of spontaneous imbibition: (1) Cocurrent (2) Countercurrent. In the cocurrent imbibition both wetting and non-wetting phases move in the same direction while during countercurrent imbibition both move in the opposite directions.

When a porous medium filled with non-wetting fluid is brought into contact with wetting fluid, then there is a spontaneous flow of the wetting fluid into the medium and a counter flow of the non-wetting fluid from the medium. This phenomenon occurs due to the difference of wetting abilities of the fluids is called countercurrent imbibition phenomenon.

The imbibition phenomenon has been investigated by many researchers such as Brownscombe and Dyes [7], Scheidegger [26], Blair [5], Verma [30], Graham and Richardson [10], Mehta and Verma [19], Tavassoli, Zimmerman and Blunt [28]. Many researchers have discussed this phenomenon with different point of views. Blair [5] has found the numerical solution of the imbibition of water and the countercurrent flow of oil in porous rocks. Bourblaux and Kalaydjian [6] have discussed experimental study of cocurrent and countercurrent flows in natural porous media. Pooladi-Darvish and Firoozabadi [24] have discussed the similarities and differences of cocurrent and countercurrent imbibition and pointed out the consequences for practical applications. Mehta [20] has discussed analytically the phenomenon of imbibition in porous media using a singular perturbation method. Yadav and Mehta [31] have discussed the mathematical model and similarity solution of countercurrent imbibition phenomenon in banded Porous matrix.Joshi, Desai and Mehta [11] have described an analytical solution of the countercurrent imbibition phenomenon arising in the fluid flow through homogeneous porous media. Parikh, Mehta and Pradhan [22] have discussed the mathematical model and analysis of countercurrent imbibition in vertical downward homogeneous porous media.

In this paper, we have discussed the countercurrent imbibition phenomenon in the inclined homogeneous porous medium. During secondary oil recovery process, when water is injected in inclined oil formatted homogeneous porous medium, at the common interface the countercurrent imbibition phenomenon occurs. The main objective of this paper is to measure the saturation of injected water at distance x and time t for horizontal ($\theta = 0^\circ$) and inclined ($\theta = 5^\circ, 10^\circ$) homogeneous porous medium. The nonlinear partial differential equation for the countercurrent imbibition phenomenon has been obtained. The homotopy analysis method has been applied to solve this governing equation by using appropriate initial and boundary conditions.

In 1992, the homotopy analysis method (HAM) has been developed by Liao [12] to obtain series solutions of nonlinear differential equations. This technique has been successfully applied to solve various partial differential equations such as solution of the linear vibration equation [1], solution of diffusion equations [23], solution has been established for the well-known Richards' equation for unsaturated flow of transports in

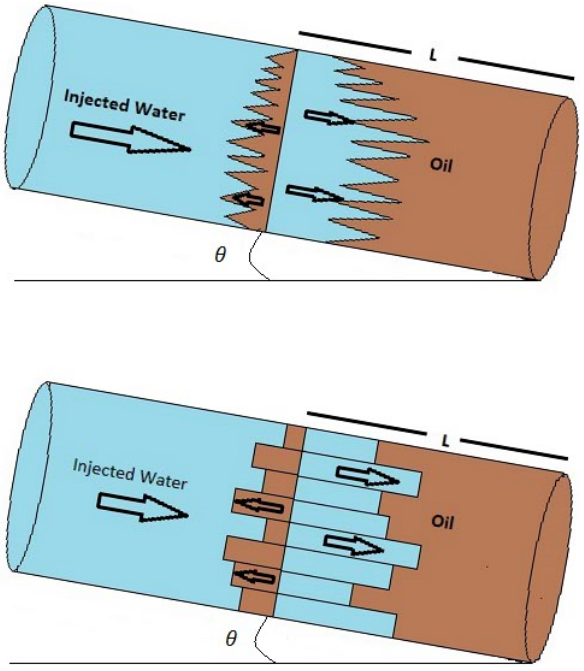

Figure 1: Schematic Diagram.

soils [9] and so on. As pointed out by Liao, the convergence for the HAM solution strongly depends on the value of the convergence control parameter c_0 which is obtained with the help of the c_0-curves.

2. Statement of the Problem

Here it is considered that water is uniformly injected in inclined oil formatted homogeneous porous medium. During the secondary oil recovery process, when water is injected in inclined oil formatted homogeneous porous medium, at the common interface the countercurrent imbibition phenomenon occurs due to the difference of wetting abilities of water and oil. For the inclined homogeneous porous medium, the velocity of oil and the velocity of water are considered under the gravitational effect. Hence the gravitational effect will be deducted during imbibition fingers of oil occurring in the opposite direction for smaller distance and short time in the inclined homogenous porous medium.

For the mathematical model of the countercurrent imbibition, it is assumed that Darcy's law is valid for the investigated flow system and only the average cross sectional area occupied by the fingers is considered, the size and shape of the individual fingers are neglected. The porosity and permeability of inclined homogeneous porous medium are considered as constant. The saturation of the injected water is then defined as the average cross-sectional area occupied by injected water at distance x and time t and is denoted by $S_w(x, t)$.

3. Mathematical Model of the Problem

Assumed that the Darcy's law is valid for the investigated flow system, the velocity of injected water V_w and velocity of oil V_o can be written as follows [3], [4], [21], [27]:

$$V_w = -\frac{K_w}{\delta_w} K \left[\frac{\partial P_w}{\partial x} + \rho_w g sin\theta \right] \tag{1}$$

$$V_o = -\frac{K_o}{\delta_o} K \left[\frac{\partial P_o}{\partial x} - \rho_o g sin\theta \right] \tag{2}$$

where V_w and V_o are the velocities of water and oil respectively, K is the permeability of the homogeneous medium, k_w and k_o are the relative permeabilities of water and oil respectively which are functions of saturation of water S_w and saturation of oil S_o, δ_w and δ_o are the constant viscosities, P_w and P_o are the pressures of water and oil respectively, ρ_w and ρ_o are constant densities of water and oil respectively, θ is the inclination of homogeneous porous medium and g is acceleration due to gravity.

The equation of continuity of injected water is

$$P \frac{\partial S_w}{\partial t} + \frac{\partial V_w}{\partial x} = 0 \tag{3}$$

where P is the porosity of the medium.

When two immiscible fluids are in contact in the interstices of a porous medium, a discontinuity in pressure exists across the interface separating them. The difference in pressure is called the capillary pressure (P_c), that is

$$P_c = P_o - P_w \tag{4}$$

For definiteness, we assume that the capillary pressure (P_c) is a continuous linear function of the form

$$P_c = -\beta S_w \quad Mehta[20] \tag{5}$$

where β is a constant quantity.

We assume the standard relationship due to Scheidegger and Johnson [27] between phase saturation and relative permeability as

$$k_w = S_w \tag{6}$$

$$k_o = 1 - \alpha S_w \tag{7}$$

In countercurrent imbibition phenomenon, the sum of the velocities of injected water and native oil is zero [26], that is

$$V_w + V_o = 0 \tag{8}$$

From (1) and (2),

$$\frac{K_w}{\delta_w}K\left[\frac{\partial P_w}{\partial x}+\rho_w g sin\theta\right]+\frac{K_o}{\delta_o}K\left[\frac{\partial P_o}{\partial x}-\rho_o g sin\theta\right]=0 \tag{9}$$

From equations (9) and (4)

$$\left(\frac{k_w}{\delta_w}+\frac{k_o}{\delta_o}\right)\frac{\partial P_o}{\partial x}-\frac{k_w}{\delta_w}\frac{\partial P_c}{\partial x}=-\left(\frac{k_w}{\delta_w}\rho_w-\frac{k_o}{\delta_o}\rho_o\right)g sin\theta \tag{10}$$

Solving equation (10) for $\frac{\partial P_o}{\partial x}$

$$\frac{\partial P_o}{\partial x}=-\left[\frac{\left(\frac{k_w}{\delta_w}\rho_w-\frac{k_o}{\delta_o}\rho_o\right)g sin\theta-\frac{k_w}{\delta_w}\frac{\partial P_c}{\partial x}}{\frac{k_w}{\delta_w}+\frac{k_o}{\delta_o}}\right] \tag{11}$$

From equation (2), we get

$$V_o=\frac{k_o}{\delta_o}K\left[\frac{\frac{k_w}{\delta_w}(\rho_w+\rho_o)g sin\theta-\frac{k_w}{\delta_w}\frac{\partial P_c}{\partial x}}{\frac{k_w}{\delta_w}+\frac{k_o}{\delta_o}}\right] \tag{12}$$

Using equation (8) and (12)

$$V_w=-\frac{\frac{k_w}{\delta_w}\frac{k_o}{\delta_o}}{\frac{k_w}{\delta_w}+\frac{k_o}{\delta_o}}K\left[(\rho_w+\rho_o)g sin\theta-\frac{\partial P_c}{\partial x}\right] \tag{13}$$

On substituting the value of V_w from equation (13) to (3),

$$P\frac{\partial S_w}{\partial t}-\frac{\partial}{\partial x}\left[\frac{\frac{k_w}{\delta_w}\frac{k_o}{\delta_o}}{\frac{k_w}{\delta_w}+\frac{k_o}{\delta_o}}K(\rho_w+\rho_o)g sin\theta\right]+\frac{\partial}{\partial x}\left[K\frac{\frac{k_w}{\delta_w}\frac{k_o}{\delta_o}}{\frac{k_w}{\delta_w}+\frac{k_o}{\delta_o}}\frac{\partial P_c}{\partial x}\right]=0 \tag{14}$$

For the investigation flow system involves water and viscous oil, therefore according to Scheidegger [26], we have

$$\frac{\frac{k_w}{\delta_w}\frac{k_o}{\delta_o}}{\frac{k_w}{\delta_w}+\frac{k_o}{\delta_o}}\approx\frac{k_o}{\delta_o} \tag{15}$$

On substituting values from (15), (7) and (5) into equation (14), we get

$$P\frac{\partial S_w}{\partial t}=\frac{K(\rho_w+\rho_o)g sin\theta}{\delta_o}\frac{\partial(1-\alpha S_w)}{\partial x}+\frac{K\beta}{\delta_o}\frac{\partial}{\partial x}\left[(1-\alpha S_w)\frac{\partial S_w}{\partial x}\right] \tag{16}$$

Using dimensionless variables

$$X = \frac{x}{L}, \quad T = \frac{K\beta t}{\delta_o L^2 P},$$

Equation (16) reduces to

$$\frac{\partial S_w}{\partial T} = \frac{\partial^2 S_w}{\partial X^2} - \alpha S_w \frac{\partial^2 S_w}{\partial X^2} - \alpha \left(\frac{\partial S_w}{\partial X}\right)^2 - \alpha A \frac{\partial S_w}{\partial X} \tag{17}$$

where $A = \dfrac{L(\rho_w + \rho_o) g sin\theta}{\beta}$ and $S_w(x, t) = S_w(X, T)$.

We choose appropriate initial and boundary conditions for imbibition phenomenon as

$$S_w(X, 0) = \frac{X + X^2}{6} \tag{18}$$

$$S_w(0, T) = 0 \tag{19}$$

$$S_w(1, T) = \frac{1 + T}{3} \tag{20}$$

Here, $S_w(X, 0) = \dfrac{X + X^2}{6}$ is the initial saturation of injected water, $S_w(0, T) = 0$ is saturation of injected water at $X = 0$ and $S_w(1, T) = \dfrac{1 + T}{3}$ is saturation of injected water at $X = 1$.

4. Solution of the Problem by Homotopy Analysis Method

To solve the equation (17) by means of the HAM [12], according to the initial and boundary conditions, we choose initial guess as

$$S_{w_0}(X, T) = \frac{(1 + T)(X + X^2)}{6} \tag{21}$$

We choose the linear operator as

$$\mathcal{L}(\phi(X, T; q)) = \frac{\partial^2 \phi(X, T; q)}{\partial X^2} \tag{22}$$

with $\mathcal{L}(f) = 0$ when $f = 0$.

Now we define a nonlinear operator as

$$\mathcal{N}(\phi(X, T; q)) = \frac{\partial^2 \phi(X, T; q)}{\partial X^2} - \alpha \phi(X, T; q) \frac{\partial^2 \phi(X, T; q)}{\partial X^2} - \alpha \left(\frac{\partial \phi(X, T; q)}{\partial X}\right)^2 - \alpha A \frac{\partial \phi(X, T; q)}{\partial X} - \frac{\partial \phi(X, T; q)}{\partial T} \tag{23}$$

The so-called zeroth-order deformation equation is

$$(1-q)\mathcal{L}(\phi(X,T;q)-S_{w_0}(X,T))=c_0 q\,H(X,T)\mathcal{N}[\phi(X,T;q)] \tag{24}$$

where $q\in[0,1]$ is the embedding parameter, $c_0\neq 0$ is a convergence control parameter, $H(X,T)\neq 0$ is an auxiliary function, $\mathcal{L}$ is an auxiliary linear operator, $S_{w_0}(X,T)$ is an initial guess of $S_w(X,T)$, $\phi(X,T;q)$ is an unknown function, $\mathcal{N}$ is a nonlinear operator.

When $q=0$ and $q=1$, it holds

$$\phi(X,T;0)=S_{w_0}(X,T) \tag{25}$$

and

$$\phi(X,T;1)=S_w(X,T) \tag{26}$$

respectively. Thus, as the embedding parameter q increases from 0 to 1, the solution $\phi(X,T;q)$ deforms from the initial guess $S_{w_0}(X,T)$ to the solution $S_w(X,T)$ of the original equation (17). Expanding $\phi(X,T;q)$ in Taylor series with respect to q we have

$$\phi(X,T;q)=S_{w_0}(X,T)+\sum_{m=1}^{\infty}S_{w_m}(X,T)q^m \tag{27}$$

where

$$S_{w_m}(X,T)=\frac{1}{m!}\frac{\partial^m\phi(X,T;q)}{\partial q^m}\bigg|_{q=0} \tag{28}$$

The convergence of the homotopy series (27) depends upon the convergence control parameter. If the auxiliary linear operator, the initial guess, the convergence control parameter c_0 and the auxiliary function are properly chosen, the homotopy series converges at $q=1$ and

$$S_w(X,T)=S_{w_0}(X,T)+\sum_{m=1}^{\infty}S_{w_m}(X,T) \tag{29}$$

Differentiating the zeroth-order deformation equation (24) m times with respect to the embedding parameter q and then dividing them by $m!$ and finally setting $q=0$, we have the so-called mth-order deformation equation

$$\mathcal{L}(S_{w_m}(X,T)-\chi_m S_{w_{m-1}}(X,T))=c_0 H(X,T)R_m(\overrightarrow{S_{w_{m-1}}}) \tag{30}$$

where

$$R_m(\overrightarrow{S_{w_{m-1}}})=\frac{1}{(m-1)!}\frac{\partial^{m-1}\mathcal{N}(\phi(X,T;q))}{\partial q^{m-1}}\bigg|_{q=0} \tag{31}$$

and

$$\chi_m=\begin{cases}0 & \text{if } m\leq 1,\\ 1 & \text{if } m>1.\end{cases} \tag{32}$$

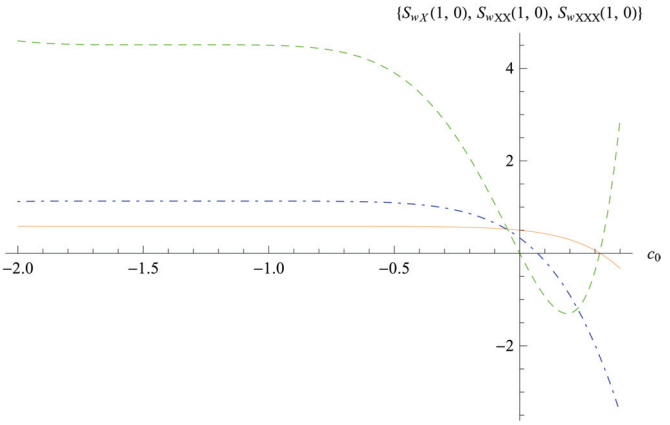

Figure 2: The c_0-curves of $S_{w_X}(1,0)$ (Solid line), $S_{w_{XX}}(1,0)$ (DotDashed line) and $S_{w_{XXX}}(1,0)$ (Dashed line) for 10th order approximation.

Assume $H(X,T)=1$, then the solution of mth-order deformation equation (30) is

$$S_{w_m}(X,T)=\chi_m S_{w_{m-1}}(X,T)+c_0\mathcal{L}^{-1}(R_m(\overrightarrow{S_{w_{m-1}}})) \tag{33}$$

subject to boundary conditions $S_{w_m}(0,T)=0$ and $S_{w_m}(1,T)=0$, $m\geq 1$. In this way, we get $S_{w_m}(X,T)$ for $m=1,2,3,\ldots$ successively. Hence,

$$\begin{aligned}S_w(X,T)=&\left(\frac{X}{6}+\frac{TX}{6}+\frac{X^2}{6}+\frac{TX^2}{6}\right)+c_0\Bigg(-\frac{X}{8}+\frac{\alpha X}{18}+\frac{5\alpha AX}{36}\\&-\frac{TX}{6}+\frac{\alpha TX}{9}+\frac{5\alpha ATX}{36}+\frac{\alpha T^2X}{18}+\frac{X^2}{6}-\frac{\alpha X^2}{72}\\&-\frac{\alpha AX^2}{12}+\frac{TX^2}{6}-\frac{\alpha TX^2}{36}-\frac{\alpha ATX^2}{12}-\frac{\alpha T^2X^2}{72}-\frac{X^3}{36}\\&-\frac{\alpha X^3}{36}-\frac{\alpha AX^3}{18}-\frac{\alpha TX^3}{18}-\frac{\alpha ATX^3}{18}-\frac{\alpha T^2X^3}{36}-\frac{X^4}{72}\\&-\frac{\alpha X^4}{72}-\frac{\alpha TX^4}{36}-\frac{\alpha T^2X^4}{72}\Bigg)+\cdots\end{aligned} \tag{34}$$

is the solution which represents the saturation of injected water at distance X for time T. The equation (34) describes the analytical expression for the saturation of injected water for the countercurrent imbibition phenomenon arising in fluid flow through the inclined homogeneous porous medium.

The values of the following constants are taken from standard literature: $L=1$, $g=9.8$, $\rho_w=0.1$, $\rho_o=0.3$, $\beta=0.1$, $\alpha=1.11$.

As discussed by many researchers such as Liao [15], Abbasbandy, Shivanian and Vajravelu [2], Saeidian and Javadi [25], Abbasbandy and Shivanian [1], Paripour, Babolian and Saeidian [23], Ghotbi, Omidvar and Barari [9], the nonzero convergence control parameter c_0 is introduced to construct the so-called zeroth-order deformation equation.

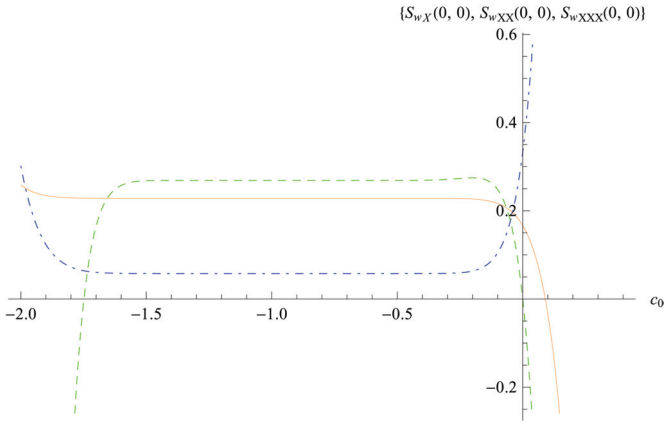

Figure 3: The c_0-curves of $S_{w_X}(0,0)$ (Solid line), $S_{w_{XX}}(0,0)$ (DotDashed line) and $S_{w_{XXX}}(0,0)$ (Dashed line) for 15th order approximation.

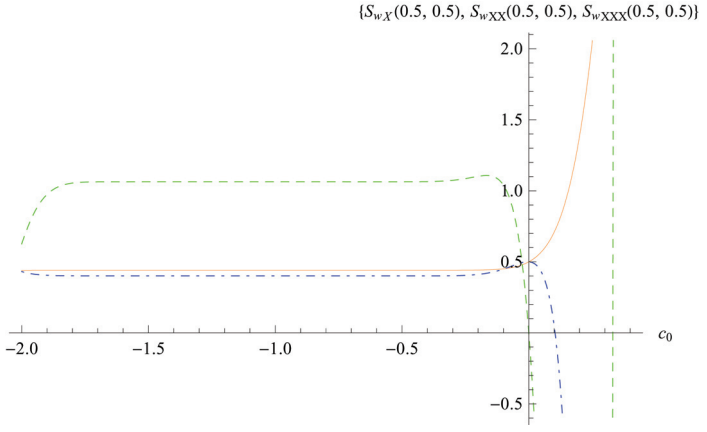

Figure 4: The c_0-curves of $S_{w_X}(0.5,0.5)$ (Solid line), $S_{w_{XX}}(0.5,0.5)$ (DotDashed line) and $S_{w_{XXX}}(0.5,0.5)$ (Dashed line) for 20th order approximation.

The convergence of the series solution is dependent upon the convergence control parameter c_0 and thus choosing a proper value for c_0 provides us with a convenient way to adjust and control convergence region and rate of solution series given by the homotopy analysis method. The so-called c_0-curves are used to find proper value of c_0 for which the solution series converges.

Using Mathematica software for BVPh [18], we plot the c_0-curves of $S_{w_X}(1,0)$, $S_{w_{XX}}(1,0)$, $S_{w_{XXX}}(1,0)$, $S_{w_X}(0,0)$, $S_{w_{XX}}(0,0)$, $S_{w_{XXX}}(0,0)$, $S_{w_X}(0.5,0.5)$, $S_{w_{XX}}(0.5,0.5)$, $S_{w_{XXX}}(0.5,0.5)$, $S_{w_X}(0,1)$, $S_{w_{XX}}(0,1)$ and $S_{w_{XXX}}(0,1)$ in the figures 2-6 for the inclination $\theta = 0°$. We choose proper value of $c_0 = -0.9$ with the help of c_0-curves.

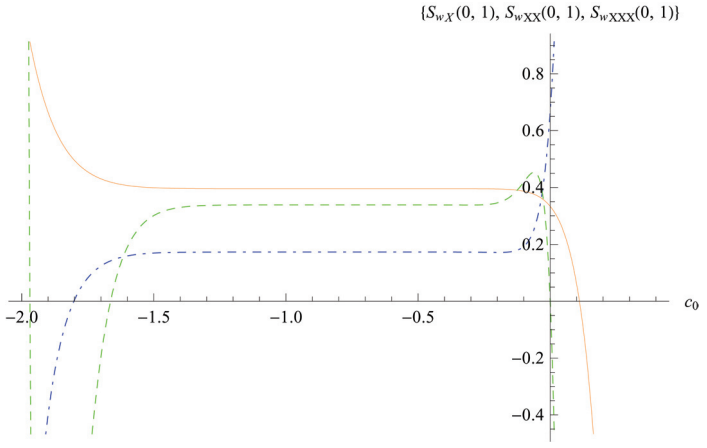

Figure 5: The c_0-curves of $S_{w_X}(0, 1)$ (Solid line), $S_{w_{XX}}(0, 1)$ (DotDashed line) and $S_{w_{XXX}}(0, 1)$ (Dashed line) for 25th order approximation.

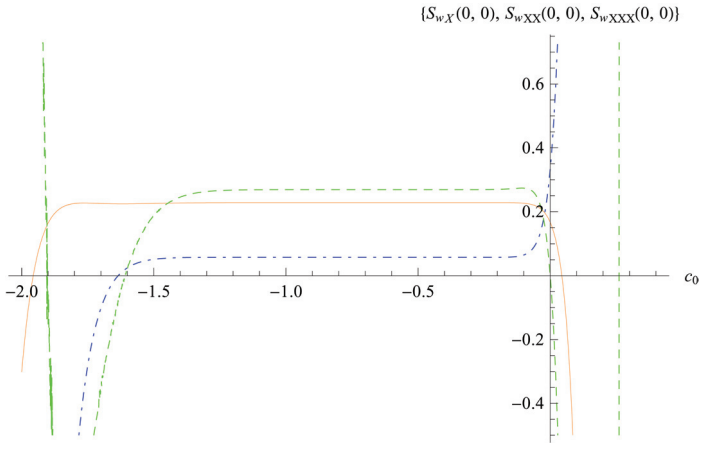

Figure 6: The c_0-curves of $S_{w_X}(0, 0)$ (Solid line), $S_{w_{XX}}(0, 0)$ (DotDashed line) and $S_{w_{XXX}}(0, 0)$ (Dashed line) for 30th order approximation.

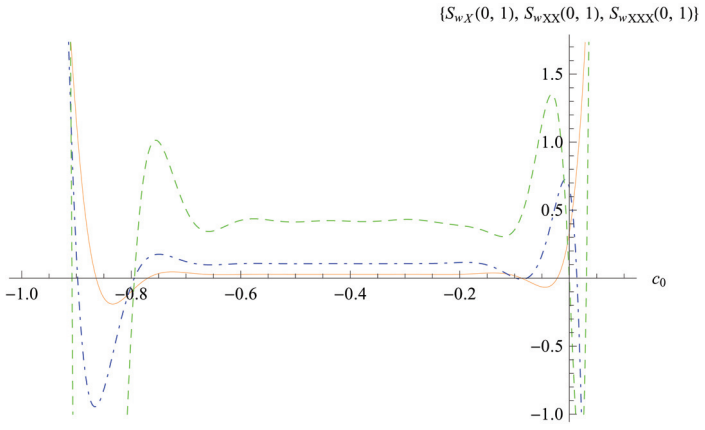

Figure 7: The c_0-curves of $S_{w_X}(0, 1)$ (Solid line), $S_{w_{XX}}(0, 1)$ (DotDashed line) and $S_{w_{XXX}}(0, 1)$ (Dashed line) for 25th order approximation.

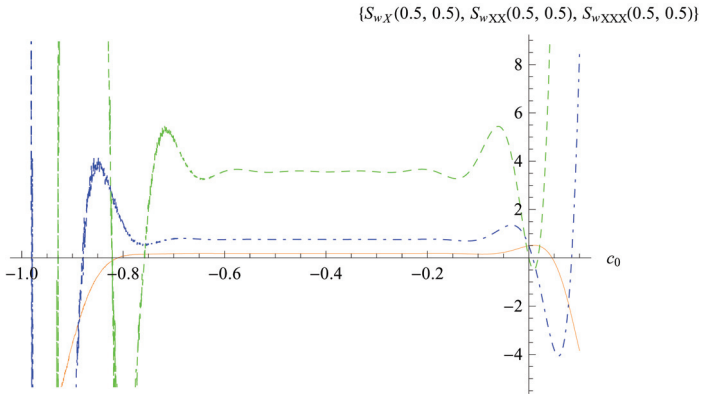

Figure 8: The c_0-curves of $S_{w_X}(0.5, 0.5)$ (Solid line), $S_{w_{XX}}(0.5, 0.5)$ (DotDashed line) and $S_{w_{XXX}}(0.5, 0.5)$ (Dashed line) for 30th order approximation.

In the case of inclination $\theta = 5^\circ$, we plot the c_0-curves for $S_{w_X}(0, 1)$, $S_{w_{XX}}(0, 1)$, $S_{w_{XXX}}(0, 1)$, $S_{w_X}(0.5, 0.5)$, $S_{w_{XX}}(0.5, 0.5)$, $S_{w_{XXX}}(0.5, 0.5)$, $S_{w_X}(0, 0)$, $S_{w_{XX}}(0, 0)$ and $S_{w_{XXX}}(0, 0)$ in the figures 7-9. With the help of c_0-curves, we choose proper value of $c_0 = -0.5$.

For inclination $\theta = 10^\circ$, we plot the c_0-curves for $S_{w_X}(0, 0)$ and $S_{w_{XX}}(0, 0)$ in the figures 10-11. We choose proper value of $c_0 = -0.25$ from these c_0-curves.

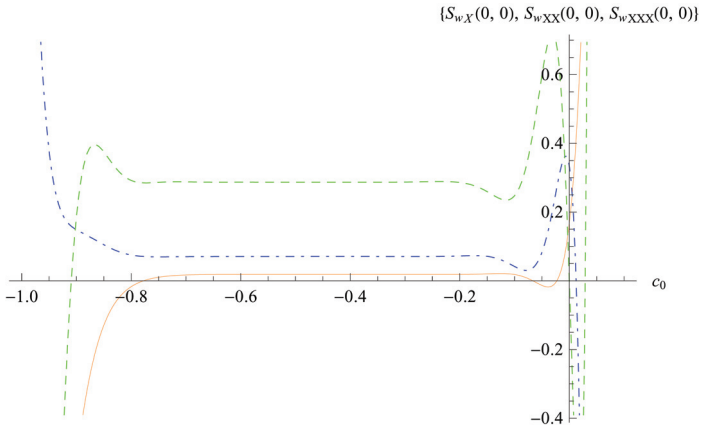

Figure 9: The c_0-curves of $S_{w_X}(0, 0)$ (Solid line), $S_{w_{XX}}(0, 0)$ (DotDashed line) and $S_{w_{XXX}}(0, 0)$ (Dashed line) for 30th order approximation.

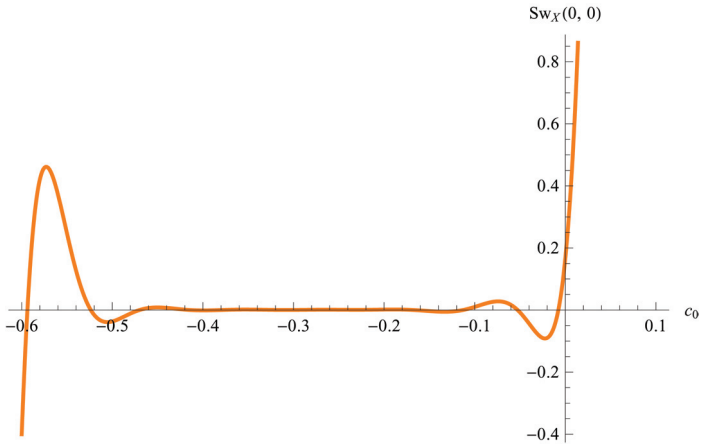

Figure 10: The c_0-curve of $S_{w_X}(0, 0)$ (Solid line) for 30th order approximation.

5. Results and Discussion

5.1. Numerical and Graphical representation without inclination ($\theta = 0°$)

For this case, we put $\theta = 0°$ in equation (34) so it represents the saturation of injected water for countercurrent imbibition phenomenon in the homogeneous porous media without inclination ($\theta = 0°$). Numerical and graphical presentations are obtained by using Mathematica software. We choose the proper value of the convergence control parameter $c_0 = -0.9$ to obtain convergent homotopy series. Table 1 indicates the numerical values of saturation of injected water for distance X and time T.

Figure 12 represents the graph of saturation of injected water vs. distance X for different time $T = 0.1, 0.2, \ldots, 1$ and figure 13 represents the graph of saturation of

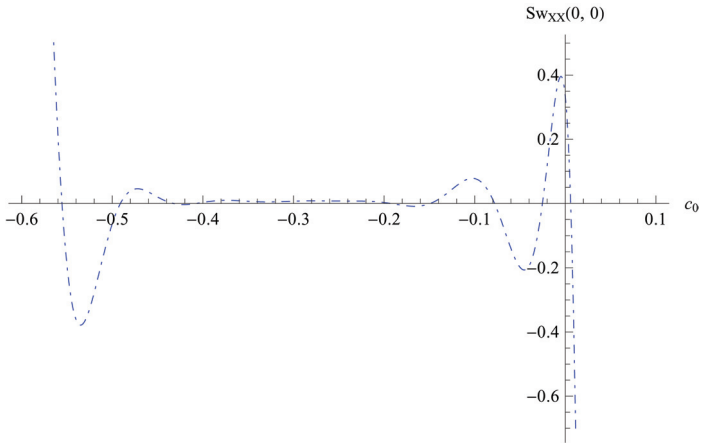

Figure 11: The c_0-curve of $S_{w_{XX}}(0,0)$ (DotDashed line) for 30th order approximation.

Table 1: Numerical values of the saturation of injected water in inclined homogeneous porous media with inclination $\theta = 0^\circ$.

T	$X=0.1$	$X=0.2$	$X=0.3$	$X=0.4$	$X=0.5$	$X=0.6$	$X=0.7$	$X=0.8$	$X=0.9$	$X=1.0$
0.0	0.0231599	0.0471921	0.0724362	0.0992933	0.1282463	0.1598903	0.1949826	0.2345284	0.2799370	0.3333333
0.1	0.0254093	0.0518122	0.0795584	0.1090685	0.1408571	0.1755716	0.2140553	0.2574587	0.3074506	0.3666667
0.2	0.0275444	0.0562090	0.0863562	0.1184278	0.1529744	0.1907019	0.2325514	0.2798426	0.3345601	0.4000000
0.3	0.0295647	0.0603800	0.0928225	0.1273579	0.1645762	0.2052483	0.2504250	0.3016224	0.3612071	0.4333333
0.4	0.0314699	0.0643225	0.0989504	0.1358455	0.1756402	0.2191763	0.2676272	0.3227338	0.3873230	0.4666667
0.5	0.0332594	0.0680341	0.1047336	0.1438776	0.1861439	0.2324508	0.2841057	0.3431054	0.4128262	0.5000000
0.6	0.0349331	0.0715126	0.1101658	0.1514414	0.1960650	0.2450354	0.2998057	0.3626584	0.4376200	0.5333333
0.7	0.0364906	0.0747557	0.1152411	0.1585248	0.2053812	0.2568935	0.3146691	0.3813058	0.4615895	0.5666667
0.8	0.0379317	0.0777617	0.1199538	0.1651157	0.2140708	0.2679879	0.3286359	0.3989530	0.4845984	0.6000000
0.9	0.0392563	0.0805287	0.1242988	0.1712029	0.2221125	0.2782818	0.3416440	0.4154975	0.5064860	0.6333333
1.0	0.0404642	0.0830552	0.1282712	0.1767756	0.2294857	0.2877385	0.3536303	0.4308301	0.5270634	0.6666667

injected water vs. time T for different distance $X = 0.1, 0.2, \ldots, 1$. Table 1 indicates the numerical values for figure 12 and figure 13.

5.2. Numerical and Graphical representation with inclination ($\theta = 5^\circ, \theta = 10^\circ$)

Equation (34) represents the saturation of injected water for countercurrent imbibition phenomenon in the inclined homogeneous porous medium. Table 2 indicates the numerical values of saturation of injected water for different values of distance X and time T in homogenous porous media with inclination $\theta = 5^\circ$. The convergence of the homotopy series is dependent on the convergence control parameter c_0. Here we choose $c_0 = -0.5$ to get convergent homotopy series.

Figure 14 represents the graph of saturation of injected water vs. distance X for different time $T = 0.1, 0.2, \ldots, 1$ in homogeneous porous media with inclination $\theta = 5^\circ$. Table 2 indicates the numerical values for figure 14.

In the case of homogeneous porous media with inclination $\theta = 10^\circ$, $c_0 = -0.25$ is used to find the numerical values of saturation of injected water for different distance X and time T. Table 3 indicates its numerical values.

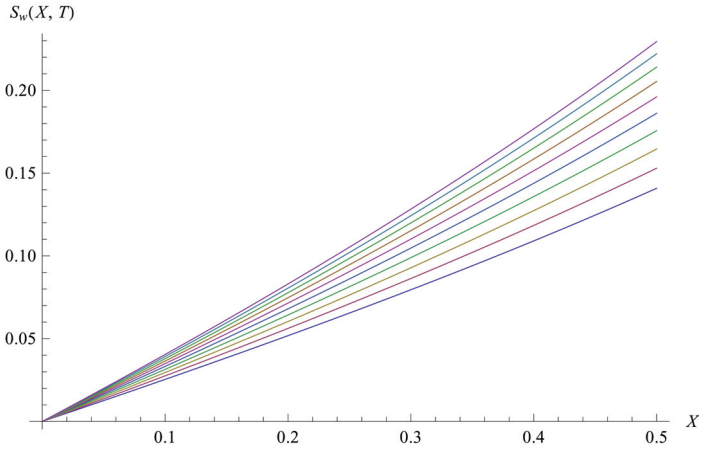

Figure 12: The graph of saturation of water v/s distance for fixed time $T = 0.1, 0.2, \ldots, 1 (\theta = 0^\circ)$.

Table 2: Numerical values of the saturation of injected water in inclined homogeneous porous media with inclination $\theta = 5^\circ$.

T	$X = 0.1$	$X = 0.2$	$X = 0.3$	$X = 0.4$	$X = 0.5$	$X = 0.6$	$X = 0.7$	$X = 0.8$	$X = 0.9$	$X = 1.0$
0.0	0.0022572	0.0055912	0.0105527	0.0179908	0.0292399	0.0464591	0.0733081	0.1164850	0.1900465	0.3333333
0.1	0.0024311	0.0060196	0.0113537	0.0193412	0.0314102	0.0498805	0.0787155	0.1252695	0.2054031	0.3666667
0.2	0.0025899	0.0064107	0.0120855	0.0205756	0.0333963	0.0530169	0.0836900	0.1334087	0.2198668	0.4000000
0.3	0.0027342	0.0067665	0.0127513	0.0216997	0.0352066	0.0558795	0.0882439	0.1409096	0.2334094	0.4333333
0.4	0.0028650	0.0070887	0.0133547	0.0227190	0.0368498	0.0584797	0.0923902	0.1477818	0.2460060	0.4666667
0.5	0.0029827	0.0073791	0.0138987	0.0236391	0.0383351	0.0608292	0.0961419	0.1540373	0.2576363	0.5000000
0.6	0.0030882	0.0076393	0.0143865	0.0244656	0.0396719	0.0629403	0.0995117	0.1596906	0.2682853	0.5333333
0.7	0.0031819	0.0078706	0.0148208	0.0252039	0.0408711	0.0648263	0.1025111	0.1647596	0.2779447	0.5666667
0.8	0.0032643	0.0080744	0.0152043	0.0258595	0.0419449	0.0665025	0.1051486	0.1692662	0.2866140	0.6000000
0.9	0.0033358	0.0082516	0.0155391	0.0264379	0.0429084	0.0679874	0.1074276	0.1732382	0.2943027	0.6333333
1.0	0.0033966	0.0084028	0.0158268	0.0269445	0.0437808	0.0693059	0.1093420	0.1767127	0.3010336	0.6666667

Table 3: Numerical values of the saturation of injected water in inclined homogeneous porous media with inclination $\theta = 10^\circ$.

T	$X = 0.1$	$X = 0.2$	$X = 0.3$	$X = 0.4$	$X = 0.5$	$X = 0.6$	$X = 0.7$	$X = 0.8$	$X = 0.9$	$X = 1.0$
0.0	0.0001494	0.0004312	0.0009835	0.0021512	0.0047436	0.0105918	0.0236846	0.0529370	0.1228759	0.3333333
0.1	0.0001731	0.0004843	0.0010749	0.0023011	0.0050114	0.0111801	0.0251603	0.0564768	0.1316964	0.3666667
0.2	0.0002023	0.0005480	0.0011799	0.0024579	0.0052527	0.0116669	0.0264483	0.0597091	0.1398476	0.4000000
0.3	0.0002387	0.0006266	0.0013066	0.0026349	0.0054820	0.0120552	0.0275404	0.0626465	0.1473343	0.4333333
0.4	0.0002840	0.0007246	0.0014644	0.0028483	0.0057194	0.0123519	0.0284247	0.0653022	0.1541616	0.4666667
0.5	0.0003400	0.0008471	0.0016637	0.0031175	0.0059912	0.0125691	0.0290851	0.0676895	0.1603343	0.5000000
0.6	0.0004086	0.0009991	0.0019163	0.0034656	0.0063318	0.0127265	0.0295012	0.0698217	0.1658559	0.5333333
0.7	0.0004915	0.0011859	0.0022344	0.0039192	0.0067846	0.0128540	0.0296475	0.0717116	0.1707268	0.5666667
0.8	0.0005902	0.0014123	0.0026310	0.0045082	0.0074038	0.0129952	0.0294939	0.0733709	0.1749431	0.6000000
0.9	0.0007060	0.0016830	0.0031189	0.0052660	0.0082555	0.0132115	0.0290053	0.0748090	0.1784942	0.6333333
1.0	0.0008396	0.0020015	0.0037107	0.0062288	0.0094193	0.0135871	0.0281430	0.0760315	0.1813605	0.6666667

Figure 15 represents the graph of saturation of injected water vs. distance X for different time $T = 0.1, 0.2, \ldots, 1$ in homogeneous porous media with inclination $\theta = 10^\circ$. Table 3 indicates the numerical values for figure 15.

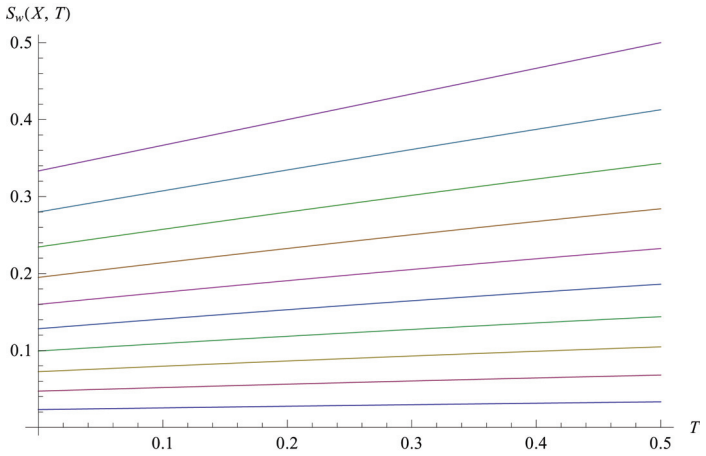

Figure 13: The graph of saturation of water v/s time for fixed distance $X = 0.1, 0.2, \ldots, 1 (\theta = 0°)$.

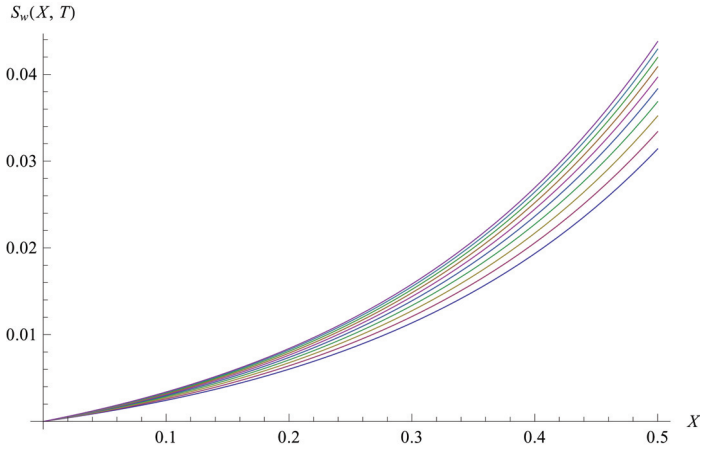

Figure 14: The graph of saturation of water v/s distance for fixed time $T = 0.1, 0.2, \ldots, 1 (\theta = 5°)$.

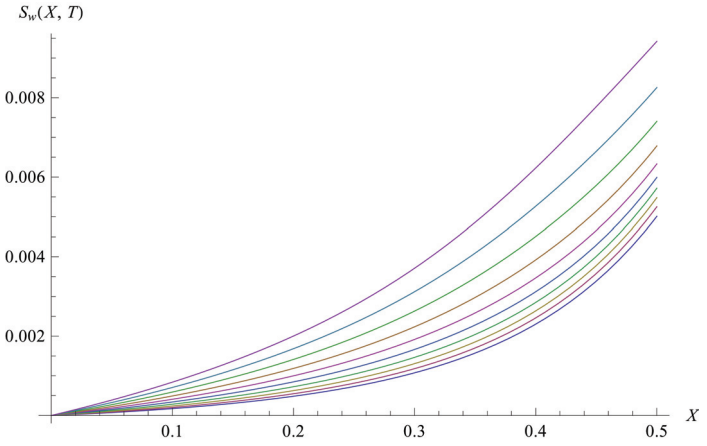

Figure 15: The graph of saturation of water v/s distance for different time $T = 0.1, 0.2, \ldots, 1 (\theta = 10^{\circ})$.

6. Conclusion

The equation (34) represents an approximate analytical solution of nonlinear partial differential equation (17) arising in countercurrent imbibition phenomenon in inclined homogeneous porous medium by homotopy analysis method which gives the saturation of injected water in inclined porous media during the countercurrent imbibition phenomenon occurred. The solution (34) satisfies both the initial and boundary conditions. The graph of saturation of injected water in the horizontal porous medium given by figure 12 increases as distance X increases for given time T. Figure 14 and 15 represent the graphs of $S_w(X, T)$ in inclined porous medium vs. distance X for time $T = 0.1, 0.2, \ldots, 1$ which show that saturation increases when distance and time increase. But due to inclination the saturation of injected water is less than the saturation of injected water without inclination.

It is concluded that when the water is injected in oil formatted homogeneous porous medium, at the common interface the countercurrent imbibition phenomenon occurs and the saturation of injected water increases as distance X increases for given time T in both inclined homogeneous porous medium and horizontal homogeneous porous medium. The saturation of injected water in the case of inclination is less comparative to the case without inclination.

References

[1] S. Abbasbandy, E. Shivanian, Solution of Singular Linear Vibrational BVPs by the Homotopy Analysis Method, *Journal of Numerical Mathematics and Stochastics*, Vol. 1(1), 77–84, (2009).

[2] S. Abbasbandy, E. Shivanian, K. Vajravelu, Mathematical properties of h-curve in the frame work of the homotopy analysis method, *Commun. Nonlinear Sci. Numer.*

Simul., Vol. 16, 4268–4275, (2011).

[3] J. Bear,Dynamics of fluids in porous media, *American Elsevier Publishing Company*, Inc., (1972).

[4] J. Bear, AHD Cheng, Modeling Ground water flow and contaminant Transport: Theory and Applications of transport in Porous Media, *Springer*, (2010).

[5] P. M. Blair, Calculation of oil displacement by countercurrent water imbibition, *Society of Petroleum Engineers Journal*, Vol. 4(3), 195–202, (1964).

[6] J. Bourblaux, F. J. Kalaydjian, Experimental Study of Cocurrent and Countercurrent Flows in Naturally Porous Media, *SPE Reservoir Engineering, Society of Petroleum Engineers*, Vol. 5(3), 361–368 (1990).

[7] E.R. Brownscombe, A.B. Dyes, A Water imbibition Displacement - A Possibility for the Spraberry, *Drilling and Production Practice, American Petroleum Institute*, 383–390, (1952).

[8] N. B. Desai, The study of problems arises in single phase and multiphase flow through porous media, Ph.D. Thesis,*South Gujarat University, Surat*, (2002).

[9] A. R. Ghotbi, M. Omidvar, A. Barari, Infiltration in unsaturated soils - An analytical approach, *Computers and Geotechnics*, Vol. 38, 777–782, (2011).

[10] J.W. Graham, J.G. Richardson, Theory and application of imbibition phenomena in recovery of oil, *Journal of Petroleum Technology, Society of Petroleum Engineers*, Vol. 11(2), 65–69, (1959).

[11] M. S. Joshi, N. B. Desai, M. N. Mehta, An analytical solution of countercurrent imbibition phenomenon arising in fluid flow through homogeneous porous media, *Int. J. of Appl. Math. and Mech.*, Vol. 7 (11), 21–32, (2011).

[12] S. J. Liao, The proposed homotopy analysis technique for the solution of nonlinear problems, Ph.D. Thesis,*Shanghai Jiao Tong University*, (1992).

[13] S. J. Liao, An approximate solution technique not depending on small parameters: a special example,*Int. J. Nonlinear Mech.*, Vol.30 (3), 371–380 (1995).

[14] S. J. Liao, A kind of approximate solution technique which does not depend upon small parameters (II): an application in fluid mechanics, *Int. J. Nonlinear Mech.*, Vol.32 (5), 815–822 (1997).

[15] S. J. Liao, Beyond perturbation: introduction to the homotopy analysis method, *CRC Press Chapman and Hall*, (2003).

[16] S. J. Liao, On the homotopy analysis method for nonlinear problems, *Appl. Math. Comput.*, Vol. 147, 499–513 (2004).

[17] S. J. Liao, Notes on the homotopy analysis method: Some definitions and theorems, *Commun. Nonlinear Sci. Numer. Simul.*, Vol. 14, 983–997 (2009).

[18] S. J. Liao, Homotopy analysis method in nonlinear differential equations, *Higher Education Press and Springer*, (2012).

[19] M. N. Mehta, A. P. Verma, A Singular Perturbation Solution of Double Phase Flow due to differential wettability, *Indian J. Pure Appl. Math.*, Vol.8(5), 523–526, (1977).

[20] M. N. Mehta, Asymptotic expansions of fluid flow through porous media, Ph.D. Thesis,*South Gujarat University, Surat*, (1977).

[21] M. Muskat, The flow of homogeneous fluids through porous media, *First edition, McGraw Hill Book Company* (1946).

[22] A. K. Parikh, M. N. Mehta, V. H. Pradhan, Mathematical model and analysis of countercurrent imbibition in vertical downward homogeneous porous media, *British J. of Math. and Comp. Sci.*, Vol. 3(4), 478–489, (2013).

[23] M. Paripour, E. Babolian, J. Saeidian, Analytic solutions to diffusion equations, *Mathematical and Computer Modelling*, Vol. 51, 649–657, (2010).

[24] M. Pooladi-Darvish, A. Firoozabadi, Cocurrent and countercurrent imbibition in a water wet matrix block, *Society of Petroleum Engineers Journal*, Vol. 5(1), 3–11, (2000).

[25] J. Saeidian, S. Javadi, Some notes on the convergence control parameter in the framework of the homotopy analysis method, *J. of Math. and Comp. Sci.*, Vol. 9, 103–110, (2014).

[26] A. E.Scheidegger, The Physics of flow through porous media, *Soil Science*, Vol. 86, (1958).

[27] A. E. Scheidegger, E. F. Johnson, The statistically behaviour of instabilities in displacement process in porous media, *Canadian J. Physics*, Vol. 39, Issue 2, 326–334 (1961).

[28] Z. Tavassoli, R. W. Zimmerman, M. J. Blunt, Analysis of countercurrent imbibition with gravity in weakly water-wet systems, *J. Petro. Sci. and Engg.*, Vol. 48, 94–104, (2005).

[29] K. Vajravelu,R. A. Van Gorder, Nonlinear flow phenomena and homotopy analysis: Fluid flow and Heat transfer, *Higher Education Press, Beijing and Springer*, (2012).

[30] A. P. Verma, Statistical behaviour of fingering in a displacement process in heterogeneous porous medium with capillary pressure, *Canadian J. Physics*, Vol. 47, Issue 3, 319–324 (1969).

[31] S. Yadav, M. N. Mehta, Mathematical model and similarity solution of countercurrent imbibition phenomenon in banded Porous matrix, *Int. J. of Appl. Math. and Mech.*, Vol. 5(5), 76–86, (2009).

***PRAJÑĀ* - Journal of Pure and Applied Sciences Vol. 24 – 25 : 15–22 (2017)**
ISSN 0975 - 2595

MATHEMATICAL MODELLING OF FINGERO-IMBIBITION PHENOMENON IN HETEROGENEOUS POROUS MEDIUM WITH MAGNETIC FIELD EFFECT

MAHENDRA A. PATEL[1] AND N. B. DESAI[2*]

[1]Government Engineering College, Gandhinagar-382028, Gujarat (India),
E-mail: mahendraapatel@yahoo.co.in. Telephone. +91-9737730526
[2] A. D. Patel Institute of Technology, New V. V. Nagar-388121, Gujarat (India),
E-mail: drnbdesai@yahoo.co.in. Telephone. +91-9327158932

ABSTRACT

The present paper discusses the mathematical model for fingero-imbibition phenomenon arising in fluid flow through the heterogeneous porous medium with magnetic field effect during secondary oil recovery process. The mathematical formulation leads to a nonlinear partial differential equation and its solution has been obtained with appropriate boundary conditions by homotopy analysis method. The solution represents the saturation of injected water for fingero-imbibition phenomenon which increases when distance increases for given time. The graphical and numerical representations of the solution are discussed.

Keywords: Fluid flow, Heterogeneous porous medium, Fingero-imbibition phenomenon, Homotopy analysis method.

AMS subject classification: 76S05, 76Txx, 65Nxx, 35Q35.

INTRODUCTION

If a porous medium filled with some phase (oil) is brought into contact with another phase (water) which preferentially wets the medium, there is a spontaneous flow of the wetting phase (water) into the medium and a counter flow of the native phase (oil) from the medium. This phenomenon occurring due to the difference of wetting abilities of the phases is called imbibition phenomenon. Besides this if a porous medium filled with one phase (oil) is displaced by another phase (water) of lesser viscosity, then instead of regular displacement of the whole front, protuberances may occur which shoot through the porous medium at relatively very high speed giving rise to the fingering phenomenon. This simultaneous occurrence of both phenomena fingering and imbibition is known as fingero-imbibition phenomenon (see fig. 1).

The imbibition phenomenon have been investigated by many researches with different aspects. Mishra and Verma [3] have discussed imbibition in the flow of two immiscible fluids (oil and water) with magnetic field. Shah and Verma [5] have obtained the numerical solution of fingero-imbibition phenomenon through homogeneous porous media with magnetic field using finite difference method. Desai [21] has discussed the imbibition phenomenon by similarity transform. Patel, Mehta and Patel [9] have discussed mathematical model of imbibition phenomenon in heterogeneous porous media. Parikh, Mehta and Pradhan [10] have discussed mathematical modeling of fingero-imbibition phenomenon in homogeneous porous medium with magnetic field effect in vertical downward direction. Patel, Rabari and Bhathawala [11] have obtained numerical solution of imbibition phenomenon in a homogeneous medium with magnetic fluid.

In the present work, we have developed the mathematical model for fingero-imbibition phenomenon in heterogeneous porous medium with magnetic field effect. The mathematical formulation leads to the governing nonlinear partial differential equation. The solution of the problem have been obtained using homotopy analysis method [20]. The main aim of this work is to find the solution (the saturation of injected water) of the fingero-imbibition phenomenon in

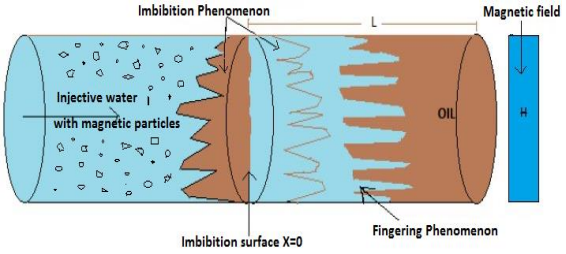

Figure 1: Fingero-imbibition phenomenon.

***PRAJÑĀ* - Journal of Pure and Applied Sciences Vol. 24 – 25 : 15–22 (2017)**
ISSN 0975 - 2595

the heterogeneous porous medium with magnetic field effect.

AIM AND SCOPE OF THE WORK

The aim with this work is to discuss the mathematical model for fingero-imbibition phenomenon arising in fluid flow through the heterogeneous porous medium with magnetic field effect during secondary oil recovery process. The solution of problem is obtain by using homotopy analysis method. This solution represents the saturation of injected water which helps us to predict the amount of water required to inject for recovering oil. This type of mathematical model is useful for predicting oil recovery from petroleum reservoir.

STATEMENT OF THE PROBLEM

Here we consider the cylindrical piece of heterogeneous porous matrix of length L which is filled with oil. During the secondary oil recovery process, the imbibition phenomenon will occur simultaneously with fingering which describes the fingero-imbibition phenomenon. It is considered that the flow of water with magnetic particles and oil in the heterogeneous porous medium under the variable magnetic field effect. In this work assumed that the injected water is conductive while the oil is non-conductive and the effect of a variable magnetic field is to increase the velocity of injected water by gradient of $\frac{\omega H^2}{8\pi}$ where ω is permeability of magnetic field H. It is assumed that the Darcy's law is valid for the investigated flow system for the mathematical model of the fingero-imbibition phenomenon and the average cross sectional area occupied by the fingers was observed.

The saturation of the injected water $S_w(x,t)$ is then defined as the average cross-sectional area occupied by injected water at distance x and time t. The porosity and permeability of heterogeneous porous medium may vary from one place to another place. Considered that the porosity and permeability of heterogeneous porous medium are the functions of variable x only.

MATHEMATICAL MODEL

The velocity of injected water V_w and velocity of oil V_o can be represented due to Darcy's law as [14, 15]:

$$V_w = -\frac{k_w}{\delta_w} K\left[\frac{\partial P_w}{\partial x} + \frac{\omega H}{4\pi}\frac{\partial H}{\partial x}\right] \tag{1}$$

$$V_o = -\frac{k_o}{\delta_o} K\frac{\partial P_o}{\partial x} \tag{2}$$

where V_w and V_o are the velocities of water and oil respectively, k_w and k_o are the relative permeabilities of water and oil respectively, δ_w and δ_o are the constant viscosities of water and oil respectively, K is the variable permeability of the heterogeneous porous medium, P_w and P_o are the pressures of water and oil respectively, ω is permeability of magnetic field H.

The equation of continuity of injected water is

$$P\frac{\partial S_w}{\partial t} + \frac{\partial V_w}{\partial x} = 0 \tag{3}$$

where $P = P(x)$ is the variable porosity of the heterogeneous porous medium.

The pressure difference is given by the capillary pressure P_c:

$$P_c = P_o - P_w\,. \tag{4}$$

The imbibition condition for countercurrent imbibition phenomenon can be expressed as [14]

$$V_w = -V_o\,. \tag{5}$$

Using equations (1), (2) and (4) in (5), we get

$$\frac{\partial P_w}{\partial x} = -\left(\frac{k_w}{\delta_w} + \frac{k_o}{\delta_o}\right)^{-1}\left(\frac{k_o}{\delta_o}\frac{\partial P_c}{\partial x} + \frac{k_w}{\delta_w}\frac{\omega H}{4\pi}\frac{\partial H}{\partial x}\right). \tag{6}$$

According to Scheidegger [14], we have

$$\frac{k_w}{\delta_w}\frac{k_o}{\delta_o}\left(\frac{k_w}{\delta_w} + \frac{k_o}{\delta_o}\right)^{-1} \approx \frac{k_o}{\delta_o}. \tag{7}$$

On substituting the value of $\frac{\partial P_w}{\partial x}$ with (7) in equation (1), we get

$$V_w = K\frac{k_o}{\delta_o}\left[\frac{\partial P_c}{\partial x} - \frac{\omega H}{4\pi}\frac{\partial H}{\partial x}\right]. \tag{8}$$

Substituting equation (8) into (3), we get

$$P\frac{\partial S_w}{\partial t} + \frac{\partial}{\partial x}\left[K\frac{k_o}{\delta_o}\frac{\partial P_c}{\partial x} - K\frac{k_o}{\delta_o}\frac{\omega H}{4\pi}\frac{\partial H}{\partial x}\right] = 0. \tag{9}$$

***PRAJÑĀ* - Journal of Pure and Applied Sciences Vol. 24 – 25 : 15–22 (2017)**
ISSN 0975 - 2595

We assume that the capillary pressure P_c is a continuous linear function of the form [19]

$$P_c = -\beta S_w \tag{10}$$

where β is a constant.

Due to Scheidegger and Johnson [1], we assume the standard relationship between phase saturation and relative permeability as

$$k_w = S_w \text{ and } k_o = 1 - \alpha S_w \tag{11}$$

where α is a constant.

For the heterogeneous porous medium, we assume the porosity and permeability as functions of x only [2],

$$P(x) = \frac{1}{a_1 - a_2 x} \text{ and } K(x) = K_0(1 + bx) \tag{12}$$

where a_1, a_2, K_0 and b are positive constants. Since $P(x)$ can't exceed unity, we assume that $a_1 - a_2 x \geq 1$.

For simplicity, we consider $K \propto P$ [17],

$$K = K_c P \tag{13}$$

where K_c is a constant.

Considering the magnetic field in the x- direction only, we write H as [4, 22]

$$H = \lambda x^n \tag{14}$$

where λ is a constant parameter and n is an integer.

Using the value of H for $n = 1$ in equation (9) with equations (13), (11) and (10), we get

$$\frac{\partial S_w}{\partial t} = \frac{\beta K_c}{\delta_o P}\frac{\partial}{\partial x}\left[P(1 - \alpha S_w)\frac{\partial S_w}{\partial x}\right] + \frac{K_c \omega \lambda^2}{4\pi \delta_o P}\frac{\partial}{\partial x}[P(1 - \alpha S_w)x]. \tag{15}$$

Using dimensionless variables

$$X = \frac{x}{L}, \qquad T = \frac{\beta K_c t}{\delta_o L^2},$$

equation (15) becomes,

$$\frac{\partial S_w}{\partial T} = \frac{1}{P}\frac{\partial}{\partial X}\left[P(1 - \alpha S_w)\frac{\partial S_w}{\partial X}\right] + \frac{\omega \lambda^2 L^2}{4\pi \beta P}\frac{\partial}{\partial X}[P(1 - \alpha S_w)X]. \tag{16}$$

Now,

$$\frac{1}{P}\frac{\partial P}{\partial X} = \frac{\partial(\log P)}{\partial X}$$

$$= \frac{\partial}{\partial X}\left(\frac{a_2 L X}{a_1} - \log a_1\right)$$

$$(neglecting\ higher\ order\ terms\ of\ X)$$

$$= \frac{a_2 L}{a_1}.$$

Equation (16) reduces to

$$\frac{\partial S_w}{\partial T} = \frac{\partial}{\partial X}\left[(1 - \alpha S_w)\frac{\partial S_w}{\partial X}\right] + A(1 - \alpha S_w)\frac{\partial S_w}{\partial X} + B\frac{\partial}{\partial X}[(1 - \alpha S_w)X] + AB(1 - \alpha S_w)X \tag{17}$$

where $A = \frac{a_2 L}{a_1}$, $B = \frac{\omega \lambda^2 L^2}{4\pi\beta}$ and $S_w(x,t) = S_w(X,T)$.

A set of suitable boundary conditions for fingero-imbibition phenomenon are considered as

$$S_w(0,T) = \frac{T}{5} \text{ and } S_w(1,T) = \frac{1 + 3T}{5} \tag{18}$$

The equation (17) is the desired governing nonlinear partial differential equation for the fingero-imbibition phenomenon in the heterogeneous porous medium with magnetic field effect. The solution $S_w(X,T)$ of equation (17) represents the saturation of injected water at distance X and time T.

APPLICATION OF HOMOTOPY ANALYSIS METHOD

In 1992, Liao [20] proposed a new technique homotopy analysis method (HAM) to obtain solutions of nonlinear differential equations. Many authors have applied the HAM for solving ordinary differential equations and partial differential equations. For example, Liao [16] has discussed solution of various ODEs by HAM. Liao [6] has obtained solution for an unsteady boundary-layer flow due to an impulsively stretched sheet by HAM. Ali and Mehmood [7] have discussed the solution of the unsteady boundary layer flow equations by HAM. Darvishi and Khani [8] have applied the HAM to solve the foam drainage equation. Patel and Desai [12, 13, 23] have applied the HAM to one dimensional

***PRAJÑĀ* - Journal of Pure and Applied Sciences Vol. 24 – 25 : 15–22 (2017)**
ISSN 0975 - 2595

partial differential equation arising in fluid flow through porous medium.

Let us consider the nonlinear partial differential equation according to equation (17) as

$$\mathcal{N}[\varphi(X,T;q)] = 0 \tag{19}$$

where $q \in [0,1]$ is the embedding parameter, $\varphi(X,T;q)$ is an unknown function and a nonlinear operator $\mathcal{N}$ is defined as

$$\begin{aligned}\mathcal{N}[\varphi(X,T;q)] = &\frac{\partial^2\varphi(X,T;q)}{\partial X^2} \\ &- \alpha\varphi(X,T;q)\frac{\partial^2\varphi(X,T;q)}{\partial X^2} \\ &- \alpha\left\{\frac{\partial\varphi(X,T;q)}{\partial X}\right\}^2 \\ &+ (A - B\alpha X)\frac{\partial\varphi(X,T;q)}{\partial X} \\ &- A\alpha\varphi(X,T;q)\frac{\partial\varphi(X,T;q)}{\partial X} \\ &- (B\alpha + AB\alpha X)\varphi(X,T;q) \\ &+ ABX + B - \frac{\partial\varphi(X,T;q)}{\partial T}\end{aligned} \tag{20}$$

According to boundary conditions (18), it is straightforward to choose initial approximation as

$$S_{w_0}(X,T) = \frac{T + X^2 + T(X + X^2)}{5} \tag{21}$$

Now we choose the linear operator as

$$\mathcal{L}[\varphi(X,T;q)] = \frac{\partial^2\varphi(X,T;q)}{\partial X^2} \tag{22}$$

which has the property $\mathcal{L}(f) = 0$ when $f = 0$.

Let $c_0 \neq 0$ be the convergence control parameter and $H(X,T)$ be a non-zero auxiliary function. Liao [20] constructed, the so-called zeroth-order deformation equation

$$\begin{aligned}(1-q)\mathcal{L}\left[\varphi(X,T;q) - S_{w_0}(X,T)\right] \\ = qc_0H(X,T)\mathcal{N}[\varphi(X,T;q)]\end{aligned} \tag{23}$$

where $S_{w_0}(X,T)$ is an initial approximation of $S_w(X,T)$. When $q = 0$ and $q = 1$, we have

$$\varphi(X,T;0) = S_{w_0}(X,T) \text{ and } \varphi(X,T;1) = S_w(X,T) \tag{24}$$

respectively. Therefore, when q increases from 0 to 1, the solution $\varphi(X,T;q)$ deforms (varies) from the initial approximation $S_{w_0}(X,T)$ to the solution $S_w(X,T)$. By Taylor's theorem, we expand $\varphi(X,T;q)$ in powers of q as

$$\varphi(X,T;q) = S_{w_0}(X,T) + \sum_{m=1}^{\infty} S_{w_m}(X,T)q^m \tag{25}$$

where

$$S_{w_m}(X,T) = \frac{1}{m!}\frac{\partial^m\varphi(X,T;q)}{\partial q^m}\bigg|_{q=0}. \tag{26}$$

Assume that the linear operator, the initial approximation, the convergence control parameter and the auxiliary function are selected such that the series (25) is convergent at $q = 1$. Then at $q = 1$, the series (25) becomes

$$S_w(X,T) = S_{w_0}(X,T) + \sum_{m=1}^{\infty} S_{w_m}(X,T) \tag{27}$$

Define the vector $\overrightarrow{S_{w_n}} = \{S_{w_0}(X,T), S_{w_1}(X,T), \ldots, S_{w_n}(X,T)\}$. Differentiating (23) m times with respect to q and then putting $q = 0$ and finally dividing them by $m!$, we have the so-called high-order deformation equation

$$\begin{aligned}\mathcal{L}\left[S_{w_m}(X,T) - \chi_m S_{w_{m-1}}(X,T)\right] \\ = c_0H(X,T)\mathcal{R}_m\left(\overrightarrow{S_{w_{m-1}}}\right)\end{aligned} \tag{28}$$

where

$$\begin{aligned}\mathcal{R}_m\left(\overrightarrow{S_{w_{m-1}}}\right) = &\frac{\partial^2 S_{w_{m-1}}}{\partial X^2} - \alpha\sum_{j=0}^{m-1} S_{w_j}\frac{\partial^2 S_{w_{m-1-j}}}{\partial X^2} \\ &- \alpha\sum_{j=0}^{m-1}\frac{\partial S_{w_j}}{\partial X}\frac{\partial S_{w_{m-1-j}}}{\partial X} \\ &+ A\frac{\partial S_{w_{m-1}}}{\partial X} - B\alpha X\frac{\partial S_{w_{m-1}}}{\partial X} \\ &- A\alpha\sum_{j=0}^{m-1} S_{w_j}\frac{\partial S_{w_{m-1-j}}}{\partial X} \\ &- B\alpha S_{w_{m-1}} - AB\alpha X S_{w_{m-1}} \\ &+ (B + ABX)(1 - \chi_m) \\ &- \frac{\partial S_{w_{m-1}}}{\partial T}, m \geq 1\end{aligned} \tag{29}$$

and

$$\chi_m = \begin{cases} 0, & when \quad m \leq 1 \\ 1, & when \quad m > 1. \end{cases} \tag{30}$$

Here we consider the auxiliary function as $H(X,T) = 1$. Then the equation (28) becomes

***PRAJÑĀ* - Journal of Pure and Applied Sciences Vol. 24 – 25 : 15–22 (2017)**
ISSN 0975 - 2595

$$S_{w_m}(X,T) = \chi_m S_{w_{m-1}}(X,T) + c_0 \mathcal{L}^{-1}\left[\mathcal{R}_m\left(\overrightarrow{S_{w_{m-1}}}\right)\right] + C_1 X + C_2 \quad (31)$$

where C_1 and C_2 are determined by the boundary conditions $S_{w_m}(0,T) = 0$ and $S_{w_m}(1,T) = 0$, $m \geq 1$. Solution of (31) gives $S_{w_1}(X,T), S_{w_2}(X,T)$ and so on. Hence the homotopy series solution of (17) is as

$$\begin{aligned} S_w(X,T) = {} & \frac{T + X^2 + T(X + X^2)}{5} + c_0 \left[-\frac{X}{20} + \frac{X^2}{10} \right. \\ & - \frac{X^3}{30} - \frac{X^4}{60} - \frac{TX}{5} + \frac{TX^2}{5} - \frac{BX}{2} \\ & + \frac{BX^2}{2} - \frac{ABX}{6} + \frac{ABX^3}{6} \\ & + \frac{A}{5}\left(-\frac{X}{3} + \frac{X^3}{3} - \frac{5TX}{6} + \frac{TX^2}{2} \right. \\ & \left. + \frac{TX^3}{3} \right) - \frac{\alpha}{25}\left(-\frac{X}{2} + \frac{X^4}{2} - 3TX \right. \\ & + TX^2 + TX^3 + TX^4 - 3T^2X \\ & \left. + \frac{3T^2X^2}{2} + T^2X^3 + \frac{T^2X^4}{2} \right) \\ & - \frac{A\alpha}{25}\left(-\frac{X}{10} + \frac{X^5}{10} - \frac{47TX}{60} + \frac{TX^3}{3} \right. \\ & + \frac{TX^4}{4} + \frac{TX^5}{5} - \frac{27T^2X}{20} + \frac{T^2X^2}{2} \\ & \left. + \frac{T^2X^3}{2} + \frac{T^2X^4}{4} + \frac{T^2X^5}{10} \right) \\ & - \frac{B\alpha}{5}\left(-\frac{X}{4} + \frac{X^4}{4} - \frac{13TX}{12} + \frac{TX^2}{2} \right. \\ & \left. + \frac{TX^3}{3} + \frac{TX^4}{4} \right) - \frac{AB\alpha}{5}\left(-\frac{X}{20} \right. \\ & + \frac{X^5}{20} - \frac{3TX}{10} + \frac{TX^3}{6} + \frac{TX^4}{12} \\ & \left. \left. + \frac{TX^5}{20} \right) \right] + \cdots \quad (32) \end{aligned}$$

The solution (32) represents the saturation of injected water at distance X and time T for the fingero-imbibition phenomenon arising in fluid flow through the heterogeneous porous medium with magnetic field effect.

As pointed out by Liao, the convergence of the homotopy series solution depends upon the value of convergence control parameter c_0. The proper value of c_0 has been obtained using c_0-curves. Many authors have discussed the convergence of the homotopy series solution. For example, Liao [6, 16], Ali and Mehmood [7], Darvishi and Khani [8], Patel and Desai [12, 13, 23] have chosen a proper value of c_0 providing us the convergent homotopy series solution of nonlinear ODEs and PDEs. With the help of Mathematica package for nonlinear BVPs [18], the so-called c_0-curves are plotted for 20th order approximation. This helps us to discover the range for the admissible values of c_0, which corresponds to the horizontal line segment. It is obvious that the valid domain of c_0 is $-1.2 \leq c_0 \leq -0.4$ from the c_0-curves (see figures 2-4). This means that the series (32) converges for these values of c_0.

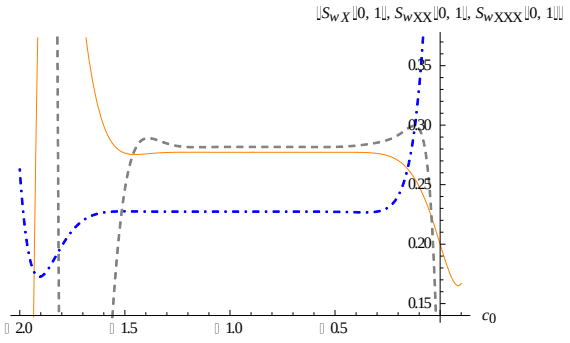

Figure 2: The c_0-curves of $S_{w_X}(0,1)$ (Solid line), $S_{w_{XX}}(0,1)$ (DotDashed line) and $S_{w_{XXX}}(0,1)$ (Dashed line).

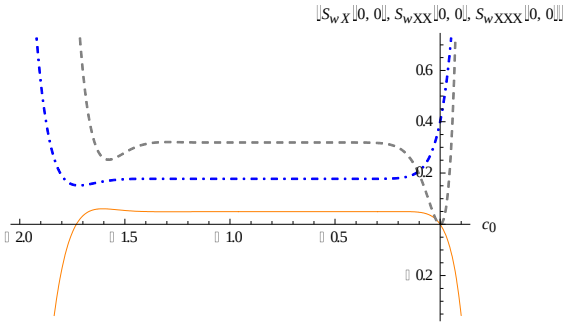

Figure 3: The c_0-curves of $S_{w_X}(0,0)$ (Solid line), $S_{w_{XX}}(0,0)$ (DotDashed line) and $S_{w_{XXX}}(0,0)$ (Dashed line).

***PRAJÑĀ* - Journal of Pure and Applied Sciences Vol. 24 – 25 : 15–22 (2017)**
ISSN 0975 - 2595

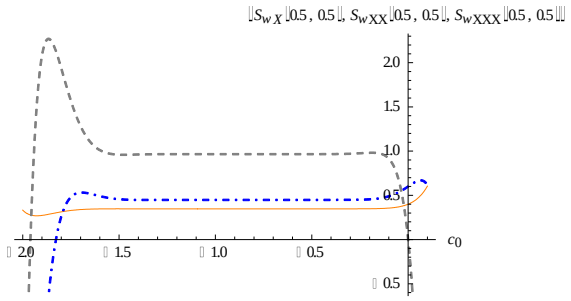

Figure 4: The c_0-curves of $S_{wX}(0.5, 0.5)$ (Solid line), $S_{wXX}(0.5, 0.5)$ (DotDashed line) and $S_{wXXX}(0.5, 0.5)$ (Dashed line).

RESULTS AND DISCUSSION

The following values of constants are considered as: $L = 1, \alpha = 1.11, a_1 = 2, a_2 = 1, \beta = 0.1, \omega = 0.1, \lambda = 0.1$ and we choose the proper value of the convergence control parameter $c_0 = -0.8$ to obtain convergent series solution. We have considered first 20 terms of series solution. Hence it gives an approximate solution of fingero-imbibition phenomenon in heterogeneous porous media with magnetic field effect. Table 1 indicates the numerical values of saturation of injected water for fingero-imbibition phenomenon at distance X for time T. Graphical presentation of the saturation of injected water is obtained by using Mathematica software. The graph of saturation of injected water versus distance X for fixed time $T = 0.1, 0.2, \ldots, 1$ is given in fig. 5 and fig. 6 represents the graph of saturation of injected water versus time T for fixed distance $X = 0.1, 0.2, \ldots, 1$

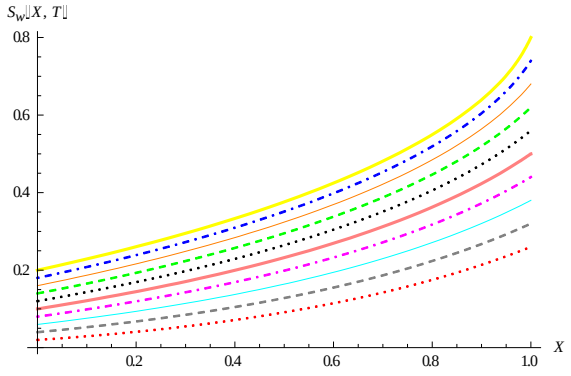

Figure 5: Saturation of water v/s distance X for fixed time $T = 0.1(lower\ most\ graph), 0.2, \ldots, 1(upper\ most\ graph)$.

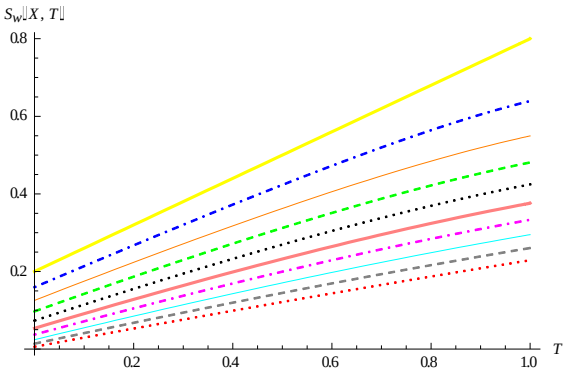

Figure 6: Saturation of water v/s time T for fixed distance $X = 0.1(lower\ most\ graph), 0.2, \ldots, 1(upper\ most\ graph)$.

COMPARATIVE STUDY WITH FINGERO-IMBIBITION PHENOMENON IN HETEROGENEOUS POROUS MEDIUM WITHOUT MAGNETIC FIELD EFFECT

Patel and Desai [13] have discussed homotopy series solution for fingero-imbibition phenomenon in heterogeneous porous medium without magnetic field effect. Table 2 shows the comparative numerical values of the saturation of injected water of fingero-imbibition phenomenon without magnetic field effect [13] and with magnetic field effect.

CONCLUSION

We have discussed the fingero-imbibition phenomenon in heterogeneous porous medium with magnetic field effect under certain assumptions. The homotopy series solution (32) represents the saturation of injected water. The solution (32) satisfies the boundary conditions (18). Numerical and graphical representations are obtained using Mathematica software. Table 1 indicates the numerical values of the saturation of injected water. Figures 5 and 6 give graphical representation. It is concluded that the saturation of injected water of fingero-imbibition phenomenon increases when the distance increases for given time T. Due to additional magnetic field effect the saturation of injected water is more increasing than the saturation of injected water without magnetic field effect. We can conclude that the magnetic field effect plays an important role in the fingero-imbibition

***PRAJÑĀ* - Journal of Pure and Applied Sciences Vol. 24 – 25 : 15–22 (2017)**
ISSN 0975 - 2595

phenomenon in the heterogeneous porous medium.

REFERENCES

[1] Scheidegger, A. E. and Johnson, E. F., (1961), The statistically behavior of instabilities in displacement process in porous media, Canadian J. Physics, 39 (2), pp. 326-334.

[2] Verma, A. P., (1969), Statistical behavior of fingering in a displacement process in heterogeneous porous medium with capillary pressure, Canadian J. Physics, 47 (3), pp. 319-324.

[3] Mishra, S. K. and Verma, A. P., (1974), Imbibition in the flow of two immiscible fluids with magnetic field, The Physics of fluids, American Institute of Physics, 17 (6), pp. 1338-1340.

[4] Verma, A. P., (1980), Instabilities in two phase flow through porous media with magnetic field, Multiphase transport: Fundamentals, Reactor Safety, Applications (Ed. T. N. Veziroglu), Hemisphere Publication Corporation, Washington, 3, pp. 1323-1335.

[5] Shah, R. C. and Verma, A. P., (1998), Fingero-imbibition phenomenon through porous media with magnetic field, Indian J. of Engg. and Materials Sciences, 5, pp. 411-415.

[6] Liao, S. J., (2006), An analytic solution of unsteady boundary-layer flows caused by an impulsively stretching plate, Commun. Nonlinear Sci. Numer. Simul., 11 (3), pp. 326-339.

[7] Ali, A., Mehmood, A., (2008), Homotopy analysis of unsteady boundary layer flow adjacent to permeable stretching surface in a porous medium, Commun. Nonlinear Sci. Numer. Simul., 13, pp. 340-349.

[8] Darvishi, M. T. and Khani, F., (2009), A series solution of the foam drainage equation, Computers and Mathematics with Applications, 58, pp. 360-368.

[9] Patel, K. R., Mehta, M. N. and Patel, T. R., (2013), A mathematical model of imbibition phenomenon in heterogeneous porous media during secondary oil recovery process, Applied Mathematical Modelling, 37, pp. 2933-2942.

[10] Parikh, A. K., Mehta, M. N. and Pradhan, V. H., (2014), Mathematical modeling and analysis of fingero-imbibition phenomenon in homogeneous porous medium with magnetic field effect in vertical downward direction, I. J. of Latest Tech. in Engg., Management & Appl. Sci., 3 (10), pp. 17-23.

[11] Patel, A. V., Rabari, N. S. and Bhathawala, P. H., (2015), Numerical solution of imbibition phenomenon in a homogeneous medium with magnetic fluid, IOSR J. of Mathematics, 11(4), pp. 11-19.

[12] Patel, M. A. and Desai, N. B., (2016), Homotopy analysis solution of countercurrent imbibition phenomenon in inclined homogeneous porous medium, Global J. Pure and Appl. Math., 12 (1), pp. 1035-1052.

[13] Patel, M. A. and Desai, N. B., (2017), Homotopy analysis method for fingero-imbibition phenomenon in heterogeneous porous medium, Nonlinear Science Letters A: Math., Phy. and Mech., 8 (1), pp. 90-100.

[14] Scheidegger, A. E., (1960), The Physics of flow through porous media, Revised edition, University of Toronto Press, Toronto.

[15] Bear, J., (1972), Dynamics of fluids in porous media, American Elsevier Publishing Company, Inc., New York.

[16] Liao, S. J., (2003), Beyond perturbation: Introduction to the homotopy analysis method, Chapman and Hall/CRC Press, Boca Raton.

[17] Cheng, Z., (2007), Reservoir simulation: Mathematical techniques in oil recovery, Society for Industrial and Applied Mathematics, Philadelphia.

[18] Liao, S. J., (2012), Homotopy analysis method in nonlinear differential equations, Higher Education Press, Beijing and Springer-Verlag Berlin Heidelberg.

[19] Mehta, M. N., (1977), Asymptotic expansions of fluid flow through porous media, Ph.D. Thesis, South Gujarat University, Surat, India.

[20] Liao, S. J., (1992), The proposed homotopy analysis technique for the solution of nonlinear problems, Ph.D. Thesis, Shanghai Jiao Tong University, Shanghai, China.

[21] Desai, N. B., (2002), The study of problems arises in single phase and multiphase flow through porous media, Ph.D. Thesis, South Gujarat University, Surat, India.

[22] Banerji, A. C. and Srivastava, K. M., (1963), Radial oscillations of variable magnetic star and the origin of the planetary system, Proceedings of the National Academy of Sciences, India, 33 (A), pp. 125-148.

[23] Patel, M. A. and Desai, N. B., (2017), A mathematical model of cocurrent imbibition phenomenon in inclined homogeneous porous medium, Kalpa Publications in Computing, ICRISET2017, Selected Papers in Computing, 2, pp. 51-61.

***PRAJÑĀ* - Journal of Pure and Applied Sciences Vol. 24 – 25 : 15–22 (2017)**
ISSN 0975 - 2595

Table-1: Numerical values of the saturation of injected water with magnetic field effect.

T	$X=0.1$	$X=0.2$	$X=0.3$	$X=0.4$	$X=0.5$	$X=0.6$	$X=0.7$	$X=0.8$	$X=0.9$	$X=1.0$
0.1	0.0294702	0.0409648	0.0548286	0.0714324	0.0911921	0.1145950	0.1422402	0.1749026	0.2136411	0.2600000
0.2	0.0528328	0.0676626	0.0848556	0.1048177	0.1280162	0.1550146	0.1865255	0.2235014	0.2672979	0.3200000
0.3	0.0759336	0.0938712	0.1141989	0.1373570	0.1638673	0.1943772	0.2297319	0.2711031	0.3202373	0.3800000
0.4	0.0987564	0.1195543	0.1427983	0.1689628	0.1986268	0.2325306	0.2716734	0.3174967	0.3722661	0.4400000
0.5	0.1212845	0.1446740	0.1705897	0.1995398	0.2321627	0.2692999	0.3121271	0.3624155	0.4231194	0.5000000
0.6	0.1435009	0.1691909	0.1975056	0.2289855	0.2643291	0.3044852	0.3508272	0.4055203	0.4724262	0.5600000
0.7	0.1653884	0.1930648	0.2234759	0.2571912	0.2949670	0.3378610	0.3874590	0.4463816	0.5196575	0.6200000
0.8	0.1869300	0.2162553	0.2484289	0.2840434	0.3239060	0.3691771	0.4216559	0.4844582	0.5640480	0.6800000
0.9	0.2081090	0.2387224	0.2722926	0.3094260	0.3509672	0.3981617	0.4529997	0.5190818	0.6044820	0.7400000
1.0	0.2289092	0.2604273	0.2949965	0.3332228	0.3759679	0.4245282	0.4810286	0.5494552	0.6393414	0.8000000

Table-2: Comparative numerical values of the saturation of injected water without magnetic field effect and with magnetic field effect.

T	$X=0.1$	$X=0.2$	$X=0.3$	$X=0.4$	$X=0.5$	$X=0.6$	$X=0.7$	$X=0.8$	$X=0.9$	$X=1.0$
0.1	0.0294301	0.0408938	0.0547358	0.0713267	0.0910823	0.1144897	0.1421481	0.1748322	0.2136012	0.2600000
0.1	0.0294702	0.0409648	0.0548286	0.0714324	0.0911921	0.1145950	0.1422402	0.1749026	0.2136411	0.2600000
0.2	0.0527940	0.0675937	0.0847656	0.1047151	0.1279096	0.1549123	0.1864359	0.2234330	0.2672591	0.3200000
0.2	0.0528328	0.0676626	0.0848556	0.1048177	0.1280162	0.1550146	0.1865255	0.2235014	0.2672979	0.3200000
0.3	0.0758961	0.0938046	0.1141118	0.1372578	0.1637642	0.1942783	0.2296453	0.2710369	0.3201998	0.3800000
0.3	0.0759336	0.0938712	0.1141989	0.1373570	0.1638673	0.1943772	0.2297319	0.2711031	0.3202373	0.3800000
0.4	0.0987202	0.1194901	0.1427143	0.1688671	0.1985275	0.2324355	0.2715902	0.3174333	0.3722302	0.4400000
0.4	0.0987564	0.1195543	0.1427983	0.1689628	0.1986268	0.2325306	0.2716734	0.3174967	0.3722661	0.4400000
0.5	0.1212496	0.1446122	0.1705089	0.1994478	0.2320674	0.2692088	0.3120477	0.3623551	0.4230855	0.5000000
0.5	0.1212845	0.1446740	0.1705897	0.1995398	0.2321627	0.2692999	0.3121271	0.3624155	0.4231194	0.5000000
0.6	0.1434674	0.1691316	0.1974281	0.2288975	0.2642381	0.3043985	0.3507520	0.4054637	0.4723946	0.5600000
0.6	0.1435009	0.1691909	0.1975056	0.2289855	0.2643291	0.3044852	0.3508272	0.4055203	0.4724262	0.5600000
0.7	0.1653563	0.1930080	0.2234018	0.2571073	0.2948806	0.3377792	0.3873886	0.4463291	0.5196290	0.6200000
0.7	0.1653884	0.1930648	0.2234759	0.2571912	0.2949670	0.3378610	0.3874590	0.4463816	0.5196575	0.6200000
0.8	0.1868992	0.2162010	0.2483583	0.2839637	0.3238244	0.3691004	0.4215907	0.4844107	0.5640233	0.6800000
0.8	0.1869300	0.2162553	0.2484289	0.2840434	0.3239060	0.3691771	0.4216559	0.4844582	0.5640480	0.6800000
0.9	0.2080794	0.2386705	0.2722254	0.3093505	0.3508905	0.3980903	0.4529401	0.5190399	0.6044621	0.7400000
0.9	0.2081090	0.2387224	0.2722926	0.3094260	0.3509672	0.3981617	0.4529997	0.5190818	0.6044820	0.7400000
1.0	0.2288809	0.2603777	0.2949326	0.3331515	0.3758960	0.4244623	0.4809749	0.5494194	0.6393273	0.8000000
1.0	0.2289092	0.2604273	0.2949965	0.3332228	0.3759679	0.4245282	0.4810286	0.5494552	0.6393414	0.8000000